UNIVERSITÀ DEGLI STUDI DELLA TUSCIA DI VITERBO

DIPARTIMENTO PER LA INNOVAZIONE NEI SISTEMI BIOLOGICI,
AGROALIMENTARI E FORESTALI
(DIBAF)

CORSO DI DOTTORATO DI RICERCA

BIOTECNOLOGIA DEGLI ALIMENTI - XXVI CICLO

Different regulation of target genes coding components of phenolics compounds biosynthesis pathways and their accumulations in apple and olive mutants

S.S.D AGR15

Author
Marco Cirilli

Coordinator of PhD course

Prof. Marco Esti

Tutor

Prof. Rosario Muleo

Co-Tutor

Prof. Vittorio Colizzi

2013-2014

SUMMARY

INTRODUCTION

Many epidemiologic studies support the association between high intake of fruit and vegetables, and low risk of many chronic diseases. The presence in plant-derived foods of a wide range of phytochemicals has been emerged as the main biologically plausible reason of such association. Phytochemicals are plant constituents characterized by bioactivities towards animal biochemistry and metabolism, which have the potential of being incorporated into foods or food supplements as nutraceutical, or into pharmaceuticals (Dillard et al., 2000). The term *nutraceutical* was coined by De Felice (1995), defining as 'any non-toxic food extract supplement that has scientifically proven health benefits for both disease treatment and prevention'. However, health effects is the result of the synergic action of numerous phytochemicals supplied by foods and/or diets at nutritional doses, rather than a simple *drug* (Fardet and Rock, 2013). Phytochemicals could regulate animal biochemistry, metabolism and physiology in different ways, as for example, they could be substrates for biochemical reactions, cofactors or inhibitors of enzymatic reactions, scavengers of reactive or toxic chemicals species, etc. (Dillard et al., 2000). Hundreds of researches have been added supporting evidences about beneficial role of phytochemicals on human health, related to the prevention of cardiovascular disease, cancer (Russo et al., 2005; Surh, 2003), diabetes, microbial, viral and parasitic infections and many other.

In the past, breeding programs were been aimed mainly to increase plant yield and productivity, with the results of lowering nutraceutical values of many common fruit and vegetables. However, the recent growing interest from nutritionist and consumers for food phytochemicals has opened new challenges for agriculture and food industries, particularly towards nutraceutical and functional foods. A functional foods is defined by Roberfroid (1999) as 'foods that should have a relevant effect on well-being and health or result in a reduction in disease risk'.

The growing knowledge about genetic mechanism regulating biosynthesis and accumulation of many important phytochemical classes in plants has speeded genetic improvement programs for increasing phytochemicals content of common fruit and vegetables crops. Plant breeders have identified a great source of genetic variation in *wild* species, often characterized by a superior ability in phytochemicals accumulation compared to cultivate ones (Hajjar et al., 2007). However, the introgression of favorable genetic traits from *wild* species through traditional breeding methods is laborious and time-consuming, since requires the *cleaning* from linkage drag caused by disturbing neighboring *wild* alleles (Collard and Mackill, 2007; Dubcovsky, 2004). OGM-based approaches could be potentially more rapid and effective compared to other breeding methods. However, the difficulty to fine-tune transgene expression might results in unbalanced accumulation of phytochemicals, negatively affecting sensorial attributes of the products. In addition, consumers often prefer OGM-free products (Aldrich and Blisard, 1998) and OGM-plants cultivation is prohibited or severely limited in some countries. Spontaneous mutants of cultivated variety for phytochemicals accumulation represent important resources both for scientific and productive purpose. At scientific

level, they represent important tools for understanding genetic and biochemical mechanisms regulating phytochemicals accumulation. At productive and agro-industrial level, these mutants might be used for direct production of functional foods or for genetic improvement of other cultivars. Indeed, spontaneous mutants could effectively speeded breeding programs, since they have only a limited number of undesired character compared to *wild* species. Moreover, respect to OGM-plants, mutated gene/s are often better integrated in transcriptional regulation network, resulting in a more fine-control of phytochemicals accumulation.

In the first part of the thesis is aimed to characterize at pomological, biological, genetic and molecular level, the new red-fleshed apples line, Italian Red Passion, obtained through traditional breeding methods. The second part of the thesis is aimed to elucidate genetic mechanism regulating anthocyanin biosynthesis in olive fruit, comparing olive cultivars showing a different pattern of drupe pigmentation. In addition, the application of NIRS technology for on-field monitoring of pigments (and other phenolic compounds) accumulation in olive, has been evaluated. In the third part of the this research work, advanced studies are reported on the small-RNAs, their presence in fruit and derived food, and their role in plant genes network regulation and human health gene regulation.

SECTION I
MOLECULAR AND BIOCHEMICAL CHARACTERIZATION OF THE ITALIAN RED PASSION APPLE LINES

1. STATE OF THE ART

1.1 EFFECT OF APPLE CONSUMPTION ON HUMAN HEALTH

Apple is a widely consumed fruit and a rich source of phytochemicals. Epidemiological studies have linked the consumption of apples with reduced risk of some disease including cardiovascular pathologies, cancer, asthma and diabetes (Boyer et al., 2004). Several studies have specifically linked apple consumption to a reduced risk of lung cancer, especially in woman (Feskanich et al., 2000). Moreover, Le Marchand et al. (2000) associated this reduced risk to flavonols intake, such as quercetin, although results were not statistically significant. The Women's Health Study (Sesso et al., 2003) found a significant reduced risk of cardiovascular disease associated with apple regular consumption. Women ingesting the highest amounts of flavonoids had a 13–22% decrease in cardiovascular disease risk. Moreover, apple consumption was also inversely associated with coronary heart disease in postmenopausal women (Arts et al., 2001). The intakes of catechins and epicatechins, both constituents of apples, were strongly and inversely associated with coronary heart disease and the same authors suggested that apple catechins could be more bioavailable than the catechin and epicatechin gallates commonly found in teas. Apple consumption has been linked with asthma and diabetes prevention (Esenkrantz et al., 2003; Knekt et al., 2002), and positively associated with general pulmonary health (Woods et al., 2003). Anthocyanin have been implicated in a diverse range of health-promoting properties (Lila, 2004) and their antioxidant properties has been established from various fruit (Smith et al., 2000; Chun et al., 2003).

1.2 APPLE FRUIT COMPOSITION AND PHYTOCHEMICALS

Apple fruit is prevalently composed by water, which represent about of 85% of fresh weight; the solid component is predominate by carbohydrates (especially fructose and fiber) which ranged from 9% to 13%, depending from many factors. Moreover, apple fruit contain a good percentage of minerals and vitamins, in particular vitamin C and very low amounts of lipids (0.4%) and protein (0.3%). In addition, apple fruit contain relevant amount of some class of secondary metabolites, such as phenolic acid and flavonoids. However, their content is variable, depending from many factors including cultivars, environmental condition and farm management. During the last 13 years, a large number of studies reporting polyphenol concentrations of apples has been published. The Phenol Explorer (Neveu et al., 2010), available at http://www.phenol-explorer.eu/website.html, is a powerful tool to get an overview of potential polyphenol contents and ranges in different apples cultivars and in different environmental and agronomical condition. In general, five polyphenol classes predominate

apples fruit, such as flavan-3-ols, phenolic acids, dihydrochalcones, flavonols and anthocyanidins. The amount of each class varied depending from tissues (Francini et al., 2013), as shown in figure 1.

The flavan-3-ols are the most abundant group of polyphenols in apples. They could be divided into monomeric, oligomeric and polymeric flavan-3-ols. The only two monomeric flavan-3-ols in apples are catechins and epicatechins. The condensation of this two monomers results in oligomeric flavan-3-ols, which are called procyanidins. The most important dimeric procyanidins in apples are procyanidin B1 and B2. Treutter at al. (2001) reported a range of 1-8.4 mg/100 g FW for procyanidin B1 and 1.5-23 mg/100 g FW for procyanidin B2 in fresh apple fruits. The content in the apple peel ranged from 10 to 100 mg/100 g of fresh weight for procyanidin B2. Additionally, oligomeric procyanidins with 5.7-7.1 average degree of polymerization seem to be the most abundant polyphenols in apples (Guyot et al., 2002). Monomeric and oligomeric flavan-3-ols are present in both flesh and peel, although peel contained higher amounts (Tsao et al., 2003).

Phenolic acids are phenols having one carboxylic acid group and thus, belong to organic acids. Hydroxycinnamic and hydroxybenzoic acids represent the main subclasses. In apples, hydroxycinnamic acids content is relevant, particularly chlorogenic acid, the ester of caffeic acid (CF) and quinic acid (QA) but also p-Coumaroylquinic acids (CQA). The concentration ranged from 0.3 to 3.5 mg/100 g of fresh weight for CQA in whole apple fruits and 0.54-3.9 mg/100 g of fresh weight for CQA in peel tissue, as reported by Treutter et al. (2001).

Dihydrochalcones are compounds exclusively present in *Pomaceae*, such as apple and pear fruit. These class of compounds have a chemical structure composed by an open ring (Crozier et al. 2009). Major dihydrochalcones contained in apples are phloridzin and phloretin-xyloglucoside, differing for substituted sugar at the superior hydroxyl group (glucose in phloridzin, xylose in phloretin). The amount varied from 0.3 to 16 mg/100 g of fresh weight for phloridzin and from 1 to 23 mg/100 g of fresh weight for phloretin, whereas major levels in apple skin are reported, ranged between 0.6-65.4 mg/100 g of fresh weight and 7-27 mg/100 g of fresh weight, respectively (Treutter et al., 2001). Additionally, dihydrochalcones represent up to 60 % of the polyphenols in the seeds (Tomàs-Barberàn et al., 2000).

Flavonols are glycosylated quercetin derivatives mainly present in apple peel. The glucosyl moiety is mainly composed by galactose, although glucose, xylose, arabinose, rhamnose and rhamnoglucose derivatives are also been reported (Treutter et al., 2001). The amounts in fresh apple fruits are very low. Instead, peel content varied from 7-95 mg/100 g FW for quercetin-galactoside (Treutter et al., 2001) to trace for the other glycosylated form.

Anthocyanins are anthocyanidins glycosides deriving from flavonols, which lack the ketone oxygen at the C4-position, the major anthocyanin found in apple skin is cyanidin 3-galactoside (Ubi et al., 2006). Other anthocyanins occur in small quantity, and include cyanidin 3-arabinoside, cyanidin 3-glucoside (Ubi et al., 2006) and di-glycosylated cyanidins. Most of the apple cultivars contain

anthocyanins only in peel tissues. However, particularly apple fruit of *Malus* wild species, accumulate anthocyanins also in flesh tissue (Volz et al., 2009).

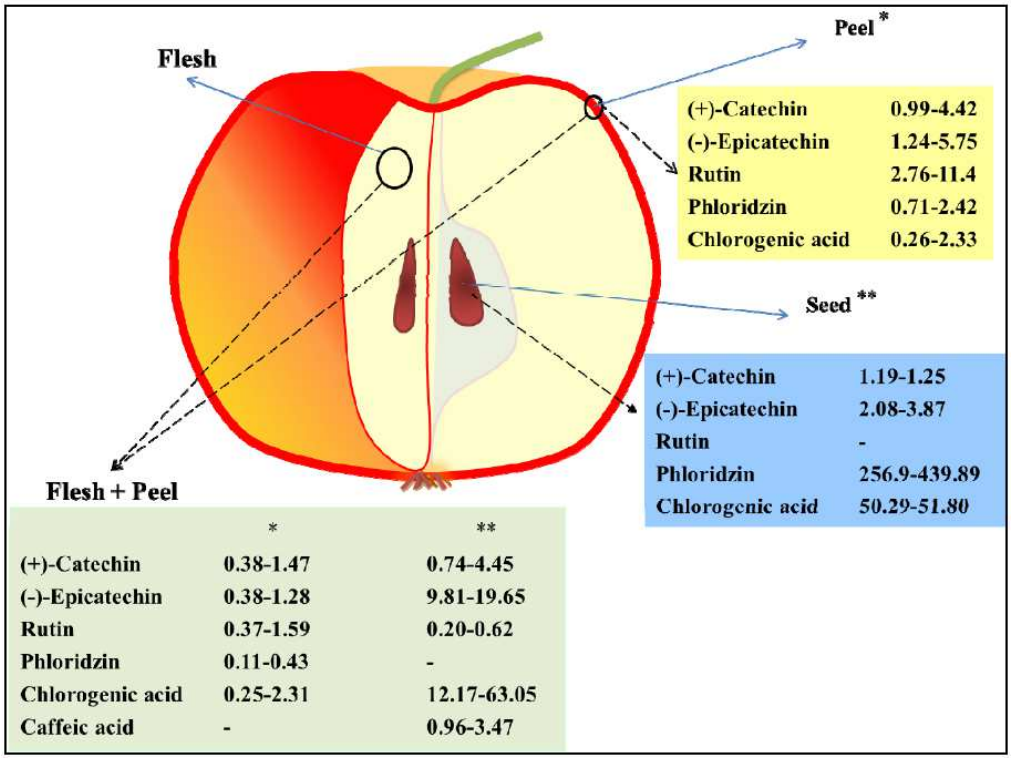

*Figure 1. Flavonoid content of flesh, peel and seed, as determined by various authors (adapted from Francini et al., 2013). * mg/g DW; ** mg/100 g FW; - not determined.*

1.3 FLAVONOID BIOSYNTHESIS

Flavonoids are synthesized by the combination of 4-coumaroyl-CoA with malonyl-CoA to yield the class of chalcones, which represent the backbone of flavonoids compounds. Flavonoids pathways (Figure 2) begin with the reaction catalyzed by the phenylalanine ammonia-lyase (PAL) enzyme, which converts the amino acid phenylalanine to cinnamic acid, which could be further utilized by phenylpropanoid enzymes to synthesize phenolic acids and lignin, or converted to chalcones by the enzyme chalcone synthase (CHS), in the presence of malonyl-CoA (malonyl Co-A). This represents the first committed step in the synthesis of flavonoid compounds. Whereas the biosynthesis of chalcones and flavonoids is well understood, the biosynthesis of closely related dihydrochalcones has been partially elucidated only recently. The high similarity of p-coumaroyl-CoA and p-dihydrocoumaroyl-CoA (required for dihydrochalcones biosynthesis) suggests that chalcone synthase enzyme could utilize both substrates. Studies of chalcone synthases from *M. domestica* confirmed this hypothesis (Gosch et al., 2009). The key unidentified enzyme is a putative carbon double-bond reductase, which acts on *p*-coumaroyl-CoA to produce the dihydro-*p*-coumaroyl-CoA precursor (Dare et al., 2013). The same authors demonstrated that the silencing of *ENRL3* and *ENRL5* genes, coding

for two enoyl-reductase isoforms, induce a reduction of phloridzin content, although the same authors speculate that even other genes could be play a relevant role in the regulation of dihydrochalcones content. The *PGT1* gene encode the glucosyltransferase enzyme which converts phloretin to phloridzin (phloretin-2-glucoside) was also identified (Judgè et al., 2010).

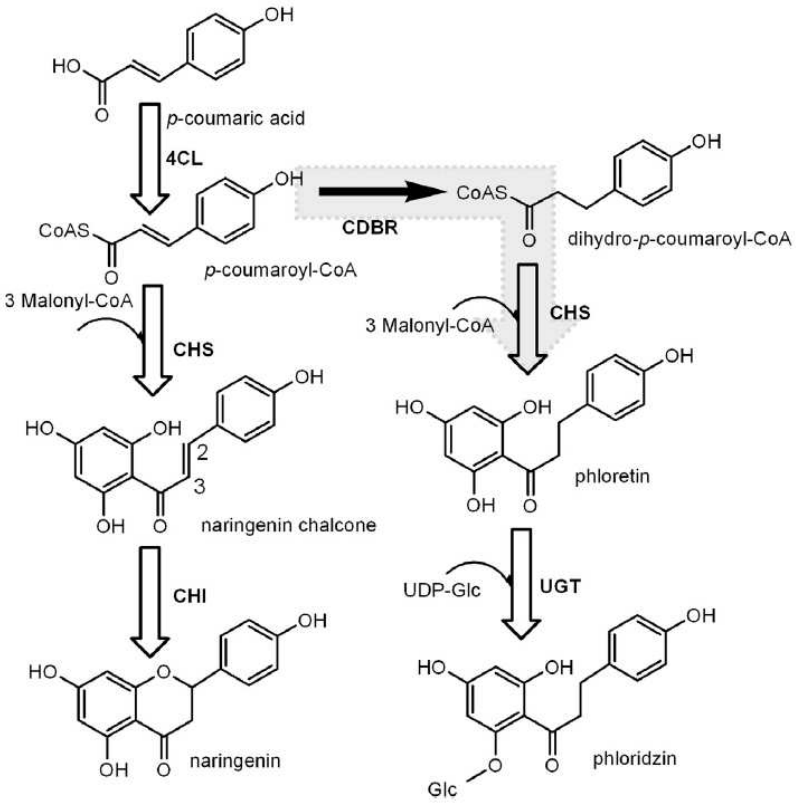

Figure 2. Flavanone and chalcones simplified biosynthesis pathway (as revised from Dare et al., 2013).

Down-stream of chalcones, biosynthesis generates the dihydrokaempferol, and the reaction is catalyzed by the 3ß-hydroxylase (F3H) enzyme (Pelletier et al., 1996). Dihydrokaempferol is hydroxylated to produce dihydroquercetin by flavonoid 3'-hydroxylase (F3'H) or flavonoid 3',5'-hydroxylase (F3'5'H) enzymes (Holton and Cornish, 1995). The conversion of the different dihydroflavonols in flavonols such as kaempferol and quercetin, is catalyzed by the flavonol synthase (FLS) enzyme (Pelletier et al., 1997). In addition to FLS, modifying enzymes such as glycosyltransferases (GTs) and methyltransferases (MTs) further contribute to the wide range of flavonol glycosides found in plants (Yonekura-Sakakibara et al., 2007). The conversion of colorless dihydroflavonols to anthocyanin pigments involves reduction of the dihydroflavonols to leucoanthocyanidins by dihydroflavonol 4-reductase (DFR) enzyme, followed by oxidation to anthocyanins by leucoanthocyanidin dioxygenase (LDOX). Anthocyanins are subsequently glycosylated by the enzyme UDP-glycosyl:flavonoid-3-O-glycosyltransferase (UFGT). Numerous

anthocyanin glycosides could be produced, depending on the dihydroflavonol substrate and the carbon atom to which the aglycone is conjugated. In addition, further modification of anthocyanin glycosides by glycosylation, methylation and acylation increases the number of different anthocyanins that occur in nature. Recently, the biosynthesis of flavan-3-ols was investigated also in apple (Henry-Kirk et al., 2012). The genes leucoanthocyanidin reductase (*LAR*) and anthocyanidin reductase (*ANR*), encoding enzymes for the synthesis of catechins (2,3-transflavan-3-ol) and epicatechins (2,3-cis-flavan-3-ol), respectively. Catechins and epicatechins both act as initial substrate for the synthesis of condensed tannins. The mechanism by which extension units are added to produce a polymeric tannin molecule remains unknown, although some polymerization theories have been presented (Zhao et al., 2010).

1.4 ANTHOCYANINS BIOSYNTHESIS IN APPLE

Many genes encoding the anthocyanin biosynthesis enzymes, such as chalcone synthase CHS, F3H, DFR, LDOX and UFGT, are coordinately expressed during apple fruit development and their transcription levels are positively correlated with anthocyanin concentration (Ben-Yehuda et al., 2005). Deduced amino acid sequences of these genes in cultivar Fuji showed high homology to corresponding protein sequences from other plants (Kim et al., 2003). The mRNAs of anthocyanin biosynthetic genes are detected preferentially in peel tissue and transcription of the genes was coordinately induced by light (Kim et al., 2003). Moreover, transcripts were detected abundantly in the skin of red-pigmented apple, but rarely in non-red pigmented apple cultivars, confirming their roles in determination of apple skin color (Kim et al., 2003). However, southern hybridization using fragments of anthocyanin structural genes as probes revealed little polymorphism between green and red cultivars, demonstrating that both green and red ones carry on anthocyanin structural genes. Interesting, Kondo et al. (2002) detected CHS, F3H, DFR, LDOX and UFGT transcripts already at early developmental stages (20 Days after full bloom) in both dark and light grown fruit. These results are in agreement with those of Ju et al. (1995) which found higher UFGT activity in red-striped areas contained more anthocyanin compared to green colored adjacent areas, but no differences in PAL and CHS activities. Moreover, Ju et al. (1997) have not been found a correlation between DFR activity and anthocyanin accumulation in apple fruit. It appears that DFR is necessary, but not a limiting point, for anthocyanin synthesis in apples.

1.5 TRANSCRIPTIONAL REGULATION OF ANTHOCYANIN BIOSYNTHESIS IN APPLE

The production of secondary metabolites in response to environmental and developmental cues is regulated by transcription factors (TFs), proteins that bind to specific DNA sequences modulating the initiation of target gene transcription. The plant MYB family protein comprises many of the most important TFs regulating phenylpropanoid and flavonoid biosynthesis, together with HELIX-LOOP-HELIX (bHLH) and WD-repeats (WDR) proteins families. The co-ordinate expression of particular flavonoid biosynthetic genes in response to developmental (Pelletier et al., 1999) and environmental

cues (Kim et al., 2003) has long been indicative that these genes are regulated at the level of transcription. Since the first plant MYB gene to be isolated, COLOURLESS1 (C1) from maize, regulating genes for anthocyanin synthesis (Paz-Ares et al., 1987), many TFs controlling flavonoid pathway has been identified and characterized in a variety of plant species, including snapdragon, petunia, Arabidopsis, grape and apple. Many species regulate flavonoid pathways branching through discrete control of specific gene subsets or individual flavonoid genes (*Figure 3*). R2R3-MYB proteins that specifically regulate anthocyanin (PRODUCTION OF ANTHOCYANIN PIGMENT1, AtPAP1), (Borevitz et al., 2000) flavonol (AtMYB11, AtMYB12, AtMYB111) (Stracke et al., 2001) or flavan-3-ols synthesis (TRANSPARENT TESTA2, AtTT2) (Nesi et al., 2001) have been identified from Arabidopsis. Transcriptional control of genes, involved in anthocyanin biosynthesis, has also been demonstrated in grape berries by VvMYBA1 (Kobayashi et al., 2004). Further research in grape has involved the discovery of more R2R3-MYB transcription factors, including VvMYBPA1 which control flavan-3-ols biosynthesis (Bogs et al., 2007), VvMYBF1 as a specific regulator of flavonol biosynthesis (Czemmel et al., 2009), and VvMYB5a and VvMYB5b which have a broad effect on a number of phenylpropanoid genes (Deluc et al., 2008).

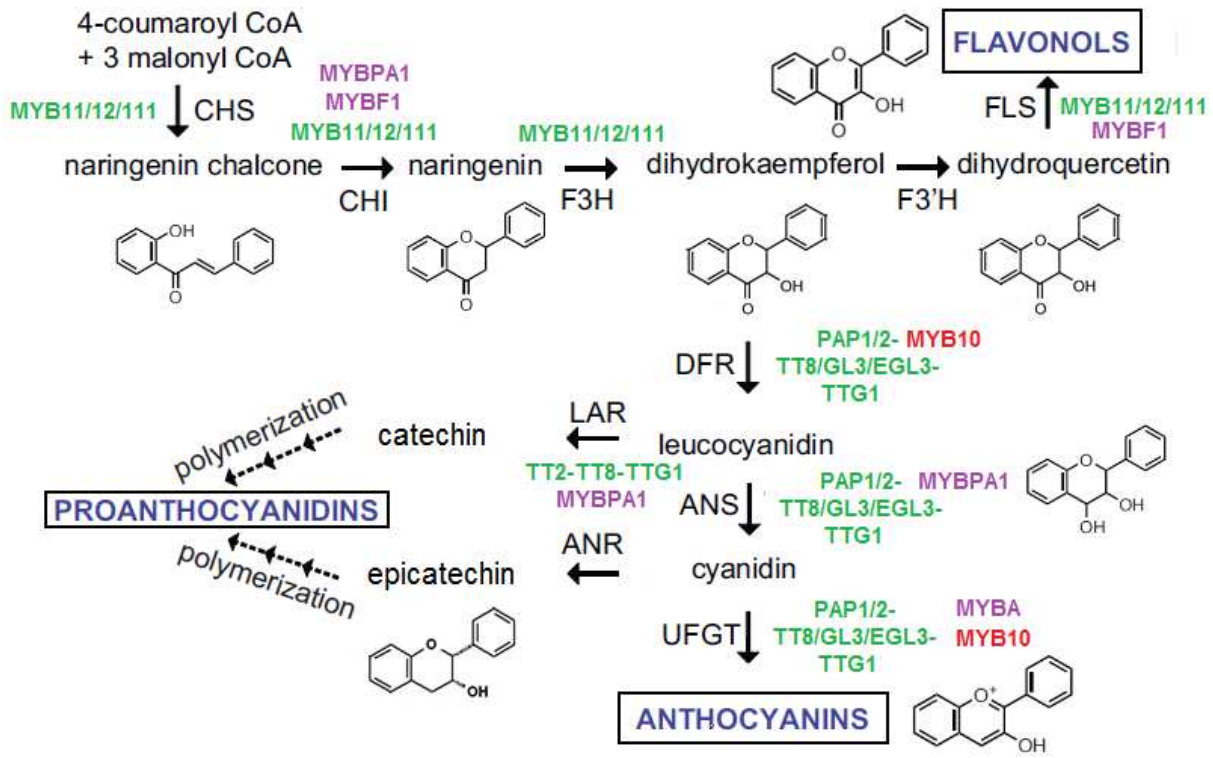

Figure 3. Main structural gene and transcription factors (TFs) regulating flavonoid biosynthesis. Green, violet and red colored TFs highlighted TFs characterized in Arabidopsis, grape and apple, respectively.

As reported by Volz et al. (2007) red-fleshed apple could be divided into two type, I and II based on the presence (type I) or absence (type II) of red pigmentation in other plant organs, such as young leaf, flowers, petiole and vasculature. Many researcher have been investigated molecular basis of these two phenotypes, ultimately leading to the identification of a R2R3 MYB, MdMYB1/10 transcription factor responsible for anthocyanin accumulation (Ban et al., 2007b; Espley et al., 2007; Takos et al., 2006a). *MdMYB10* transcript levels strongly correlate with peel anthocyanin levels, and this gene is able to induce anthocyanin accumulation in heterologous and homologous systems (Espley et al., 2007). In addition, *MdMYB10* cosegregates with the Rni locus, mapped in long arm of chromosome 9 of apple genome, a major genetic determinant of red foliage and red color in the flesh of apple fruit (Chagne et al., 2007). Type I red-fleshed apples are characterized by a 101 bp insertion in promoter region at *MdMYB10* gene (*Figure 4*), composed by 5 tandem duplication of a 23 bp microsatellites (Espley et al., 2007), forming the so called R_6 domain, to distinguish from the 23-bp sequence motif, named R_1, present in wild type *MdMYB10* allele (*Figure 4*). Transient assays and electrophoretic mobility shift assays demonstrated that this 23-bp sequence motif is a target of the MYB10 protein itself, and the number of repeat units correlates with an increase in trans-activation by MYB10 protein.

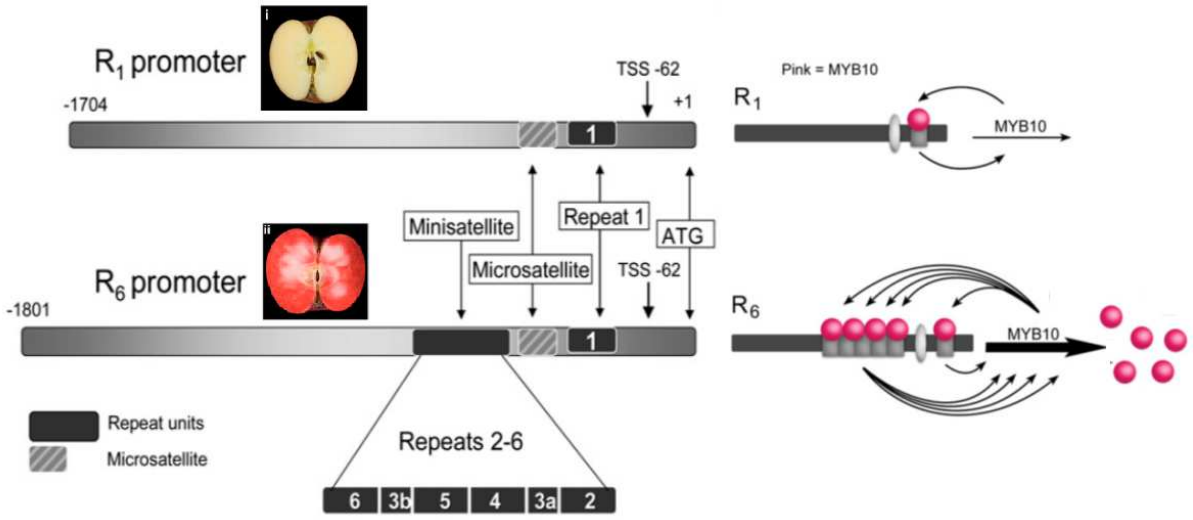

Figure 4. The 121 bp minisatellites insertion within MdMYB10 promoter R_6 MYB10, confer trans-activation of MYB10 protein itself, inducing anthocyanins accumulation in apple flesh.

Other apple MYBs, such as MYB1 and MYBA, were also reported to regulate genes in the anthocyanin pathway. Takos et al. (2006) identified three alleles of *MdMYB1*. The *MdMYB1-1* allele was found to be expressed in red apple skin, whilst green or yellow apple skin possessed the *MdMYB1-2* and *MdMYB1-3* alleles type. Although functional assays did not revealed differences among the three types of *MdMYB1* alleles, important differences were found regarding promoter region and first intron of *MdMYB1-2/3* alleles, suggesting that these mutations could affect their

transcriptional regulation. *MdMYBA* is also more highly expressed in redder peels and the redder cultivars and its transcription is induced by UV-B light and low temperature (Ban et al., 2007). As *MdMYB1* and *MdMYBA* share identical sequences, and *MdMYB10* and *MdMYB1* genes are located at very similar positions on linkage group 9, it was concluded that these genes were allelic (Lin-Wang et al., 2010). In contrast, the type 2 red-flesh apple phenotype does not cosegregate with molecular markers linked to *MdMYB10* (Volz et al., 2006) and Chagnè et al. (2013) demonstrated that the red-flesh cortex type II phenotype is associated with enhanced expression of *MdMYB110a*, a paralog of *MdMYB10*. Both *MdMYB10* and *MdMYB110a* have conserved function in some cultivars, but they differ in their expression pattern and response to fruit maturity. The expression of several anthocyanin pathway genes was found to be regulated by both *MdMYB10* and *MdMYB1*. Transient assay demonstrated the ability of MYB10 to induce DFR promoter activity, while ectopic expression of *MdMYB10* in transgenic plant enhance also expression of UFGT and CHI genes (Espley et al., 2007). A similar results was found by Takos et al. (2006), which demonstrated the ability of MYB1 to activate UFGT and DFR promoters. Although MYB1/10/A play a pivotal role in orchestrating anthocyanin accumulation, an excellent survey of van Nocker et al. (2011) highlighted that the presence of the R_6 allele alone was, at least in some cases, insufficient to drive development of pigmented flesh. Analyzing red-color patterning in hundreds of different accession, authors identified genotype carry on R_6 allele yet did not develop significant pigmentation. In addition, although R_6 allele is associated to red-flesh pigmentation, many of these accessions produced fruit exhibiting various internal coloration patterns, unrelated to whether R_6 was heterozygous or homozygous. Collectively, these observations suggest that the effect of R_6 is extensively modified in a genotype-specific manner. Finally, as reported by Espley et al. (2013), ectopic *MdMYB10* expression in transgenic Royal Gala plants induced a strong increase in total polyphenol content, suggesting a broad role for MYB10 in general flavonoid pathways regulation. However, Volz et al. (2007), analyzing cross populations carry on mutated MYB10 allele, did not observe a tight association between R_6 mutation and total polyphenol content, suggesting that mutation could affect polyphenol content only in genotype-dependent manner.

1.6 A PROTEIN COMPLEX IS REQUIRED FOR INITIATION OF TRANSCRIPTION

In some cases, the binding of a MYB factor to a target gene promoter is sufficient to activate transcription of the gene. The Arabidopsis flavonol regulator AtMYB12, for example, is capable of transcriptional activation that is independent of a bHLH partner (Mertens et al., 2005). However, more commonly a protein complex is required for transcriptional activation of target genes (Larkin et al., 1999). In species analyzed to date, regulatory proteins isolated include those from the *MYB*, *bHLH* and *WD40* gene families. Yeast one- and two-hybrid assays have indicated these proteins can interact with each other, and that MYB domains can bind to the promoters of target genes (Aharoni et al., 2001). Functional specificity of these regulatory complexes appears to reside with the MYB factors, which

display different binding specificities as determined by sequences within the DNA binding domain. On the other hand, proteins belonging to the bHLH and WD40 families are more highly conserved and are consequently often involved in regulation of several processes (Koes et al., 2005). Early studies in maize demonstrated that pigments production requires the interaction of the R/B family and a member of the C1/Pl family (Cocciolone and Cone, 1993). The R/B gene family of transcription factors encodes proteins with homology with the basic helix-loop-helix (bHLH) motif in the MYC transcription activator (Chandler et al., 1989). In Arabidopsis, the WD40 protein TRANSPARENT TESTA GLABRA1 (TTG1) works together with AtPAP1 (MYB) and GLABRA3 (AtGL3, bHLH) or ENHANCER OF GL3 (AtEGL3) to regulate anthocyanin synthesis (Zhang et al., 2003), and works in combination with the AtTT2 (MYB) and AtTT8 (bHLH) to control tannin production (Baudry et al., 2004). In addition to the activators, transcriptional repressors may modulate flavonoid biosynthesis, in particular members of C2-repressor motif MYB subclade 4. In Arabidopsis, C2-repressor clade include *AtMYBL2* gene, which could inhibit anthocyanin synthesis in transgenic plants (Matsui et al., 2008). In kiwifruit, ectopic expression and suppression of the persimmon *MYB4* gene (an orthologs of *AtMYBL2*) negative regulate tannin synthesis (Akagi et al., 2009). The strawberry R2R3-MYB transcription factor *FaMYB1* is capable of lowering the expression of anthocyanin and flavonol biosynthetic genes in transgenic tobacco (Aharoni et al., 2001).

1.7 EPIGENETIC REGULATION OF FLAVONOIDS BIOSYNTHESIS

MicroRNAs (miRNAs) are a class of 21-24 nucleotides non-coding RNAs involved in post-transcriptional gene silencing in eukaryotes (Reinhart et al., 2002). MicroRNAs are generated from single-stranded RNA precursors (transcribed from the genomic loci-microRNA genes) forming an imperfect stem-loop secondary structure (Reinhart et al., 2002) which is processed to a mature miRNA duplex in two steps by the Dicer Like enzyme1 (DCL1). After being exported to the cytoplasm, the mature miRNAs are loaded onto the Argonaute (AGO) proteins (*Figure 5*), the catalytic centers of plant RNA-induced silencing complexes (RISC) (Vaucheret et al., 2004). The miRNA loaded RISC binds to the target mRNA in a sequence specific manner that cleaves the target (the predominant mechanism in plants) or prevents the translation (Brodersen et al., 2008). The plant miRNA world has expanded with the cloning of numerous miRNAs from various plant species and different environmental conditions, revealing highly conserved nature of miRNAs across the plant kingdom (Willmann & Poethig, 2007). Plant miRNAs are involved in a plethora of function, regulating plant growth and development. MYB gene family are target by at least three miRNA classes, *miR858*, *miR828* and *miR159* in model species *Arabidopsis* (Dubos et al., 2010). Recently, Xia et al. (2012) demonstrates that *miR858* potentially target up to 53 different *MYBs*, many of them expressed in fruit and putatively involved in proanthocyanidin biosynthesis, such as, for example, *MdMYB9* and *MdMYB12* (orthologs of *AtTT2* and *VvMYB5a*, previously described) or some putative anthocyanins repressor, such as *MdMYB16*, belonging to the *MYBC2*-repressor clade.

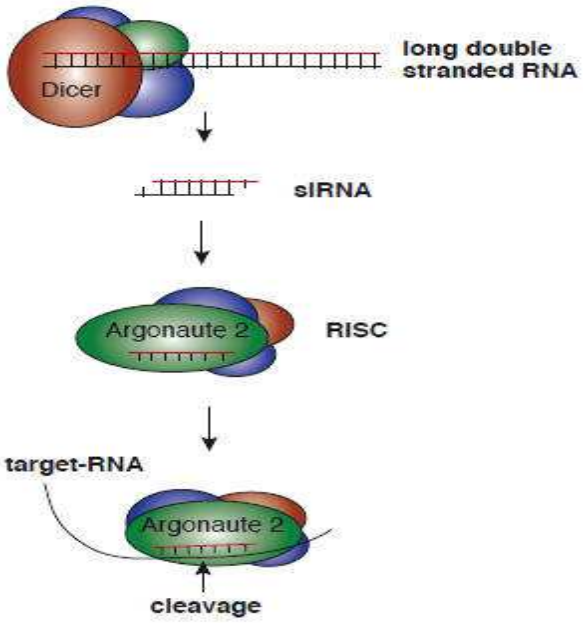

Figure 5. RNA silencing machinery. The mature miRNAs are loaded onto the RNA-induced silencing complexes (RISC) and binds to the target mRNA in a sequence specific manner.

1.8 BREEDING FOR RED PIGMENTATION IN APPLE FLESH

The most used breeding strategy in apple to achieve red-flesh color or polyphenol content increase is based through the cross of selected cultivars with *Mauls wild* species, such as *M. niedzwetkyana*, *M. sieverisii* or *M. kirghisorum*. The fruits of *M. niedzwetzkyana* Dieck. are violet-purple in colour with a waxy bloom while their flesh is pink to purple in colour (Dzhangaliev et al., 2003). The fruit are normally large sized and usually astringent. This wild species has been used in many breeding programs and some of its accession include cultivars such as Redfield and Redflesh. *M. sieversii* fruit show a variable fruit peel and flesh colour, from yellow to red and white to yellow, respectively. Skin colour of Kirghiz apple (*M. kirghisorum*) is green, yellow or reddish and the flesh colour is white with a flavor that is sour-sweet, acid to bitter and astringent. Despite wild apples species are mainly used in breeding programs due to their resistance to a range of diseases such as apple scab, recently they are also used to incorporate novel colour, aroma, flavour, size, and texture into breeding programs (Forsline et al., 2003). However, wild apples are often acidic and high in tannins, which make them astringent (Dzhangaliev, 2003). Some of the wild apples have low sugar levels. The difference in flavour is due to the differences in tannin levels and high acidity. Wild apples also vary in fruit size ranging from small to large fruits (Dzhangaliev, 2003).

Since 1944, some red-flesh cultivar have been released (*Figure 6*). The first cultivar, Pink Pearl, was released for commercial cultivation by Albert Etter, an apple breeder from California, after crossing the pink/red-fleshed cultivar Surprise with a white-fleshed cultivar. Other seven red-fleshed cultivars derived from Pink Pearl were released, under the Rosetta^{TM} brand, such as Rubayat,

Grenadine and Pink Pearmain. Apples of Weirouge cultivars represent a red-fleshed German cultivar, bred in Weihenstephan (Germany) primarily for processing purposes and officially registered in 1997. Plant & Food Research in New Zealand has conducted research on red-fleshed apples since 1998 (Volz et al., 2009). High quality white fleshed apples were crossed with accessions of red-fleshed cultivars to give rise to progenies with various colors (Volz et al., 2006, Volz et al., 2009). However, no red-fleshed cultivar has yet been released from this breeding programme. In 2008, Next Fruit Generation (NFG) introduced a red-fleshed cultivar, Redlove, after 12 years of breeding by Swiss researchers, starting with a small, bitter red-fleshed apple from eastern Germany (Freshplaza, 2008). Annurca apples, is an old Italian variety that is used in this research thesis with Italian Red Passion to highlight the general perception that apples are good for health.

Annurca apple fruit is one of the most important cultivars of southern Italy (Scalzo, et al., 2001). The apple is not very sweet, but has an average amount of aroma and good flavor characteristics, it can be recommended, for example, in a low-sugar diet. It represents 60% of the Campania County apple production (D'Abrosca et al., 2006) and 5% of the national apple production and it has recently obtained the official designation of Protected Geographical Indication (PGI) from the European Council (Commission Regulation, EC, No. 417/2006). The Annurca variety is characterized by a strong antioxidant activity (Cefarelli et al., 2006; Napolitano et al., 2004) as a function of catechins and phloridzin concentrations. This phenomenon was found in other apple varieties, but is more evident in the Annurca, probably due to its genetic background.

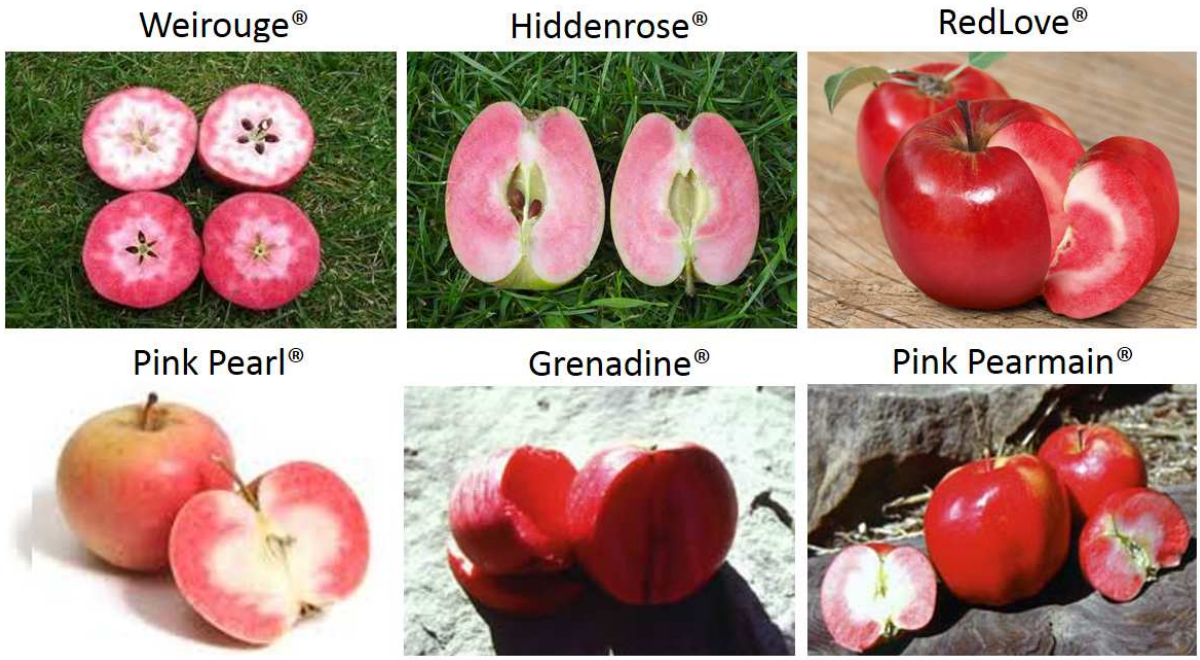

Figure 6. Most important red-fleshed apple cultivars released in the last sixty years.

1.9 SENSORY EVALUATION OF APPLE AND OTHER FRUITS

Consumers use sensory analysis to determine the degree of liking, preference and acceptability of different products. It is a scientific tool used to investigate measure and explain the difference in the properties of food as these are recognized through sight, hearing, taste, smell and touch (Lawless and Heymann, 1998). Two types of sensory analysis are common used: 1) Analytical sensory evaluation, for evaluate the degree of variation in products or food through a trained panel, and 2) consumer sensory analysis to determine the degree of liking, preference and willingness to purchase a product by using the target consumers (Lawless and Heymann, 1998). Sensory attributes mostly evaluated for apple include texture traits, such as crunchiness, crispness, juiciness, mealiness and flavor traits, such as sweetness, sourness, astringency, aroma, odour (*Table 1*). Texture mainly depend from the rearrangement of the primary wall and middle lamella in apple cells during ripening. However, starch content and turgor may also result in texture loss. Flavor is a combination of taste and aroma. Assess consumer preference for taste is difficult, due to the effect of different characteristic such as sugar, organic acids and phenolic compounds. Descriptive sensory analysis represent an economic and powerful tools to aid breeders in plant selection, providing good prediction of consumer's response, in some cases, even better of instrumental measurement.

Flavour	**Definition**
sweetness	Intensity of sweet taste. Depend from total soluble sugar (TSS)
sourness	Intensity of sour taste. Depend from titratable acidity (TA)
bitterness	Bitter taste. Mainly depending from some phenolic acids
astringency	Intensity of dry sensation in the mouth. Depend from condensed flavan-3-ols
odour	Intensity of aroma
Texture	**Definition**
juiciness	Amount of juice released when chewing for a long time
mealiness	Intensity of granular dry structure
crunchiness	The amount of noise produced when chewing with the back teeth
crispness	Sound produced when biting with the front teeth and chewing once
peel toughness	Intensity of skin residual in the mouth before swallowing

Table 1. Apple sensorial attributes

According to Harker et al. (2003), quality is the combination of all the attributes that makes the product satisfactory or acceptable to the consumer. As demonstrated by Peneau et al. (2006) appearance and taste represent the major driver for consumer preference for apples. In particular, color and price mainly affect consumers' purchase decision (pre-purchase) an apple market (McCracken et al., 1994). Flavour and texture, as well their reciprocal interaction, represent the most important

attributes in determining the after purchase evaluation (Harker et al., 2008). With regard to flesh colour, Janick et al. (1996) indicated that consumers prefer a clear yellow flesh colour in apples, but have shown intolerance towards red flesh and slight bleeding in apple flesh. Familiarity also seems to play a role in preference for flesh colour since in regions were 'McIntosh' is regarded as the standard apple, consumers prefer a white compared to the more yellow flesh colour of some other cultivars.

1.10 CONSUMERS' PREFERENCES FOR IRP RED-FLESH APPLE LINES

Successful marketing for fresh apples requires accurate knowledge of consumers' preferences and perceptions, particularly in the last years, characterized by substantial decrease of apples per capita consumption, especially in European country (FAO, 2011). The loss of market share by apple fruit could be mainly imputed to the relative static varietal landscape, dominated by traditional varieties and by often-inadequate marketing strategy of new positioned cultivars (O'Rourke et al., 2011). In addition, the mounting demand of consumers for high-quality fruit has generated an increasing competition between apple industries and a growing awareness of brand differentiation (Axelson & Axelson, 2000). Therefore, understanding consumers' preference for apple cultivars is a strategic necessity for apple breeders and suppliers (Reid & Buisson, 2001; Jaeger et al., 2003; O'Rourke, 2011) and consumer research should be carried out since early stages of the breeding process (Hampson et al., 2000). Fruit quality should not be considered as an absolute variable, but rather a concept that changes dynamically across time along with consumers' expectations (Harker et al., 2003). Indeed, quality is a combination of all attributes that makes a product acceptable to consumers. In fruit market, consumers' preferences is generally driven by appearance and/or taste (Pre-Aymard et al., 2005). Appearance includes the external fruit colour, shape and cosmetic appeal, as well as flesh colour, whereas taste includes flavour, textural and mouth-feel attributes (Harker et al., 2008). In addition to appearance and/or taste, there is a growing interest from consumers even for nutritional and healthy values of fruits, including apples. Recent apple breeding programs have focused on the development of red-fleshed cultivars, with the presumption that red-fleshed apples will created a new market segment due to the novel appearance of the fruit, often, but not ever, associated to its high antioxidant capacity and thus, higher healthy value (Freshplaza, 2008). In this way, Italian Red Passion apple lines represent a new brand composed by different apple varieties, characterized by different peel colors, pink to red color of flesh, higher polyphenols content and, above all, higher antioxidant potential compared to commercial apples, such as the typical Italian cultivar Annurca.

1. AIMS OF THE STUDY

Aims of this study is the analyses of Italian consumer's preferences for the internal appearance and taste of Italian Red Passion apple line. The main objective of the survey was to gain knowledge about consumer's acceptance, the level of interest and the purchasing decision of new red-flesh apple

products. Indeed, the survey was focused on the so-called pre-purchase factors (McCracken et al. 1994), such as appearance and price, which represent the main factors influenced consumer's decision to purchase in apple market. However, considering the relevance of nutritional property of IRP lines, an informative background was also added, further remarking this not negligible aspect. In addition to market analysis, a panel test descriptive sensorial analysis was also conducted, to assess the sensory qualities of fruits and to acquire detailed information about the main traits that influence consumer perception and general preference for the distribution pattern and intensity of red pigmentation in the flesh.

1. MATERIALS AND METHODS

PLANT MATERIAL

The investigations were performed on apple seedlings of Italian Red Passion line, obtained from a free-pollinated cross of unknown mother plant belonging to Center Italian germplasm. The C2, C8 and C15 seedlings (C group) were grafted on M26 rootstock and planted in rows at 2.0-m and X 4.0-m spacing in the experimental orchard of University of Tuscia (Viterbo, Italy). The M3, M4 and M5 seedlings (M group) were grafted on MM111 and planted in rows 3.0-m X 4.5-m spacing, in the same location of C series seedlings. Soil and fertilizer management were conducted according to commercial guidelines. All trees were sprayed with pesticides according to a minimum programme of pest control against *C. pomonella* and apple scab.

DETERMINATION OF TOTAL SOLUBLE SOLID, PH AND TITRATABLE ACIDITY

For qualitative analysis, apples of IRP lines and cv Annurca were randomly divided into 4 batches. Three fruit from each batch were sampled for determination of total soluble solids (expressed in ° Brix), pH and titratable acidity of the juice, for total of 20 measurements per line. The titratable acidity, the soluble solids and pH were determined after extraction of the juice from the fruits through homogenization and subsequent centrifugation at 10,000 rpm for 10 minutes. The soluble solids was measured with the aid of ATAGO digital refractometer PR-101; for the determination of titratable acidity, after reading of the pH of the juice with the aid of digital pH-meter, the neutralization was performed with a solution of 0.1 N sodium hydroxide (NaOH) to pH 8.1. The titratable acidity was then expressed as grams per liter of malic acid equivalent.

FRUIT FIRMNESS

Fruit firmness was determined sampling 20 fruits per line and by performing two measurements on the two opposite sides of each fruit with a TR penetrometer, TURONI Ltd. (Forli, Italy) with 11 mm tip. After removing a thin slice of peel (about 1 mm thick), the tip was placed perpendicular to the surface of the fruit and gently pushed up to the mark placed on tip. The force required was expressed in kg/cm^2.

STARCH TEST

Twenty fruits for each line were subjected to starch test. Briefly, each fruit were dissected along the equatorial diameter and the two halves immersed for 1 minute in a container containing 30 ml water solution containing 8.8 grams of potassium iodide and forming a layer of 5-8 mm. After this first phase, 2.2 grams of iodine crystals

were added and mixed until completely dissolution. Maturity index has been determined by visual comparison of each fruit with guideline cultivars (Red Delicious and McIntosh), following a visual scale ranging from 1 to 9.

COLORIMETRIC ANALYSIS OF APPLE FRUIT

A total of 10 fruits for each lines and for each sampling data were harvested for colorimetric analysis. Color was recorded using a Minolta CR-400 Colorimeter (Minolta Camera Co., Ltd., Ramsey, NJ) tristimulus color analyzer equipped with an 8-mm diameter measuring area and diffuse illumination of a 2° standard observer. The L* coordinate indicates darkness or lightness of color and ranges from black (0) to white (100). Coordinates, a* and b*, indicate color directions: +a* is the red direction, –a* is the green direction, +b* is the yellow direction, and –b* is the blue direction. Chroma is the saturation or vividness of color. As chromaticity increases, a color becomes more intense; as it decreases, a color becomes duller. Hue angle is the basic unit of color and can be interpreted, for example, as 0° = red and 90° = yellow. Both chroma and hue are derived from a* and b* using the following equations: metric chroma: $C^* = \sqrt{(a^*)^2 + (b^*)^2}$ and metric hue angle: $h = \tan^{-1}(b^*/a^*)$ (degrees).

TOTAL PHENOLIC CONTENT

Total phenolic content was determined spectrophotometrically according to the Folin–Ciocalteu's method (Singleton et al., 1999), opportunely modified. Briefly, 1 mL of Folin–Ciocalteu's, previously diluted with 10ml of distilled water, was added to 100µl of apple extracts, diluted in methanol: water 70:30. Then, 900 µl of 7.5% Na_2CO_3 solution and stored on dark. During the oxidation of phenolic compounds, phosphomolybdic and phosphotungstic acid, contained in the Folin–Ciocalteu's reagent, was reduced to blue-colored molybdenum and tungsten oxides. After 1.30 hours, the absorbance of blue coloration was measured at λ = 765 nm against a blank sample. The measurements were compared to a standard curve of prepared gallic acid solutions (in the range 25 to 500 mg L^{-1}) and expressed as milligrams of gallic acid equivalents (GAE) per 100 g ± SD. All measurements were performed in triplicate.

TOTAL ANTHOCYANINS CONTENT

The content of total anthocyanins was determined using the method developed by Mancinelli et al. (1975); 5 grams of finely ground plant tissue were extracted in 50 ml of methanol acidified with 0.1% HCl and placed in agitation, in the dark, for 24 hours at 4° C. The extract was then centrifuged to collect supernatant, subsequently filtered for spectrophotometric analysis. Sample absorbance was determined at 530nm, compared to a standard curve of prepared cyanidin-3-glucoside (Extrasynthese, France) solution and expressed as cyanidin-3-glucoside equivalent per 100g FW.

EXTRACTION AND HPLC ANALYSES OF APPLE FRUIT

Finely ground apple fruit tissues were immediately freeze-dried in an 'EDWARDS *modulyo'* freeze-dryer, weighted and extracted in 5 ml of slightly acidified 70% methanol (pH 4.00) for each gram of freeze-dried apple powder. The solution was sonicated for 10 min, vortexed and centrifuged at 15.000 rpm for 15 min. The pellet was separated from the supernatant, re-extracted in 5 ml per gram of slightly acidified 70% methanol (pH 4.00), vortexed and centrifuged again under the same centrifugation condition. The resulting supernatant was added to

the supernatant previous obtained, filtered by 0.45 µm Whatman filters (GE Healthcare, US) evaporated by Rota-vapor (Buchi, Canada) at 35°C under low pressure condition, and the remaining aqueous part of the solution was freeze-dried again. Freeze-dried polyphenols were suspended in 3 ml of pure methanol for each gram of initial freeze-dried apple powder. The content of main apple phenolics compound were identified and quantified using high-performance liquid chromatography with photodiode array detection. The instrument was composed by a HPLCP680 pump (DIONEX), two thermo stated (30° C) columns, TCC-100 inverse column (DIONEX) and Acclaim® 120 C18 column (5µm 120Å, 4.6X 250 mm) (DIONEX), and a photodiode detector PDA-100 (DIONEX). Optimized conditions were determined by flow injection analysis (FIA) of standard solutions of the analyses at three different concentrations, ranging from 0 to 100 mg/L. System control and data processing were carried out by chromeleon software (DIONEX) running on a desk computer. Separations were performed by multistep gradient, using A) a solution of 50 mM of dihydro-ammonium phosphate acidified at pH 2.6 by ortophosphoric acid. B) 20% of phase A and 80% of acetonitrile. C) a solution 0.2 M of ortophosphoric acid basified at pH 1.5 by NaOH at a flow rate of 0.5 mL/min. Samples were introduced into the column using a single injection with a 20 µL sample loop. Catechin, epicatechin, procyanidin B1 and B2, quercetin-3-glucoside, cyanidin-3-glucoside, phlorizin and chlorogenic acid, were purchased at Extrasynthese (France).

RADICAL SCAVENGING ACTIVITY

The radical scavenging ability or hydrogen donating of the extracts was monitored using the stable free radical DPPH, following the method described by Brand-Williams et al. (1995), lightly modified as follows. Different dilutions of crude extract (in 0.4 ml of methanol) were mixed in a 1 cm disposable cuvette with 3 ml of freshly prepared methanolic solution of DPPH (0.06 mM). A control was prepared with 0.4 ml of pure methanol; its initial absorbance was between 0.716 and 0.720. The cuvette was capped and left to stand in the dark at room temperature for 180 min (time required to reach the steady state). At this time, the decrease in absorbance was measured at 515 nm against a blank of pure methanol, with a Perkin–Elmer Lambda 3 UV/vis spectrophotometer (Perkin–Elmer Inc., Wiesbaden, Germany). For each extract at least five different concentrations were tested. The radical scavenging activity was expressed in terms of IC50 (inhibitory concentration %) which is the amount of extract or pure antioxidant necessary to decrease the initial DPPH concentration by 50%; EC50 (efficient concentration) and antiradical power (ARP).

NUCLEIC ACIDS EXTRACTION

Nucleic acids extraction was performed using methods described by Muleo et al. (2009). Vegetal tissues were frozen in liquid nitrogen and ground with mortar and pestle to obtain a fine powder. Then, 1 ml of extraction buffer (Tris / 100mM HCl pH 8.0, 20 mM EDTA pH 8.0, 1.4 M NaCl , CTAB 3 % w / v) was added to 100mg of tissue and incubated at 60° C for 30 minutes, stirring every 10 minutes. After this step, 1 ml of chloroform:isoamyl 24:1 was added to the mixture and subsequently centrifuged at 14,000 rpm for 5 minutes at 4° C. To the surnatant, 0.7 volumes of isopropanol and 0.1 volumes of sodium acetate 3 M pH 5.2 were added and incubated at -20° C for 1 hour. Subsequently, the samples were centrifuged for 15 minutes at 14,000 rpm and resuspended in TE buffer. After these step, total RNA and DNA were respectively purified using RNeasy Plant Kit and DNeasy Plant Kit (Qiagen, Germany), following manufacturer's instruction. Nucleic acids were resolved on a 1% (w/v) agarose TBE gels (in 1x TBE buffer), using standard protocol (Sambrook et al., 1989).

Nucleic acids were visualized by ethidium bromide staining and photography of gels under UV light (240nm). Size and quantity of nucleic acid bands were estimated by comparison to Lamda Hind (Invitrogen) and 100bp (GeneAid) molecular markers. A more accurate quantification of nucleic acids was performed using a QUBIT spectrophotometer (Invitrogen, USA) using manufacturer's protocol.

PRIMER DESIGN

For MYB10 molecular analysis oligonucleotide primers designed by Espley et al. (2007) and Takos et al. (2006) were used (Table 1), except for forward primer used in quantitative High resolution Melting Analysis (qHRMA), designed using Primer3 software, available at www.primer3.org website.

MdMYB10 Gene	Primer (5' – 3')		Size (bp)	Description
	Forward	Reverse		
-431 to -181	GGTGGTGTAATCAGCTTGACCCCTG	CACAGAAGCAAACACTGACAAGT	250-351	MYB10 promoter region
+39 to +580	TGCCTGGACTCGAGAGGAAGACA	CGTGTTTCCCAAAAGCCTGTGAA	542-475	I° intron
CDS +39 to +626	TGCCTGGACTCGAGAGGAAGACA	AACCAAAAACTTGTGAAGAGTTC	587	MYB10 cDNA isolation
CDS +529 to +626	GATTGGTGGGAGACCTTGTTAGAA	AACCAAAAACTTGTGAAGAGTTC	98	qHRMA analysis
CDS +39 to +257	TGCCTGGACTCGAGAGGAAGACA	CCTGTTTCCCAAAAGCCTGTGAA	219	qPCR

Table 1. List of primer pairs used for MdMYB10 PCR analysis

Primer pairs for Real-Time PCR analysis of transcripts coding structural enzyme and transcription factors regulating flavonoid biosynthesis were, taken from previously published work (*Table 2, references*) or designed ex novo (*Table 2*) searching inside apple genome assembly (Velasco et. al., 2010) at www.rosaceae.org, website. Annealing temperature was comprised in the range 57-60° C for all primer pairs.

Gene	qPCR Primer (5' – 3')		Size (bp)	Efficency	Reference
	Forward	Reverse			
MdCHS	TATCCCAGCATTGAGTTAGAGGA	ACACATGCTAGATGGTACCAC	121	1.97	Espley et al. (2007)
MdF3H	TGGAAGCTTGTGAGGACTGGGGT	CTCCTCCGATGGCAAATCAAAGA	115	1.92	Espley et al. (2007)
MdDFR	GATAGGGTTTGAGTTCAAGTA	TCTCCTCAGCAGCCTCAGTTTTCT	116	1.97	Espley et al. (2007)
MdLDOX	CCAAGTGAAGCGGGTTGTGCT	CAAAGCAGGCGGACAGGAGTAGC	157	2.01	Espley et al. (2007)
MdUFGT	CTAGACAAGCAAGAGGCTCCAT	CAATGCTTTTGTCAAGAACTCA	221	1.89	
MdPAL	CACATACTTCAAATGCGGTGGAG	CGATGAAAGGTGGGATTGTAAGG	140	1.97	
MdC4H	CGCAGAGCTTCGATTACAACTAC	GAATCCTCTTCTCCTTCACTTCC	102	2.00	
MdC3H	ATGGCTCTCTCTGGACTACTTCTC	CTGTATCTGGTAGAGGTTACCGAC	144	1.99	
MdFLS	TTCTTACAGGGAAGCTAATGAA	GAGGACATGGTGGGTAGTAGTT	123	1.91	
MdLAR1	TAGAGCTACTGCAAGAGGAGG	CCTCGAAGAAACCCTAGAAAC	121	1.95	
MdHQT	CACATACTTCAAATGCGGTGGAG	CGATGAAAGGTGGGATTGTAAGG	140	1.96	
Md4CL	CCCAAGGGAGTCATTCTAACACAC	CACAATACGACATCGTCCTCCTTC	107	1.98	
MdPGT1	GAAGGGTGTGTTGCCAGAAGGGT	GTCACGAACCCACCAACCGACT	135	1.98	
MdMYB9	CCTGGACTGCCTTGGAAGATAAA	GTTGCCTCTCTTTATGTCTGGTCTC	161	1.92	
MdMYB12	GATAAGCCAAGGCATAGATCCCAG	GATGGACAAGACGATCAGAAGGAG	182	1.90	
MdMYB16	CTCATCATCAAACTCCATAGCCTCC	CAGATTCCTGAGGTGTCTCGTTG	181	1.89	
MdMYB22	CCTACTCTACCACCAAACCCAAAG	CTCCATTAGTAGCACGTAACCGTC	191	1.93	
MdbHLH3	AGGGTTCCAGAAGACCACGCCT	TTGGATGTGGAGTGCTCGGAGA	194	1.90	Telias et al. (2009)

MdbHLH33	ATGTTTTTGCGACGGAGAGAGCA	TAGGCGAGTGAACACCATACATTAAAG	143	1.96	Telias et al. (2009)
MdWDR	CATCGACACCACCTGCACAATTTG	CACTGGCATCGTCGGCGATCGG	162	1.90	An et al. (2012)
MdACT	TGACCGAATGAGCAAGGAAATTACT	TACTCAGCTTTGGCAATCCACATC	155	1.98	

Table 2. List of primer pairs used for real time PCR analysis

PCR ANALYSIS AND SEQUENCING OF MYB10 LOCUS IN IRP APPLE LINES

PCR amplification were performed on a thermal cycler PTC -100 (MJ Research) with the following protocol: 8 minutes of initial denaturation at 95 ° C and 34 cycles each consisting of 40 sec of denaturation at 95 ° C , 30 sec of annealing at 60 ° C and 45 sec of amplification at 72 ° C. The reaction mixture was as follows: 2.5 µl 10x Buffer; 2.5 µl 10 mM dNTPs; 2.5 µl 10 mM forward and reverse primer; 0.2 µl Taq Polymerase; 0.2ul of 25mM $MgCl_2$; 40 ng of template and DEPC water up to a total volume of 25 µl. PCR products were loaded on 1.2% agarose gel. Bands of interested PCR products were excised from the gel and purified with the GeneMatrix Agarose-Out DNA Purification Kit (EURX) following manufacturers' instructions. Once purified and quantified, DNA samples were sequenced by PRIMM (Milano) service.

cDNA SYNTHESIS

RNA samples concentration was quantified using QUBIT (Invitrogen, USA) and 1 µg for each sample was used for cDNA synthesis. Reactions were performed using a Superscript III cDNA synthesis kit (Invitrogen, USA), according to the manufacturer's instructions. To maximize the RNA conversion both random hexamers and oligo (dNTs) were used in each reaction. To offset the variability of the efficiency of individual reactions, three replicate reactions for each RNA sample were synthesized and pooled before qPCR analysis.

REAL-TIME PCR ANALYSIS

Real-time PCR analysis was conducted using the thermal cycler LC480II® (Roche, Italy). Each reaction (20 µL) contained 10 µL of Light Cycler 480 SYBR Green I Master (Roche, Cat. No. 04 707 516 001, Italy), 0.5 µM of each primer (Tab. 1), 1 µL of cDNA and 7 µL of water PCR-grade. The PCR reaction was conducted using the following conditions: 95° C for 10 min; 45 cycles at 94° C for 20 sec, 58° C for 30 sec and 72° C for 30 sec, followed by a melting cycle from 65° to 95° C. Quantitative Real-time PCR was performed using three biological replicates, with three technical replicates for each sample. Data were expressed with the $2^{\Delta\Delta Cp}$ method using *ACTIN* as an endogenous reference gene for the normalisation of expression analysis. After PCR amplification, all products were sequenced to confirm their identity. The amplification efficiency (E_{target}) of each primer set was calculated by the method of Kubista et al. (2006), using the cycle threshold values obtained from Real Time PCR of a series of dilutions of control cDNA. Expression levels of the analyzed genes were calculated by using the methods of Kubista et al. (2006). For all analyses, the signal obtained for the gene of interest (target) was normalized against the signal from the constitutively expressed apple *Actin* gene. Where relative changes in gene expression are shown, transcript abundance was plotted as a fold increase above the expression of a particular time point or treatment. One-way ANOVA and Student-Newman-Keuls test were used to *post hoc* comparison of multiple groups, considering $p < 0.05$ as statistically significant.

EXTRACTION AND QUANTIFICATION OF CANDIDATE APPLE miRNA BY REAL-TIME PCR ANALYSES

Total RNA was extracted using TRIzol (Invitrogen), purified without smallRNAs enrichment using miRNeasy kit (Qiagen, Germany), and quantified using QUBIT fluorometer, according to respective manufacturers' instructions. Generation of cDNA for RT-qPCR was done using the Qiagen miRNA first-strand synthesis and qPCR kit (miScript II; Qiagen) according to the manufacturer's instructions. In particular, 2 μg of total RNA were reverse transcribed using HiFlex buffer and modified oligo-dT primers which have a 3' degenerate anchor and a universal tag sequence on the 5' end, allowing amplification of both mature miRNA and precursor in the real-time PCR step. The combination of polyadenylation and the universal tag addition ensures that miScript Primer Assays do not detect genomic DNA. Specific primers for mdo-miR168 and mdo-miR858 were designed based on sequences of their most abundant isoform in fruit tissue, according to Xia et al., (2012). Primer sequences was the follow: *mdo-miR168* 5'-TCGCTTGGTGCAGGTCGGGAA-3' and *mdo-miR858* 5'-TTCGTTGTCTGTTCGACCTGA-3'. Real-time PCR detection was performed using the same procedure above descripted for quantitative real-time PCR, however, using the follow PCR conditions: 95° C for 10 min and 40 cycles of 94° C for 15 s, 57° C for 20 s, and 70° C for 20 s. PCR products were subsequently analyzed by a melting curve analysis. Relative miRNA expression, determined by real time RT-PCR, was normalized to the expression of the reference mdo-miR168 using the ΔΔCt method above described in Real Time PCR analysis paragraph.

5' RLM-RACE FOR mdo-miR858 TARGET IDENTIFICATION

Following manufacturers' instruction, FirstChoice® RLM-RACE Kit (Ambion, Austin) was used for RNA ligase mediated—5′ rapid identification of cDNA ends of putative *MdMYB10* and *MdMYB16* (MDP0000950559) *mdo-miR858* target. The gene *MdMYB9* (MDP0000210851), already confirmed mdo-miR858 target by degradome sequencing (Xia et al., 2012) was used as further control. Briefly, RNA adapter was ligated to the free 5′ phosphate of an uncapped mRNAs population produced from nucleolytic activities. The ligation product was reverse transcribed using a forward primer directed against the linker and gene specific reverse primers, which is subsequently amplified and identified by sequencing. Reverse specific PCR primers were the follows: *MdMYB10*, 5'-AACCAAAAACTTGTGAAGAGT-3' expected PCR products about 334bp; *MdMYB16*, 5'-AAGGTCAAGATTCAAGTCAGGGCA-3', products about 248 bp; *MdMYB9*, 5'-AGAGGTTGAGCAGCGGCAGTTGATG-3', product about 192 bp.

HIGH RESOLUTION MELTING BASED DAE (DIFFERENTIAL ALLELIC EXPRESSION) OF MYB10 GENE

According to Nguyen-Dumont et al. (2011), primers pair was designed to amplify a C/T SNP located in the position +555 from *ATG* site of *MdMYB10* gene. The differences in melting temperature (T_m) of two different allele in heterozygous individuals, measured by derivative fluorescent signal, correlated to the relative abundance of each transcript. Therefore, for DAE-HRM analysis, a range of melting curves associated with known allelic imbalance were created, using respective homozygous alleles amplified from genomic DNA. PCR amplification were performed in capillaries on Light Cycler (Roche, Germany) using SensiMix kit (Quantace, USA) and LC-Green II plus dye (Idaho Technology, USA), in a 20 μl total volume containing: 4 μl Mix Buffer, 100 nM of each primer, 1 μl of LC-Green dye, 1.5 μl of Taq polymerase and 20 ng of template. The

amplification profile was set to 10 min at 95° C, 50 cycles of 10s at 95° C, 10s at the primer annealing temperature and 10s at 72° C. High resolution melting analyses were performed separately on HR1 instrument (Idaho Technology, USA) setting with temperature ramp from 70° to 90° C, rising by 0.10° C/s. All reactions were performed in triplicate. The melting curves were normalized using the software provided with HR1 instrument and visualized using Derivative Plot tool.

APPLE SENSORIAL ANALYSIS

Eleven judges were trained in descriptive sensory analysis according to the procedure described by Lawless and Heymann (1998) and tested for consistency. Apple used for panel test were preserved for one week at 4° C. Anonymous apple samples were removed peel and placed in special food trays. Eight judges were trained for descriptive sensory analysis. The judge were blindfolded and water were used as pallet cleaners between the tastings. Following criteria of Quantitative Descriptive Analysis (QDA), sensorial analysis was performed using eight descriptors, four regarding flavour attributes (sweetness, sourness, astringency and aroma) and four regarding texture attributes (mealiness, crunchiness, crispness and juiciness). An unstructured 1-10 scale was used for analysis with the left side of the scale representing low values and the right side of the scale representing higher values of the respective attributes. Samples were presented in a complete randomized order and marked with a three digit codes. Each judge tested one samples per session with size of 1/8 apple. Tasting was conducted in a controlled room temperature of 21 ºC. All data were subjected to test-retest analysis of variance (ANOVA) using SigmaPlot software v10.0.

CONSUMERS' PREFERENCES AND MARKET ANALYSIS

The survey was conducted at mall located in Viterbo (Italy) on January 2013. The consumers were recruited adopting the quota sampling method, stratifying respondents in different age classes, each composed by a pre-established number of individuals with equal representation of males and females. Participation in the study was voluntary. Data collection was completed within one week and in different daytime slots, in order to guarantee homogeneity of data gathering conditions and to obtain the best representative sample. The questionnaire consisted of thirteen questions divided into three main areas of analysis: (i) customer profile, containing the customer socio-demographic characteristics necessary to identify individual attributes, such as sex, age and profession; (ii) customer behavior for the consumption of apples in general; (iii) consumer consumption habits and level of interest for IRP red-flesh apple lines, based on fruit appearance and explained healthy value. Consumer response modalities were structured on the basis of a Likert scale, with assigned score between 1 and 6, representing, respectively, the highest positive response (very much) and the least (not at all). Likert scale allow avoiding consumer's indifference with respect to the question. For cluster analysis, Ward hierarchical clustering method was used (Fabbris, 1997; Bracalente et al., 2009), determining the number of clusters according to Caliski-Harabasz index (Calinski and Harabasz, 1974). Ward hierarchical clustering method is particularly useful for hypermarkets costumers' analysis, allowing identifying smaller costumers group becoming object of target marketing activities. This methods is based on the decomposition of total variance within groups and between groups, considering at every iteration, the sum of all possible pairs and the pair with lesser variance between groups. STATA software was used for data processing, descriptive statistic and multivariate analysis. The questionnaire was supplemented with a poster (*Figure 7*) contained different

photographs of one representative red-flesh IRP apple, and simple slogan about its higher antioxidant potential and healthy value. The symbol of 'OGM-free products' was also included in the poster. In addition, entire and sectioned fruits representative of red-flesh apples lines, were shown during questionnaire administration.

Figure 7. Poster shown during the survey, containing different photographs of one representative red-flesh IRP apple, simple slogan about its healthy value and the symbol of OGM-free products.

1 RESULTS

1.1 PHENOTYPICAL OBSERVATION OF ITALIAN RED PASSION SEEDLINGS

The six apple lines of Italian Red Passion (IRP) group, named M3, M4, M5, C2, C8 and C15 were generated by free-pollination of an unknown red apple mother plant, native from Center Italy. The phenotypic observations of wide red colour distribution in tissues and organs of IRP lines suggest that they belong to type I group of red apple, except C8 line, which did not display a 'reddish phenotype' (*Figure 1*). The type I group, described by Volz et al. (2009), is characterized by red coloration of apple fruit flesh and peel, young leaf, petiole and venatures of mature leaf, petals, styles, stamens and vascular tissues. All these phenotypic characters are present in IRP lines (Figure 1).

Figure 1. Phenotypic observation of red characters in the all organs of M5 line plant. The 'reddish' phenotype is present in the young leaf and did not disappear completely in the mature leaf.

1.2 MOLECULAR ANALYSIS OF ITALIAN RED PASSION LINES

Type-I red apple phenotype is conferred by a mutation in *MdMYB10* gene promoter region, consisting in a six-time repeated 23-bp minisatellites insertion (Espley et al., 2007). To confirm the belonging of IRP lines to type-I red apples, a couple of primers was designed to amplify promoter region comprised between -431 to -181 from *ATG* site of *MdMYB10*. Visualization of PCR products

visualized onto agarose gel have confirmed the presence of two fragments of 250 and 351 bp in M3, M4, M5, C2 and C15 lines (*Figure 2, a*). The 250-bp fragment derived from the amplification allelic *wild type (wt) form of MdMYB10* resulted to be also present in white-flesh apple of cv Annurca and C8 line; while the 351-bp amplified fragment of the *mutated* (*m*) *MdMYB10* allele is characterized by the 100bp insertion, which confer *MdMYB10* trans-activation (Espley et al., 2007). Coherently with the phenotypic detection, in C8 line only one amplified product is visualized onto agarose gel, since the $MdMYB10_m$ allele is absent.

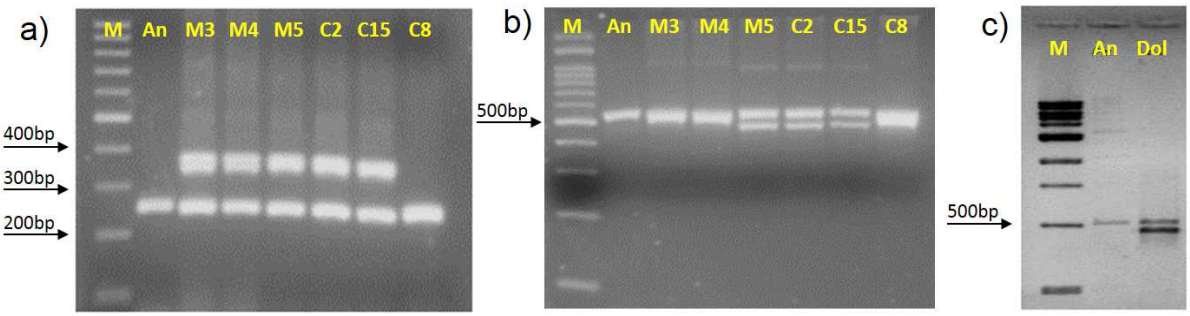

Figure 2. a) Visualization of PCR product amplified from MdMYB10 promoter region in IRP lines and cv Annurca, through gel electrophoresis running. b) Visualization of PCR product amplified from MdMYB region comprised between first and second exon in MdMYB10 promoter region in IRP lines and cv Annurca, through gel electrophoresis running. c) MYB10 first and second exon region in cv Annurca and cv Dolce.

To confirm that the increased size of 350-bp amplified fragment of the $MdMYB10_m$ allele is due to the insertion, we have sequenced the amplicon amplified from M3 line (*Figure 3*). The analysis of sequence confirms that the insertion depend on 4-times repeated 23-bp minisatellites, and one 23-bp repeat is broken into two parts and reinserted in the opposite orientation (*Figure 4*, STATE-OF-THE-ART). Moreover, *MdMYB10* first intron structure was also sequenced. Primers were designed to amplify the region comprised between the first exon (+39 from *ATG* site) and the end of second exon (+580 from *ATG* site). The visualization onto agarose gel of amplified products (*Figure 2, b*) has highlighted the presence of two type of fragments, one of 541-bp and the other of 475-bp. Both fragments resulted to be only present in C2, C15 and M5 lines, while M3, M4, C8 and cv Annurca, which carry only on the 541-bp fragment. The 475-bp fragment has been also found in cv Dolce (*Figure 2, c*).

Figure 3. Sequence alignment of M3 line, Royal Gala (accession number EU518249.2) and cv Niedwetskiana (accession number GQ500894.1) MdMYB10 promoter region (-431 to -181 from ATG site).

Sequence analysis of the region comprised between -481 to +580 from *ATG* site in IRP lines and cv Annurca revealed, the presence of at least three different *wild type MdMYB10* alleles, named 1, 2 and 3, in addition to the *MdMYB10*$_m$ allele (*Figure 4*).

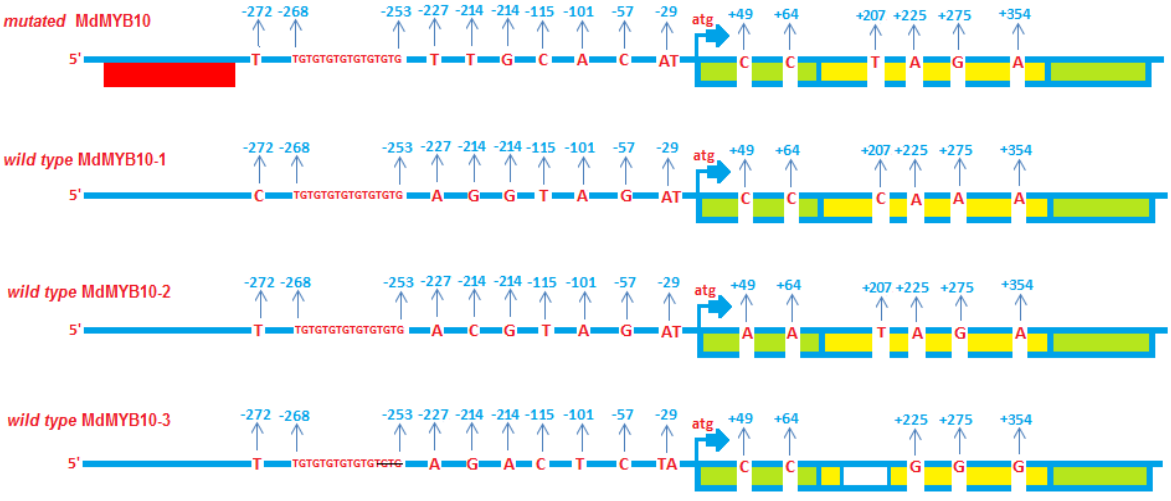

Figure 4. Landscape Representation of theMdMYB10 gene region comprised between -431 and +580 from ATG site in the four allele types. The substitution of bases are indicated with the letters, on the same position among the four sequences. Boxes colored in green represent the exons, while the box colored in yellow represent the intron. The two alleles MdMYB10-1 and -2 are present in cv Annurca, in the IRP lines is always present MdMYB10$_m$*, mutated in the promoter region, and one of the other 3 alleles. In C8 line the MdMYB10*$_m$ *is absent.*

MdMYB10-1 and *MdMYB10-2* both alleles have an analogous sequence. However, two silent SNPs mutations C/A (transversion) are present in first exon (position +49 and +64 from *ATG* site), two SNPs in the first intron (C/T – transition, in position +207 and A/G – transition, in position +275) and two SNPs in promoter region (C/T -transition- and G/C -transversion-, respectively in position -272 and -214). On the contrary, *MdMYB10-3* allele is characterized by a 67-bp deletion in the first intron, by deletion of two repeats in promoter TG minisatellites, and other SNPs mutations in promoter region and first intron. This allele is also present in the Center Italian autochthonous cultivar Dolce and similar to *MdMYB1-3* type allele described by Takos et al. (2006). Instead, *MdMYB10-1* and *MMdYB10-2* are more similar to *MdMYB1-1* and *MdMYB1-2* types, described by the same author. The analysis of sequence of a large portion of *MdMYB10*$_m$ coding region of M3 lines has revealed a conspicuous number of SNPs respect to cv Niedwetskiana *MdMYB10* of (*Figure 5*) and a broad homology (only two SNPs are present) to Royal Gala *MdMYB10 wt allele*.

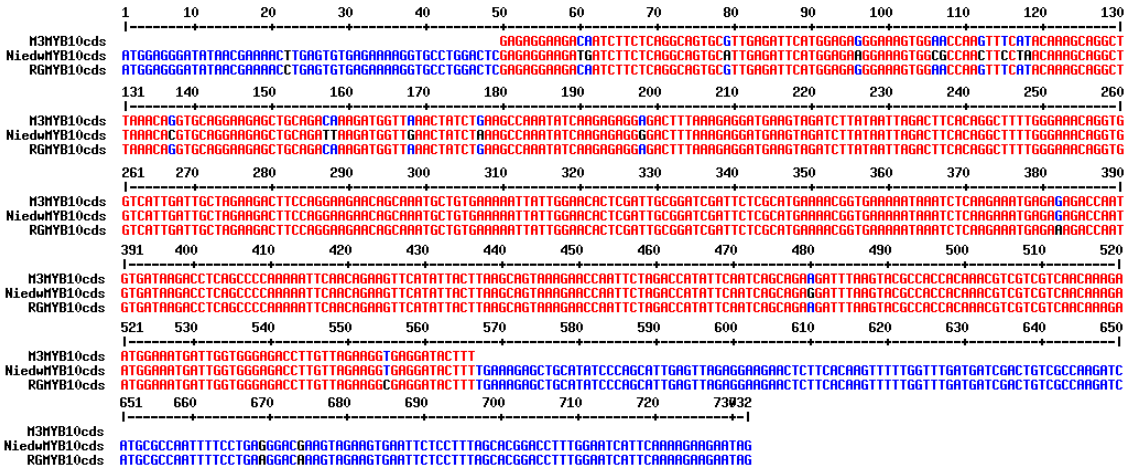

Figure 5. Sequence alignment of M3 line, Royal Gala (accession number EU518249.2) and cv Niedwetskiana (accession number GQ500894.1) MdMYB10 coding region (+50 to -565 from ATG site).

To resume, allelic composition at *MdMYB10* locus in IRP lines and cv Annurca is the following: C8 line, is characterized by *wtMYB10-1* and *wtMYB10-2* alleles identical to cv Annurca allelic form; M3 and M4 lines are characterized by *MdMYB10*$_m$ and *MYB10-1* wt alleles; in C2, C15 and M5 lines are present *MdMYB10*$_m$ and *MdMYB10-3* alleles.

1.12 IRP LINES APPLE GROWTH AND DEVELOPMENT

Apple fruit growth have been monitored at weekly intervals during season 2013 in IRP lines and cv Annurca, measuring fresh weight and equatorial diameter. Developmental stages have been defined by days after full bloom (DAFB). Full bloom were reached in IRP lines and cv Annurca approximately during the first decade of April, and apples were harvested in the second decade of September (about 160 DAFB). Mean apple fresh weight at harvest (*Figure 6a*) ranged from ~ 100g of Annurca, C15, C2

and M3 to ~ 120g of C8. Apple of M4 and M5 fresh weight ranged around 110g. The equatorial diameter of IRP apple and Annurca ranged around 70-75 mm (*Figure 6b*).

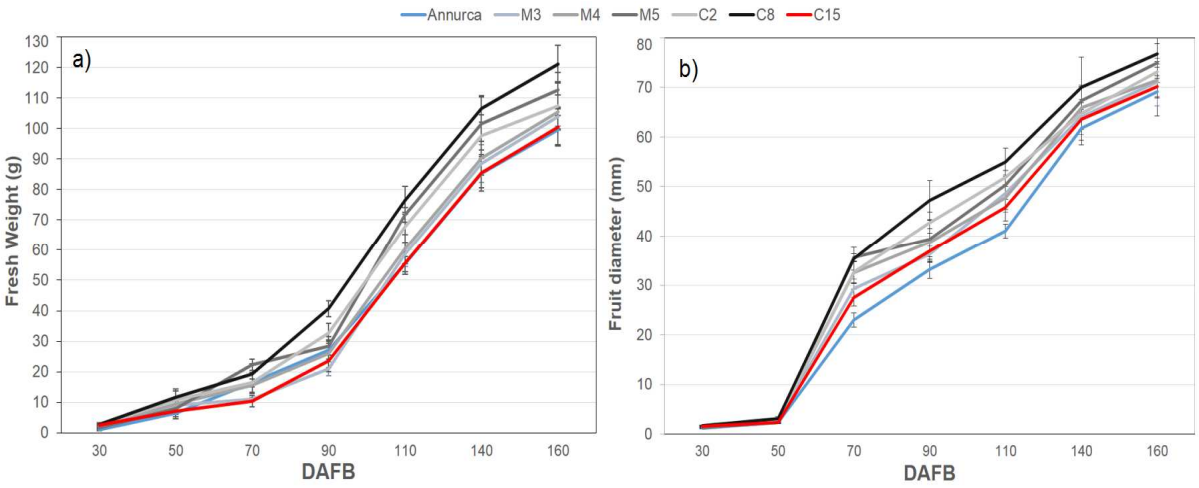

Figure 6. IRP apples fruit growth dynamics as function in terms of a) fresh weight (g) and b) equatorial diameter (mm). Histogram represents the average, bar represents ±SD.

To better define IRP apples maturity degree at harvest, apple firmness and starch index have been evaluated. Fruit firmness, determined by penetrometric measurements, resulted to be significant different among IRP lines and cv Annurca (*Figure 7a*). Apples of M3, C2 and C15 lines have shown higher firmness (9 Kg/cm^2, 10 kg/cm^2 and 9.4 kg/cm^2, respectively) compared to Annurca (7.30 Kg/cm2), M5 and M4 lines (6.54 and 5.61 kg/cm^2, respectively). The values of starch index (*Figure 7b*) resulted higher in apple of C2 line and Annurca, with not statistically different values of 7.8 and 8.6, respectively. In the fruit of the other lines a lower starch content has been found, however not statistically different from C2 line. Following apple harvest guideline (Peck and Merwin, 2011), starch index values indicate an advanced maturity degree for all IRP line apples and also for cv Annurca, thus indicating that apple are ready to fresh consume or short-term cold storage. Firmness values, however, highlighted important differences among IRP apples. In particular, the high firmness of C2 and C15 appear to be a genotypic characteristic that could make these lines suitable for medium-long term CA preservation.

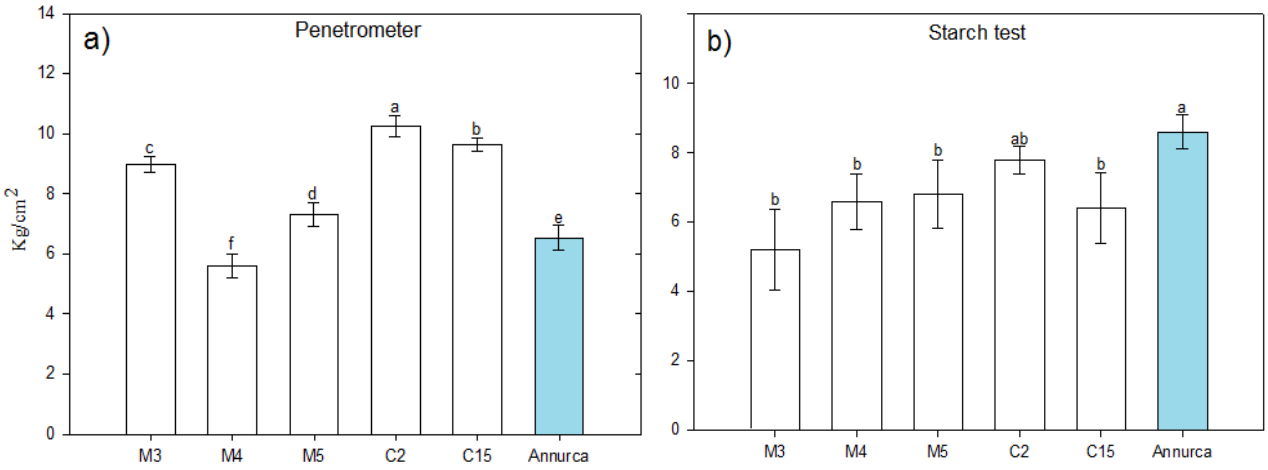

Figure 7. a) Starch *index measured in the flesh of apple fruit of IRP lines and Annurca. b) Firmness values as determined by penetrometric measurement, expressed in Kg/cm2. Histogram represents the average, bar represents ±SD. Different letters indicate statisti cally significant difference at p < 0.05 (Duncan's test).*

On season 2013, at harvest, IRP apples of M lines have shown a higher total soluble solid (TSS) content, expressed as °Brix, than C lines and Annurca (*Table 1*). In particular, apple of M3 and M5 lines have shown the highest TSS content of 15.8 and 15.7 °Brix, respectively, followed by M4 and C2 (14.7° and 14.5° Brix, respectively). The lowest TSS has been observed in apple of C8 and C15 line, 13.9 and 13.5, respectively. The highest titratable acidity (TA), expressed as mg malic acid eq. /L, has been found in fruit of M4 and M5 lines (6.8 and 6.1 mg/L, respectively), although pH value resulted to be similar to the other IRP apples and Annurca (*Table 1*). In contrast, fruit of M3 line have shown a very low acidity, ~ 2.4 g/L, and the lowest pH value (4.3). Apple of C15 line has shown the lowest TSS content (13.5° Brix) and, together with C2, the lowest pH value (3.28). The TSS/acidity (*Table 1*) resulted particularly high in apples of M3 line, mainly due to its low acidity level. Instead, apples of the other IRP lines have shown a lower value, ranged from 2.5 to 3.0 and similar to Annurca. A similar trend for TSS, TA and pH values has been also observed during season 2011 and 2012.

Genotype	Total Soluble Solid (Brix°)			pH			Titratable Acidity (malic acid eq. g/L)			TSS/Acidity		
	2011	2012	2013	2011	2012	2013	2011	2012	2013	2011	2012	2013
M3	15.3±0.4	15.4±1.0	15.8±1.1	4.59±0.09	4.60±0.13	4.37 ±0.17	2.5±0.4	1.7±0.2	2.4±0.4	6.0	9.1	6.4
M4	14.8±0.2	15.5±1.1	14.7±0.9	3.36±0.05	3.48±0.11	3.40 ±0.09)	7.0±0.4	5.8±0.4	6.8±0.3	2.1	2.6	2.1
M5	15.7±0.3	16.6±0.9	15.7±0.6	3.59±0.05	3.47±0.12	3.77 ±0.11	6.2±0.5	7.2±0.5	6.1±0.5	2.5	2.3	2.5
C2	14.2±0.5	14.4±0.5	14.5±0.5	3.29±0.03	3.22±0.07	3.33 ±0.11	5.6±0.4	6.2±0.2	5.8±0.2	2.5	2.3	2.5
C8	13.7±0.4	-	13.9±0.3	3.59±0.07	-	3.44±0.04	4.8±0.3	-	4.7±0.1	2.8	-	2.9
C15	13.2±0.4	12.9±0.5	13.5±0.4	3.28±0.06	3.22±0.09	3.38 ±0.14	4.2±0.3	4.4±0.2	4.9±0.1	3.0	2.9	2.7

cv Annurca	14.3±0.5	14.2±0.5	14.9±0.6	3.52±0.03	3.48±0.04)	3.6 7±0.20	5.4±0.2	5.2±0.2	6.0±0.2	2.6	2.7	2.4

Table 1. Total soluble solid (TSS), pH value, titratable acidity (TA) and Brix°/Acidity ratio of IRP lines apples at harvest, on seasons 2011-2013.

1.13 COLOR EVOLUTION DURING APPLE FRUIT DEVELOPMENT

Preliminary observation of red colour intensity in peel and flesh tissue suggested important differences among the six IRP lines. Therefore, red colour evolution were monitored along six fruit development stages: 30 DAFB (stage I), 50 DAFB (stage II), 70 DAFB (stage III), 90 DAFB (stage IV), 110 DAFB (stage V) and 160 DAFB (stage VI, harvest).

Peels lightness parameter (*Figure 8b*) resulted to be highest in cv Annurca and C8 line until 70 DAFB. After this stage, lightness sharply decreased until maturity (stage VI, about 160 DAFB), particularly in cv Annurca. Red-coloured peels have characterized the IRP lines C2, C15, M3, M4 and M5 already at early stage of fruit development. In these lines, lightness progressively increased until maturity, reaching higher values than cv Annurca, except for M4 line. A similar trend was also observed for flesh tissue (*Figure 8a*). The values of lightness parameter resulted to be the highest in cv Annurca and C8 line, until stage III of fruit development. Subsequently to this stage, differences among lines disappeared and at maturity, red and white flesh lines had a similar lightness value.

The hue angle value was expressed using the formula *2π-hue angle* to directly correlate values with red colour intensity. As expected, in fruit peel of C8 line and cv Annurca a low value of this parameter as been detected (*Figure 8d*) until stage IV, and after that the value has started to increase. The highest values were reached at stage VI, in agreement with the appearance of peel red coloration. On the contrary, in IRP lines an inverse trend has been detected. Hue angle parameter resulted to be high during early stage of fruit development (until stage III), and after that progressively decreased in all lines except M4, characterized by values similar to cv Annurca. Regarding hue angle values of flesh tissues (*Figure 8c*), in fruit of C8 line and cv Annurca, characterized by white colored flesh, the lowest values, with very little variability along developmental stages, has been relived. Fruits of lines of IRP group, characterized by red colored flesh, instead have shown the highest values of this parameter. Interestingly, significative differences were detected both among IRP lines and among developmental stages. At early stages of fruit development, until stage II, hue angle values resulted higher in all lines, in agreement with strong red flesh coloration. Starting from stage III, differences among lines become more evident as well the general reduction of hue angle values, probably due to environmental condition. However, fruit of C2, C15 and M4 lines have shown higher values than fruit of M3 and M5 lines, even if in this last a strong variability of the value has been found. Interesting, at stage VI of fruit development, we have observed a strong reduction of C2 hue angle values, while M4 and C15 retained the highest values. M3 line has shown the lowest intensity of red coloration, together with M5, although both have shown the highest variability.

As observed for lightness, values of chrome parameter in peel tissues (*Figure 8f*), were characterized by a decreasing trend during fruit development in cv Annurca and C8 line, on the contrary an increasing trend of these values have characterized the IRP lines. Flesh chrome parameter (*Figure 8e*) have shown a decreasing trend along fruit development in all studied lines and cv Annurca, indicating a general reduction of colour intensity.

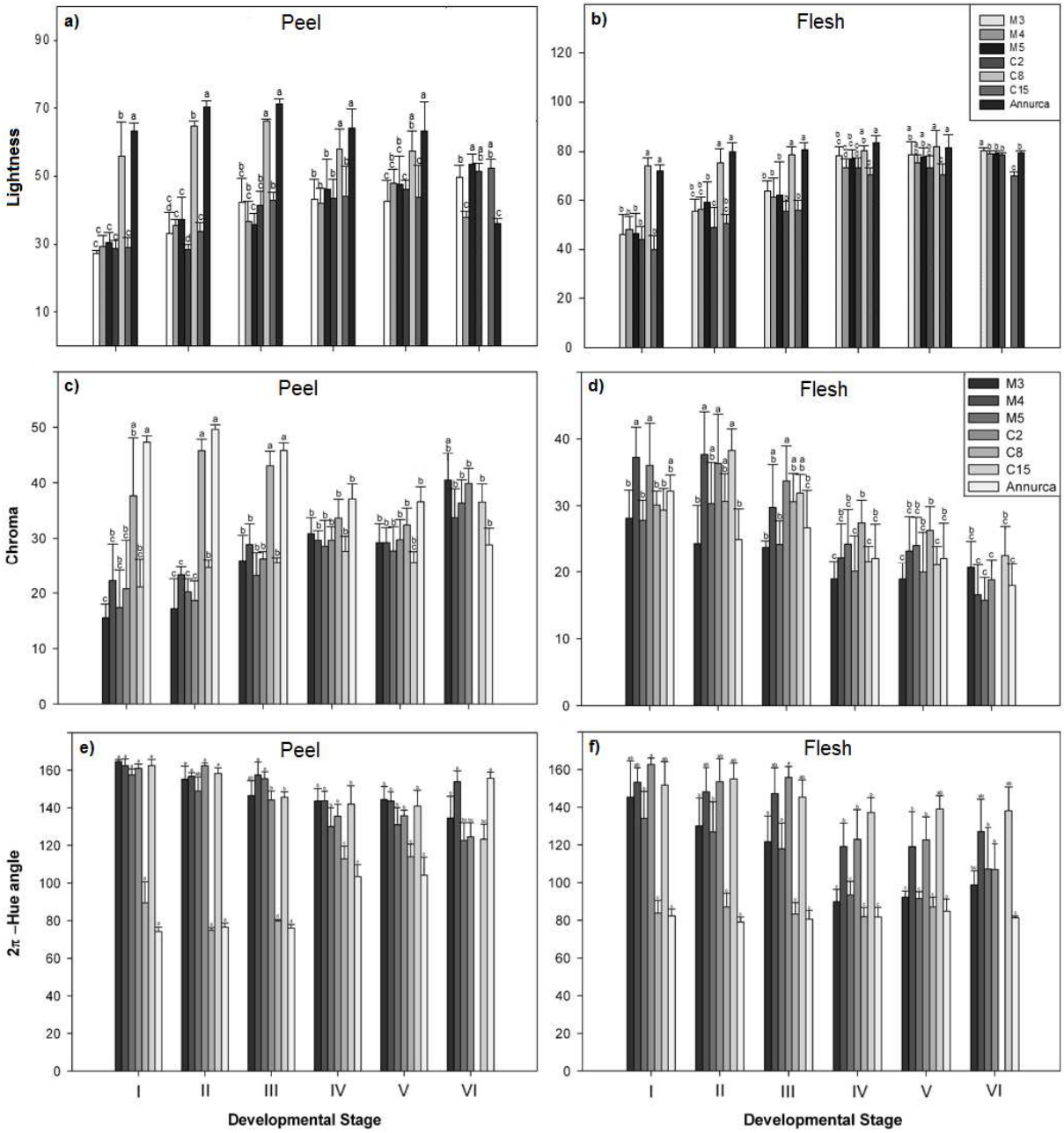

Figure 8. Mean values of lightness (a, b), chroma (c, d) and hue angle (e, f) parameters detected in peel and flesh tissues of IRP lines and cv Annurca. Histogram represent the average, the bar the standard deviation, and different letters indicate statistically significant differences at $p < 0.05$ (Duncan's test).

All colorimetric data suggests important differences among IRP lines, particularly for flesh tissues. C15 and M4 lines appeared to have the highest flesh red colour intensity, with reduced variability among fruit. In contrast, C2 and M5 line were characterized by the highest variability in flesh red

colour intensity, even if they have retained acceptable level of coloration. Finally, M3 line have shown only a reduced red-coloration, usually restricted to the central core or sub-epidermal tissues. A representative picture of peel and flesh colour evolution during IRP apple development are shown in *Figures 9* and *10*.

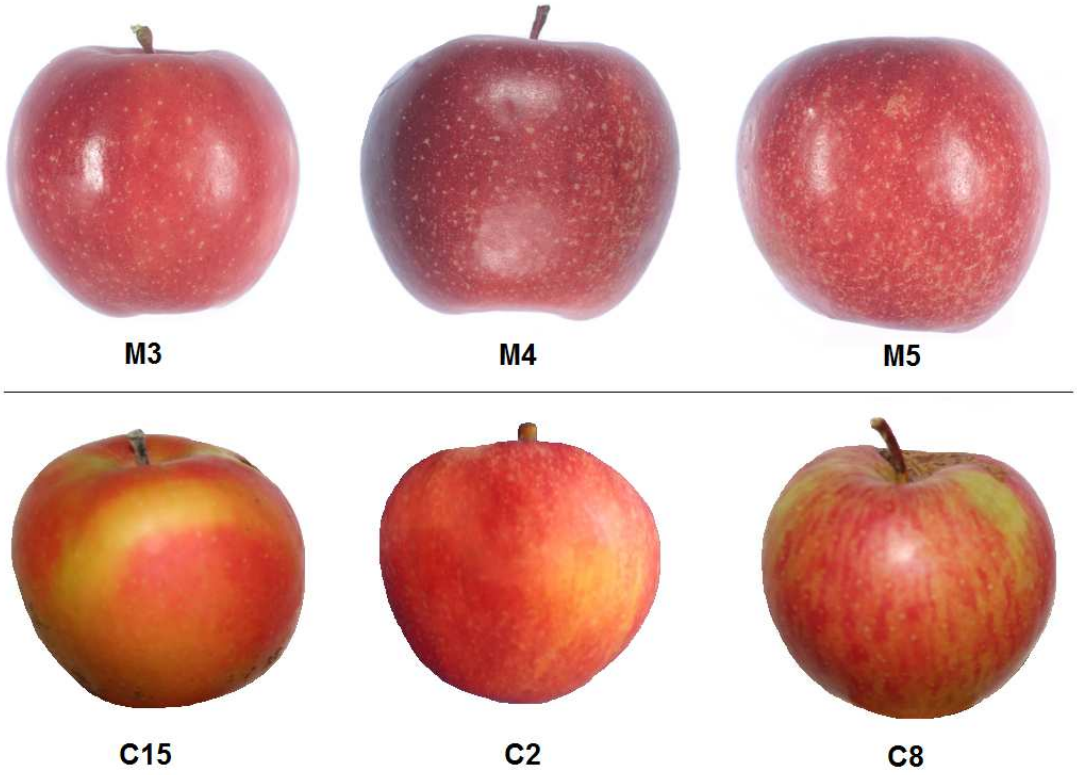

Figure 9. Mature apples of Italian Red Passion lines.

Figure 10. Colour evolution in flesh tissue of IRP apple during development.

1.14 TOTAL POLYPHENOL AND ANTHOCYANINS CONTENT IN FLESH AND PEEL TISSUES OF ITALIAN RED PASSION APPLE LINES

At 2013 harvest, total polyphenol content of apple flesh varied significantly among lines of IRP group (*Figure 11, a)*. The content ranged from 87 to 172 mg eq. GAE/100g FW. Apple flesh of IRP lines contained a higher content respect to Annurca, and M lines a higher content respect to C lines. Total polyphenol content of M4 and M5 flesh (172 and 159 mg, respectively) was almost double compared to Annurca (87 mg), while in flesh of the other IRP lines the content resulted to be lower: 139 mg in M3, 119 mg in C2 and 125 mg in C8. Among the lines of IRP group, the lowest value has been detected in the flesh of C15, although this content resulted to be higher than Annurca.

Peel total polyphenol content (*Figure 11, b*) resulted to be more similar among the fruits of IRP lines and about 2 to 3-fold higher compared to flesh content. In peel of M4 line has been detected the highest total polyphenol content, ~ 290 mg eq. GAE/100g FW, while the content in fruit peels of M3 and M5 lines has been 265 and 253 mg, respectively. The whole C lines have shown a slightly lower content than M lines, but it resulted to be similar to that of Annurca (around 220 mg), except for the peel of C8 line, where the content detected resulted to be up to 247 mg.

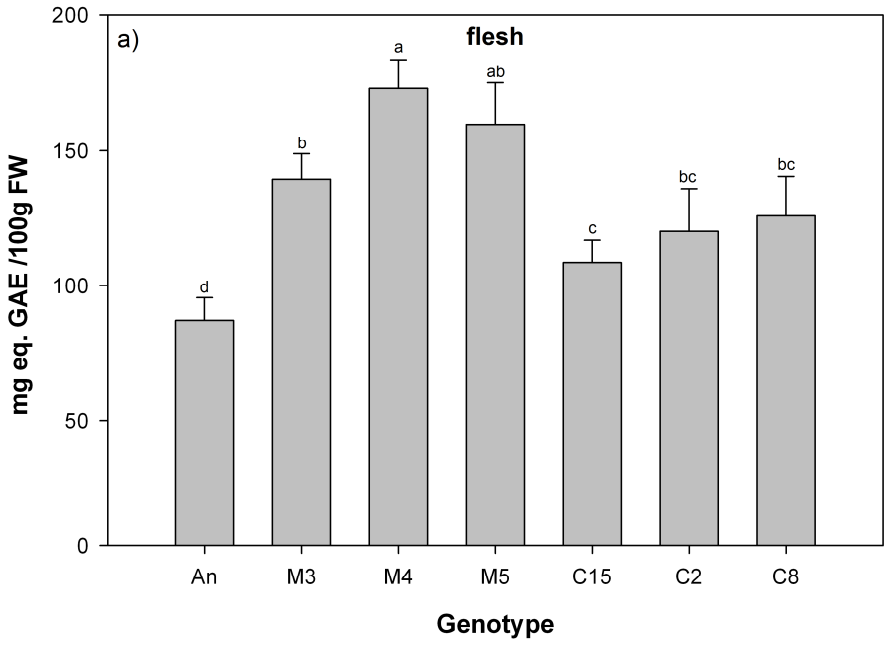

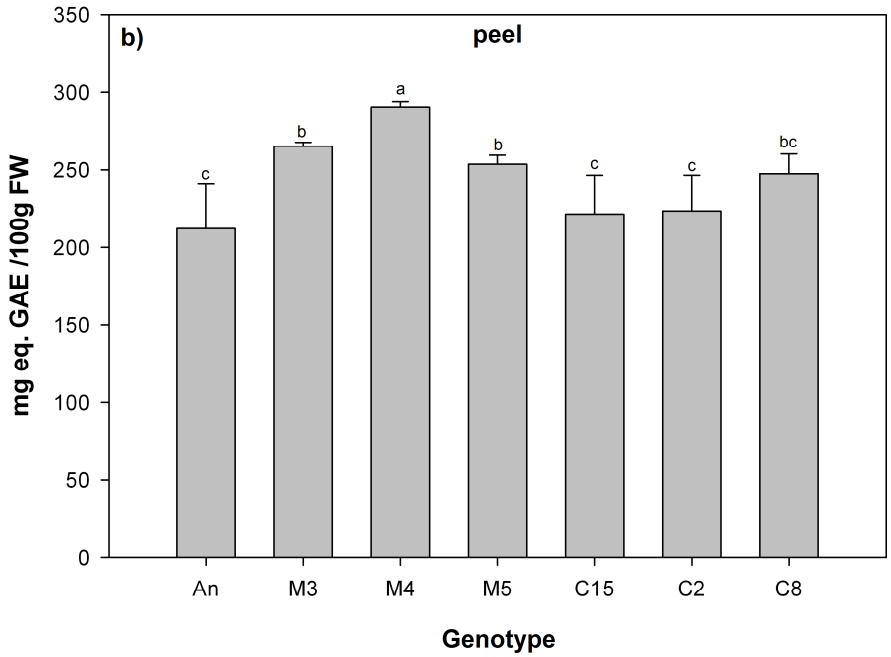

Figure 11. Total polyphenols content in flesh (a) and peel tissue (b) of fruit of IRP lines and cv Annurca. The value are expressed in mg of gallic acid eq. /100g fresh weight (FW). Histogram represents the average, bar represents the SD and different letters indicate statistically significant difference at p < 0.05 (Duncan's test).

At 2013 harvest, total anthocyanins content of flesh tissues resulted different among IRP lines and between those and cv Annurca (*Figure 12a*). The highest content has been detected in flesh of C15 (5.1 mg/100g FW) and M4 (4.4 mg/100g FW), which resulted to be the most intense colored lines. In the flesh of C2 line has been detected a content of 3 mg/100g FW, while in M3 and M5 lines the detected content resulted to be the lowest among IRP lines (1.3 and 1.9 mg/100g FW, respectively). As expected, in flesh of Annurca and C8 only detectable anthocyanins amount have been detected. Peel colour resulted to be different among IRP lines (*Figure 12b*) and total anthocyanins content resulted to be generally lower compared to Annurca peel, except for M4 line. Among the IRP apple group, the highest content have been observed in M4 line, about 10 mg/100g FW, while M3 and M5 had a similar content of 7.6 and 6.9 mg, respectively. The peel of C lines resulted to be less rich in anthocyanins: 4.9 mg in C8, 3.9 mg in C2 and 3.6 mg in C15. It is worth noting that in the last line has been detected the lowest peel anthocyanin content but the highest flesh one.

The content of anthocyanins was been also determined in the flesh of apple harvested from seedlings of IRP group prior to their grafting on selected rootstock (MM111 for M lines and M26 for C lines), to explore the effect of scion-rootstock combination on anthocyanin accumulation (*Figure 12a*). Indeed, for example, M5 seedlings have shown the highest flesh anthocyanin content among M lines (season 2010) while the same M5 line grafted on MM111 rootstock accumulate only minor content (2013). The reduction of flesh anthocyanins content in grafted M5 seems to not depend from environmental condition, since M3 and M4 lines have shown a comparable content between the two

different seasons 2010 and 2013. On the contrary, grafting seems to not affect flesh anthocyanins content in the other lines. The effect of scion-rootstock combination will be further investigate in the future.

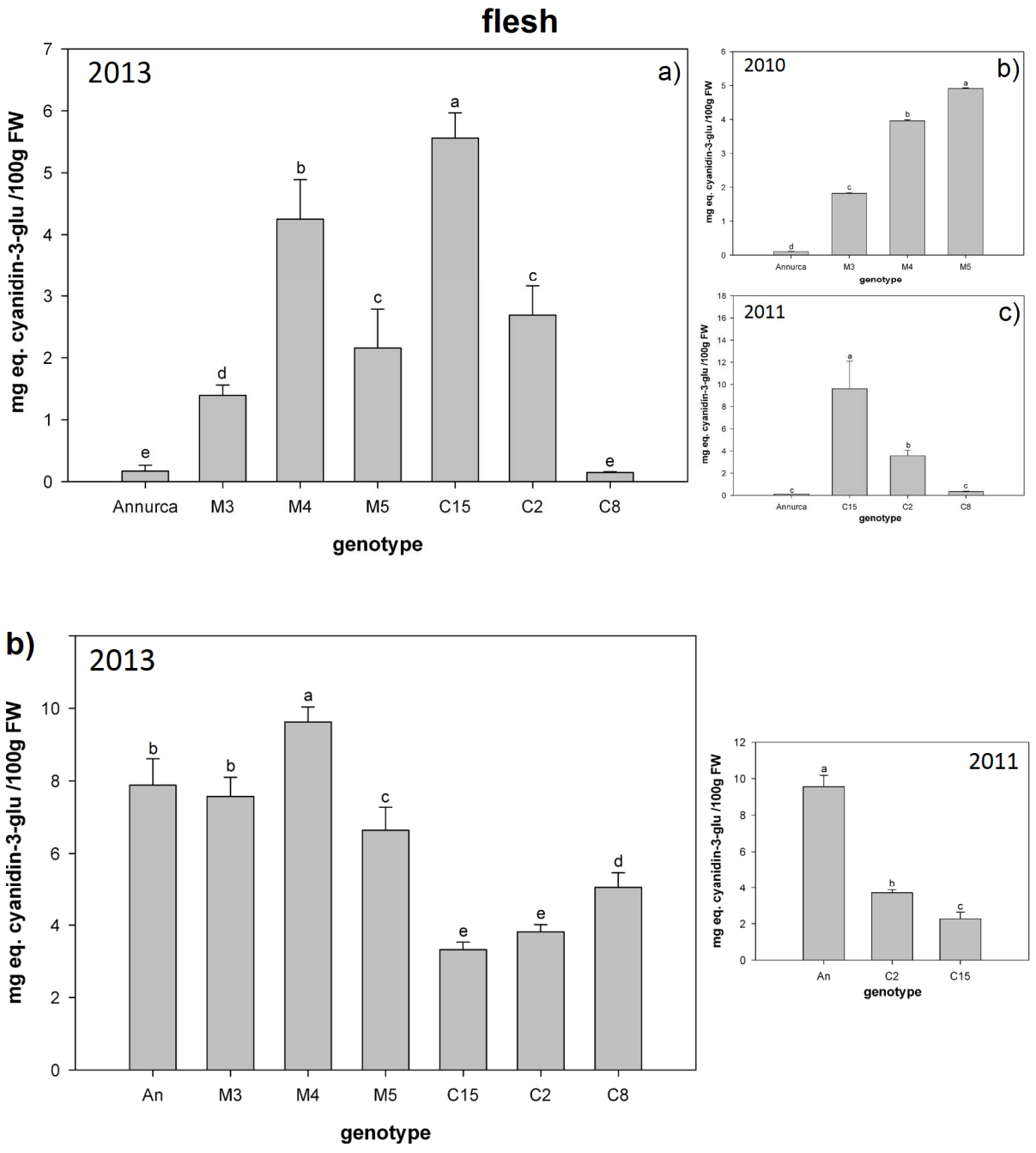

Figure 12. Total anthocyanins content in flesh and peel tissues of IRP lines and cv Annurca apples, expressed in mg cyanidin-3-glucoside eq. /100g fresh weight (FW) determined in seedlings (season 2010 and 2011) and grafted plant (season 2013). Histogram represents the average, bar represents the SD and different letters indicate statistically significant difference at $p < 0.05$ (Duncan's test).

1.15 ANALYSIS OF MAIN PHENOLICS COMPOUNDS CONTENT IN APPLE FLESH AND PEEL OF IRP LINES

The HPLC analysis of specific polyphenol provides a more detailed information on apple flesh composition of IRP lines. In general, we observed large differences on polyphenol content and profile (*Table 2*). Two major classes of polyphenols, flavan-3-ols, composed by mono- and dimeric flavan-3-ols, and phenolic acids, mainly composed by chlorogenic acid, dominate polyphenol profile of IRP lines apples.

Apple flesh of M3 accumulate a higher amount of chlorogenic acid (127 mg/100g FW) respect to the other IRP lines, which ranged from 40 mg in M5 to 54 mg in C15, and also respect to flesh of Annurca (32 mg).

Flesh of C15 accumulated the lowest amount of flavan-3-ols. Indeed the sum of catechins, epicatechins, procyanidin-B1 and -B2 (*Figure 13*) ranged from the highest content of ~120 and 110 mg, respectively in apple flesh of M4 and M5 to the lowest of Annurca (~30 mg). Regarding individual flavan-3-ols compound, in flesh of M4, C2 and C8 lines has been detected the highest catechins content, ranging from 20 to 25 mg, followed by M5 with ~16 mg. Flesh of Annurca and C15 apples accumulated the lowest amount of catechins. Epicatechin content resulted to be the highest in flesh of M group, ~30 mg, while Annurca the lowest, ~8 mg. A general higher content of procyanidin-B2 respect to procyanidin-B1 has been detected. Fruit flesh of M4 and M5 lines accumulated the highest amount of procyanidin-B1, ~15 mg, while C15 the lowest (~1 mg). Flesh of M4 and M5 accumulated also the highest amount of procyanidin-B2, ~45 mg while Annurca the lowest (~9 mg).

Cyanidin-3-galactoside resulted absent in white flesh of C8 line and Annurca. The observed content of cyanidin-3-galactoside seems to confirm the previously described data on total anthocyanins accumulation: in flesh of C15 and M4 has been found the highest content (~4 and ~2 mg, respectively) and M3 the lowest (0.95 mg), while the other lines had a similar content around 1.3 mg. Relevant amount of cyanidin-diglucoside have been found in M lines, while this compound resulted to be undetectable in C lines and Annurca.

The amount of phloridzin, resulted highest in M3 and M4 apple flesh followed by M5 and C lines, with a similar content around 1 mg/100g FW, and lowest in cv Annurca. Instead, flesh of C2, C8 and Annurca accumulate the highest amount of phloretin (~0.4 mg), which resulted to be undetectable in M5 flesh. In addition, other classes of phenolics compounds resulted to more abundant in flesh of IRP lines compared to Annurca, as deduced by HPLC peaks area (data not shown). Among these classes putative phenolics acids, such as caffeic, *p*-coumaric and hydroquinic acids, have been observed, as well as differently glycosylated form of anthocyanins.

Compound (mg/100g FW)	Genotype						
	Annurca	**M3**	**M4**	**M5**	**C15**	**C2**	**C8**
Hydroxycinnamic acids							
Chlorogenic acid	32.04±2.01 c	127.1±16.6 a	46.72±5.77 b	40.88±3.45 b	41.40±13.3 b	48.19±12.2 b	54.70±12.7 b
Dihydrochalcones							
Phloridzin	0.610±0.09 c	2.180±0.48 a	1.985±0.32 a	1.224±0.18 b	1.225±0.07 b	0.975±0.23 c	1.375±0.45 b
Phloretin-xyloglucoside	0.451±0.13 a	0.138±0.05 c	0.044±0.02 d	n.d.	0.092±0.01	0.448±0.09 b	0.447±0.02 b
Flavan-3-ols							
Procyanidin B1	3.53±0.47 c	5.50±0.73 b	13.90±1.42 a	15.30±1.70 a	1.026±0.27 d	2.16±0.53 e	6.53±1.48 b
Procyanidin B2	8.56±0.82 d	28.56±3.64 b	46.16±5.42 a	43.10±6.31 a	18.31±5.53 c	15.77±4.86 c	23.77±4.68 bc
Epicatechin	8.109±1.43 d	29.20±3.78 a	36.85±4.46 a	34.66±5.50 a	11.50±2.36 cd	13.86±4.32 c	22.55±8.89 b
Total catechins	9.009±1.24 cd	11.17±0.99 c	24.97±6.25 a	16.82±2.36 b	6.665±1.40 d	24.28±0.96 a	20.86±6.50 ab
Flavonols							
Total Quercetins	0.013±0.001 b	0.06±0.023 a	0.0441±0.01 a	0.0158±0.01 b	n.d	n.d	n.d
Anthocyanins							
Cyanidin-3-galactoside	n.d	0.955±0.226 d	1.936±0.375 b	1.292±0.159 c	3.93±1.42 a	1.317±0.85 c	n.d
Cyanidin-diglucoside	n.d	0.108±0.014 c	0.235±0.05 b	0.325±0.04 a	n.d	n.d	n.d

Table 2. Main apple flesh phenolics compounds concentration, expressed in mg/100g FW detected in IRP lines and cv Annurca. Histogram represent mean values and standard deviation of three biological replicates. Histogram represents the average, bar represents the ± standard deviation and different letters indicate statistical significant difference at p < 0.05 (Duncan's test).

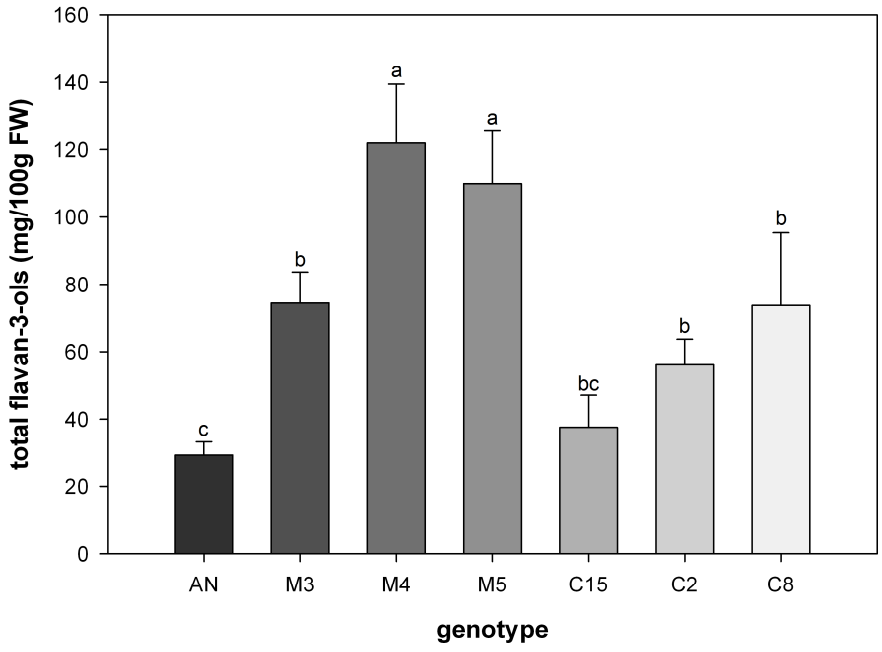

Figure 13. Table 1. Sum of detected flavan-3-ols fractions, expressed in mg/100g FW, detected in IRP lines and cv Annurca. Histogram represents the average, bar represents the standard deviation and different letters indicate statistical significant difference at p < 0.05 (Duncan's test).

The content of some important phenolics classes have been also analyzed in peel tissues of C2 and C15 lines and compared to cv Annurca (*Table 3*). Differently respect to that detected for flesh tissues, the total polyphenol content of peel did not resulted to be different in C2 and C15 lines, and compared to Annurca. Despite this, some difference have been detected regarding to the content of some specific compound. Peel of C2 line accumulate the highest amount of both monomeric and dimeric flavan-3-ols, and chlorogenic acid respect to Annurca and C15 apples. Instead, peel of Annurca accumulate the highest amount of flavonols (about 30 mg/100g FW), phloridzin and phloretin xyloglucoside compared to C2 peel. On the opposite, a greater content of flavan-3-ols have been detected in peel of C2.

Compound (mg/100g FW)	**Genotype**		
	Annurca	**C2**	**C15**
Hydroxycinnamic acids			
Chlorogenic acid	16.1±1.0 a	27.2±2.8 b	15.4±4.4 a
Dihydrochalcones			
Phloridzin	16.3±1.71 a	9.59±5.64 b	5.20±3.42 b
Phloretin-xyloglucoside	3.76±0.59 a	1.95±0.62 b	0.42±0.11 c
Flavan-3-ols			
Procyanidin B1	4.22±1.2 a	3.80±0.3 a	0.94±0.2 b
Procyanidin B2	75.4±7.9 b	118±17 a	39.9±8.0 c
Epicatechin	46.1±11 a	44.6±10 a	21.5±6.3 b
Total catechins	21.0±4.8 a	25.7±3.8 a	10.7±3.1 b
Flavonols			
Total Quercetins	31.16±4.17 a	19.72±2.75 b	10.05±2.03 c
Anthocyanins			
Cyanidin-3-galactoside	9.78±0.32 b	17.3±2.9 a	5.22±0.3 c
Cyanidin-diglucoside	n.d	n.d	n.d

Table 3. Content of specific classes of phenolics compounds, expressed in mg/100g FW, detected in apple peel of C2, C15 lines and cv Annurca. Histogram represents the average, bar represents the ± standard deviation and different letters indicate statistical significant difference at $p < 0.05$ (Duncan's test).

1.16 ANTIOXIDANT ACTIVITY

Antioxidant activity was evaluated in the fruit extract of IRP lines and cv Annurca (*Figure 14*) by using DPPH test, which measures radical scavenging ability. The inhibitory concentration (IC50), the efficient concentration (EC50) and the antiradical power (ARP) were calculated, as already has been described in Materials and Methods. In general, more less it is the value of EC50, higher it is the

antioxidant capacity and greatest is the value of ARP, therefore more efficient is the antioxidant properties of fruit.

Fruits of all IRP lines have shown higher radical scavenging activity than that of cv Annurca. The value of EC50 ranged from 11.89 mg/mg DPPH of cv Annurca, with the highest value, to 4.00 mg/mg DPPH of M3 genotype, with the lowest. In agreement with EC50, fruits of the M line have almost 2-fold higher ARP values than that evaluated in the fruits of C lines and 2.5-fold than that of cv Annurca. Moreover, extract of fruits from M3 and M4 lines have shown the highest ARP value, (25 and 24, respectively; while for the C15 line has been determined the lowest value of ARP (11), even if not significative different from cv Annurca with ARP value of 6.75. The antioxidant activity, expressed as anti-radical power value of apple extracts, resulted to be correlated with the total phenolics content (R^2 value of 0.92), expressed in mg GAE/100g FW (*Figure 15*) and, to a lower extent, with sum of flavan-3-ols fraction (R^2 value of 0.76). Instead, the ARP value appear uncorrelated with anthocyanin content (R^2 value of 0.14, data not shown).

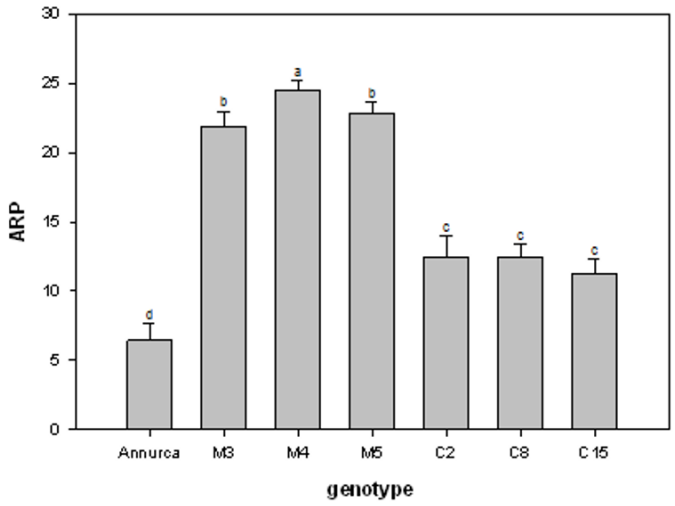

Genotype	IC50 (mg/ml)	EC50 (mg/mg_{DPPH})	ARP
Annurca	3.84±0.52	16.29±2.24	6.75±0.92
M3	1.05±0.12	4.48±0.51	22.30±0.70
M4	0.96±0.03	4.07±0.12	24.40±0.74
M5	1.03±0.03	4.37±0.13	22.87±0.71
C2	1.92±0.26	8.15±1.12	12.42±1.61
C8	1.90±0.14	8.06±0.60	12.45±0.91
C15	2.11±0.19	8.93±0.81	11.26±1.08

Figure 14. Antioxidant activity, expressed as anti-radical power value (ARP) of apple extracts of IRP lines and cv Annurca. Histogram represents mean values and standard deviation of three biological replicate, bar represents the SD. Different letters indicate statistical significant difference at p < 0.05 (Duncan's test). In table were reported numerical data of IC50, expressed in mg/ml, EC50, expressed in mg/mg DPPH and ARP value.

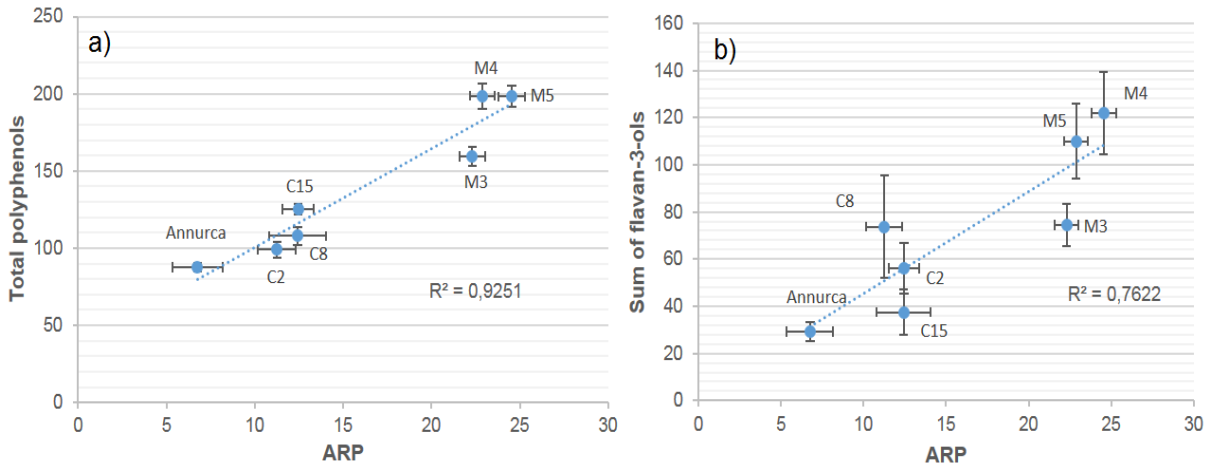

Figure 15. *Linear regression obtained by plotting a) total polyphenol content (mg/100 g FW) and b) total flavan-3-ols content (mg/100g FW) versus ARP values.*

1.17 APPLE SENSORY EVALUATION USING HEDONIC SCALE

It is well known by apple breeders that the very high polyphenols content of red-flesh apple fruit negatively affect their sensorial attributes (Thovogi, 2009). In particular, the astringency often induces repulsion in the acceptance consumers. Therefore, becoming important for commercial purpose evaluate the sensory properties of the fruits of the IRP lines, particularly for fresh consumption. The comparison with commercial apple cultivars, such as Golden Delicious, Royal Gala and Granny Smith, could give clear information about IRPs fruits consumer acceptance.

In *Figure 16* are represented the mean values for each fruit attributes and of each apple lines and cultivars. Apple fruits of C15 line, characterized by the most intense reddish flesh, were administered two times (named C15-1st and C15-2nd) to account for taste coherence.

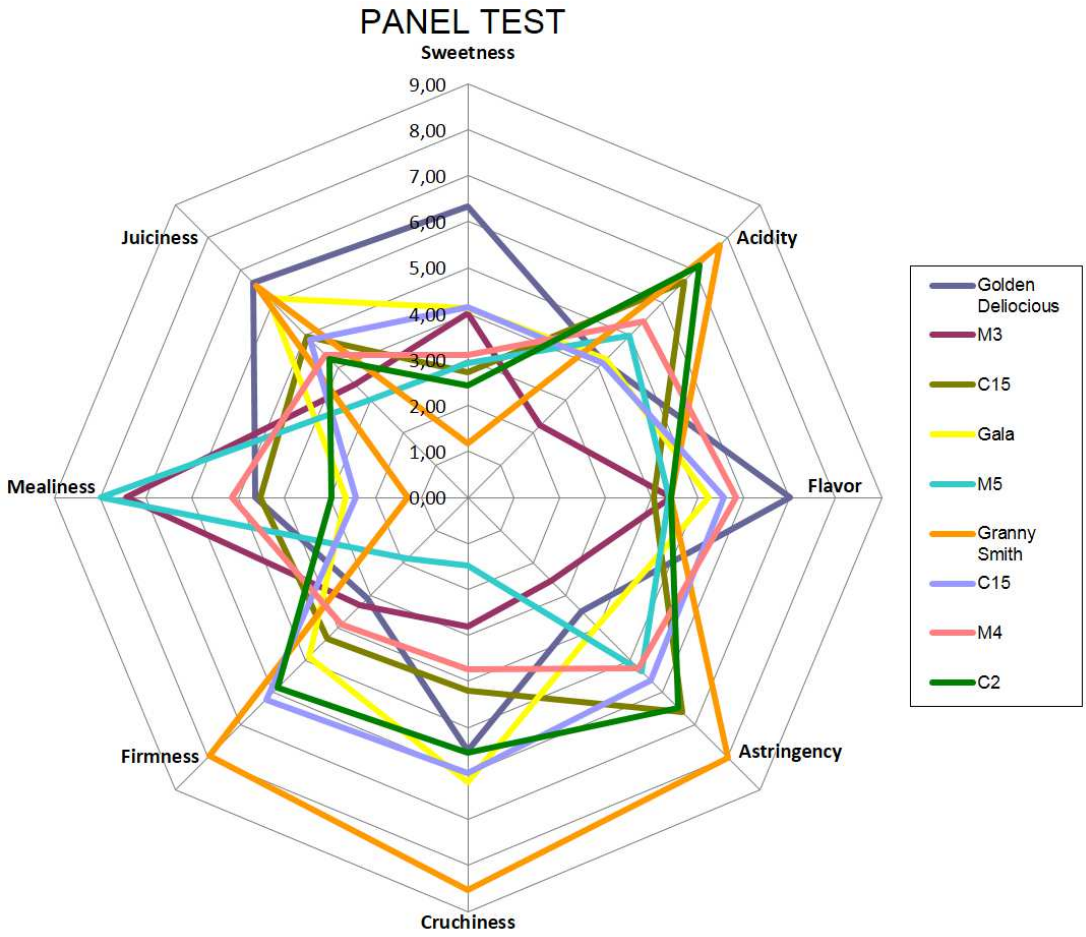

Figure 16. Mean score of each sensorial attribute in the fruits of IRP lines as compared to commercial apple cultivars Golden Delicious, Granny Smith and Royal Gala.

Regarding taste sensation (*Table 4*), sweetness perception resulted to be the highest for Golden Delicious (6.33) and, as expected, the lowest for Granny Smith (1.18). IRP lines have scored intermediate values, ranged from 2.45, in C2, to 4.00, in M3, similar to that found in Royal Gala (4.11). Although, in the C15-2nd test a high value has been scored it did not resulted to be statistically significant. Sourness attribute resulted to be the highest in Granny Smith, with a score of 7.75, followed by C2 and C15-1st test, with a value proximally similar, 7.13 and 6.65, respectively (*Table 4)*. Except for M3, characterized by the lowest acidity value score (2.22), the other lines have shown a similar values, around 4-5. Golden Delicious scored the highest flavor value (7.02), while the other lines and cultivars have scored a similar value, around 4-5 (*Table 4*). Important, astringency has resulted to be the highest for Granny Smith, with a score of 8.01 and lowest for M3 line, with 2.55. As expected, astringency score was generally higher in IRP lines than Golden Delicious (3.50) and Royal Gala (3.97), ranged from 6.61 for C15-1st to 5.25 of M4.

Genotype	Taste sensation			
	Sweetness	**Acidity**	**Flavor**	**Astringency**
Golden Delicious	6.33±1.16 a	4.17±1.48 de	7.02±0.96	3.50±1.53 cd
M3	4.00±1.37 b	2.22±1.46 e	4.42±1.57	2.55±1.86 d
C15	2.73±1.21 bc	6.65±1.33 ac	4.05±1.19	6.61±1.40 ab
Royal Gala	4.11±1.44 b	4.26±1.21 de	5.24±1.64	3.97±1.10 cd
M5	2.92±1.05 b	4.98±1.78 cd	4.38±1.60	5.35±1.86 bc
Granny Smith	1.18±0.49 c	7.75±1.56 a	4.42±1.81	8.01±0.98 a
C15	4.14±1.09 b	4.15±1.08 e	5.57±1.43	5.62±1.65 bc
M4	3.10±0.88 b	5.41±1.65 bd	5.84±1.50	5.25±1.54 bc
C2	2.45±0.87 bc	7.13±0.65 ab	4.43±1.21	6.47±1.21 ab

Table 4. Mean values and ± SD of taste sensations for red-flesh IRP apple lines compared Golden Delicious, Granny Smith and Royal Gala apples. Letters indicate statistically significant difference for $p<0.05$ (Duncan's test).

Regarding structural sensation (*Table 5*), Granny Smith has scored the highest value for crouchness (8.54) and firmness (7.95), while lines of M group has scored the lowest one. For these attributes, the fruit of C lines resulted to be similar to Golden Delicious and Royal Gala. M3 and M5 have shown the highest mealiness score (7.45 and 7.99, respectively), while juiciness attribute resulted generally highest in the three commercial cultivar and lowest in IRP lines, although by not statistically significant differences of one to each other. Resuming, the lines of IRP could be classified into two main commercial classes on the basis of structural sensations: the first class represented by fruits from C2 and C15 lines, characterized by high crunchiness and firmness; the second one represented fruits

from M3, M4 and M5, characterized by high mealiness. Moreover, M3 could be considered the 'sweet line', in contrast to C2, sour and slightly astringent, while fruits of M4, M5 and C15 lines have a more balanced sweet/sour taste. In the Figure 21, the overall enjoyment of fruits from the panelist resulted to be the highest for Golden Delicious and Royal Gala (7.0 and 6.4, respectively), altough the values scored by C2 and C15-2nd lines (5.3 and 5.6, respectively) did not resulted to be statistically different. Instead, M3 and M4 ranked with Granny Smith (4.5). Finally, fruits of M5 line have shown a very low overall enjoyment score of 2.1.

Genotype	Structural sensation			
	Crouchness	Firmness	Mealiness	Juiciness
Golden Delicious	5.50±1.57 bc	3.09±1.19 de	4.62±1.72 bc	6.60±1.28 a
M3	2.80±1.07 de	3.32±1.62 de	7.45±1.01 a	3.46±1.12 c
C15	4.21±1.44 bd	4.34±1.53 bd	4.51±1.84 bc	4.95±1.31 ac
Royal Gala	6.19±1.17 b	4.90±1.37 bd	2.65±0.75 cd	6.13±1.31 ab
M5	1.47±0.57 e	1.88±0.96 e	7.99±1.00 a	3.01±0.94 c
Granny Smith	8.54 ±0.66 a	7.95±0.74 a	1.30±0.60 d	6.53±1.38 a
C15	5.98±1.50 b	6.21±1.15 ab	2.43±1.20 d	4.85±1.60 ac
M4	3.74±1.65 cd	3.89±1.93 cd	5.15±1.96 b	4.38±1.41 bc
C2	5.55±1.54 bc	5.85±1.40 bc	2.96±1.13 cd	4.26±1.64 bc

Table 5. Mean values and ±standard deviation of structural sensations for red-flesh IRP apple lines and Golden Delicious, Granny Smith and Royal Gala apples. Different letters indicate statistically significant difference at for $p < 0.05$ (Duncan's test).

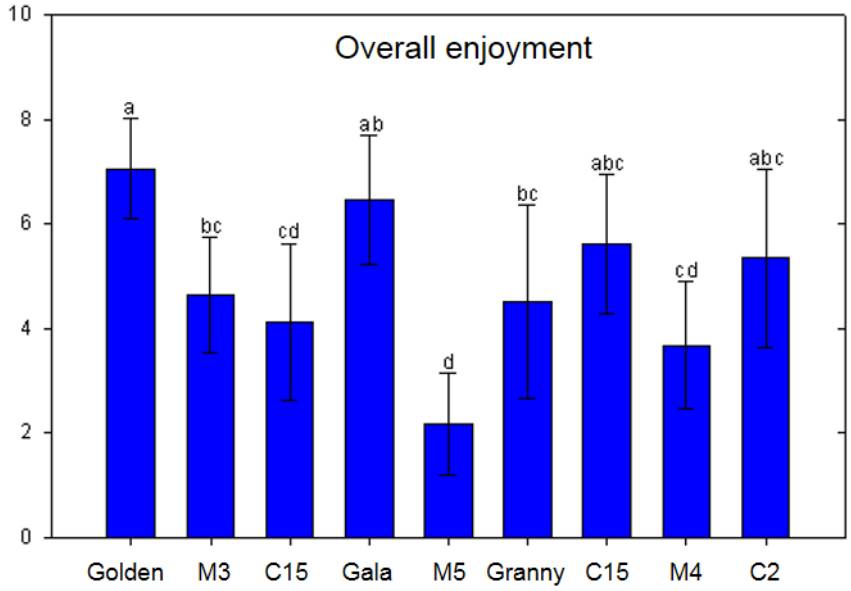

Figure 17. Overall enjoyment values for red-flesh IRP apple lines compared to Golden Delicious, Granny Smith and Royal Gala apples. Histogram represent the average and the bars ± standard deviation. Different letters indicate statistically significant difference at $p < 0.05$ (Duncan's test).

1.18 CONSUMERS' PREFERENCES AND MARKET ANALYSIS

The main objective of the survey was to gain knowledge about consumer's acceptance, the level of interest and purchasing decision of new red-flesh apple products. Indeed, the survey have been focused on the pre-purchase factors (McCracken et al. 1994), such as appearance and price, which represent the main factors influenced consumer's decision to purchase in apple market. Considering the relevance of nutritional property and the genetic origin of IRP lines, an informative background has been also provided, further remarking both not negligible aspects. A total of 485 consumers were surveyed, almost equally divided into male and female, 242 and 243, respectively. Most of the respondents (285) lived in Viterbo, where 70,000 residents live inside, while the remaining respondents lived out of city in countryside of the same province or in neighboring provinces, characterized by small town under 10,000 residents. Respondents belong mainly to age classes ≥ 50 (years), for almost 50%, to age classes comprise between 20-49 years, for almost 37%, while the remaining 13% belong to teenager, ranged from 15 to 19. Regarding the professional categories, pensioner (21.5%), student (14.5%), homemaker (14.5 %) and employed (11%) resulted the most represented, on a total number of twelve categories. About 60% of the respondents stated to consume habitually apple fruit. However, surprisingly, 95% of respondent stated they are not informed of about red-flesh apple nor Italian Red Passion apple lines. The level of interest of respondents to taste the new red-flesh apple product was evaluated through a Likert scale (score 1-6). The last question ha inherent in itself a possible dichotomous response, and based on assigned score, ≤ 3 and ≥ 4, two different questions were introduced. As shown in figure 18 about 64% of respondents assigned a score ≥ 4, indicating a general propension to taste the products, although the mean value scored around 4.05 and the variability oscillated between ranged from 3 to 5.

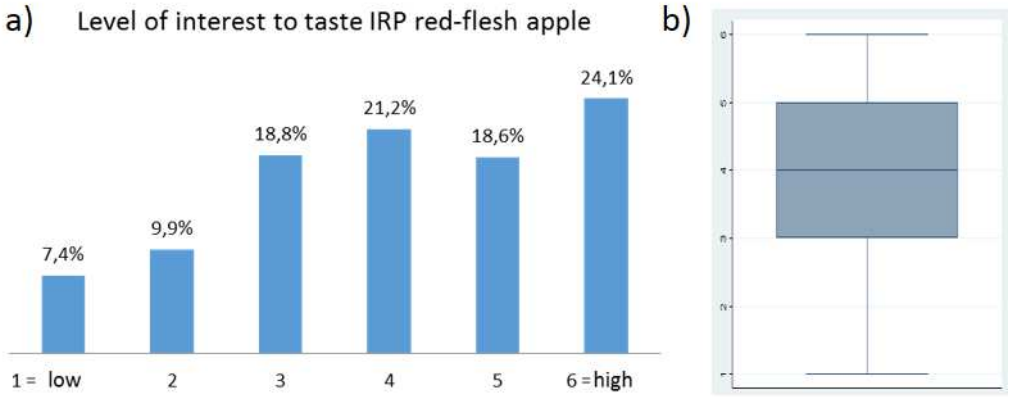

Figure 18. Level of interest to taste Italian Red Passion apples, expressed as percentage of Likert score (a). b) Box plot of mean Likert scores variability among respondents.

Respondents that have assigned a score ≥ 4, they have stated that curiosity represented the main factor that influencing their decision, with mean score of 5.02, although nutraceutical properties and visual attributes have totalized a slightly low score of 4.81 and 4.41, respectively (*Figure 19*). Instead,

respondents that have assigned a score ≤ 3 have clearly explained that their decision was not influenced by the diffidence about novelty and genuineness of product, mean score of 3.36 and 3.22, respectively.

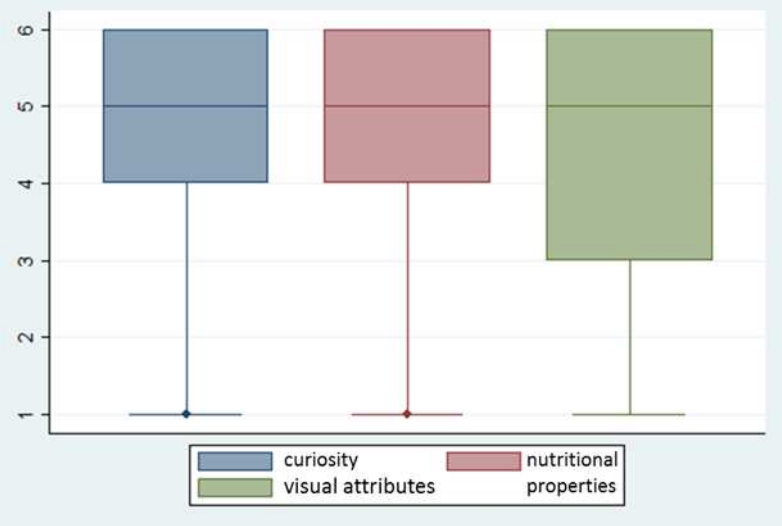

Figure 19. Box plot of variables 'curiosity', 'nutritional properties' and 'visual attributes' for respondents assigned a score ≥4 to the level of interest to taste the product.

Independently from their propensity to taste red-flesh apples, to the respondents was asked their most impressive appearance attributes of the products. Interesting, and about 52% of them was mainly impressed by the red colour of flesh, judging as attracting or unusual (rum), 27% and 24.9% scored, respectively; while about 45% of respondents was mainly influenced by the fruit shape, judging small or attracting, 12.4% and 22.9% scored, respectively.

Remarking the higher nutritional property of IRP apple varieties respect to commercial cultivars, to the respondents have been asked their propensity toward buying red-flesh apples. Surprisingly, 73% of them would be willing to purchase the apples (*Figure 20a*); among them, 35% would be willing to pay a higher price respect to other apple varieties (*Figure 20b*). Moreover, among the last group of the respondents 76% were willing to pay 25% more than the normal price (*Figure 20c*). Among the 27% of respondents not interested to purchase the product, 54% of them did not consider red-flesh apple superior than commercial ones, while 28% of them were not simply interested to the red flesh apples. Interesting, a small percentage (11%) of not interested have been stated to do not believe what affirmed by researchers about the product.

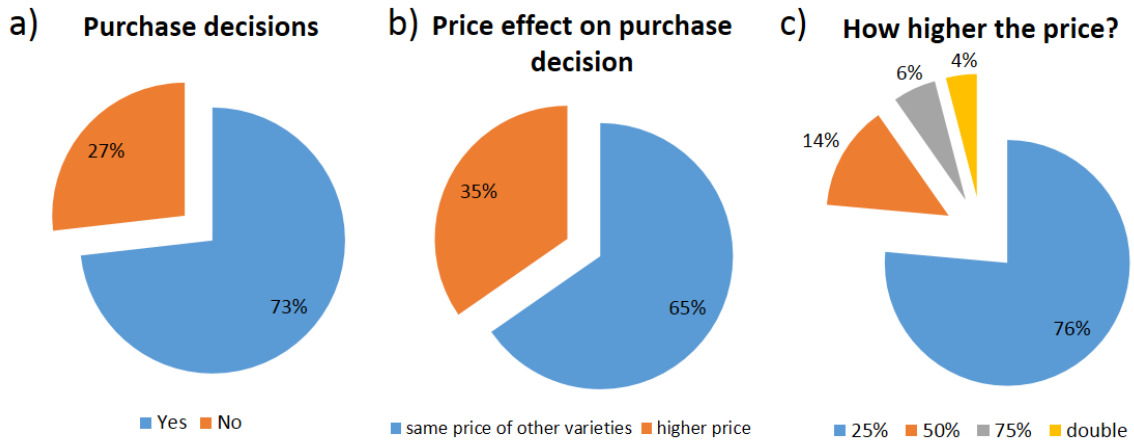

Figure 20. a) 2D pie chart of purchase decisions, b) pie chart of price effect on purchase decision and c) additional cost which respondents state to pay for red-flesh apples.

To assess the relationship between socio-demographic respondent members and respondent's behavior toward their **real interest to consume the novelty**, a cluster analyses have been performed, gathering them in segments, in agreement with their high or less homogeneity. Cluster analysis about the level of interesting to taste the apple, showed three distinct respondents clusters, identified as the *excited*, *health-conscious* and *unmotivated*. The cluster *excited* explains 56.6% of variability, among the all analyzed variables the curiosity, nutritional properties and visual attributes scored the best means, although, they resulted to be similar one to each other (5.53, 5.14 and 5.48, respectively). The cluster was prevalently composed by women, belonged to age class ≥ 60 and to professional categories of pensioner, homemaker and shop assistant (*Table 5*). The cluster *health-conscious* (Table 5) was prevalently composed by respondents that were strongly interested to nutritional properties of the red flesh apple (5.21 was scored), although, the respondents that have manifested curiosity have also score high mean value, 4.80. Although, women have mainly composed this cluster, the most representative age classes ranged from 20-49 result the, and the professional categories more present were that of employee, student and entrepreneur.

The cluster *unmotivated* was composed by respondents that did not manifested any differences among the three variables, scoring similar low values, and prevalently composed by member of age class 50-59, mainly men, belonging to the professional categories of teacher, employee and worker (*Table 6*).

Cluster name	Freq.	Cluster size	Variables scores			Sex	Age Class	Professional category
			curiosity	nutraceutical properties	visual attributes			
excited	175	56.6%	5.53	5.14	5.48	W	15-19; 40-49; **≥60***	homemaker; shop assistent; pensioner
health-conscious	67	21.7%	4.80	5.20	2.14	W	20-29; 30-39; 40-49	student; employee; entrepreneurs

unmotivated	67	21.7%	3.91	3.53	3.86	M	20-29; 30-39; **50-59***	teacher; worker; employee
	Tot 309	mean profile	5.02	4.80	4.41			

Table 5. Cluster analyses of respondents assigned a score ≥ 4 to the level of interest to taste the apples.

Cluster analysis of the respondents **not interest to the product** (*Table 7*) have individuated two clearly distinguishable clusters: the *indifferent* (42.20%) and *traditionalist* (57.80%). Surprisingly, the *indifferent* cluster was mainly composed by the younger member of the population (age ≤ 39), mainly men, and belonging to professional category of unemployed and student. This cluster was not influenced by any factor, since the suggested motivations scored very low values. Instead, the cluster *traditionalist was prevalent* composed by the older member of population, age class ≥ 40, composed by mainly women and pensioner, with a clear predominance of the variable diffidence for the novelty, which scored the highest value of 4.55. Cluster analysis of *purchase decisions* did not highlight relevant significant differences respect to human genus, age class and/or professional category (data not shown).

Cluster name	**Cluster size**	**Variables scores**		**Sex**	**Age class**	**Professional category**
		Diffident product genuinity	**Diffident new product**			
indifferent	42.2%	2.59	1.41	M	**15-19***; 20-29; 30-39	students; unemployed
traditionalist	57.8%	3.89	4.55	W	40-49; 50-59; **≥ 60***	pensioners
mean profile		3.34	3.23			

Table 7. Cluster analysis of respondents assigned a score ≤3 to the level of interest to taste the product.

DISCUSSION

Together with size, shape, colour and taste of the fruit, the presence of bioactive compounds is becoming more required by the consumers (Schirrmacher and Schempp, 2003). Apple fruits contain a wide range of phytochemicals compounds that are effective in the prevention of many human diseases (Boyer et al., 2004). The challenges for agriculture and food industries, therefore, is the production of functional foods with a relevant effect on well-being and health to reduce disease risks (Roberfroid, 1999). Apples of the Italian Red Passion group as resulted from these studies represent an example of functional food. Indeed, flesh and peel fruits contain high polyphenols content compared to Annurca cultivar, including flavan-3-ols, chlorogenic acids and anthocyanins, these last compounds conferring the red pigmentation of IRP apple flesh. Considering the health benefits associated to dihydrochalcones consumption (Ehrenkranz et al., 2003) it is relevant 2 to 3-fold high amount of

phloridzin found in the flesh of IRP lines. Contrary to what is observed by Espley et al. (2013), IRP lines did not accumulate significant amount of flavonols in the flesh, while they accumulated amount of anthocyanins, mainly in the form of cyanidin-3-galactoside, at different degree and localization inside the fruit. However, other glycosylated form has also found, including cyanidin-diglucoside and cyanidin-glucoside. We speculate that the different accumulation of anthocyanins in flesh tissue might be dependent by the different glycosylated form, could be responsible for the observed red shades of each IRP line, oscillating from light pink to intense red. The increase polyphenol content is highly correlated to the higher antioxidant activity shown by the extracts from IRP apple flesh, which resulted highest that that detected in extracts from Annurca fruits, reported as one of the higher antioxidant apple cultivar (Cefarelli et al., 2006).

Since the understanding of consumers' preference for apple fruit represent a strategic necessity for the positioning of new cultivars, a panel test and a survey have been conducted to assess the general good likely of Italian consumers to taste and purchase Italian Red Passion apples product. Sensorial analysis highlighted that the very high amount of flavan-3-ols, often conferring bitter and astringent taste, seems to be not affect the liking of IRP apples lines, which have shown, as expected, general high scores for this attribute. This aspect is particularly evident considering the higher overall enjoyment score assigned to the apples of C2 and C15 lines, which shown also the highest scores for astringency degree. Regarding sensorial attributes, apples of M4, M5 and C15 resulted more balanced in sweet/tart while M3 apple could be considered the 'sweet apple', in contrast to C2, characterized by more pronounced sourness and astringency. Notably, good scores for aroma attributes characterized all IRP apples. Regarding structural sensation, C2 and C15 apples, characterized by high crunchiness and crispness, resulted more similar to Granny Smith type, on the contrary, M3, M4 and M5 apples represent the typical mealy apple. Therefore, sensorial attribute of IRP apples might cover many segments of general consumer's preference for apple.

Regarding to the market analysis, a very consistent part of respondents resulted to be clearly excited from all features of the novelty Italian Red Passion apple product, including the important component of curiosity about this unusual apple type. Others important aspects, emerged from the survey. For example, only few consumers (less than 20%) did not consider red color of flesh *per se* a predominant factor orienting their purchase decisions, rather a characteristic making the product unusual and so exciting to taste and purchase. Instead, the high nutraceutical and healthy value appear to be the major driver for consumers' preference, independently from age, gender and professional categories. On the other hand, a moderate percentage of consumers with scarce interest to product was somewhat expected, particular for consumers belonging to the older group of population, clearly more traditionalist and diffident towards novelty product in general. The indifference of the younger member of population, mainly teenager and students, was surprisingly; although the explanation could be associated to their general low interest on food quality. The innovative characteristics of IRP red-flesh apples make this product potentially able to open up new segments in apple market, although, the

successful introduction of this products requires the developing of a marketing strategy, not only focused to flesh red-color but also and above all to its higher nutritional values.

MOLECULAR ANALYSIS

1.19 TRANSCRIPT LEVEL OF STRUCTURAL GENE AND TRANSCRIPTION FACTORS REGULATING PHENYLPROPANOID AND FLAVONOID PATHWAYS IN APPLE FLESH TISSUE OF IRP LINES

Comparing phenotypic and biochemical data of the intensity and intensity and distribution red colour in peel and flesh tissues of fruits of IRP lines with their genetic background, we did not apparently detect strong association (*Table 8*). For example, C15 line, characterized by *mutMdMYB10/wtMdMYB10-3* alleles showed the highest intensity of flesh red colour and the lowest intensity of peel red colour; on the opposite, M3 line, characterized by *mutMdMYB10/wtMdMYB10-1* alleles, showed a very faintly coloration in flesh tissues but high intensity of peel red colour. Therefore, we analyzed expression pattern of *MdMYB10*, *MdbHLH3*, *MdbHLH33* and *MdWDR* genes (*Figure 21*) in apple flesh tissues, sampled at harvest maturity, in C2, C15, M5, M4 and C8 lines, and cv Annurca.

genotype	flesh red color	peel red color	MYB10 alleles
M3	*	***	mutMYB10 wtMYB10.1
M4	***	***	mutMYB10 wtMYB10.1
M5	**	**	mutMYB10 wtMYB10.3
C2	**	*	mutMYB10 wtMYB10.3
C8	-	**	wtMYB10.1 wtMYB10.2
C15	***	*	mutMYB10 wtMYB10.3
Annurca	-	***	wtMYB10.1 wtMYB10.2

Table 7. Allelic composition at MYB10 locus in IRP lines compared to an arbitrary scale of flesh and peel red colour intensity, derived from phenotypic and biochemical analysis.

Transcript levels of *MdMYB10* gene resulted to be highest in M4 and lowest in C15, while intermediate levels among the first two has been detected in flesh fruit of C2 and M5 lines (*Figure 21a*). As expected, *MdMYB10* resulted to almost undetectable in C8 line and cv Annurca, characterized by white flesh colour. In contrast, *MdbHLH3* transcripts resulted to be 3-fold higher in

C2 and C15 lines than cv Annurca, M5 and C8, while M4 showed only very low transcript level (*Figure 21b*). A similar expression pattern has been also observed for *MdbHLH33* gene, which resulted to be 2-fold higher in C2 and C15 lines than M4, M5, C8 and cv Annurca (*Figure 21c).* Differences have been found for the level of *MdWDR* transcripts among the fruits of all genotypes, and the highest levels of transcripts have been detected in fruit of C15 and M5 lines (*Figure 21d*).

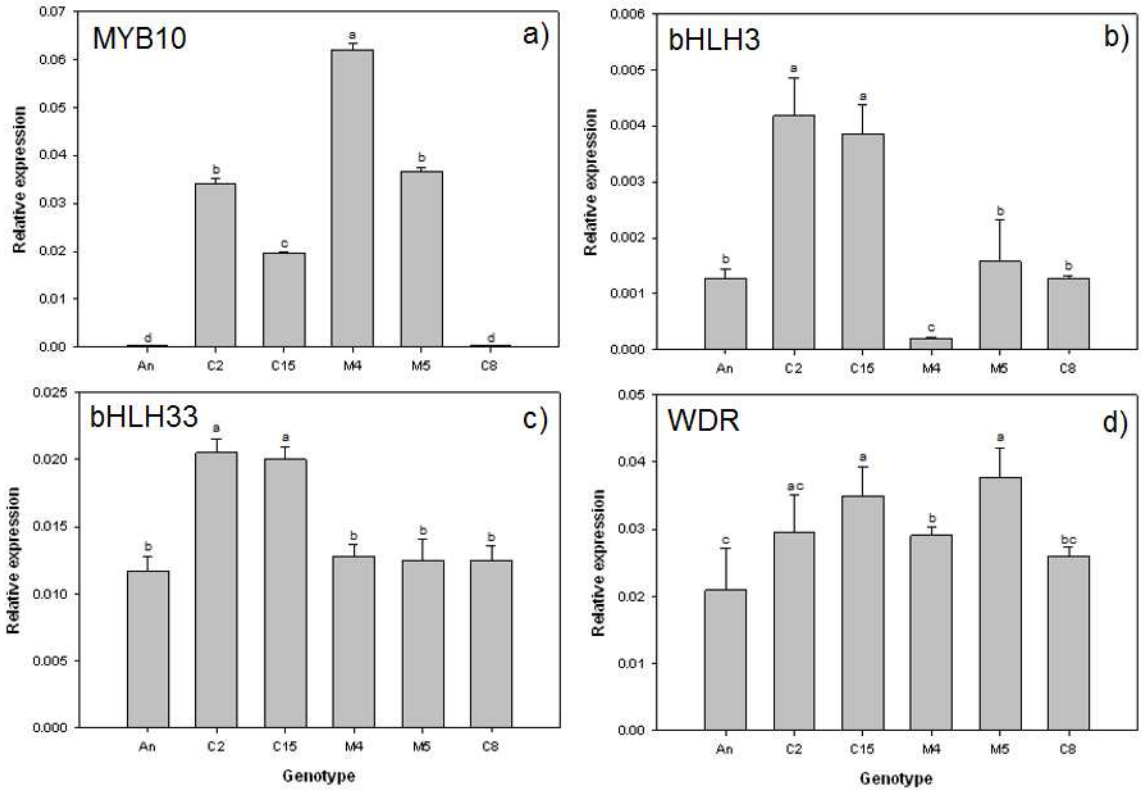

Figure 21. Expression pattern of MYB10, bHLH3, bHLH33 and WDR genes in flesh tissues of mature apple in IRP lines and cv Annurca. Histograms are the mean of three biological replication and bar represent the standard deviation. Letters indicate statistical significant difference at p < 0.01 (SNK test)

Moreover, to unravel whether the *wild type MdMYB10* allele contributes to the level of total amount of *MdMYB10* transcripts, we have tested this hypothesis through primers designed in the region located on 3rd exon, which includes a C/T SNP in position +555 from *ATG* site. At this position, *MdMYB10$_m$* is characterized by the presence of T nucleotides while all the three *wt MdMYB10* alleles are characterized by the presence of C nucleotide. The C/T SNP *situ* allow to employ quantitative high resolution melting analysis (qHRMA) to discriminate between the two types of alleles. However, this approach require standard amplicons to quantify allelic proportion. The amplicon composed by the single *MdMYB10$_m$* allele (100 %) has been obtained through digital PCR approach from DNA of M4 line, while the amplicon of the *wt MdMYB10* (100 %) has been obtained by amplification of the DNA from C8 line, which doesn't carry on the mutated allele. The two different standard fragments were

mixed in 1:1 ratio to simulate equal contribution of both *MdMYB10* alleles. HRMA analysis of *MdMYB10* amplicons (*Figure 22*) obtained by amplification from cDNA template of flesh tissues of M4, C15 and M5 apple lines has highlighted the presence of an identical melting peaks corresponding to 100% $MdMYB10_m$ allele. Thus, we conclude that *wt MdMYB10* did not affect global *MdMYB10* expression level.

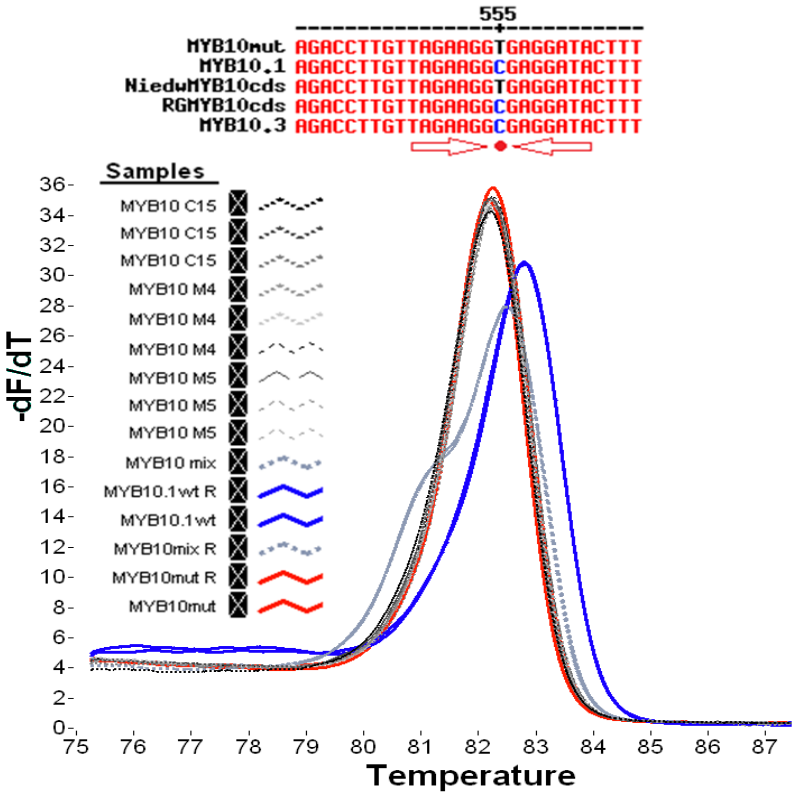

Figure 22. Qualitative detection of wtMYB10 alleles, to identify the composition of transcripts in the reddish flesh through qHRMA analysis in M4, M5 and C15 lines. Curves with single peak are the pure allele, while the other curves represent the derivate values of melting curve of mixed allele.

1.20 TRANSCRIPT LEVEL OF GENES CODING FOR STRUCTURAL ENZYME OF PHENYLPROPANOID AND FLAVONOID PATHWAYS IN APPLE FLESH TISSUE OF IRP LINES

Transcriptional regulation of gene coding for structural enzyme of phenylpropanoid pathways resulted to be differently regulated between fruits of IRP lines and cv Annurca (*Figure 23*).

The highest level of transcripts of *PAL* gene has been detected in M5 line flesh fruit, and a similar levels has been also detected in C8 and cv Annurca (F*igure 23a*). Compared to M5 line, in flesh fruit of C2 and C15 lines 2-fold less *PAL* transcript levels has been found, while in flesh fruit of M4 the levels *decreased to about* 4-fold. Cinnamate-4-hydroxylase (*C4H*), cinnamate-3-hydroxylase (*C3H*) and coumarate-4-ligase (*4CL*) transcripts, encoding early structural enzyme of phenylpropanoid pathway, resulted to be very similar in the amount in flesh fruits (*Figure 23b, c, d*). However, their levels resulted to be highest in all red-flesh IRP lines and less levels have been detected white-flesh C8

line and cv Annurca. Among the fruits of IRP lines, the highest transcript levels of *C4H* and *4CL* has been detected in C2 fruit of line, while the level of both transcripts genes did not result significantly different among the fruit of C15, M5 and M4 lines, except in the fruit of the last line where *4CL* transcript levels found did not differed from that of C8 line and cv Annurca. Instead, about 2-fold higher *C3H* transcript levels has been detected in C15 and M5 lines than C2 and M4. A very complex expression pattern has been detected for *HQT* gene (*Figure 23e*), encoding hydroxycinnamoyl-CoA quinate transferase, involved in chlorogenic acid biosynthesis. The highest transcript levels has been detected in flesh fruit of C15 lines, while HQT transcripts resulted 2-fold reduced in flesh fruit of C8 and cv Annurca, 4-fold reduce in C2 and M5 lines, and barely detectable in M4 line. The *PGT1* gene, coding for phloretin glucosyltransferase, the last step of phloridzin biosynthesis, resulted up-regulated in all IRP lines, including C8 and less regulated in flesh fruits of cv Annurca (*Figure 23f*). Moreover, C2 line showed the highest transcript levels. Very low transcript levels of chalcone synthase gene (*CHS*) were found in all IRP lines and cv Annurca, except in flesh fruit of M5 line (*Figure 23g*).

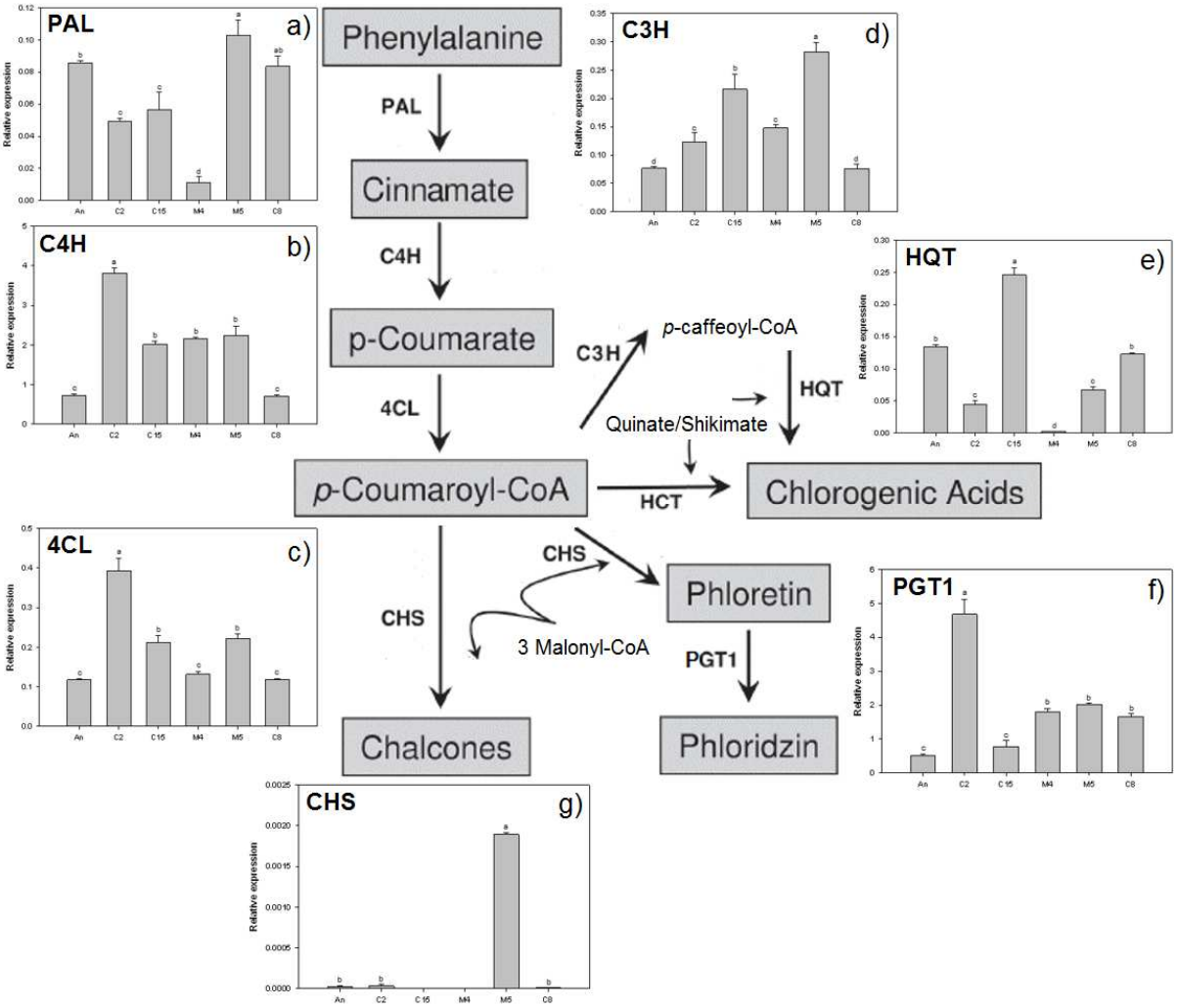

Figure 23. Expression pattern of genes coding structural enzyme of early phenylpropanoid pathways in IRP lines and cv Annurca. Histograms represent the average of three biological replications and bar represent the standard error. Different letters indicate statistical significant difference at p < 0.01 (SNK test)

Regarding transcriptional regulation of genes encoding structural downstream enzyme of flavonoid pathways, particularly for the biosynthesis of catechins and anthocyanins, important differences have been detected in flesh fruits among genotypes (*Figure 24*). A strongly induction of *DFR* and *LDOX* gene expression (*Figure 24b, d*) has been detected in IRP lines carry on *MdMYB10*$_m$ allele compared to that of C8 line and cv Annurca. Interesting, M5 line showed about 6-fold higher *DFR* and *LDOX* transcript levels than C2, C15 and M4. A similar trend has been observed for the pattern of *F3H* gene expression (*Figure 24a*), which resulted to be up-regulated in the four IRP lines and particularly in M5, altough the values of transcript levels resulted generally lower respect to *DFR* and *LDOX*. *UFGT* transcript levels resulted to be the higher in flesh fruit of C15 line and M4 lines, which are both characterized by the highest flesh anthocyanin content. On the contrary, except for M4 line, no relevant differences have been detected for *LAR1* transcript levels, suggesting that this gene is not target of the complex transcription factor with the MdMYB10*m* protein.

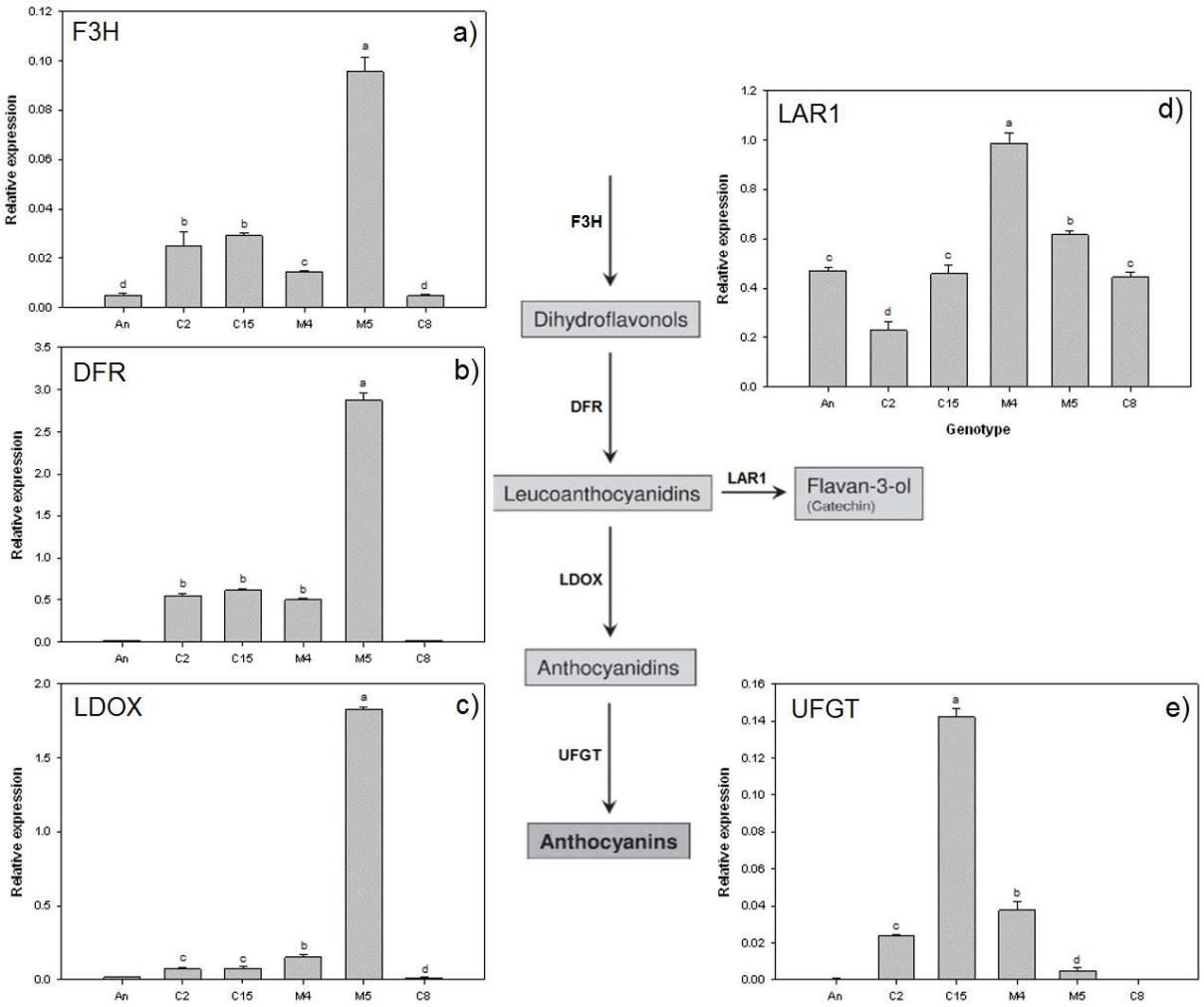

Figure 24. Expression pattern of genes coding structural enzyme of downstream flavonoid pathways in IRP lines and cv Annurca. Histogram represent the average of three biological replication and bar represents the standard error. Different letters indicate statistical differences at p < 0.01 (SNK test)

Transcript levels of *MdMYB1*0 gene, the master regulator of anthocyanin biosynthesis, resulted to be higher in peel of C2 and C15 lines compared to cv Annurca (*Figure 25b*). However, relative abundant of *Md*MYB10 transcript resulted uncorrelated with peel anthocyanin content, this last higher in cv Annurca compared both to C2 and C15 lines (*Figure 25a*). Instead, *MdUFGT* transcript levels appear more correlated with anthocyanin content, and resulted higher in cv Annurca (*Figure 25f*). As previously observed in flesh molecular analysis, transcripts level of MYB10 resulted strongly correlated with *MdDFR* one and, according to this, *MdDFR* transcripts level resulted higher in peel of C2 and C15 lines (*Figure 25e*). However, abundance of both *bHLH* transcripts (*Figure 25c, d*) was lower in peel of C2 and C15 lines, compared to cv Annurca, as observed even for *MdUFGT* transcript. Therefore, at least in peel, the accumulation of anthocyanins appear to be mainly depend from the transcript levels of *bHLH3* and *bHLH33*, both able to form a regulative complex with MYB10 protein.

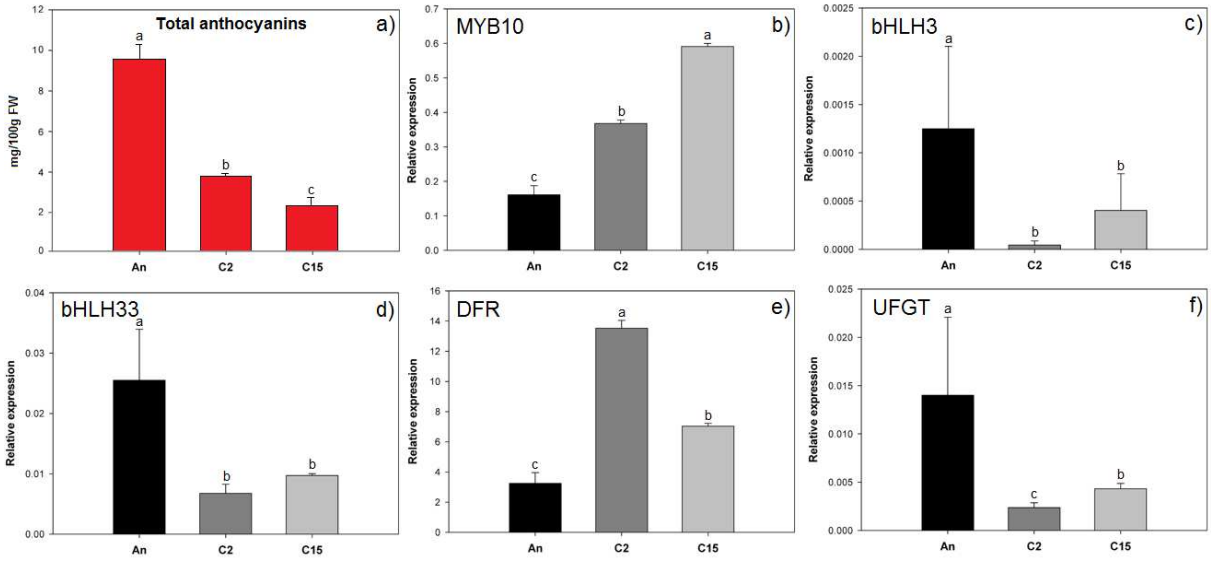

Figure 25. Anthocyanins content (a) and expression pattern of genes coding MdDFR and MdUFGT enzymes, and MYB/bHLH3/bHLH33 transcription factors, in peel tissue of C2, C15 and cv Annurca. Histograms are the mean of three biological replicates and bar represent standard deviation. Letters indicate statistical significant difference at p<0.01 (SNK test) for expression analysis and at p<0.05 (Duncan's test) for anthocyanins content.

1.21 MAIN PHENOLICS CONTENT OF C2 AND C15 'WHITE AND RED ISLANDS' COMPARED TO CV ANNURCA

Phenotypic observations highlights that the red on flesh apple fruit is not spread in all area. Indeed in the flesh the red area (red island) are surrounded by and/or adjacent to white area (white island) (*Figure 26*), which size and location varied depending from IRP line. Moreover, 'red islands'

appeared located in sub-epidermal tissues, central core and near vascular tissues, while 'white islands' appeared located in the internal part of flesh tissues. Thus, we analyzed phenolic composition of flesh white and red islands and peels of the two promising IRP lines, C2 and C15, which totalized the best overall enjoyment scores in panel test.

Total polyphenol content detected, expressed as mg GAE eq. /100g FW, did appear to be coherent with the type of island. In fact, in the red islands of C2 flesh line has been detected the highest content total polyphenol; on the contrary the highest value of total polyphenol in C15 flesh line has been detected in white islands (*Figure 26*).

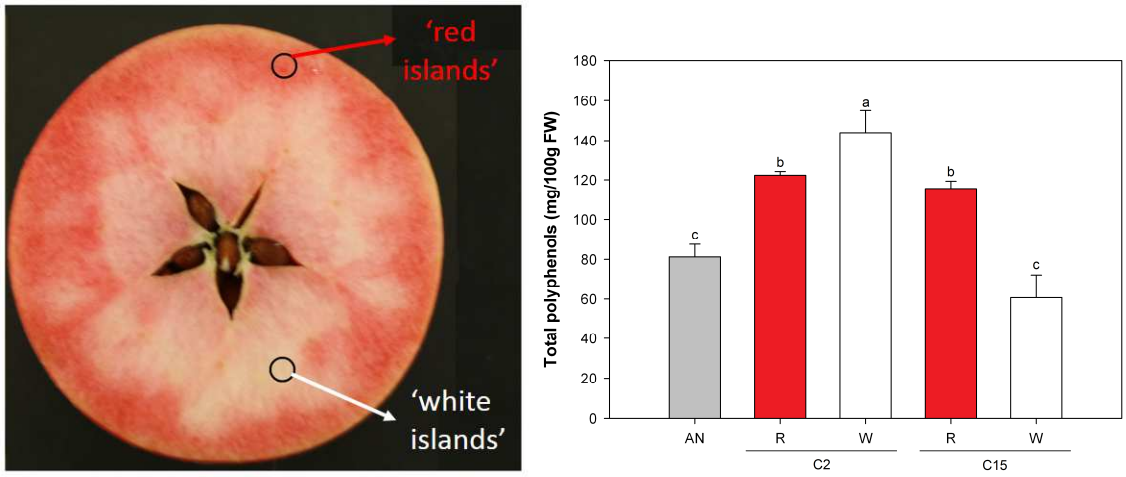

Figure 26. Total polyphenol content, expressed as mg GAE eq. /100g FW, in red and white islands of C2 and C15 IRP line compared to cv Annurca. Histograms are mean of three biological replications, bar represent standard error. Different letters indicate statistical significant difference at p < 0.05 (Duncan's test).

Important differences were found in phenolics content between white and red islands in both lines. The content of monomeric flavan-3-ols, such as epicatechins and total catechins (*Table 8*) resulted higher in the two IRP lines compared to cv Annurca, and the content resulted higher in white islands respect to the red ones, even if differences were more evident in C15 line. The same pattern was even observed for dimeric flavan-3-ols such as Procyanidin-B1 and –B2, altough for B2-type the differences was not statistically significative in C2 line. Interesting, a higher content of chlorogenic acid was found in white islands respect to the red ones and in both line. As expected, red islands had a higher content of cyanidin-3-galactoside, which resulted to be just detectable in white islands and cv Annurca. Regarding phloretin and phloridzin compounds, we found a higher content in red islands of C2 line, while, on the contrary, an higher content in white islands of C15 line.

Compound (mg/100g FW)	Genotype				
	Annurca	C2		C15	
		white islands	*red islands*	*white islands*	*red islands*
Hydroxycinnamic acids					
Chlorogenic acid	34.97±0.91 b	48.93±2.53 a	37.14±8.87 b	55.90±6.97 a	19.61±2.31 c
Dihydrochalcones					
Phloridzin	0.538±0.12 c	1.267±0.12 b	3.406±0.44 a	3.189±0.54 a	1.296±0.22 b
Phloretin xyloglucoside	0.902±0.22 a	0.017±0.002 d	0.790±0.09 a	0.254±0.04 b	0.079±0.01 c
Flavan-3-ols					
Procyanidin B1	2.801±0.55 a	2.092±0.41 b	1.810±0.39 b	2.492±0.43 a	0.592±0.18 c
Procyanidin B2	8.559±1.43 b	14.19±0.43 a	15.32±3.17 a	16.81±1.32 a	6.714±0.31 b
Catechin	1.481±0.64 c	6.724±0.50 a	6.268±0.77 a	6.559±0.98 a	2.290±0.22 b
Epicatechin	5.278±0.79 b	13.75±3.32 a	10.45±2.80 a	12.20±1.89 a	5.152±0.73 b
Total catechins	11.09±2.81 b	25.12±2.71 a	23.81±6.01 a	27.64±6.69 a	11.39±1.50 b
Flavonols					
Total Quercetins	n.d	n.d	n.d	n.d	n.d
Anthocyanins					
Cyanidin-3-galactoside	n.d	n.d	1.080±0.05 a	n.d	0.660±0.02 b
Cyanidin-diglucoside	n.d	n.d	n.d	n.d	n.d

Table 8. Main apple flesh phenolics compounds concentration, expressed in mg/100g FW, detected in flesh red and white islands of C2 and C15 lines compared to cv Annurca. Histogram represent mean values and standard deviation of three biological replicates. Different letters indicate statistical significant difference at $p < 0.05$ (Duncan's test).

1.22 MOLECULAR ANALYSIS OF RED AND WHITE ISLANDS

To assess the role of genes that coding for transcription factor proteins (*Figure 28*) and the structural enzymes (*Figure 27*) involved in flavonoid biosynthesis on the polyphenols composition of white and *red islands*, transcriptional regulation studies have been performed by Real-Time in the fruits of both lines.

Transcript levels of *DFR* gene, the main target of MdMYB10 transcription factor protein, resulted to be highest in *red islands* of flesh of both lines, and faintly detectable transcripts have been found in flesh of cv Annurca (*Figure 27a*). An analogous trend has been also observed for the expression of *LDOX* gene (*Figure 27b*), although in the *red islands* of flesh fruits of C15 line 2-fold quantity of transcripts resulted to be present compared to that of C2 line. *UFGT* transcript levels (*Figure 27c*) resulted to be very low in cv Annurca, and, surprisingly, no significant differences have been found

between white and *red islands* of C2 and C15 line. However, overall in the fruits of the last line 3-fold higher transcript levels have been found respect to C2. Noteworthy, *LAR1* gene transcripts (*Figure 27d*), involved in catechins biosynthesis, resulted higher in *white islands* than *red islands* in fruits of C2 and C15 lines; anyway, generally less transcript levels of this gene have been found in cv Annurca. In the last genotype, the observed *ANR* gene expression (*Figure 27e*), involved in epicatechins biosynthesis, resulted to be up regulated significant more than that observed in *red islands* of flesh fruits of C2 and C15 lines, and higher that that observed in the *white islands* of the same IRP lines.

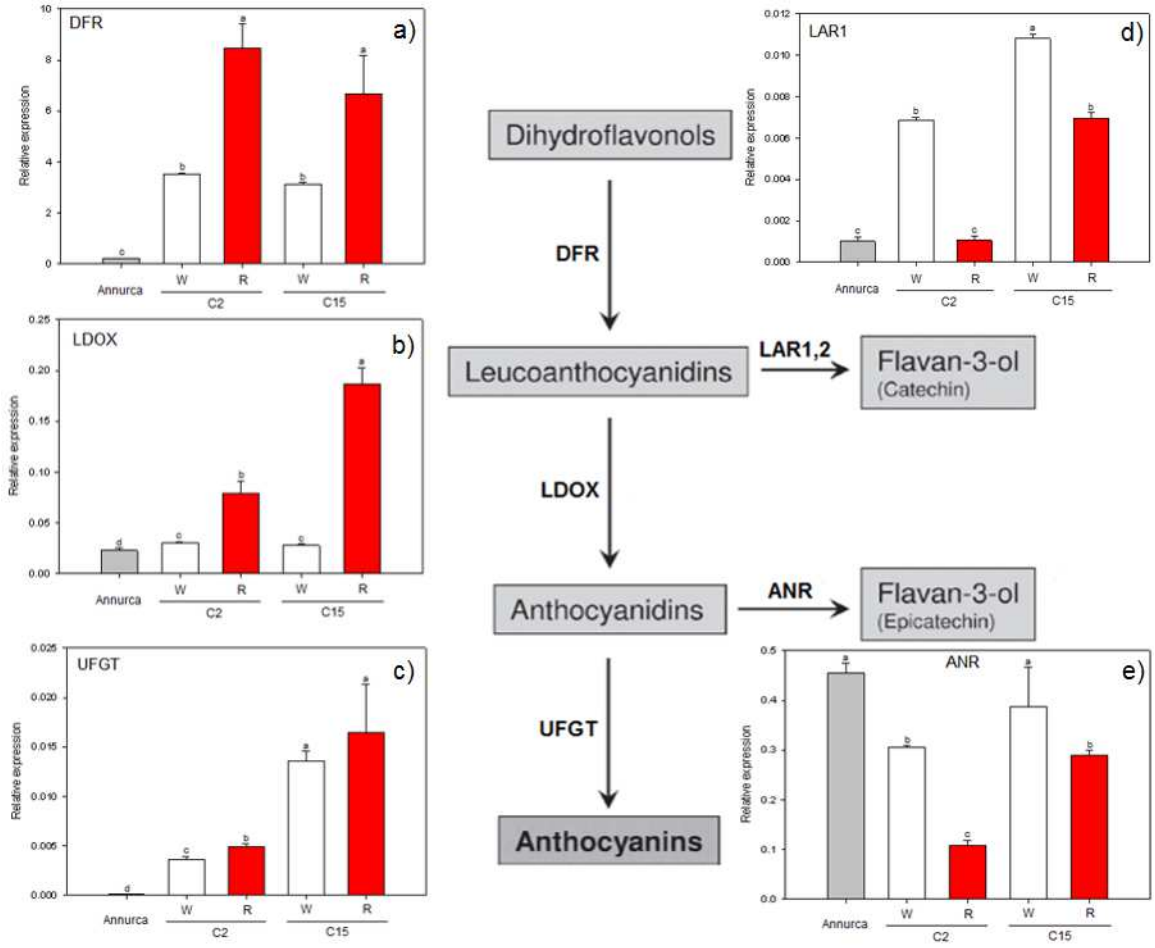

Figure 27. Expression pattern of genes coding structural enzyme of flavonoid pathway in flesh red and white islands of C2 and C15 lines, and cv Annurca. Histograms are the mean of three biological replications and bar represent standard error. Different letters indicate statistical significant difference at p < 0.01 (SNK test)

The highest transcripts levels of *DFR* and *LDOX* genes may be correlated with up-regulation of the *MdMYB10$_m$* gene (*Figure 28a*) detected in red islands of C2 and C15 lines, while the transcript of this gene resulted to be undetectable in cv Annurca. A similar trend of the previous gene was observed for *MdbHLH33* transcript levels (*Figure 28c*) in *red islands*, which resulted to be reduced in the *white islands*, and a reduce levels of this gene has been also detected in cv Annurca. On the opposite, no significant differences have been detected for *MdbHLH3* (*Figure 28b*) transcript levels between *white*

and *red islands*, and between the previous lines and cv Annurca. The transcripts levels of *MdWDR* gene fond in the *white islands* of C15 line resulted to be the lowest, while the highest has been found in the cv Annurca. Although, less content of transcripts has been found in the *red islands* of C2 and C15 lines, however their values did not resulted to be significant different from that of Annurca (*Figure 28d*). In the *white island* of flesh fruit of C2 line a high variability levels of transcripts has been detected in the biological replications, so that no significant differences resulted between this fruit samples and all other ones.

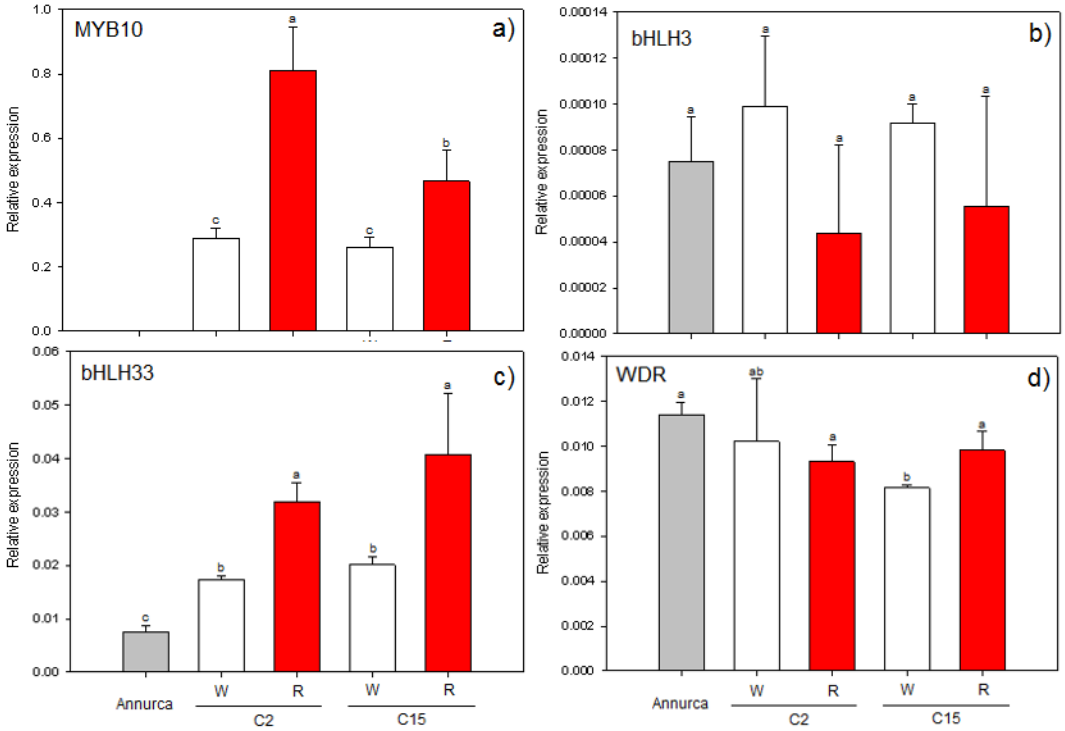

Figure 28. Expression pattern of genes coding transcription factors regulating anthocyanins biosynthesis in flesh red and white islands of C2 and C15 lines, and cv Annurca. Histograms are the mean of three biological replications and bar represent standard error. Different letters indicate statistical significant difference at p < 0.01 (SNK test)

1.23 EPIGENETIC REGULATION OF MYB TRANSCRIPTION FACTORS OF POLYPHENOL PATHWAY

The possible role of epigenetic regulation system has been also evaluated in the specific context of *MdMYB* genes. In particular, the expression level of *mdo-miR858* has been evaluated, since this miRNA is involved in the regulation of high number *MdMYB* apple target (Xia et al., 2012), including MYBs putatively involved in flavan-3-ols biosynthesis, as for example *MdMYB9*, belonging to Arabidopsis *AtTT2* clade. In Arabidopsis, *AtTT2* regulates structural enzymes such as *AtLAR1*. A bioinformatic analysis has been performed to verify if *mdo-miR858* might target other specific apple MYBs, such as *MdMYB10*, *MdMYB12* and *MdMYB16*, this two last belonging to Arabidopsis MYB5 and MYB4 clades, respectively. In particular, *AtMYB5* and its grape orthologs *VvMYB5*, are general

regulator of flavonoid pathways. Instead, the MYB4 clade is composed by C2-repressor domain proteins, involved in the repression of anthocyanin biosynthesis (Jin et al., 2000). As reported in *Figure 29*, the *mdo-miR858* did not show general high level of sequence identity with their MYB target. For example, *MdMYB9*, a validated *mdo-miR858* target, show only 17/21 identical nucleotides (nt). The *miR858:MYB* identity is only slighty lower in *MdMYB12* (16/21 nt), *MdMYB16* (15/21 nt) and *MdMYB10* (15/21 nt). Therefore, we analyzed transcripts level of *mdo-miR858*, the validate target *MdMYB9* and the putative target *MdMYB12* and *MdMYB16* in white and red flesh islands of C2 and C15 apple. Expression pattern of *MdMYB10*, as well as main gene coding for structural enzymes, have been already described in the previous *paragraph 1.25*.

	miRNA:mRNA alignment		identity
	Mdo-miR858	3′-UCAGGUCGAACAGACAACGAA-5′	
(MDP0000125457)	MdMYB12	5′-CCAGGUCGUACGGACAAUGAG-3′	16/21
(MDP0000950559)	MdMYB16	5′-CCUGGAAGAACAGACAAUGAG-3′	15/21
(MDP0000210851)	MdMYB9	5'-CCGGGGCGAACAGACAAUGAA-3'	17/21*
(MDP0000574942)	MdMYB10	5'-CCAGGAAGAACAGACAAAGCU-3'	15/21

*Figure 29. Results of bioinformatic analysis of putative apple MYBs target of mdo-miR858. NCBI accession number for MYB genes are the follow: MdMYB16 (HM122617.1), MdMYB9 (DQ267900.1), MdMYB12 (HM122616.1)*validate by degradome sequencing (Xia et al., 2012).*

The *mdo-miR858* resulted more expressed in red islands compared to the white ones and in both C2 and C15 lines, altough it was expressed at comparable level also in cv Annurca (*Figure 30a*). Interesting, high *mdo-miR858* transcripts level is associated to low level of *MdMYB16* in red islands of both C2 and C15 line (*Figure 30c*), while *MdMYB12* (*Figure 30b*) and *MdMYB10* seems to not be related with *mdo-miR858* transcript level. Controversial are the results for *MdMYB9*, a validated *mdo-miR858* target. Low transcript level of *MdMYB9* are associated to high *mdo-miR858* level only in C2 flesh, while only little differences have been found in C15 flesh.

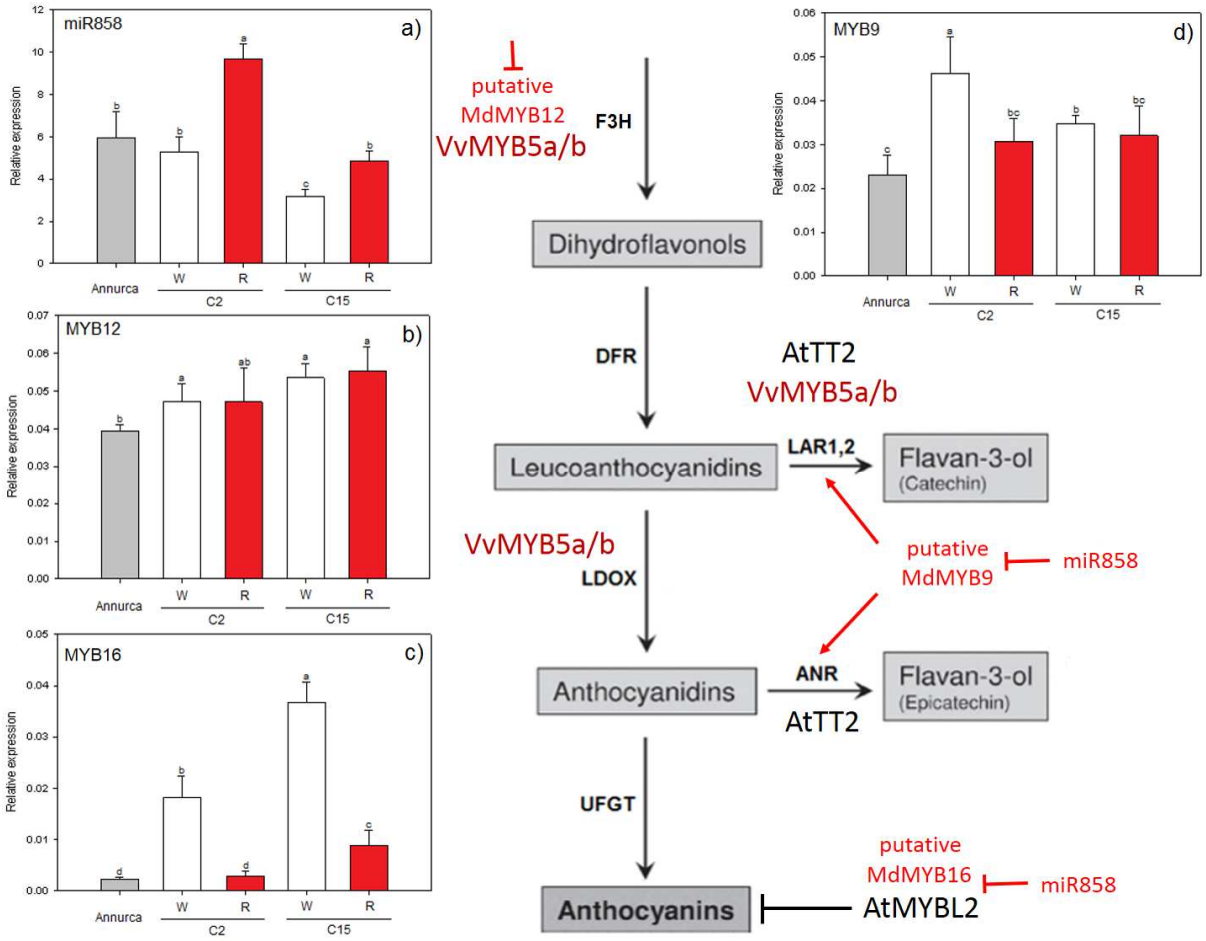

Figure 30. Expression pattern of mdo-miR858 and MdMYB9, MdMYB12, MdMYB16 transcription factors in red and white islands of C2 and C15 apple flesh, and cv Annurca. Histograms are the mean of three biological replicates and bar represent standard error. Letters indicate statistical significant difference for p<0.01 (SNK test).

1 DISCUSSION

Plant of IRP apple lines produce functional food and, meantime, are an important scientific tool for the comprehension of genetic and biochemical mechanism regulating the anabolism, catabolism and accumulation of phenolic compounds in all tissues of apple fruit. Molecular analysis confirm that IRP lines belonging to type I red-flesh apple group, except C8 line. These lines are characterized by the microsatellite insertion in *MdMYB10* promoter region, which confers trans-activation of *MdMYB10* itself (Espley et al., 2007), inducing the activation of structural genes that in the ultimate leading to anthocyanins accumulation in many organs and tissues, including apple flesh. Although, M3, M4, M5 and C2 red-flesh apple lines present the same mutated $MdMYB10_m$ allele, however, they differed regarding total anthocyanins accumulation exclusively in flesh and probably in peel tissues.

In flesh tissues, the intensity and localization of red pigmentation is diverse inside of each single fruit and among the fruit of the lines. Apples of C15 line accumulate the highest amount of anthocyanin in flesh, with red coloration diffuses in external and internal cortex (flesh) tissues, and

central core. Apples of M3 line accumulate the lowest anthocyanin amount in cortex tissues, mainly located in central core and in peel, where the highest amount was detected. Moreover, apples of M4 line accumulate high amount of anthocyanins in both flesh and peel. Therefore, the presence of the *MdMYB10*$_m$ single mutation alone seems to be not able to explain the different apple phenotypes of IRP lines. Although anthocyanins accumulation are extensively regulated by environmental factors, such as light and temperature (Lin-Wang et al., 2010), however, the observed phenotype is only under genetic control. The extension and intensity of the phenotype appear to be regulate by environmental and physiological internal factors.

The transcriptional analysis of many genes encoding structural genes of flavonoid pathways demonstrated wide difference among the mutated M3, M4, M5, C2 and C15 IRP apple lines, when compared to Annurca and C8 line. In agreement with results obtained by Espley et al. (2007), a general strongly up-regulation of *MdDFR* gene, encoding dihydroflavonol reductase enzyme, was observed in IRP lines. In addition, the expression of the others downstream genes (*MdUFGT*, *MdF3H* and *MdLDOX*) of flavonoid pathway resulted to be higher expressed when compared to cv Annurca e C8 line.

It is remarkable the results obtained from the expression analysis of gene activated upstream of phenylpropanoid pathway that never have studied before, in any of the red flesh mutated apple. *MdC3H*, *MdC4H*, *Md4CL*, coding all for enzyme that produce the substrate for flavonoid compounds resulted up regulated in all red flesh IRP lines. This result seems to be coherent with anthocyanin accumulation and it is coherent with the high accumulation of total polyphenols, as it was detected in all fruits of IRP lines. We have also found that lateral branches of the pathway would seem to be more up-regulate. Indeed, *MdHQT* gene, which enzyme play a pivotal role in the synthesis of phenolics acids, resulted more up-regulate in some IRPs lines, as well as, MdPGT1 gene, which enzyme play a pivotal role in the synthesis of phloridzin, resulted more up-regulate even in C8 line, a white flesh IRP line.

The MdMYB10 protein play a role of transcription factors only when is liked to others two proteins, WDR and bHLH, to form MBW complex. Therefore a direct relation between level of transcript of *MdMYB10*$_m$ and others structural functional genes might be dependent on the concomitant expression of the genes of the other two transcription factors (Cocciolone and Cone, 1993; Zhang et al., 2003). We have studied the gene expression of *MdbHLH3*, *MdbHLH33* and *MdWDR*, coding the bHLH3, bHLH33 and WDR, and relevant differences were detected in flesh tissue of IRP apple, suggesting they might be differently involved in the regulation pattern observed for many genes of flavonoid pathway. In particular, *MdbHLH33* gene resulted strongly up regulated compared to *MdbHLH3* genes, this last reported by Espley et al. (2007) as the main MYB10 cofactors for activating anthocyanins structural genes. Therefore, the different expression of *MdbHLH3* and *MdbHLH33* genes between IRP apples might indicate a functional diversity not directly associated with the mutation found the promoter of *MdMYB10* gene. However, it is not possible to exclude that a different

maturation stage reached by fruit could affect expression of genes, independently from the accumulation of anthocyanin and/or total polyphenol. In fact, the commercial ripening stage of fruit is different among the genotypes studied.

Anthocyanin accumulation in flesh and peel appear independent, suggesting that *MdMYB10*$_m$ is regulate in its transcription in a tissue-specific manner. In apple peel, as demonstrated by Takos et al. (2006), *wt MdMYB10* allele strong influence the coloration pattern. In peel of IRP apples, C2, M5 and C15 line carry on the *MdMYB10-3* allele, similar to *MYB1-3* allele, which characterized no-red peel apple cultivars. In contrast, M4 and M3 carry on *MdMYB10-1/2* alleles, similar to *MYB1-1/2* alleles that characterized red peel cultivars. As expected from the genetic background, M3 and M4 have shown an almost uniform red-colored peel and the colorimetric analysis assign to the fruit of both lines the highest and uniform coloration. More complex appears the peel coloration pattern in M5, C2 and C15 fruits. The detection of anthocyanin amount in the fruit peel of M5, although resulted different from M3 and M4, its trend appear more similar to the last lines respect to C2 and C15 lines. In the fruit peel of the last two lines, a half amount of anthocyanins was detected. These data were confirmed by the colorimetric determinations.

Although, among the IRP lines in the fruits of C2 and C15 the peel coloration appeared reduced respect to that observed in cv Annurca, but the expression of *MdMYB10* alleles (wt type form plus *MdMYB10*$_m$ form) in the former lines resulted 2 to 3-fold higher compared to Annurca. In contrast, a very low gene expression level was detected for *bHLH3* and *bHLH33* in the two IRP lines. As consequence of this different expression pathway might the assembling of the MBW–complex, as could be supposed by the strong down regulation of *MdUFGT* found in C2 and C15

The fundamental role played by MYB10 cofactors such as bHLH and/or WDR proteins is further highlight by the transcriptional analysis of their genes in red and white flesh islands of C2 and C15 line. HPLC analysis revealed the presence of cyanidin only in the red islands and a higher content of flavan-3-ols in the white islands. Transcripts level of *MdMYB10* and *MdDFR* resulted highest in red islands, and low expression level of *MdbHLH33* resulted in white islands. Thus, bHLH33 might be the limiting factors for the activation of *MdDFR* gene, because no significant differences have found for *MdbHLH3,* leading so to anthocyanins biosynthesis. In the case of apples of C2 and C15, *MdUFGT* gene could be not limiting for anthocyanins biosynthesis, as no significative differences between red and white islands were detectable. Altough, some differences were found regarding WDR transcripts (Brueggerman et al., 2010), however, in our studies, the protein appears to play any constricting role in the regulation of anthocyanins biosynthesis.

Further study will be required and evidences in this work came from the role that are played by microRNAs, such as *mdo-miR858*, in the regulation of *MdMYB* genes, because they might regulate both general and specific branches of flavonoid pathway (Xia et al., 2012). In particular, the specific targets played by MYB transcriptional repressor are currently unknown in apple fruit. Transcript levels observed of *mdo-miR858* resulted to be consistent with its putative function in the negative regulation

of *MdMYB16*. Altough, the function of *MdMYB16* is currently unknown in apple, its sequence homology give support to the function similarity with other well-characterized negative regulator of anthocyanins biosynthesis (Matsui et al., 2008). We suggest that *mdo-miR858* play a role in determining the formation of white islands, maybe down-regulating anthocyanins biosynthetic genes and up-regulating those for flavan-3-ols.

1 CONCLUSION AND PERSPECTIVE

In this research, we demonstrate that apples fruits of lines of Italian Red Passion group possess the characteristics to be an excellent functional food, due to their high nutraceutical value. The increased polyphenols content, compared to the other commercial cultivars, is not associated with reduced organoleptic qualities, as resulted by sensorial and market analyses. Consumers have manifested a good propensity to taste and purchase red-fleshed apples of IRP group. Molecular studies about transcriptional regulation of many genes encoding structural enzyme and transcription factors demonstrates the complexity of flavonoid biosynthesis pathway in apple, and the needs to explore genetic factors other than *MdMYB10*, such as *bHLH* and/or *WDR*, and to unravel the role of epigenetic regulators such as *mdo-miR858* and its *MdMYB* target. The better comprehension of the regulative network regulating not only anthocyanins biosynthesis but also general phenolics content might improve the selection of apple plant able to satisfy consumer's preferences and at the same time to give them the health benefits of a functional food.

Section II

Color development in olive fruit

2. STATE-OF-THE-ART

Olive is one of the most important fruit cultivated in Mediterranean areas, particularly in Italy, where it is cultivated over 1.1 million hectares. The Italian olive production is directed towards mainly to extra virgin olive oil and table olive.

Olive drupe is mainly composed by water (50-70% of fresh weight), lipids (16-25%), carbohydrates (15-20%) and fiber (5-6%). The minor fraction, also known as the unsaponifiable, is composed by pigments, such as chlorophylls and carotenoids, phenolic compounds (secoiridoids and flavonoids, prevalently), terpenes and tocopherols. In particular, main phenolic compounds present in olives, conventionally characterized as 'polyphenols', belong to the class phenolic acids, lignans, flavonoids and secoiridoids.

2.1 OLIVE FRUIT DEVELOPMENT AND RIPENING

According to the botanical classification, olive fruit is a drupe composed by pericarp (skin), which represent about 1.5-3.5% of fresh weight, mesocarp (pulp) representing about 70-80% and endocarp (pit), which enclosed seed, representing about 15-25% of drupe fresh weight. Percentage of the three different drupe tissues ranged depending from cultivars and environmental condition. Olive fruit growth have shown the typical double-sigmoid pattern and comprised 5 developmental stages (Conde et al., 2008):

- fertilization and fruit set (I)
- seed development (II)
- pit hardening (III)
- mesocarp development (IV)
- ripening (V)

Ripening stage is the major factor influencing olive oil quality, and could be further divided into 4 stages: 1) green maturation stage, 2) pericarp color change 3) ripening stage and 4) over-ripening stage. In the first phase, fruits are green and firm, are photosynthetically active, their content of soluble sugars reaches its maximum values and tocopherols and phenolic could be found in high concentrations. When fruit colour shades off into yellowish-green due to changes in pigment profiles (mainly chlorophyll breakdown) the second phase (pericarp color change) starts, photosynthesis slows down and small purplish spots appear on fruits' surface due to the accumulation of anthocyanins in the pericarp; in the third phase, consisting of the actual ripening, drupes reach their maximum size and oil content. In the last phase, which is over-ripening, fruits lose water and chemical reactions that can worsen oil quality take place (e.g. lipolysis, aldehydes and tocopherols degradation).

2.2 TEXTURAL CHANGES IN RIPENING OLIVES

Olive ripening is associated with a change of texture that results in drupes softening. The loss of fruit firmness is the result of enzymatic activities involved in the degradation of structural cell wall polysaccharides (reviewed by Prasanna et al., 2007) such as pectins, cellulose, hemicellulose and lignin. The two enzymes mainly involved in these processes are glycanases, such as polygalacturonase (PG) and pectin methyl esterase (PME or PE). PG enzymes causes a hydrolysis of polygalacturonic acid, whilst PME removes methoxyl groups from methylated pectin determining a release of methanol. Among the other enzymes involved in cell wall loosening, b-galactosidase, a glycosidase, is responsible for the degradation of both pectic and hemicellulosic components and is likely related to late-ripening events (Prasanna *et al.*, 2007). In olive it has been demonstrated that the major changes in drupe texture in the transition between green and purple fruits are driven by the solubilization of homogalacturonans, a fraction of pectic polysaccharides, and the decrease of tightly bound hemicelluloses. In the transition between purple and black stages, cell wall modifications are caused primarily by a decrease of hemicelluloses and cellulose, and only secondly by changes in the pectic fraction consisting of release of rhamnogalacturonan. In this ripening stage a high endoglucanase activity is observed, involved in hemicelluloses and cellulose degradation (Jiménez et al., 2001a). An increase in hemicellulose-related sugars, such as xylose, mannose, galactose, and glucose, is observed in the last phases of olive ripening (Jiménez et al., 2001b).

2.3 PIGMENTS IN OLIVE FRUITS

The quantity and quality of pigments found in fruits depend on different factors, among which developmental and ripening stages are of primary importance. As stated before, olive fruits undergoes a colour shift during ripening, and this variation is due mainly to a change in ratio and quality of pigments found in the drupes. When the ripening process progresses, photosynthetic activity of olive drupes decreases in parallel with the decrease of chlorophyll and carotenoid content, followed by the appearance of anthocyanins that confer the fruits the typical purple and violet colors. The latter are anyway water-soluble pigments, so they do not give any contribution to virgin olive oil colour. Chlorophylls and carotenoids are soluble in lipids and have been studied historically for their contribution to oil colour, but scientific interest is lately raising because these compounds may be considered quality markers since they are present in stoichiometric ratios due to their functions in photosynthetic membranes (Aparicio-Ruiz *et al.*, 2009). Moreover, these compounds can have nutraceutical and functional properties since β-carotene is a precursor of vitamin A, whilst chlorophylls can protect oils form oxidative processes together with phenols if oils are stored in darkness, but may work as pro-oxidants if oils are stored in daylight (Cimato *et al.*, 2001). A study has been carried out on Arbequina and Farga cultivars with the purpose of monitoring chlorophyllase

activity and the general pigment profile (Criado *et al.*, 2006). Chlorophyllase is the enzyme involved in the hydrolysis of the ester bond between chlorophillide and phytol, but it still unclear if this enzyme is involved only in catabolism or also in pigments biosynthesis (Criado et al., 2006). This study pointed out that the main pigments were chlorophyll *a* and *b*, and the carotenoids neoxanthin, violaxanthin, lutein, antheraxanthin, and trans-b-carotene, were presents with slight differences between the two cultivars, although and strong decrement was appeared with the ripening. In drupes of Arbequina, chlorophyllase activity decreased during ripening, and then slightly increased in the last stages. Moreover, in Arbequina drupes an unusual pigment biochemistry pathways was observed, in fact, the carotenogenesis occurs together with the synthesis of anthocyanins in the last ripening stages (Roca and Mínguez-Mosquera, 2001), and the synthesis of esterified xanthophylls was observed in the turning stage (Criado *et al.*, 2007).

2.4 CHANGES IN THE PHENOLIC PROFILE

It is well known that during the ripening process occurs a decrease in the phenolic content in olive fruits. It has been stated that the content of oleuropein increases steadily during early stages of olive fruit growth in cultivars Lucques, Salonenque and Picholine (Amiot *et al.*, 1986), reaching a maximum between the end of August and the beginning of September (depending on cultivar) and then it sharply decreases in the subsequent stages. In young fruits, oleuropein can reach 14% of the dry matter, decreasing to 3-6% before the purple stage. It has been also pointed out that this decrease is not caused by a dilution effect during fruit growth. The authors have deduced that oleuropein could be reused biochemistry events occurring during ripening, since no degradation compounds could be found in the studied samples. Rotondi et al. (2004) have observed a clear decrease in phenols in Nostrana di Brisighella cultivar during ripening. Recently, Alagna et al. (2012) evaluated the accumulation profile of phenolic compounds during different stage of olive fruit development in many typical Italian cultivars. Authors found a trend of decrement of phenols accumulation during drupe development, both in ‘high phenols’ and ‘low phenols’ cultivar.

2.5 EVALUATION OF FRUIT RIPENING

The evaluation of optimum harvest period is crucial for superior-quality olive oil production, since olive drupe ripening degree strongly affect many physiological processes, including texture and colour changes, regulation of enzymatic pathways, oil accumulation, and evolution of the phenolic profiles. Therefore, the evaluation of olive fruit ripening is a paramount of importance and should be executed in an objective, easy, and repeatable way. The scientific community has tried to evaluate ripening stages in many different ways, designing ripening indices with the purpose of finding the best balance between oil quantity, for its obvious economic importance, and oil quality. One of the most known and used ripening indices is the so-called Jaén or Ripening Index (RI), proposed by Uceda and Frías (1975). This index can be calculated dividing olive into color classes, each characterized by a different

score (0-7) and calculating the mean score of a pool of 100 picking olives. The authors established that a RI of 3.5 is the best harvesting period, even if this value has a geographical dependent meaning and cannot therefore be easily applied everywhere. Moreover, a strong dependence on fruit yield and cultivar has been demonstrated by Dag et al. (2011), highlighting that this index can be useful for a quick and easy evaluation of ripening, but also that many other factors have to be taken into account if the best results in production and quality must be achieved. Drupes colour has been used as a ripening marker also by Yousfi *et al.* (2006), considering the colorimetric spectra of fruit according to the CIE *L*a*b** system. These parameters have been used by the authors to calculate a colour index (CI) that has been also useful to evaluate table degreening drupe. Roca et al. (2001) proposed to use chlorophyll/carotenoid ratio as ripening marker, since chlorophylls and carotenoids showed a decreasing trend along fruit maturation. Loss of fruit firmness, a phenomenon that occurs in ripening fleshy fruits due to structural changes in cell wall polysaccharides, has been evaluated throughout olive ripening by some authors, such as García et al. (1996), showing a ripening-dependent trend. Cherubini *et al.* (2009) used sugar concentration in drupes as a ripening marker, and it gave interesting results since it was reproducible, objective, and correlated to oil content.

2.6 SECOIRIDOIDS AND PHENOLICS ACIDS

Secoiridoids are a class of compounds specific of *Oleaceae* family and composed by oleuropein, ligustroside, demethyloleuropein and nuzhenide. Oleuropein and ligustroside, the most important olive phenolic compounds, are the esters of elenolic acid with hydroxytyrosol (3,4-DHPEA) and tyrosol (*p*HPEA), respectively, that are further hydroxylated and glycosylated (Servili et al., 2002). Hydroxytyrosol can be further present as simple phenolic acids or as part verbascoside molecule, a phenylethanoid (Servili et al. 1999). Other phenolic acids are also present in olives, including caffeic, vanillic, syringic, and p-coumaric (Montedoro, 1972). Biosynthetic steps leading to formation of the terpenic and phenolic portions of secoiridoids are still not clarified in olive, despite many putative transcript encoding structural enzymes have been identified (Alagna et al., 2012). Feeding experiments on *Syringa* and *Fraxinus* (other genera within the *Oleaceae* family) showed that the biosynthesis of oleoside-type secoiridoids proceeds via iridodial, converted to deoxyloganic acid aglycone or to 7-epi-loganic acid to 7-ketologanic by unknown NADH-dehydrogenase. Glucosyltransferase enzymes are required to transfer glucosylic groups to deoxyloganic aglycones for the formation of deoxyloganic acid, the conversion of oleoside 11-methyl ester to 7-ß-1-D-glucopyranosyl 11-methyloleoside and the formation of oleuropein from oleuropein aglycone, which is the last step of the pathway. The position of 3,4-DHPEA-EDA along the secoiridoid pathway remains controversial. It has been considered either as a derivative of oleuropein, produced by its enzymatic degradation by endogenous β-glucosidases (Servili et al., 2002) or as the intermediate compound of an alternative biosynthetic pathway leading to oleuropein formation (Obied et al., 2008; Ryan et al., 2002). In *O. europaea* both epoxides of secologanin and secoxyloganin could be precursors of oleuropein (Chiou et al., 2012). The

methylation of 7-ketologanic acid might be catalyzed by an enzyme similar to loganic acid Omethyltransferase (LAMT), which converts loganic acid to loganin (epimers of 7-ketologanic acid and 7-ketologanin, respectively), as indicated by the functional characterization in *C. roseus* (Murata et al., 2008).

2.7 LIGNANS

Lignans are phenylpropanoid dimers in which the phenylpropane units are linked by the central carbons of the side chains. In particular, pinoresinol and 1-acetoxypinoresinol, represented the most important lignans in olive oil, ranging from 0.04-0.99 and 0.02-3.62 µg/100g FW, respectively (Phenol Explorer database). Enzymes involved in pinoresinol and 1-acetoxypinoresionol in olive are unknown. However, some of the enzymes involved in their biosynthesis have been elucidated in other species, including *Forsythia x intermedia*, belonging to *Oleaceae* family. Biosynthesis originates from phenylpropanoid pathways and involve many enzymes of lignin biosynthesis pathways. In particular, pinoresinol derived the stereospecific coupling of two units coniferyl alcohol in the presence of a dirigent protein (DIR), then further metabolized by certain biosynthetic enzymes, resulting in a high level of structural diversity of lignans molecules (Davin and Lewis 2003).

2.8 FLAVONOIDS

Olive fruit contain an appreciable amount of flavonoids, mainly flavones, flavonols and anthocyanins. Among the class of flavones, luteolin, luteolin-7-glucoside and apigenin-7-glucoside are the most important compounds in olive, ranging 0.1-7.4, 0.5-29 and 0.6-18 mg/100g FW as reported by Romani et al. (1999). These compounds were also found in olive oils, as reported by many authors (Carrasco-Pancorbo et al., 2006; Brenes et al., 1999; Murkovic et al., 2004). The compound quercetin-3-rutinoside, also known as rutin, represent the most abundant olive flavonols, ranging from 11.12-78.70 mg/100g FW (Phenol Explorer). Cyanidin glycosides, in particular cyanidin-3-rutinoside (Romani et al., 1999) are the main anthocyanins in olive. The main enzymes (and gene coding for) of flavonoids pathways, particularly those involved in anthocyanin biosynthesis, have been well elucidated in several fruit species and has been previously described (see section I). In olive fruit, Martinelli and Tonutti (2012), analyzing expression pattern of genes coding for enzymes involved in anthocyanins biosynthesis pathway during olive drupe development, observed an increasing expression of DFR and ANS genes during olive ripening, concomitantly with increase of anthocyanins content. Interesting, UFGT gene, involved in anthocyanidin glycosylation, the last step in anthocyanins biosynthesis, resulted constitutively expressed throughout fruit developmental stages. Flavones biosynthesis has been characterized in detail from several legume plants. The introduction of a double bond at C-2/C-3 of (2S)-flavanone molecule to yield flavones is accomplished by flavone synthase I or II (FNS I and II), a membrane-bound cytochrome P450 (Cytochrome P450) monoxygenase (Schwinn et al., 2004). FNS I was characterized as a 2-oxoglutarate-dependent dioxygenase (2-ODD) and has been reported

from species of the *Apiaceae* family (Martens et al., 2005). In contrast, the Cyt P450 monooxygenase FNS II was expected to be more widely distributed than FNSI and has been described from various plant families (Martens et al., 2005). The flavonol quercetin-3-rutinoside derived from dihydroflavonol precursors by the action of flavonol synthase (FLS) which again belongs to the 2-ODD class of enzymes. The further biosyntetic steps leading to quercetin-3-rutinoside are regulated, in *A. thaliana*, by a flavonoid-3-glycosiltransferase (UFGTD2) and a flavonol-3-glycosiltransferase (UFGT36C) (Jones et al., 2003).

2.9 HEALTH ASPECTS LINKED TO PHENOLS IN VOO

Many studies have been conducted to assess healthy properties of virgin olive oil (VOO), one of the most important ingredients of the Mediterranean diet. Accumulating evidence suggests that VOO consumption reduce risk of coronary heart disease, as well aid in the prevention of several types of cancers (Knoops et al., 2004). VOO could be considered a functional food, with a variety of components that may contribute to its overall therapeutic characteristics. Its nutritional and healthy arises from high levels of oleic acid, and from minor components such as phytosterols, carotenoids, tocopherols and hydrophilic phenols (Servili et al., 2009). VOO contains at least 30 phenolic compounds and among them, oleuropein derivatives are strong antioxidants and radical scavengers. Several studies demonstrated the important role of olive biophenols in increasing LDL resistance to oxidation, both *in vitro* and *ex vivo* as well the improvement of glucose metabolism in diabetes, anti-inflammatory effects, and prevention of some kinds of cancer (Obied et al., 2012).

2 AIMS OF THE STUDY

The aim of this research is a wide study of ripening related aspects in olive drupes with particular attention to genetic and biochemical mechanisms which regulate the accumulation of pigments such as chlorophylls, carotenoids, anthocyanins and flavonols. For this study, three different olive varieties have been chosen, each characterized by a specific color evolution pattern. Moreover, differences in terms of firmness and phenolic compounds content have been also evaluated together with expression profiles of genes and transcription factors putatively involved in their biosynthesis. In addition, NIR spectroscopy has been applied to measure some important olive quality attributes with the objective to explore the potential application of this non-destructive method for on-fields evaluation.

2 MATERIALS AND METHODS

PLANT MATERIAL

Olive plants of cv. Leccino and cv. Leucocarpa were cultivated in the experimental farm of University of Tuscia (latitude 42°250' N, longitude 12°080' E, altitude 300 m). For the molecular and biochemical analysis, olive fruit from cvs Leccino and Leucocarpa were sampled during the seasons 2011-2013. Fruit of cultivar Buscionetto were sampled from plant cultivated in the ARSIAL field collection, located at Montopoli in Sabina (Rieti). All samples, except those used for firmness measurement and NIRS acquisition, were frozen in liquid nitrogen, and stored at −80°C until their utilization.

TOTAL CHLOROPHYLL AND CAROTENOIDS QUANTIFICATION

Total Chlorophyll concentration was determined in olives picked during 2012-2013 seasons as described by Moran and Porath (1980), with slight modifications. Briefly, extraction of total chlorophylls was performed by incubating 100 mg of olive flesh in *N, N* dimethylformamide (Sigma-Aldrich, Milano, Italy), using a 1:10 volume/weight ratio, for 24 hours at 4° C. The liquid phase was then filtered and absorbance values were obtained at 625.0, 664.0 and 647.0 nm by means of a spectrophotometer (Thermo Scientific, Milano, Italy) in 1 cm quartz cuvettes. Total chlorophylls concentration was determined by the sum of *Chl a* and *Chl b*, calculated by Inskeep and Bloom (1985) equation: Chl *a* = 12.70**A664.5* – 2.79**A647* and Chl *b* = 12.70**A664.5* – 2.79**A647* and expressed as mg/g fresh tissue. Analyses were performed in triplicate.

TOTAL ANTHOCYANIN QUANTIFICATION

Total anthocyanin were quantified using protocol described by Martinelli et al. (2012). Briefly, 100mg of fruit tissue was ground with pre-chilled mortar and pestle and extracted with 5 ml methanol: HCl (1%) solution and incubated overnight at 4° C in darkness. Supernatant was obtained by centrifugation at 5000 RCF, filtered and used for spectroscopic analysis, measuring absorbance at 530nm. Serial dilution of cyandine-3-glucoside standard (SIGMA) were used to generate a standard curve. Anthocyanin concentration was expressed in µg g^{-1} FW.

TOTAL FLAVONOIDS EXTRACTION AND QUANTIFICATION

One gram of ground olive tissues was mixed with 40 ml of hexane and agitated for 4 min; the upper phase was recovered and the extraction was repeated twice successively with the lower phase. Flavonoid compounds were extracted with 80 ml of 80% (v/v) methanol containing 0.04% (w/v) sodium metabisulphite. The mixture was agitated for 5 min, and then centrifuged for 5 min at 3000 RCF to separate the hydromethanolic phase. This procedure was repeated three times using the same tissue; the hydromethanolic phases were then combined and filtered. Flavonoid content was measured using different dilutions of catechins as a standard. The test was performed in a 5-ml final solution containing: 500 ml MilliQ water, 150 ml NaNO2 5%. After 5 min, AlCl3 10% was added. The reaction was ended with 1 ml of 1M NaOH after 6 min of incubation, and absorbance measured at 510 nm. The analysis was repeated three times for each developmental stage.

SAMPLE PREPARATION AND HPLC ANALYSIS

Fruit were frozen in liquid nitrogen, stored at −80° C, and successively used for phenolic determination. The phenols were extracted from the olive pulp according to the procedure published previously by Servili et al. (2012) modified as follows: 10 g of frozen olive pulp was homogenized with 100 mL of 80% methanol

containing 20 mg/L butylated hydroxytoluene (BHT); the extraction was performed in triplicate. After methanol removal, the aqueous extract was used for the extraction by solid-phase separation (SPE) of phenols. The SPE procedure was applied, for the phenolic extracts, by loading a 1000 mg Bond Elut Jr-C18 cartridge (Agilent Technologies, USA) with 1 mL of sample, using 50 mL of methanol as the eluting solvent. After solvent removal under vacuum at 30° C, the phenolic extract was recovered and then dissolved in methanol (1 mL) and filtered through a polyvinylidene fluoride (PVDF) syringe filter (0.2 μm).The HPLC analyses of the phenolic extracts were conducted according to Selvaggini et al. (2006) with a reversed-phase column using an Agilent Technologies system Model 1100 (Agilent Technologies, Santa Clara, CA, USA) which was composed of a vacuum degasser, a quaternary pump, an autosampler, a thermostated column compartment, a DAD and a fluorescence detector (FLD). The C18 column used in this study was a Spherisorb ODS-1 250 x 4.6 mm with a particle size of 5 μm (Waters, Milford, MA, USA); the injected sample volume was 20 μL. The mobile phase was composed of 0.2% acetic acid (pH 3.1) in water (solvent A)/methanol (solvent B) at a flow rate of 1 mL/min and the gradient changed as follows: 95% A/5% B for 2 min, 75% A/25% B in 8 min, 60% A/40% B in 10 min, 50% A/50% B in 16 min and 0% A/100% B in 14 min; this composition was maintained for 10 min, then returned to initial conditions and equilibration in 13 min; the total running time was 73 min. Lignans were detected by an FLD operated at an excitation wavelength of 280 nm and emission at 339 nm, while the other compounds were detected by DAD at 278 nm.

ANTHOCYANINS AND FLAVONOLS HPLC**:** An aliquot (5 mL) of the aqueous extract was acidified with 75 μl of formic acid and filtered through a cellulose acetate (CA) syringe filter (0.2 μm). The HPLC analyses of the anthocyanins and flavonols were conducted with the same instrumentation reported above. The C18 column used was Inertsil ODS-3, 150 m with a particle size of 5 mm (GL Sciences Inc.), was used. The volume of injected sample was 20 mL. The mobile phase was 5% formic acid in water (A)/acetonitrile (B) at a flow rate of 0.9 mL min 1. The total running time was 64 min, and the gradient changed as follows: 95% A/5% B for 5 min, 35% A/65% B in 50 min, 0% A/100% B in 3 min, return to initial conditions in 2 min which was maintained for 4 min. The flavonols and anthocyanins were detected by DAD at 360 nm (Quercetin-3-Orutinoside) and 525 nm (anthocyanins). Identification of flavonols was performed using a LC/MS Quadrupole - Time of Flight (LC/MS Q-ToF) (mod. 6530) equipped with a Dual-ESI (Agilent Technologies) coupled to a 1260 series liquid chromatograph which was composed of a vacuum degasser, a binary pump, an autosampler, a thermostated column compartment and a DAD (Agilent Technologies). The HPLC separation was carried out on the Agilent Zorbax Extend-C18 Rapid Resolution HT 2.1 x 50 mm, 1.8 μm (Agilent Technologies, California, USA), the injected sample volume was 1 μL, the column temperature was 25º C. The mobile phases was composed of 1% formic acid in water (solvent A) and acetonitrile (solvent B) and the flow rate was 0.350 mL/min. The elution gradient changed as follow: 5% B a time 0, then increased to 30% (B) in 20 min, then increased to 100% (B) in 3 min and this composition was maintained for 7 min, then return to initial conditions in 4 min. The mass spectrometer was operated in negative ion mode and a mass range from 50 to 3200 m/z was selected. The ESI conditions were: fragmenter voltage 200 V, skimmer voltage 60 V, nebulizer pressure 20 psi, drying gas 7 L/min with temperature of 325º C. The acquisition and processing of data was performed using the Agilent MassHunter Workstation Software v. B.05.01.

RIPENESS INDEX (IC)

Ripeness index was determined according to the proposals of Hermoso et al. (1991), based on the assessment of the skin color of 100 olives randomly sampled and divided into three groups according to the pigmentation extent (0–7) of the pericarp and mesocarp of the drupes: intense green, yellowish-green, green with reddish spots, reddish-brown, black with white flesh, black with 50% purple flesh, black with 50% purple flesh, and black with 100% purple flesh. The index is expressed as Σ(Ni ni)/100, where N is the group number and n is the fruit number in that group.

FRUIT FIRMNESS MEASUREMENT

Olive firmness measurements were performed by Universal Testing Machine (UTM) TAxT2i Texture Analyser (Stable Micro System, Godalming, Surrey UK). A quasi-static loading device determined the mechanical properties for one compression axis (in line with the longitudinal). The device consists of a lower plate where fruit was placed and 32 mm diameter probe with plane tip, a constant 5N force load, and fixed speed of 25 mm min^{-1} with initial distance of 10 mm from the surface of sample compressing.

NIR SPECTRA COLLECTION

Laminar 5030 miniature Hand-held NIR Analyzer (Brimrose Corporation, Baltimore, 92 MD), based on the AOTF-NIR principle, was used for spectral detection.30 This is a portable device which can be used directly in the field on-tree, even though in this specific case spectral detections were conducted under laboratory conditions. Two different measurements were performed on each intact olive through contact between the external gun of the NIR device and the pericarp of the fruit, using the diffuse reflectance method of detection, while the raw spectra were detected and recorded in transmittance, as reported by Santos et al. (2005). Detection was conducted in the 1100−2300 nm range, with 2 nm wavelength increments and 10 spectra per average, which represented a single measurement. The average of the two measurements was the spectral response of the fruit.

NEAR INFRARED SPECTROSCOPY ANALYSIS AND CHEMOMETRICS

Raw spectra were statistically pretreated for absorbance (log 1/T) transformation using SNAP 2.03 software (Brimrose). Before the calibration and building up of the prediction models, the spectral variations of the data sets were analyzed through Principal Component Analysis (PCA). The absorbance spectra, obtained as spectral average of each olive subset, were used as X-variables for the final models. Partial Least Squares (PLS) models were obtained on the full spectrum, considering the spectral significant variables at specific wavelength intervals. The mean values and the ± Standard Deviation (SD) values obtained by the analysis of HPLC measurements were used as Y-variables in the PLS matrices in which they were contrasted with the averaged spectra as previously reported. Models were developed for the specific phenols and for total phenols, calculated as the sum of the measured compounds. Models were built combining data of all three cultivar by employing the total sample set of data (n = 33). No outlier identification and elimination was applied. The statistical indexes R^2 (coefficient of multiple determination) in calibration, cross-validation and prediction; Root Mean Standard Error Calibration, Cross-Validation and Prediction (RMSEC, RMSECV, RMSEP) and bias were used to determine the significance of the calculations. PCA, statistical pretreatments, and PLS models were performed using Unscrambler v9.7 software (CAMO ASA, Oslo, Norway); graphs, score plot, and scatter plots were performed, after data exportation from Unscambler, using SigmaPlot v. 10.0 (Systat Software Inc., San Jose, CA, USA).

IDENTIFICATION OF CANDIDATE GENE TRANSCRIPT

Sequences of transcripts have been identified by tBLASTn approach (implemented in BioLign v3.0 software), using amino acidic sequences of enzymes already characterized in other plants species, including *A. thaliana*, *M. domestica* Borkh, *V. vinifera* L.. Search of orthologous olive genes has been performed searching in the olive fruit EST database (Alagna *et al.*, 2009) (http://140.164.45.140/oleaestdb/search.php - 44,299 sequences), an in-house *Olea europaea* flower EST database (unpublished data – 57,600 sequences) and an in house SSH flower library. Identified transcripts have been annotated by BLASTx (http://blast.ncbi.nlm.nih.gov/Blast.cgi) against NCBI-*nr* database. Identified sequence with *e-value* > 1 $e10^{-30}$ were retained and used to design specific primers (Tab. 1) by Primer3 software, available at www.Primer3.com website. Full coding sequence of MYBs, bHLHs and WDR transcription factors proteins have been obtained through further searching inside Olive Genome assembly, available for private users at www.oleagenome.org website. Following isolation of nucleotide sequence, the GENESCAN web server at http://genes.mit.edu/GENSCAN.html (Burge and Karlin, 1997) have been used to predict peptide sequences.

PRIMER DESIGN

Primer for quantitative real-time PCR analysis have been designed using the previously described methods (see section I material and methods) and resumed in Table. The values of amplification efficiency have been also showed.

Gene	qPCR Primer (5' – 3')		Product Size (bp)	Efficency
	Forward	Reverse		
OeF3H	CACGTTCGCAGAAATGTATAAGAG	TTGATCAAGCAAGAATATCCTCAA	164	2.01
OeFLS	GTTGAAGATTAACTACTATCCGCC	GTGAACGATTAGAGCATTGGGAAC	178	1.94
OeDFR	CCAAGAAAATGACTGGATGGATGT	CGTGATGAATGGACCAACTACTAA	134	1.97
OeANS	CTTGTGAATAAAGAGAAGGTGAGG	CATGATATGCTGAGAAAAGGTACG	147	1.97
OeCHI	CTGGCTCCTCTATTCTATTCACTC	CTAAACTTTGTTTTGCTTCAGGGG	180	1.96
OeCHS2	CACTCACCTCGTCTTCTGCACCAC	GGGCTCCTTTGTTGTTCTCCGCT	182	2.00
OeUFGT	ACCGCACCACAACCTGAAGAACTG	CGGAGCCCATGACACGATCATTCC	159	1.99
OePAL	CTTATTAGGTTCTTGAATGCTGGG	ATGGAGTGATGTTGCTGTTTAGGA	184	1.98
OeF3'H	GATGATGAGCAGGGGGAGGAAGGG	GGTGTCGAAGGAGTTCCGCAATGG	133	1.99
OeF3'5'H	TCCGGCCAGTTAGAACCACAGAGA	GCATCGCCTTCATTCTCCGAACAC	175	1.90
OeUGT73C6	TTTAATCCAGGCTCGGCGGATGTG	CCAATGCACCAAACCTTTCCCCCT	158	1.95
OeLDOX	CTTGAGGAGAAACAAAAGTATGCG	CCTGAGAGAAATGGGAAGATAATG	135	1.96
Oe4CL	AGTGAGGATGTAATGCTGTGTGTT	AAGGGAACAATATCAAATTTCTGC	125	2.02
OeUFGT2	CTCACCTCTTTTATTCATCTCTCC	AACGTGTGGAACAGTTATCGGTAT	150	1.98
OeCHS1	CAGAAGGCTCTCCAACAATTAAAC	CTAAGTTCACTGGCAAGGTAAAGA	193	1.98
OeMYBPA-1	CTTAACCTGTTGTCTCTGTTTGAG	GAAGAATCCGAATAATGAAATGGG	122	1.93
OeMYBPA-2	AACGAAGAAGGAAAGGAACGGTAC	CAGACGATGCAGCACTCAACAAAC	131	1.92
OeMYBPA-3	GCCAGGTCGAACGGACAATGAGAT	CGGGAGGGGTTGACTTCTTTGGTT	128	1.89
OeMYBF1	TTACATTCAAGCTAATGGAGAAGG	TAACGATAATTTCTTCCTCTTGGG	158	1.96
OeMYBC2	GGAAACTTTTGAGCAGAGGTATTG	CCGGGATAATTTCTTCTTTGTTGG	168	1.98
OeMYB10gh	GCATGGACTGCTGCTGAAGACAAA	AGCCTGCAACTCTTTCCACATCTC	125	2.00
OeMYB2gh	TATGTTGCCTCTCTTGATATTGGG	TGTATGGACAGCTGAAGAAGATAG	166	1.93
OebHLH	CGGAAAATAATGGACCTAACCAAG	GACACGTTCTTATCATCAGCATCA	163	1.93

OeTT8	CCTAGTTCCGGTGCTGGACGGCGG	TGGCATGCCTTTGCGGAAGCTGGA	121	1.97
OeWDR	CATTGAGAAGGGTGTTGTGGAAAC	GAATGCTCCTTATCCCTCAAATCA	144	1.94
OeACT	AGGTTGGGATGGGACAGAAGGATGC	TGAGAGGTGCCTCAGTGAGAAGCA	200	1.88
OeEF-1α	ACCACTGGTGGTTTTGAAGC	GAAACCAGAGATGGGGACAA	234	1.91

Table 1. List of primer used in real-time PCR analysis.

PHYLOGENY RECONSTRUCTION AND BOOTSTRAP ANALYSIS

Phylogeny reconstruction was performed with full-predicted amino acid sequences of olive *MYB*, *bHLH* and *WDR* genes and then integrated with orthologs of other species, including *A. thaliana*, *V. viniferae* and *M. domestica*. Alignments were performed using the BLOSUM matrix (Gap opening and extension penalties of 25 and 1, respectively) using the ClustalW algorithm-based AlignX module from Mega4 software (Kumar et al., 2008). The phylogenetic tree was constructed using the Neighbour Joining Tree Method implemented in Mega4 software. Tree nodes were evaluated by bootstrap analysis for 1000 replicates. All positions containing gaps and missing data were eliminated from the dataset. Evolutionary distances were computed using the Poisson correction method and are represented as amino acid substitutions per site.

MOLECULAR ANALYSIS

Total RNA was extracted from fruit tissues using Trizol (Invitrogen), following manufacturer's guidelines. Samples were DNase treated using RNeasy Plant Mini Kit (Qiagen, Cat. No. 74904, Italy), and purified Total RNA quantified using QUBIT® 2.0 Fluorometer (Invitrogen, Cat. No. Q32866, Italy). First-strand cDNA was synthesized using Ready-To-GOTM RT-PCR Beads (GE HealthcareTM IllustraTM, Cat. No. 27-9267-01, Italy), following the manufacturers' guidelines. Real-time PCR analysis was conducted using the thermal cycler LC480II® (Roche, Italy). Each reaction (20 µL) contained 10 µL of LightCycler 480 SYBR Green I Master (Roche, Cat. No. 04 707 516 001, Italy), 0.5 µM of each primer (Tab. 1), 1 µL of cDNA and 7 µL of water PCR-grade. The PCR reaction was conducted using the following conditions: 95° C for 10 min; 45 cycles at 94° C for 20 sec, 57-59° C for 30 sec and 72° C for 30 sec, followed by a melting cycle from 65° to 95° C. Quantitative Real-time PCR was performed using three biological replicates, with three technical replicates for each sample. Data were normalized using geometric mean of two endogenous reference genes, the Elongation Factor-1 alpha (*OeEF1-α*, no. AM946404.1) gene and Actin (*OeACT7a* Accession No. AM946404) as described by Kubista et al., 2006. After PCR amplification, all products were sequenced to confirm their identity.

5'- 3' RACE-PCR

5'-3' RACE PCR was done using FirstChoice RLM-RACE kit (Ambion) according to the manufacturer's instructions, in combination with two antisense primers. In brief, total RNA, extracted from mature fruit tissue of cv Leucocarpa, was dephosphorylated by incubation with calf intestinal phosphatase and decapped by incubation with a tobacco acid pyrophosphatase. An RNA oligo was ligated to the 5' end of the mRNA, then sample was reverse transcribed and amplified using the *OeMYBPA1* gene-specific reverse primer (5'-GTACGATGAATATCTTCAGCTGCTG-3') and a primer targeting the RNA oligo, ligated to the 5' end of mRNA. For the 3' RACE total RNA was reverse transcribed using the poly-A adapter primer provided with the RLM-RACE kit. This template was subsequently used in 3' RACE-PCR using supplied 3'-outer primer and 5' specific *OeMYBPA1* primer (5'- ATGGGAAGATCTCCTTGTTGTTCA-3'). PCR products were cloned using

PCR Purification kit (QIAGEN), cloned into pGEM-T vector system (Promega, Madison, WI, USA) and sequenced using universal primers.

2 RESULTS

2.11 DEVELOPMENTAL OBSERVATION OF OLIVE FRUIT IN CULTIVARS LECCINO, LEUCOCARPA AND BUSCIONETTO

The biochemical and molecular bases of flavonoid accumulation and colour development in olive fruit have been studied on three cultivars, Leccino, Leucocarpa and Buscionetto, which display different phenotypes on the temporal evolution and accumulation, location on the pericarp and type of polyphenols:

- ripe drupes of cv Leccino show the typical purple-black colour of olive fruit
- ripe drupes of cv Leucocarpa show a white-ivory colour
- drupes of cvs Buscionetto are characterized by a particular ripening pattern: at the onset of ripening, drupes show the same white-ivory colour observed in cv Leucocarpa and only later they acquire the typical purple-black colour of olive drupes

Obviously, intrinsic differences of ripening pattern among the three studied cultivars do not allow to use only the character “changing colour” as ripening marker. Thus, we consider the loss of drupes green-colour as additional marker for the analysis of ripening process.

Fruit growth dynamics were monitored at weekly intervals in cvs Leccino and Leucocarpa during season 2013, detecting drupes fresh weight and diameter. Drupes of cvs Buscionetto have been only monitored at the ripening period, measuring fresh weight at commercial harvest. Developmental stages were defined by days after full bloom (DAFB). Full bloom was reached in cv Leccino and Leucocarpa during the first week of June during season 2013. However, since early stage of drupes development and until maturity, a marked difference in drupes size has been observed between the two cultivars. Fruit fresh weight at harvest was 1.5-fold higher in cv Leccino (3.779 g) respect to cv Leucocarpa (2.529 g). Instead, drupe of cv Buscionetto had the highest fresh weight of 5.48 g. In cv Leccino, the drupe colour change started about 110-115 DAFB (end of September) and reached the harvest maturity at about 135 DAFB (middle-October). Instead, the drupe of cv Leucocarpa started to loss green colour about 130-135 DAFB and progressively acquired a uniform complete white-ivory colour at 160 DAFB. As already previously described, the drupe of cv Buscionetto was monitored starting from green maturation stage and until full-ripening, occurring in last decade of November. At the onset of ripening, drupes showed a rapid loss of green colour becoming firstly white-ivory and only later acquired reddish-purple colour. Biochemical and molecular analysis have been performed in cv Leccino e Leucocarpa, selecting five stages of drupe development:

-**stage I** (early fruit development) corresponding to 50 DAFB and BBCH stages 73-74 for both cultivars. At these stages, drupe reached about 50% of their final size.

-**stage II** (green maturation), corresponding to 100 and 120 DAFB (BBCH stage 79) for cv

Leccino and cv Leucocarpa, respectively,. At this stage, table olive were usually harvested.

-**stage III** (colour change), corresponding to 115 and 135 DAFB (BBCH stage 81) for cv Leccino and cv Leucocarpa, respectively. At this stage, drupe begin to loss their intense green colour, becoming lighter, and red spot appear on pericarp of typical olive cultivars, but not for Leucocarpa.

-**stage IV**, corresponding to 125 and 145 DAFB (BBCH stage 85) for cv Leccino and cv Leucocarpa, respectively. At this stage, pericarp of cv Leccino drupe acquire an almost uniform black-purple coloration.

-**stage V** (ripe fruit), corresponding to 135 and 160 DAFB (BBCH stage 89) for cv Leccino and cv Leucocarpa, respectively. At this stage, oil drupes were usually harvested.

As previously reported drupes cv Buscionetto were sampled only during the last stages of ripening, corresponding to stage III-V.

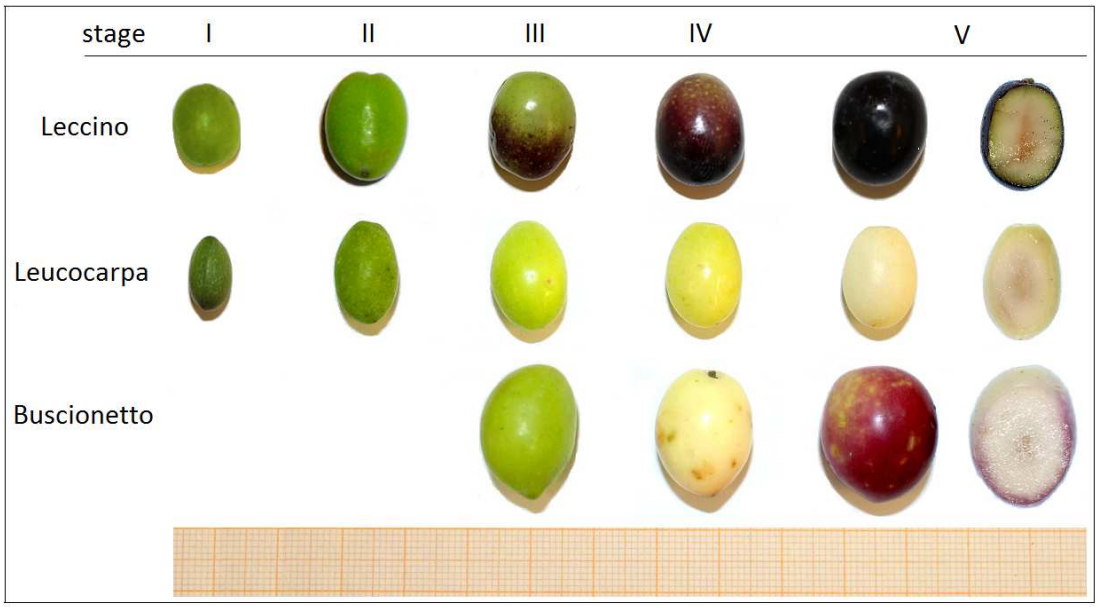

Figure 1. Colour evolution in olive fruit during growth and development as observed in cvs Leccino, Leucocarpa and Buscionetto. See text for a complete description of the five sampling stage.

2.12 PIGMENTS ACCUMULATION DURING OLIVE FRUIT RIPENING

The accumulation pattern of total chlorophyll (Chl), carotenoids (Carot) and anthocyanins has been monitored starting from green maturation until ripening of drupes, and their content has been expressed as μg/g fresh weight of drupe.

The content of total chlorophyll and carotenoids shown an analogous trend during drupe ripening (*Figure 2 and 3*) and in the three analyzed cultivars: the concentration strongly decreased along olive fruit maturation. However, the *chlorophyll:carotenoid* ratio (*Figure 4*) the chlorophyll degradation was higher than that of carotenoids. At stage II, green coloration of pericarp, the content of total chlorophyll (Figure 2) resulted to be similar in cv Leccino and cv Leucocarpa (100 and 104 μg g^{-1} FW,

respectively), while it resulted to be approximately 3/4-fold higher than total content of carotenoids (Figure 3), 24 and 30 μg g^{-1} FW in cv Leccino and cv Leucocarpa, respectively. Instead, at stage III, pericarp colour change, chlorophyll content strongly dropped down in both cultivars to 59 and 63 μg g^{-1} FW, in Leccino and Leucocarpa, respectively (*Figure2 and 3*), while total carotenoids only decreased with minor extent. At this stage, in cv Buscionetto, total chlorophyll and total carotenoids content resulted to 69 and 19 μg g^{-1} FW, respectively, quite similar to cv Leccino and cv Leucocarpa. At stage IV, *Chl: Carot* ratio (*Figura 4*) dramatically decreased from about 4 to 2.90 in cv Leucocarpa and 2.11 in cv Buscionetto, while still remained up in cv Leccino (4.12). The reduction of this value of ratio in cv Leucocarpa and cv Buscionetto could be ascribed to the rapid degradation of chlorophylls, which dropped to 23 and 21 μg g^{-1} FW, respectively. In agreement with *Chl:Carot ratio*, the colour pericarp and mesocarp of drupe changed from light-green to yellow in both cultivars, probably due to the absence of anthocyanins accumulation at this stage. Instead, cv Leccino retained a higher content of chlorophylls (43 μg g^{-1} FW) and sub-epidermal tissues remained light-green colored, although pericarp tissues had almost completely acquired the typical reddish-black colour. Finally, in ripe drupes of cv Leucocarpa, *Chl: Carot* ratio further decreased reaching the value of 1.99, while remaining quite stable in cv Buscionetto (2.30). In contrast, drupes of cv Leccino continued to maintain a higher pigment ratio (3.36).

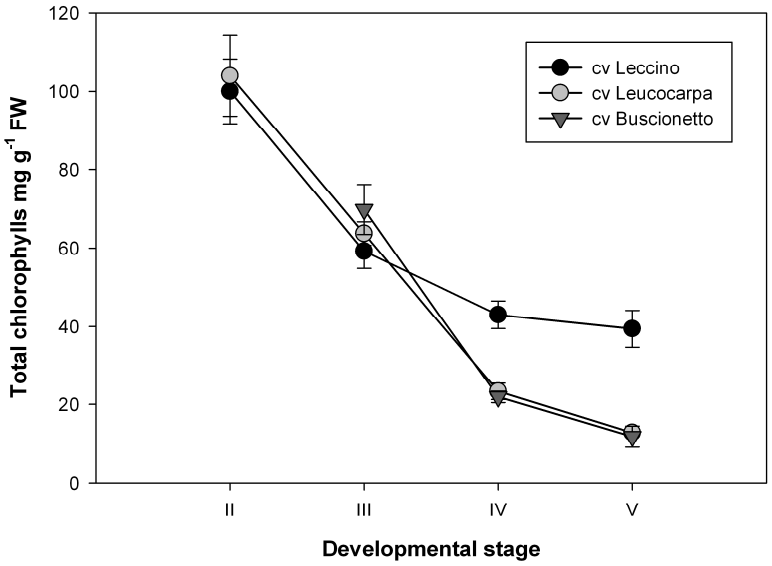

Figure 2. Content of total chlorophylls during fruit ripening in cvs Leccino, Leucocarpa and Buscionetto. The content was expressed as μg g^{-1} FW and resulted from mean of three biological replications. The symbols represent the averages and the bars ± standard deviation.

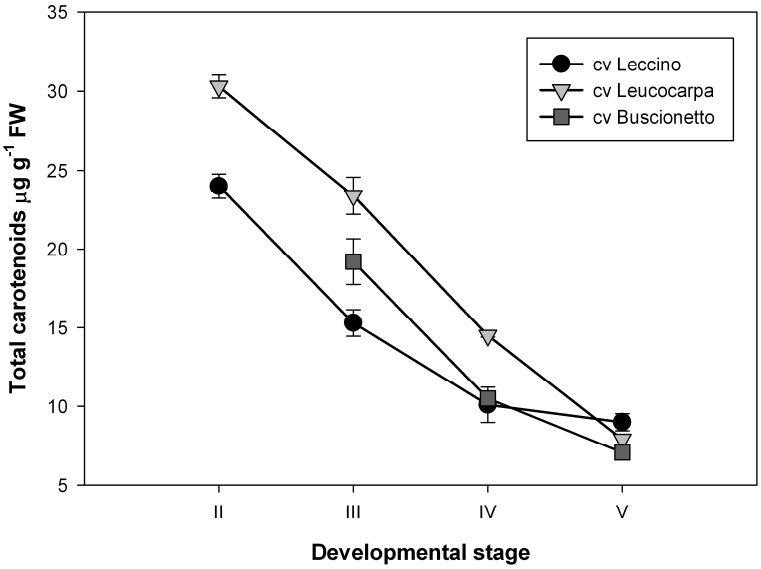

Figure 3. Content of total carotenoids during fruit ripening in cvs Leccino, Leucocarpa and Buscionetto. The content is expressed as µg g^{-1} FW and resulted from mean of three biological replications. The symbols represent the averages and the bars ± standard deviation.

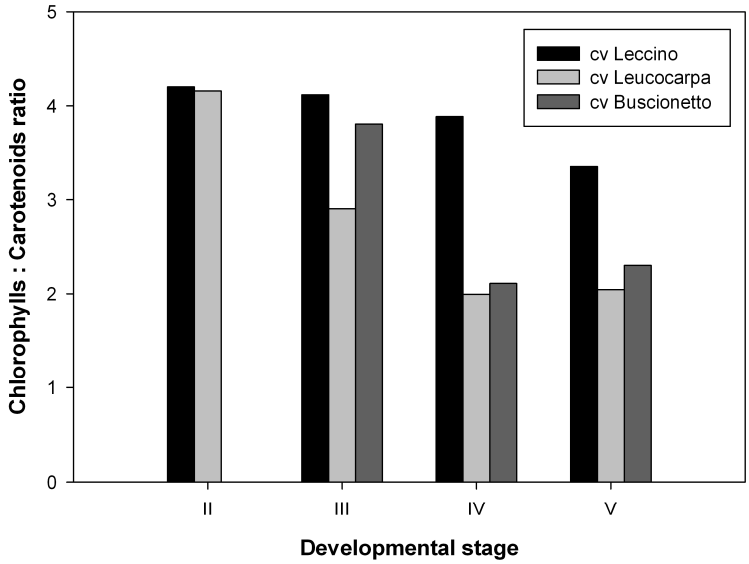

Figure 4. Total chlorophylls and total carotenoids ratio as calculated during olive fruit ripening in cvs Leccino, Leucocarpa and Buscionetto.

Anthocyanin accumulation was analyzed both in whole drupe tissues (*Figure 5a*), excluding endocarp, and in pericarp and mesocarp tissues separately (*Figure 5b*). Anthocyanin content resulted different in the drupes of the three studied cultivars. As expected, in cv Leccino, anthocyanins content started to increase in pericarp tissues at stage III (colour change), when red spot appear on the olive fruit (Figure 5b), reaching the highest concentration in ripe drupes (stage V) of about 610 µg g^{-1} FW. In cv Buscionetto, anthocyanin content begin to increase only at stage IV, reaching at stage V the content of

about 490 μg g^{-1} FW (Figure 5a). Moreover, in both cultivars, pericarp anthocyanins content was about 3-fold higher respect to mesocarp tissues (*Figure 5 a, b*). Interesting, only detectable amount of anthocyanins were detected in drupes of the ivory-white cultivar Leucocarpa.

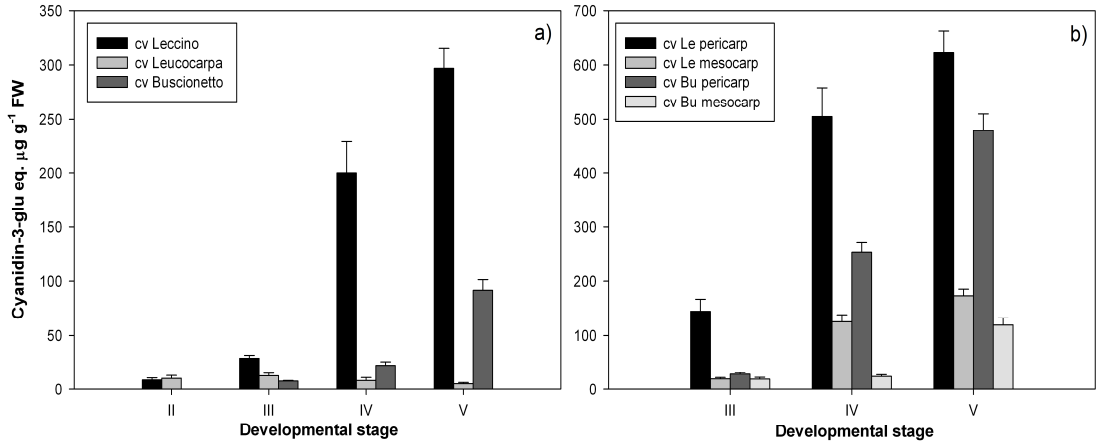

Figure 5. Olive fruit anthocyanins content during ripening stages in whole fruit (a) and pericarp-mesocarp tissues (b), expressed in μg g^{-1} fresh weight of cyanidin-3-glu equivalents. The content resulted from mean of three biological replications. Histograms represent the averages and bars the standard deviation.

2.13 MAIN PHENOLICS COMPOUNDS IN RIPE DRUPE OF CULTIVARS LECCINO AND LEUCOCARPA

Explorative HPLC analyses were performed on ripe drupes of cvs Leccino and Leucocarpa during the seasons 2011 and 2012, to obtain a general survey of secondary metabolite accumulation (*Table 1*). Moreover, the comparison of the accumulated metabolites between reddish-black colored cv Leccino and white-ivory coloured cv Leucocarpa could give information about biochemical bases on the mutant phenotype of the last cultivar. In *Table 1* are reported the accumulation profile (mg g^{-1} FW) of most important olive drupe phenolic compounds. The sum of total phenolic fractions did not significative differ in both seasons between the two analyzed cultivars: in cv Leccino only a slightly greater content than in cv Leucocarpa has been found (21.2 *vs* 17.1 mg g^{-1} FW), on season 2011, while in cv Leucocarpa, on season 2012, has been detected the highest content 2012 (28.9 *vs* 23.6 mg g^{-1} FW). The secoiridoids, oleuropein and demethyloleuropein resulted to be the most abundant phenolic compounds in cv Leccino (8.2 and 8.0 mg g^{-1} FW on season 2011, and 4.7 and 9.7 mg g^{-1} FW on season 2011, respectively). In cv Leucocarpa, oleuropein resulted to be the most abundant phenolic compound (10.5 and 11.7 mg g^{-1} FW, for 2011 and 2012, respectively), while demethyloleuropein was barely detectable in both years (0.70 and 0.13 mg g^{-1} FW). Among other phenolics, 3,4-DHPEA, 3,4-DHPEA-EDA and verbascoside did not show relevant differences, while *p*-HPEA was absent in both cultivars. The lignans acetoxypinoresinol and pinoresinol have been detected in both cultivars, with the highest content detected in cv Leccino. Regarding flavonoids compounds, important differences

have been detected between the two cultivars. Interesting, flavones such as luteolin-7-glucoside, have been not detected by HPLC analysis both in cvs Leccino and Leucocarpa, while flavonols (such as quercetin-3-rutinoside also known as rutin) and anthocyanins (cyanidin-3-glucoside) resulted to be no detectable only in cv Leucocarpa.

Compounds	***cv Leccino***		***cv Leucocarpa***	
(***mg/g FW***)	**2011**	**2012**	**2011**	**2012**
HPLC				
Phenolic alcohols				
3,4 DHPEA	0,95 ± 0,02	1,2 ± 0,01	1,09 ± 0,1	2,60 ± 0,01
p-HPEA	n.d.	0,3 ± 0,02	n.d.	0,55 ± 0,03
Hydroxycinnamic acid				
Verbascoside	1,98 ± 0,03	5,49 ± 0,01	2,82 ± 0,01	1,75 ± 0,02
Secoiridoids				
Demethyloleuropein	8,05 ± 0,01	9,78 ± 0,02	0,70 ± 0,2	0,13 ± 0,01
3,4-DHPEA-EDA	1,49 ± 0,02	1,78 ± 0,04	1,71 ± 0,02	10,6 ± 0,04
Oleuropein	8,21 ± 0,003	4,71 ± 0,05	10,5 ± 0,1	11,7 ± 0,14
Lignans				
(+)-1-Acetoxypinoresinol	0,21 ± 0,02	0,18 ± 0,01	0,11 ± 0,03	0,14 ± 0,01
(+)-1-Pinoresinol	0,13 ± 0,05	0,15 ± 0,01	0,13 ± 0,04	0,13 ± 0,01
LC-MS Q-TOF				
Flavonols				
Quercetin-3-O-Rutinoside	-	0,18 ± 0,01	-	trace
Anthocyanins				
Cyanidin-3-glucoside	-	0,05 ± 0,003	-	n.d.

Table 1. Phenolics compound in ripe drupes of cvs Leccino and Leucocarpa. The phenolic content are reported as values of the means of three independent experiments ± standard deviation. Flavonols and anthocyanins content have been quantified by LC/MS Q-TOF.

Moreover, phenolics extract of cvs Leccino and Leucocarpa were further analyzed in mass spectrophotometer LC-MS-QTRAP to identify the possible flavonoid intermediates that are not possible detected by HPLC for the low level of resolution. Surprisingly, trace amount of rutin have been found in cv Leucocarpa (*Figure 6*), while flavones and anthocyanins were confirmed to be absent. Collectively, metabolic data profile comparison between cv Leccino and Leucocarpa allow us to exclude the possibility that a mutation occur in early step of phenylpropanoid biosynthesis, as lignans and secoiridoids were found in both cultivars at comparable level. Indeed, the very low amount or even the absence of rutin and cyanidin, respectively, suggest that a block could occur in the early step of flavonoid biosynthesis, even if chalcones and/or flavononols intermediates were not found by mass-spectrophotometric analysis (data not shown). Despite we did not succeed in the identification of such flavonoid intermediate, the hypothesis could be still valid considering that in Arabidopsis mutant *tt6* (leaky lesion in *F3H* gene), naringenin (the intermediate expected to

accumulate) was never detected in mutant or *wild type* seedlings, suggesting it could be very unstable compounds (Peer et al. 2001).

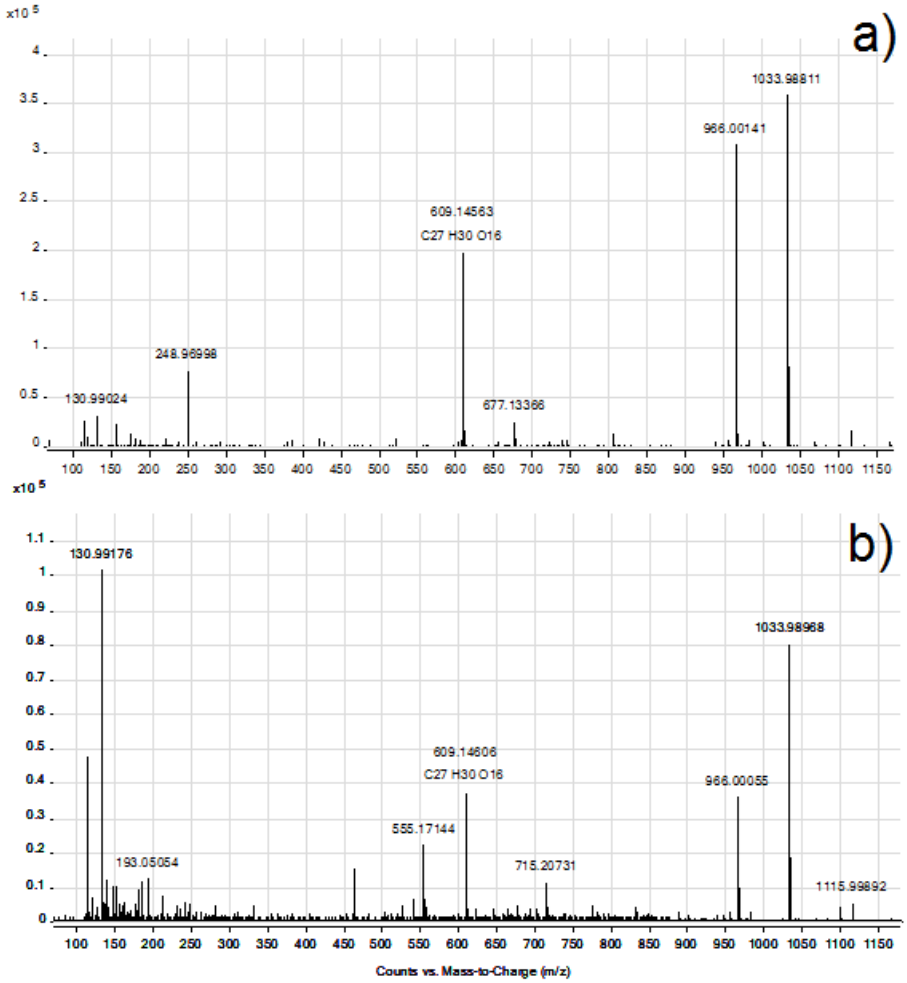

Figure 6. Accurate MS spectra for mass confirmation of quercetin-3-O-rutinoside (theoretical $[M-H]^-$ = 609.14611). A: spectrum of standard compound; B: spectrum of leucocarpa.

2.14 TOTAL FLAVONOIDS CONTENT DURING OLIVE FRUIT DEVELOPMENT IN CULTIVARS LECCINO AND LEUCOCARPA

The content of total flavonoids (*Figure 7*) detected by spectrophotometer technique, in olive drupes collected in the season 2013, have shown a general decreasing trend along development stages in cv Leccino and Leucocarpa. Total flavonoids content was the highest in both cultivars during the stage I, reaching the amount of 23 and 12 mg g^{-1} FW, respectively. The content of these compounds progressively decreased in both cultivars with an analogous trend, although since the stage II in the Leucocarpa drupes the lowest values of flavonoid compounds have been already found. In the Leccino drupes the decrement of the amount of flavonoids has been resulted to be progressive (*Figure 7*).

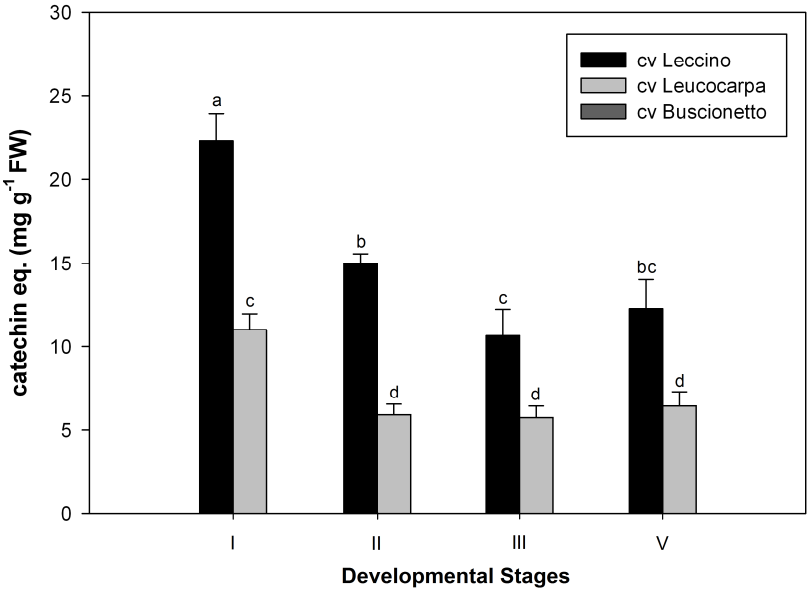

Figure 7. Dynamic of total flavonoids content in drupes of cvs Leccino and Leucocarpa during different stages of fruit development. Histograms represent the mean value (mg g^{-1} FW) of three biological replications and bars the standard deviation. Different letters represent significant difference at $p < 0.05$ (Duncan's test).

2.15 EVOLUTION OF METABOLIC ACCUMULATION PROFILE DURING OLIVE DRUPE DEVELOPMENT

Metabolic accumulation profile has been detected during drupes development of the cv Leccino, cv Leucocarpa and cv Buscionetto, during the season 2013. The dialdehydic form of elenolic acid linked to hydroxytyrosol, (3,4-DHPEA-EDA, *figure 8a*) resulted the most abundant compound at stage II (green maturation) and progressively dropped down until the end of stage V in cvs Leccino and Leucocarpa. Drupes of cv Leucocarpa in all stages contained almost 2-fold amount of this compound respect to that found in drupes of cv Leccino, and this difference has been retained even at the stage V (6.6 vs 3.2 mg g^{-1} FW, respectively). This difference has been already observed in the sample drupes collected in season 2011-2012, therefore, this event could be a particular feature of cv Leucocarpa. In ripe drupes of Buscionetto a very low amount of 3,4-DHPEA-EDA has been detected (0.6 mg g^{-1} FW). Tyrosol (*p*-HPEA,) content resulted to be not dissimilar in the drupes of the three cultivars (*Figure 8 b*), even if in the cv Leucocarpa a slightly major content has been detected in ripe drupes (0.08 mg g^{-1} FW). The hydroxytyrosol (3,4-DHPEA), on the contrary of what we have detected for 3,4-DHPEA-EDA, increased during the stages of drupe growth and maturation (*Figure 8c*), and the lowest value was detected in Leccino (0.30 mg g^{-1} FW) respect to that detected in ripe fruit of cvs Buscionetto and Leucocarpa (0.89 and 0.81 mg g^{-1} FW, respectively). Surprisingly, ripe drupes of cv Buscionetto did not accumulate detectable amount of verbascoside (*Figure 8d*), while in ripe drupes of cvs Leccino and Leucocarpa a similar content of this compound has been detected, 0.9 and 1.1 mg g^{-1} FW, respectively.

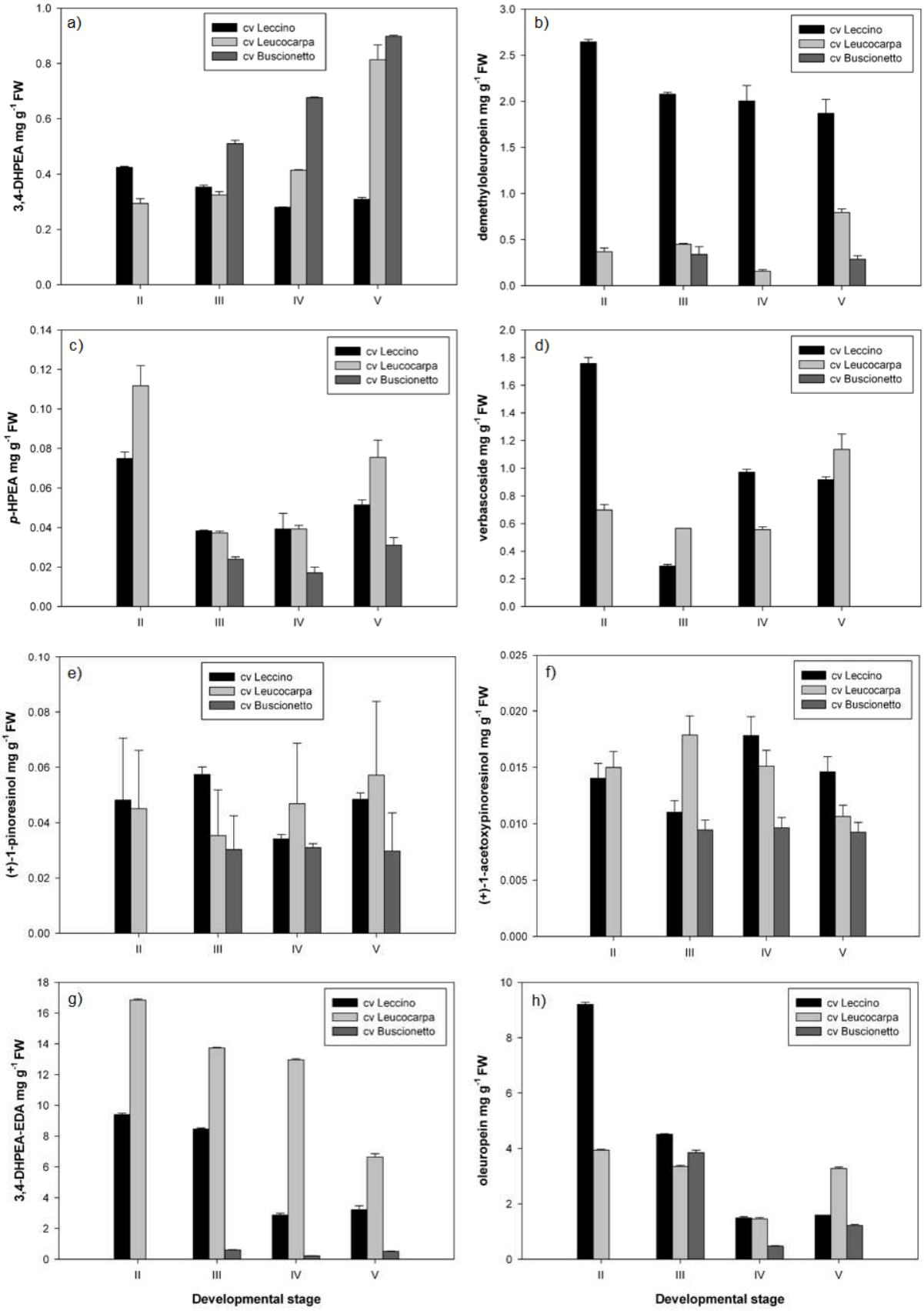
a)
3,4-DHPEA mg g-1 FW
b)
demethyloleuropein mg g-1 FW
c)
p-HPEA mg g-1 FW
d)
verbascoside mg g-1 FW
e)
(+)-1-pinoresinol mg g-1 FW
f)
(+)-1-acetoxypinoresinol mg g-1 FW
g)
3,4-DHPEA-EDA mg g-1 FW
h)
oleuropein mg g-1 FW
cv Leccino
cv Leucocarpa
cv Buscionetto
II
III
IV
V
Developmental stage

Figure 8. Polyphenol amount found in the drupes during the stages of growth and maturation as detected in the cvs Leccino, Leucocarpa and Buscionetto. The content has been expressed as mg g-1 FW and histograms represent the averages, bars represent the standard deviation, of three biological replications.

However, the dynamic determination of the quantity of this compound along the different stages of drupe growth resulted different between the last two cultivars: in cv Leccino, verbascoside content strongly decreased along drupe maturation, while in cv Leucocarpa slightly increased (*Figure 8d*). The oleuropein content progressively decreased along all of stage of drupe growth and ripening (*Figure 8e*), although in ripe drupes of Leucocarpa 2-fold higher content (3.2 mg g^{-1} FW) than in Leccino and Buscionetto, has been detected. The greatest value of the demethyloleuropein content has been found in cv Leccino (*Figure 8f*), while very low amount in cvs Leucocarpa and Buscionetto, during all developmental stages. Controversial appeared the results on the lignans detected: pinoresinol and acetoxypinoresinol (*figure 8f, g*). Any clear dynamic content has been found for pinoresinol (*Figure 8*), because the oscillation of the amount of this compound resulted to be very high in all fruit development stages. The values of the amount of acetoxypinoresinol found in the drupes of Buscionetto (*Figure 8g*) seems to be very different from that found in cv Leccino and Leucocarpa (*Figure 8g*). Surprisingly, the flavones luteolin-7-glucoside (luteolin) resulted to be no detectable in any of the drupes of the three cultivars. Regarding to the quercetin-3-rutinoside compound (rutin), as previously reported, it resulted to be no detectable in cv Leucocarpa (*Figure 9*), by HPLC procedure. Instead, in cv Leccino, rutin decreased at colour change (stage III) and then remained quite stable until the end of ripening, reaching a concentration of 0.70 mg g^{-1} FW. Although we did not tested stage II, rutin accumulation pattern in cv Buscionetto seems to have the same trend observed in cv Leccino, although content in ripe fruit was lower (0.42 mg g^{-1} FW).

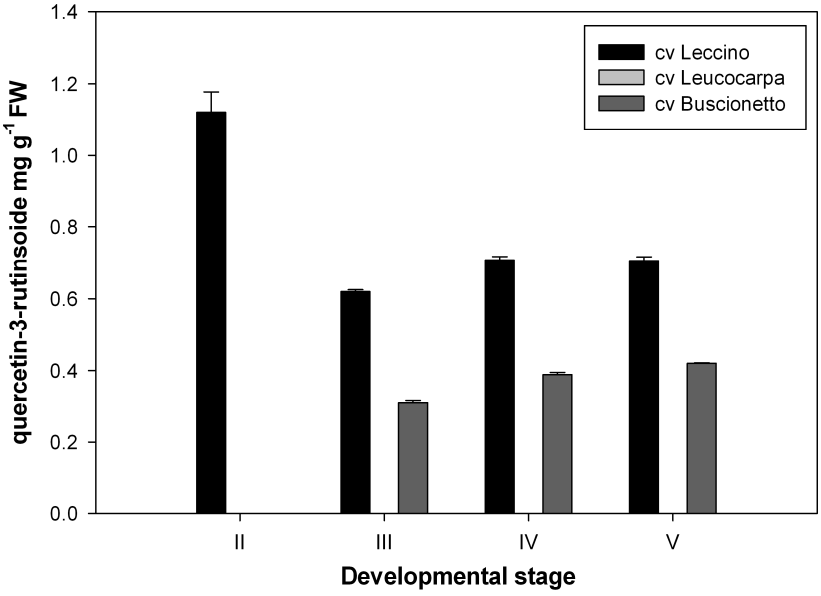

Figure 9. Rutin amount found in the drupes during the stages of growth and maturation as detected in the cvs Leccino, Leucocarpa and Buscionetto. The content has been expressed as mg g-1 FW and histograms represent the averages, bars represent the standard deviation, of three biological replications.

2.16 FRUIT FIRMNESS

Firmness has been evaluated during drupe ripening by using Universal Testing Machine instrument (Instron), applying a constant force and measuring drupe deformation (mm). Drupe fresh weight, polar and transversal diameter have been also measured, to appropriately set Instron parameters (*Table 2*). Firmness, expressed as force/deformation (N/mm), decreased in olive drupe of the three cultivar with the progression of ripening, as expected for fleshy fruits, although it occurred in a cultivar-dependent manner (*Figure 9*). At stage II (green maturation), drupes of cv Leucocarpa have shown the highest firmness value respect to that found in drupes of cv Leccino. The difference detected between the two cultivars disappeared at stage III (color change). After this stage, firmness dramatically dropped down in drupes of cv Leucocarpa and reached the minor value of the firmness at the stage V. In the drupes of cv Leccino the firmness did not varied between the stage III and stage IV, and between the last stage and the stage V a decreased has been detected (*Figure 9*). Drupes of cv Buscionetto were monitored only during advanced stage of ripening. The trend of firmness loss in the drupe of this cultivar appeared more similar to cv Leccino (*Figure 9*), therefore the firmness of the drupes scored the same values of that of cv Leucocarpa, both lower than values found in the drupes of cv Leccino.

cultivar	fresh weight (g)	polar diameter (mm)	transversal diameter (mm)	Instron	
				load (N)	deformation (mm)
Leccino	2.89±0.15	24.60±0.69	16.49±0.36	5	0.379±0.015
	3.01±0.21	24.53±0.53	16.41±0.33	5	0.457±0.021
	2.84±0.11	23.89±0.26	16.29±0.18	5	0.514±0.061
	2.73±0.18	24.28±0.22	16.67±0.40	5	0.873±0.083
Leucocarpa*	1.69±0.12	18.16±0.31	10.82±0.26	5	0.326±0.011
	1.57±0.25	19.32±0.42	10.93±0.35	5	0.443±0.056
	1.78±0.16	20.86±0.38	11.08±0.38	5	0.821±0.59
	1.83±0.16	19.79±0.67	11.17±0.21	5	1.035±0.033
Buscionetto	5.23±0.44	26.87±0.81	21.54±0.52	5	0.559±0.030
	5.07±0.28	27.29±0.75	21.85±0.64	5	0.644±0.048
	5.02±0.31	26.45±0.62	21.49±0.49	5	1.118±0.014

Table 2. Resuming table of cv Leccino, Leucocarpa and Buscionetto olive fruit fresh weight (g), polar and transversal diameter (mm), load (N) and deformation (mm).

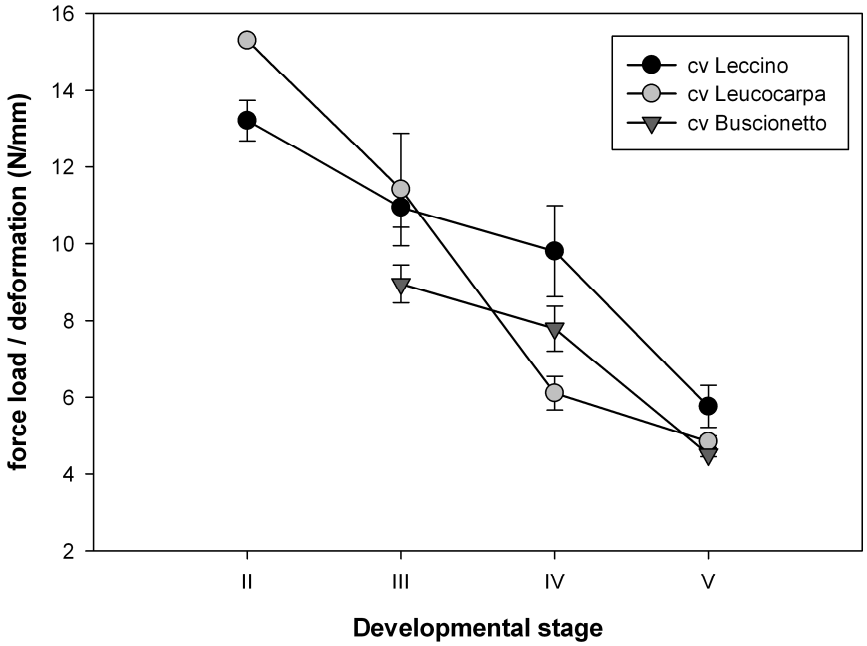

Figure 9. Mean value of drupe firmness in cvs Leccino, Leucocarpa and Buscionetto during ripening. Firmness was expressed as force load / deformation (N/mm) and resulted from mean of three biological replicates, each one composed by 10 drupes. Symbols represent the averages and the bars ± standard deviation

2.17 APPLICATION OF NIR-AOTF TECHNOLOGY FOR ON-FIELD PREDICTION OF PIGMENT AND PHENOLIC COMPOUNDS DURING THE RIPENING OF OLIVE DRUPE

Among the different factors influencing olive oil quality, the choice of the best harvesting period is one of the most important. Knowledge about the olive ripening process is, therefore, necessary to define the more profitable balance between positive features, desirable in olive oil, and negative characteristics that may arise from olives harvested at a late picking up period. Monitoring fruit quality through reflectance measure possesses many advantages over traditional destructive approaches, as simplicity, sensitivity, reliability and high-throughput. Various authors have demonstrated the useful of NIRS technology to measure some olive quality attributes. Cayuela et al. (2010), obtained good predictive models for olive moisture, dry matter, oil content, oil free acidity and maturity index. Marquez et al. (2005) applied on-line NIR sensor for real-time olive oil evaluation during processing, allowing the estimation of acidity, bitter taste and fatty acids composition. Moreover, NIR spectroscopy has also been successfully applied to detect fraudulent addition to olive oil of other vegetables ones (Wesley et al., 1995), to determine olive oil geographical origin or for authentication (Galtier et al., 2007; Inon et al., 2003; Tapp et al., 2003). For the assessment of olive fruit and oil quality, phenolics composition is considered to be of paramount importance as they affect its sensorial and healthy characteristic. Nevertheless, the low content of phenolics compounds makes it difficult to monitor with rapid and cost-effective methods, particularly in wide-scale cultivation system. In a recent publication, Bellincontro et al. (2012) evaluated the application of NIRS to

measure total phenolics content of olive fruit during ripening, and other specific metabolites, such as oleuropein, verbascoside and 3,4-DHPEA-EDA, demonstrating the potential of this methods for on-field assessment of olive phenolics composition, for a more complete evaluation of the optimal harvesting period. As reported in table 3, color index progressively increased along drupe ripening in cvs Leccino and Buscionetto, due to anthocyanin biosynthesis. However, this parameter could not be used in cv Leucocarpa, since this cultivar did not accumulate anthocyanins at any ripening stage. As previously described, chlorophylls and carotenoids progressively decreased during drupe maturation, although it occurs in cultivar-dependent manner. A decreasing trend was also observed for total phenolics content and for specific metabolites, such as oleuropein or 3,4-DHPEA-EDA, while a more complex accumulation pattern was observed for verbascoside and rutin. In particular, considering that the variability in the content of each phenolic compounds is favorable for modeling coming from multivariate regression, it was interesting to observe the absence of rutin and verbascoside, respectively in cv Leucocarpa and Buscionetto.

cultivar	ripening index (0-7)	total chlorophylls (mg g FW)	total carotenoids (mg g FW)	Total anthocyanins (mg g FW)	oleuropein (mg g^{-1})	verbascoside (mg g^{-1})	DHPEA-EDA (mg g^{-1})	rutin (mg g^{-1})	total phenolics (mg g^{-1})
Leccino	0.26	0.100±0.008	0.024±0.007	0.008±0.001	9.20±0.08	1.75±0.04	9.38±0.10	1.12±0.05	24.6±0.15
	1.97	0.059±0.004	0.015±0.001	0.028±0.003	4.51±0.02	0.29±0.01	8.45±0.07	0.61±0.01	16.3±0.08
	3.28	0.043±0.004	0.010±0.001	0.200±0.029	1.48±0.04	0.97±0.02	2.86±0.11	0.70±0.01	8.43±0.21
	3.68	0.039±0.005	0.008±0.001	0.297±0.018	1.58±0.01	0.91±0.02	3.20±0.26	0.70±0.01	8.70±0.30
Leucocarpa*	-	0.104±0.010	0.030±0.007	0.010±0.003	3.94±0.03	0.69±0.04	16.8±0.07	0.0	22.3±0.1
	-	0.063±0.003	0.023±0.001	0.012±0.003	3.35±0.03	0.56±0.01	13.7±0.04	0.0	18.5±0.1
	-	0.023±0.002	0.014±0.001	0.008±0.001	1.45±0.05	0.55±0.02	12.9±0.07	0.0	15.6±0.1
	-	0.012±0.001	0.007±0.001	0.005±0.001	3.27±0.05	1.13±0.11	6.63±0.22	0.0	12.7±0.3
Buscionetto	0.38	0.069±0.007	0.019±0.002	0.007±0.001	3.84±0.09	0.0	0.60±0.03	0.30±0.01	5.67±0.12
	2.07	0.021±0.001	0.011±0.002	0.022±0.003	1.22±0.03	0.0	0.21±0.02	0.41±0.01	3.39±0.05
	3.47	0.011±0.002	0.007±0.001	0.091±0.009	0.46±0.01	0.0	0.50±0.02	0.38±0.01	1.80±0.02

*Table 3. Mean values of color index, total chlorophylls, carotenoids, anthocyanins and main phenol content previously determined during different stages of olive fruit ripening in cultivars Leccino, Leucocarpa and Buscionetto, and used to models the NIRS data spectrum. *Color index was not determined in drupe of cv Leucocarpa since they did not showed the typical pericarp red color.*

As reported by Bellincontro et al. (2012), many wavelengths of NIR spectrum affect the PLS modelling, and thus, the entire spectrum (1100-2300nm) was considered to build calibration model for each class of compounds and for deformation values obtained by Instron. Moreover, for the regression models and related chemometric application, original NIR raw spectra were transformed in absorbance (log 1/T). The principal component analysis (PCA) calculated on all spectral dataset was able to well discriminate the three different cultivars, although a better separation was obtained for cv Buscionetto

(*Figure 10*). In particular, variance resulted well explained by PC1 and PC2, which accounting for about 98% of the observed variability.

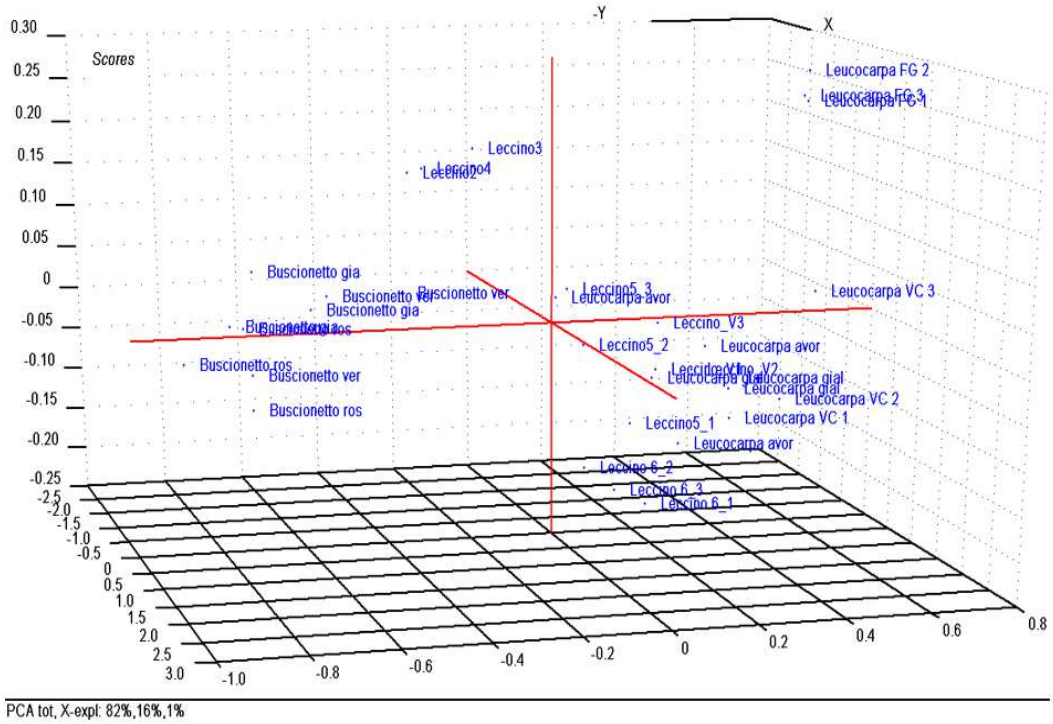

Figure 10. Score plot of the principal component analysis (PC1 vs PC2) carried out on the absorbance NIR-AOTF spectra values detected in grouped samples collected separately from the olive cvs Leccino, Leucocarpa and Buscionetto. Percentage of the explained variance is reported in parentheses on the axes.

The PLS models accuracy was described by the coefficient of determination in calibration (R^2) and cross-validation or prediction (R^2cv, R^2p), the root mean square error of calibration (RMSEC) and the root mean square of cross-validation (RMSECV) or prediction (RMSEP). The number of latent variables (LVs) was selected in correspondence to the RMSECV or RMSEP minimization, In general, good models were characterized by R^2 higher than 0.9 and low RMSEC and RMSEP values, however, with reduced differences each other. Indeed, higher differences between RMSEC and RMSEP values indicate the introduction of too many latent variables in the model.

Except for total chlorophylls content PLS model, which scored 0.86 R^2, all other PLS models have scored R^2 values close or up to 0.9, range of values that are necessary to calculate a valid quantitative information (*Table 4*, 5). In particular, as result of calibration procedure, the highest R^2 value has been obtained for firmness (0.99) parameter, determined with Instron, while for the other parameters, 0.96 has been scored for the total phenols and verbascoside content, 0.93 for 3,4-DHPEA-EDA content, 0.93 for rutin content and 0,91 for total anthocyanins content (*Table 4, 5*). Although low R^2 value has been found for the other parameters, still acceptable R^2 results have been calculated for oleuropein (0.89) and total carotenoids (0.88). The RMSEC index, expressed as mg/g FW, varied from

the lowest value of 0.002 for total carotenoids to the highest of 1.44 for 3,4-DHPEA-EDA, while the number of LVs resulted to be comprised in the range 4-8 except for verbascoside, with 10 LVs.
The cross-validation calculated as *ex-novo* built PLS models (*Table 4*) has shown a reduction of R^2cv coefficient, particularly high for total anthocyanins and rutin, 0.80 and 0.83 respectively, and low for total chlorophylls and carotenoids, 0.82 and 0.85, respectively. Despite this, the RMSEC and RMSECV indexes showed very similar values, indicating that an optimum number of factors are included in the models.

	n	Calibration				cross-validation	
		R^2	RMSEC	LVs	Bias	R^2	RMSECV
chlorophylls	33	0.86	0.011	5	-1.411 e^{-09}	0.82	0.013
carotenoids	33	0.88	0.002	4	-1.016 e^{-09}	0.85	0.003
anthocyanins	33	0.91	0.027	6	-1.814 e^{-08}	0.80	0.042
rutin	33	0.92	0.098	6	-1.066 e^{-07}	0.83	0.14
firmness	33	0.99	0.015	4	9.031 e^{-09}	0.99	0.019

Table 4. Calibration and Cross-Validation results in PLS models for total chlorophylls, carotenoids and anthocyanins, rutin and firmness, calculated on the data sets generated from PLS on parameters of three cultivars Leccino, Leucocarpa and Buscionetto.

For the parameter oleuropein, verbascoside, 3,4-DHPEA-EDA and total phenols it has been used Calibration models (*Table 5*), already generated by Bellincontro et al. (2012), to validate PLS models of this research. A substantial reduction was observed for predicted R^2, ranging from the lowest 0.74 calculated for oleuropein to the highest 0.85 for the total phenols. Moreover, the RMSEP index showed a 2-fold increased error compared to RMSEC.

compound	n	calibration				prediction	
		R^2	RMSEC	LVs	Bias	R^2	RMSEP
oleuropein	33	0.89	0.74	8	-1.210 e^{-07}	0.74	1.2
verbascoside	33	0.96	0.09	10	-6.954 e^{-08}	0.82	0.23
3,4-DHPEA-EDA	33	0.93	1.44	7	-1.350 e^{-07}	0.84	2.28
Total phenols	33	0.96	1.35	5	-1.210 e^{-07}	0.85	2.82

Table 5. Values of determination coefficient generated from Calibration and Prediction for oleuropein, verbascoside,3,4-DHPEA-EDA and total phenols used in PLS models. The calculated values have been done on the data sets generated from PLS on parameters of three cultivars Leccino, Leucocarpa and Buscionetto.

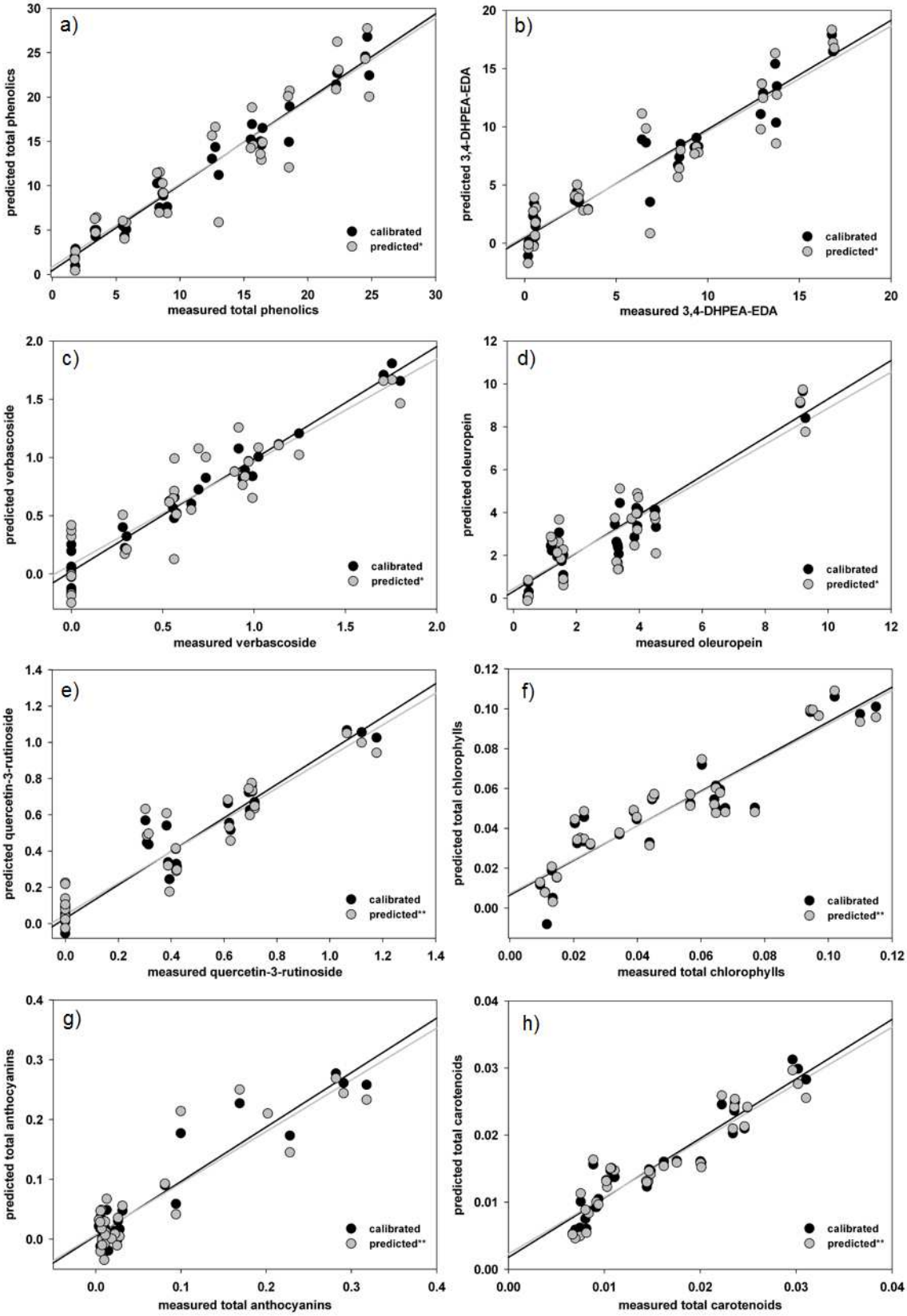

*Figure 11. Scatter plots of calculated and predicted models for all classes of parameters, generated on the global data set of olive samples (sum of the three cultivars). For each compound measured, calculated values are plotted versus predicted values. *cross validated **predicted*

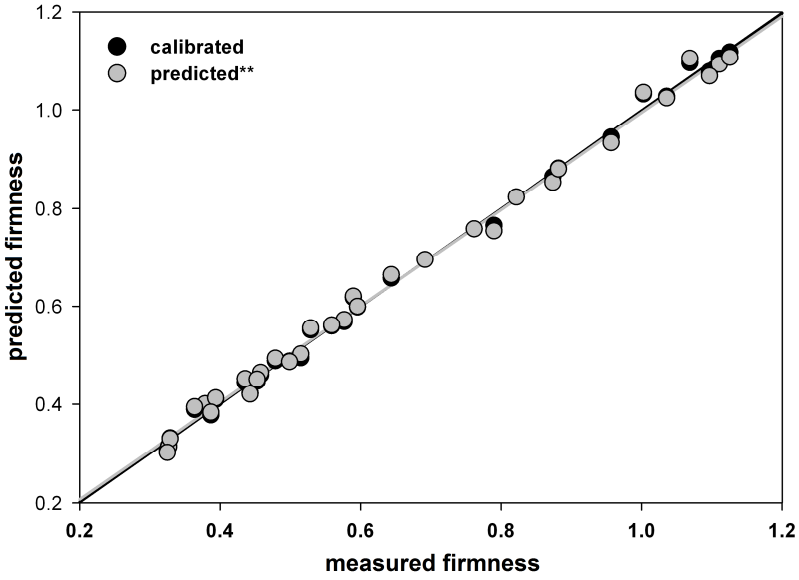

Figure 12. Scatter plots of calculated and predicted models for the firmness, generated on the global data set of olive samples (sum of the three cultivars). Calculated values are plotted versus predicted values.

BIOINFORMATIC ANALYSIS

2.18 BIOINFORMATIC IDENTIFICATION OF CANDIDATE FLAVONOID GENES FROM OLIVE FRUIT EST DATABASE

The expression of flavonoid structural genes, as well as transcription factor genes, and the accumulation of metabolites has proven to be useful in the identification of candidates controlling specific branches of the flavonoid pathway, particularly in Arabidopsis (Borevitz *et al.*, 2000; Nesi *et al.*, 2001; Mehrtens *et al.*, 2005). Therefore to unravel genetic bases of olive drupe colour regulation a Blast-based approach were used to identify candidate genes and transcripts coding for flavonoids biosynthesis enzymes, searching in olive fruit EST Database available at www.oleadb.org website and a local olive flower EST library (under submission). Identified genes or EST have been subjected to further confirmation, searching inside an advanced assembly of Olive Genome, available to our laboratory because member of partnership of Olive Genome Project (www.oleagenome.org website). Annotation of the putative genes and EST to properly attribute the physiological function has been done by Blast approaches, using BioLign software.

A general high degree of sequence homology between putative olive flavonoid gene sequences found and those present in NCBI have used as tools to annotate the identified sequences. Identified gene encompass all the principal branch of flavonoid pathways, starting from Phenylalanine ammonia lyase gene, herewith named *OePAL and* coding for the correspondent enzyme, which catalyze the first and committed step for flavonoid biosynthesis, to the flavonoid-3-O-glucosyltransferase enzyme codified

by the respective gene (*OeUFGT1*), which regulates anthocyanins biosynthesis. In particular, besides main structural genes (*Table 6*), we have identified more the one transcript coding for two different chalcone synthase isoform, named *OeCHS1* and *OeCHS2*, and two putative isoforms of anthocyanidin synthase/leucoanthocyanidin dioxygenase gene, which regulate the bi-directional synthesis of anthocyanidins or dihydroflavonol, respectively named *OeANS* and *OeLDOX*. Moreover, we have identified three putative flavonoid-glucosyltransferase genes: the flavonol-3-O-glucosyltransferase named *OeUFGT73C6 and* involved in last step of quercetin-3-rutinoside (also called rutin) biosynthesis, the main flavonol present in olive fruit; the anthocyanidin-3-glucosyltransferase, named *OeUFGT1*; and the anthocyanidin-3-glucosyltransferase, named *OeUFGT2* and putatively involved in di-glycosylation of anthocyanidins.

Name[a]	Similarity[b]	EST ID[c]	Length (bp)	BlastX [d] E-value	Function
OeF3H	Flavanone-3-beta-hydroxylase [*Capsicum annuum*] ACL54955.1	OLEEUCl024163 OLEEUCl024207 E8NTSAO04I0RKA	852 573 141	1e-97	Flavanonols biosynthesis
OeFLS EC 1.14.11.23	Flavonol synthase [*Petunia x hybrida*] Q07512.1	OLEEUCl011185 E8NTSAO03GKZS6	1,915 161	0.0	Flavonols biosynthesis
OeDFR	Dihydroflavonol reductase [*Forsythia x intermedia*] CAA70345.1	OLEEUCl084535	623	7e-101	Leucoanthocyanidins biosynthesis
OeANS EC:1.14.11.19	Anthocyanidin synthase [*Forsythia x intermedia*] CAA73094.1	OLEEUCl021221	1,302	0.0	Anthocyanidins biosynthesis
OeCHI	Chalcone isomerase [*Camelia nitidissima*] ADZ28513.1	OLEEUCl008312 E8NTSAO04IL6B7 E8NTSAO03GTD9T	1,204 168 135	7e-111	Flavanones biosynthesis
OeCHS2 EC:2.3.1.74	Chalcone synthase [*Misopates orontium*] CAJ44127.1	OLEEUCl009021 OLEEUCl009022	1,419 795	0.0	Chalcones biosynthesis
OeUFGT1 EC:2.4.1.115	Flavonoid-3-O-glucosyltransferase [*Forsythia x intermedia*] AAD21086.1	OLEEUCl016582 OLEEUCl088496 OLEEUCl016582 OLEEUCl023104	900 698 519 476	4e-121	Anthocyanins biosynthesis
OePAL EC:4.3.1.24	Phenylalanine-ammonia-lyase [*Olea europaea*] AFS28702.1	OLEEUCl011172 OLEEUCl006618 E8NTSAO03F1AYP OLEEUCl039145	1,046 648 325 246	0.0	Phenylpropanoid biosynthesis
OeF3'H EC 1.14.13.21	Flavonoid 3'-hydroxylase [*Ipomoea lutea*] ACL26687.1	OLEEUCl005685 E8NTSAO04JLR8N OLEEUCl073264	1007 490 410	2e-20	Flavonols biosynthesis
OeFNSII EC 1.14.11.22	Cytochrome P450 [*Antirrhinum majus*] BAA84071.1	OLEEUCl033485 E8NTSAO02C2YDP OLEEUCl023103	759 527 462	8e-96	Flavones biosynthesis
OeUGT73C6 EC: 2.4.1.159	UDP-glucosyltransferase [*Ricinus communis*] XP_002519419.1	OLEEUCl033042 E8NTSAO01AWJXC	252 118	2e-24	Flavonols biosynthesis
OeLDOX EC:1.14.11.19	Leucoanthocyanidin	contig01948*	984	6e-147	Anthocyanidins biosynthesis

	dioxygenase [Ricinus communis] XP_002533635.1				
Oe4CL	4-coumarate ligase [Paulownia fortunei] ACL31667.1	OLEEUCl051455	564	3e-97	Phenylpropanoid biosynthesis
OeUFGT2 EC:2.4.1.115	Anthocyanidin 3-O-glucosyltransferase [Medicago truncatula]	OLEEUCl086039 E8NTSAO02ENIED OLEEUCl015298	385 250 391	1e-55	Anthocyanins biosynthesis
OeCHS1 EC:2.3.1.74	chalcone synthase 2-like [Solanum tuberosum] XP_006359643.1	contig00521*	1,472	0.0	Chalcones biosynthesis

Table 6. Putative genes identified in O. europaea fruit and flower library. [b] NCBI Blast similarities. [c] Transcripts identification code. [d] Transcript length. [e] Overall Blast e-values. [f] putative assigned function. EC number

2.19 IDENTIFICATION OF CANDIDATE TRANSCRIPTION FACTORS UPSTREAM REGULATORS OF FLAVONOID BIOSYNTHESIS

Several Tentative Consensus (TC) sequences coding for transcription factors putatively involved in upstream regulation of flavonoid pathways were identified in olive fruit and flower EST library (*Table 7*). They belonged to MYB, bHLH and WDR family protein. Identified transcripts were used for a detailed research inside Olive Genome assembled, to define accurately their genetic structure. Putative MYB TFs identified in this research all encode putative R2R3-type MYB factors, where the N-terminal MYB DNA-binding domain consists of two repeats. The number and position of introns within the MYB sequences were generally conserved when compared with other species. Based on the bioinformatic analyses, the deduced *O. europaea* MYB proteins were assigned putative functions (*Table 7*). Briefly, we identified three olive orthologs of the grape gene *VvMYBPA1*, involved in the regulation of flavan-3-ols biosynthesis, named *OeMYBPA1-1*, *1-2* and *1-3*, an orthologs of the *Gossypium* gene *GhGHMYB10*, named *OeMYB10*, a putative flavonol-related MYB named *OeMYBF1* and a putative MYB-C2 supposed toe a potential repressor motif, named *OeMYBC2*.

Sequence Name[a]	**Best BLAST hit[b]**	**% Identity/Similarity**	**Length (aa)**	**BlastP [d] E-value**
OeMYBF1	MYBF1 [V. vinifera] ACV81697.1	43.9 / 56.9	350	1e-80
OeMYBPA1-1	MYBPA1 [V. vinifera] NP_001268160.1	47.3 / 59.8	267	4e-81
OeMYBPA1-2	MYBPA1 [V. vinifera] NP_001268160.1	41.5 / 54.7	300	1e-75
OeMYBPA1-3	MYBPA1 [V. vinifera] NP_001268160.1	49.8 / 59.8	253	4e-80
OeMYB2	MYB2 [G. hirsutum] AFN53770.1	54.2 / 67.7	201	6e-64

OeMYB10	GHMYB10 [T. cacao] EOY30297.1	45.6 / 54.1	268	1e-78
OeMYBC2	MYB4a [V. vinifera] NP_001268129.1	78.7 / 86.6	250	3e-132
OebHLH	DELILA [A. majus] AAA32663.1	51.7 / 65.1	589	0.0
OeTT8*	MYC1 [Diospyros kaki] AEC03343.1	47.9 / 60.3	440	7e-114
OeWDR	TTG2 [N. tabacum] ACN87316.1	84.2 / 90.5	348	0.0

Table 7. Putative flavonoid-related transcription factors identified in O. europaea fruit and flower library.

Surprisingly, we did not succeed in the identification of putative olive anthocyanin-related R2R3-MYB in all olive EST library queried. Using the conserved R2R3-MYB domain of *VvMYBA1*, *AtPAP1*, *MdMYB10* and *AmROSEA*, as input for BLAST search, we identified only one sequence which shown a similarity to *G. hirsutum* MYB2 protein (*GhMYB2*), belonged to *A. thaliana* GL1/WER subgroup 15 clade and involved in trichome development (Wang et al. 2004). The research conducted to explore the olive genome assembled gave similarly negative results. In particular, the motif ANDV and KPRPR[S/T][F/L] both privative of MYB associated with anthocyanin regulation (Quattrocchio et al., 1999; Borevitz et al., 2000; Stracke et al., 2001; Peel et al., 2009) seems to be absent in all identified olive putative R2R3-MYB genes. However, results of bioinformatic research do not allow to exclude the presence of *O. europaea* MYB10/MYBA/PAP1 orthologs and further analysis should be required.

Olive putative flavonol biosynthesis regulator OeMYBF1 has the conserved flavonol-specific motif DNEIKNYNSHLSRK into the R2R3-MYB domain, and outside, close to COOH terminal region, the conserved subgroup 7 motif GRTxRSxMK, which in OeMYBF1 *presents an amino acid substitution* (GRTxQSxKK) and the subgroup 7-2 motif WLLS. *OeMYBF1* gene encodes a 350 amino acid predicted protein with a similar size to the well-characterized homologs flavonol regulators proteins of *A. thaliana*, *V. vinifera* and *L. esculentum*, which size ranging from 326 to 369 amino acids. Full-length protein sequence comparison showed the best similarities with *VvMYBF1* (56.9%). The similarities strongly increase when the R2R3-MYB domain (93.9%) is only compered. All data from bioinformatics analysis suggest that *OeMYBF1* gene could be functionally related with other MYB-flavonol regulator.

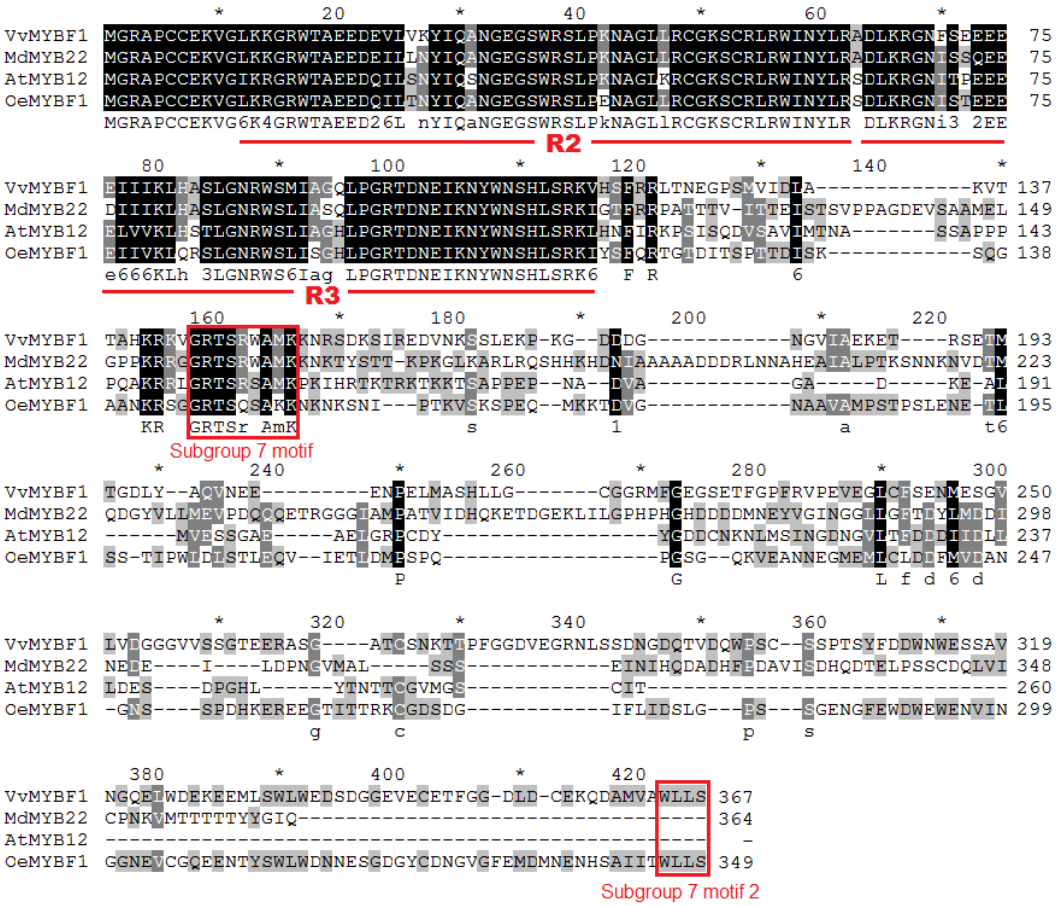

Figure 13. Aminoacidic alignment and conserved domain of the putative flavonol-regulator OeMYBF1 with functional characterized orthologs of A. thaliana (AtMYB12), M. domestica (MdMYB22) and V. vinifera (VvMYBF1).

The complete identified ORF of *OeMYBPA1-1*, *OeMYBPA1* and *OeMYBPA1-3* encoded proteins of 267, 300 and 253 amino acid residues, respectively. Analyses of the deduced amino acid sequence revealed that the three proteins contain an N-terminal R2R3-MYB domain with the conserved motif [D/E]Lx2[R/K]x3Lx6Lx3R, functional related to the interaction with bHLH proteins, however, it show the *VvMYBPA1* conserved motif EYLQLL (Bogs et al. 2007) functional involved in the flavan-3-ols biosynthesis and privative motif of the subclade 5. Full-length protein sequence comparison of OeMYBPA1-1, OeMYBPA1 and OeMYBPA1-3 shown the best similarities to *VvMYBPA1* (Bogs *et al.*, 2007), wherewith share of 47.3%, 41.5% and 49.8%, respectively, sequence identity (Table 3.3). OeMYB10 is similar (45.6% of identity) to other flavan-3-ols regulators, such as GhGHMYB10 and TaMYB14 (Hancock et al., 2012). this protein contains a nine-residue consensus sequence, V[I/V]R[T/P][K/R]A[I/L/V][R/K]C, in the highly variable C-terminal region (Fig. 2) that is also present in other flavan-3-ols-regulating TFs such as *AtTT2* (Nesi et al., 2001), *TaMYB14* (Hancock et al., 2012) and *VvMYBPA2* (Terrier et al., 2009). The previously described C-terminal motif EYLQLL found in *VvMYBPA1* is absent.

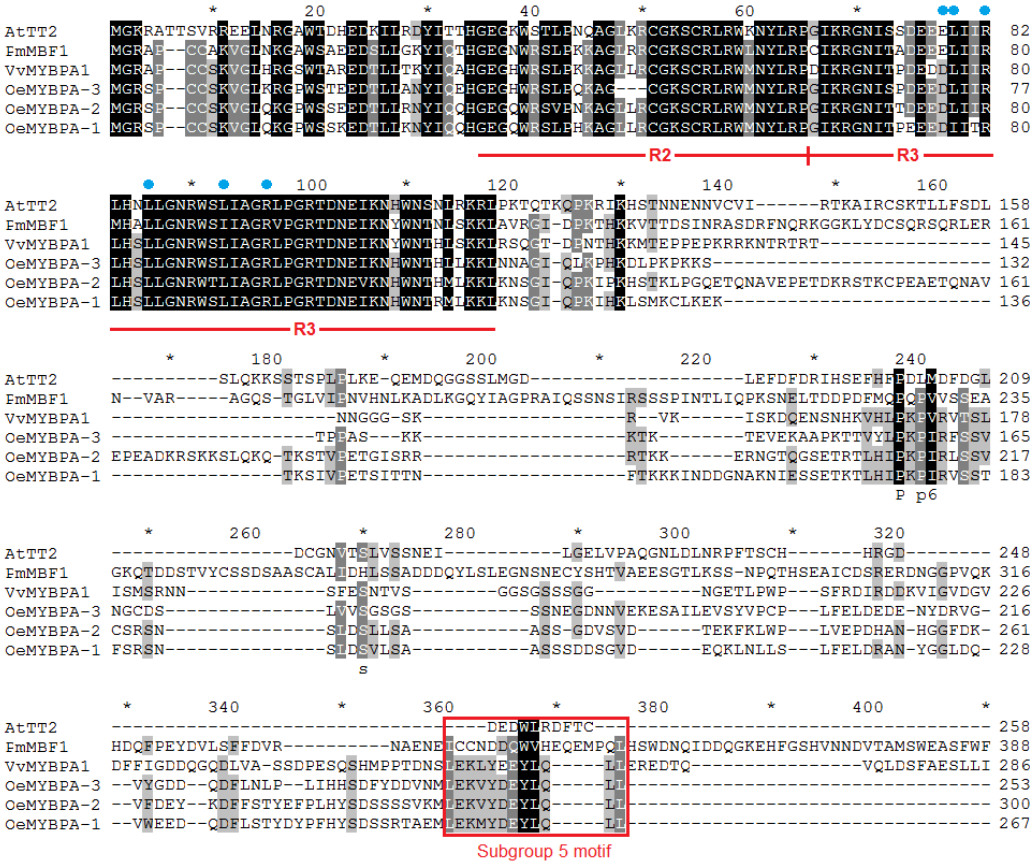

Figure 14. Aminoacidic alignment and conserved domain of the putative flavonoid pathway regulators OeMYBPA1-1, OeMYBPA1-2 and OeMYBPA1-3 with functional characterized orthologs of A. thaliana (AtTT2), V. vinifera (VvMYBPA1) and P. mariana (PmMBF1). Blue circle represent aminoacidic residues involved in the interaction with bHLH proteins.

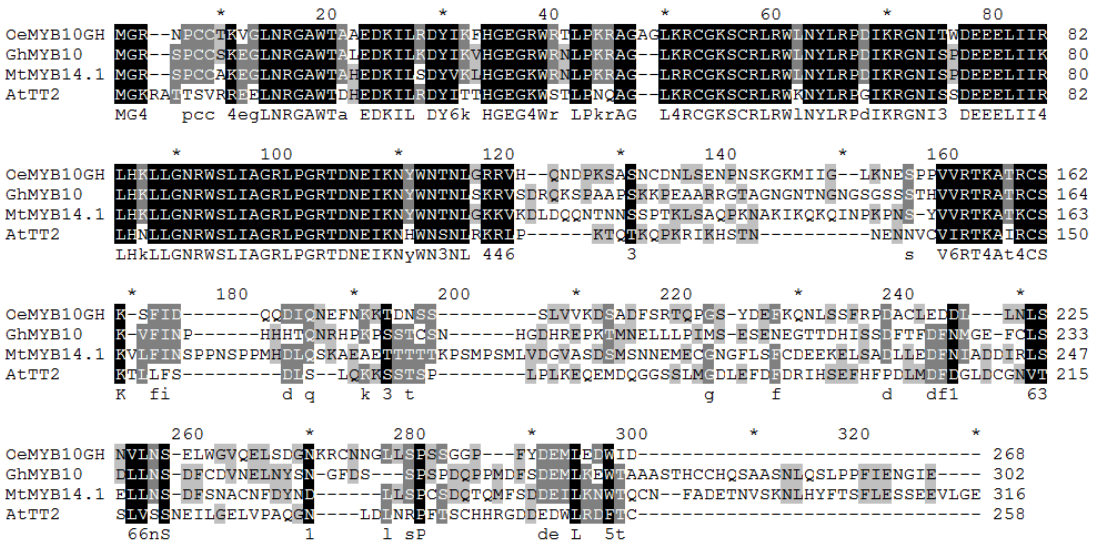

Figure 15. Aminoacidic alignment of the putative olive tannin-regulator OeMYB10gh, with functional characterized orthologs of G. hirsutum (GhMYB10), M. truncatula (MYB14.1) and A. thaliana (AtTT2).

In addition to the putative transcriptional activators, an R2R3-MYB (named *OeMYBC2*) was identified, displaying high degree of similarity to known negative regulators such as *VvMYB4* and *AtMYBL2*. The 250 amino acid deduced *OeMYBC2* protein share 78.7% identity with VvMYB4 and 60.4% with AtMYBL2, the last one has been shown to control the production of sinapate ester sunscreens through repression of the phenylpropanoid gene *cinnamate 4-hydoxylase* (*C4H*) (Jin *et al.*, 2000), and Dubos and collaborators (2008) clearly demonstrated, through silencing technology, that this TF strictly regulate the synthesis of Anthocyanins in *A. thaliana*.

Besides the R2R3-MYB transcription factors mentioned, other important flavonoid related genes of the bHLH and WDR families were also identified in olive. We identified two flavonoid-related bHLH genes: a full-sequence of 589 aminoacidic residues, named *OebHLH* and a partial sequence of 440 aa, named *OeTT8. OebHLH* had the conserved bHLH domain, the N-terminal domain described for proteins belonging to sub-groups IIId, e, f (Heim et al., 2003) involved in binding a MYB-type interaction partner (Goff et al., 1992; Grotewold et al., 2000; Pattanaik et al., 2008, An et al., 2012) and a sequence rich in acidic amino acids (*Figure 16*). Full-length protein sequence comparison shown the best similarities with *A. majus* DELILA gene (51.7% identity). The partial protein OeTT8 share 60.1% amino acid identities and 47.9% similarities with a MYC1 protein of *Diospyros kaki* (*Table 7*).

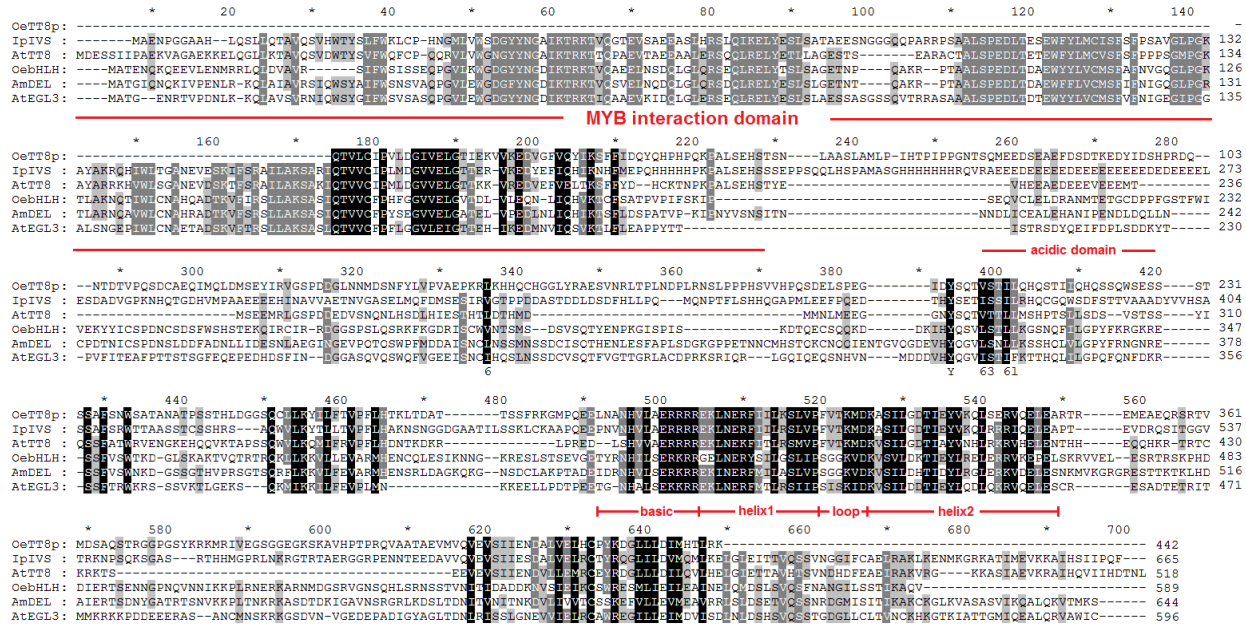

Figure 16. Aminoacidic alignment of the two identified olive bHLHs genes, OeTT8 and OebHLH, with functional characterized bHLH family protein of I. purpurea (IpIVS), A. thaliana (AtTT8 and AtEGL3), and A. majus (AmDEL)

Finally, we identified an olive WDR family protein of 348 aminoacidic residues, named OeWDR. The identified protein had the conserved four WD-repeat motif (*Figure 17*), a 40-60 residue sequence composed by glycine-histidine (GH) dipeptide at the N-region and a WD dipeptide at the C-region (Smith et al. 1999). OeWDR protein had best similarity (84.2%) with *N. tabacum* TTG2-like proteins. Besides the identification of best olive candidates R2R3-MYB for regulating flavonoid other putative MYB with unknown function were also identified.

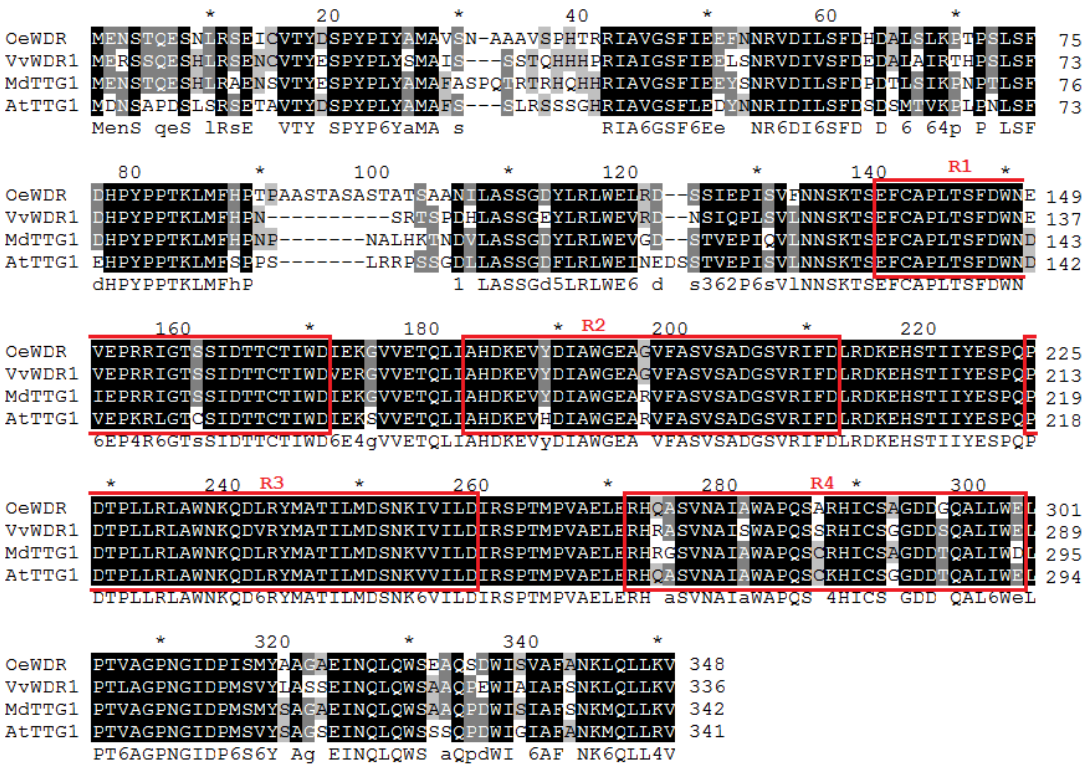

Figure 17. Aminoacidic alignment and conserved domains of the best identified olive WDR gene with already functional characterized WDR genes of V. vinifera (VvWDR1), M. domestica (MdTTG1) and A. thaliana (AtTTG1).

2.20 PHYLOGENETIC CLUSTERING OF CANDIDATES WITH CHARACTERIZED REGULATORS

Phylogenetic analysis of olive R2R3-MYB transcription factors were performed to further confirm their putative roles in flavonoid pathway. As expected from the previously described sequence homology, olive MYB proteins fell into functional clades with characterized and putative branch-specific flavonoid pathway regulators from different plant species (*Figure 18*). In particular, the three identified OeMYBPA1-3 proteins, all together, clustered in a clade of R2R3-MYB subgroup 5, which includes VvMYBPA1 and DsMYBPA1, while OeMYBF1 clustered with other flavonol-regulator such as VvMYBF1 and AtMYB12. As expected, the putative favan-3-ols-related R2R3-MYB OeMYB10 clusters in the clade of AtTT2, closely to uncharacterized grape homologs VvTT2-like. Interesting, the most closely olive anthocyanins-related R2R3-MYB (OeMYB2) clusters in the same

clade of WEREWOLF and GLABRA, proteins involved in trichome development and tissue-specific anthocyanins biosynthesis. Finally, OeMYBC2 clusters with other transcriptional repressors, such as *VvMYB4a* and *AmMYB308*. The presence of motifs supports the putative assignments of function to the olive MYB factors. Conserved motifs in the C-terminal region were used to classify MYB factors into subgroups (SGs), within which the TFs often share similar functions (Stracke *et al.*, 2001). However, this classification undergone to revision and extension, to include motifs characterized in other plant family such as *Rosaceae*, *Vitaceae* and others. Bioinformatic analysis of *O. europaea* MYB proteins suggest a broad similarity with grape MYB homologs, such as MYBPA1, MYBF1 and MYB4a

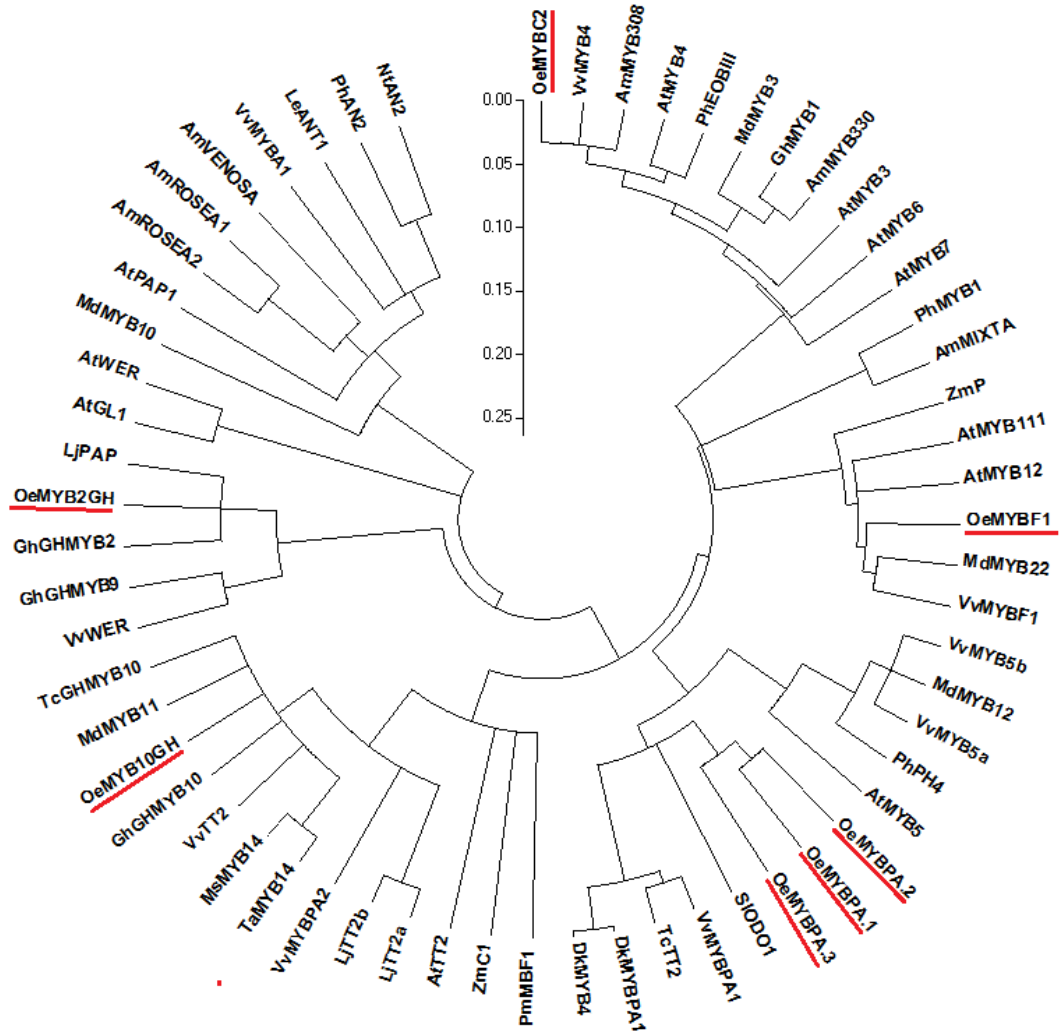

Figure 18. Consensus circular rooted tree of phylogenetic relationships among selected flavonoid-related MYB in plant species. The scale bar represents the number of substitutions per site.

Protein accession were obtained from NCBI database: VvMYBA1 (ABD72953.1), ZmP (P27898.1), ZmC1 (AAA33482.1), AtPAP1 (AAG42001.1), PhAN2 (AAF66727), LeANT1 (AAQ55181.1), OsMYB4 (O23892), NtAN2 (ACO52470.1), AtMYB5 (U26935), PhMYB1 (CAA78386.1), MdMYB10 (BAJ24837.1), AmMIXTA (CAA55725.1), AtMYB12 (CAB09172), AtMYB111 (AAK97396.1), VvMYBPA1 (AM259485), AtGL1 (P27900.2), AtTT2 (Q9FJA2), PhPH4 (AAY51377), AtWER (CAC01874.1),VvMYB5b (Q58QD0), VvMYB5a (AAS68190),

PmMBF1 (AAA82943.1), AmVENOSA (ABB8828.1), AmROSEA2 (ABB83827.1), AmROSEA1 (ABB83826.1), MdMYB22 (AAZ20438.1), VvMYBF1 (ACV81697.1), GhMYB1 (AAA33067.1), GhMYB10 (ABR01222.1), AtMYB6 (NP192684.1), AtMYB3 (NP_564176.2), AtMYB4 (NP_195574.1), AmMYB330 (P81395.1), VvWER (XP002279941.1), LjPAP (BAH28879.1), GhGHMYB9 (AAK58020.1), VvTT2 (XP002275148.1), GhGHMYB2 (AAU12248.1), LjTT2a (BAG12893.1), LjTT2b (BAG12894.2), GhGHMYB10 (AAK19615.1), MdMYB11 (AAZ20431.1), MdMYB12 (ADL36755.1), TcTT2 (ADD51352.1), DkMYBPA1 (AEC11088.1), SlODO1(XP004244728.1), AmMYB308(P81393.1), AtMYB7 (NP179263.1), TcGHMYB10 (EOY30297.1), PhEOBIII (ADK12668.1), VvMYB4 (NP001267938.1), TaMYB14 (AFJ53053.1), VvMYBPA2 (ACK56131.1), MsMYB14 (AFJ53055.1), DkMYB4 (BAI49721.1).

Phylogenetic analysis of identified olive bHLH family proteins (*Figure 19*) highlighted a difference between the two putative olive flavonoid-related bHLH, *OebHLH* and *OeTT8*. Indeed, *OebHLH* protein clusters with the clade of *A. majus DELILA* (*AmDEL*), grape *MYCA1* and Arabidopsis *GLABRA3* (*AtGL3*) and *ENHANCER OF GLABRA3* (*AtEGL3*) genes, involved in trichome-specific regulation of anthocyanin accumulation. Partial protein sequence of *OeTT8*, instead, clusters very closely to Arabidopsis *TRANSPARENT TESTA8* (*AtTT8*), grape *MYC1* and the recently characterized gene *IVORY SEED* (*IpIVS*) of Ipomea. Finally, *OeWDR* protein clusters (*Figure 20*) in a subclade of Arabidopsis TRANSPARENT TESTA GLABRA1 protein (*AtTTG1 gene*) and it is closely related to grape and petunia orthologs VvWDR and PhAN11.

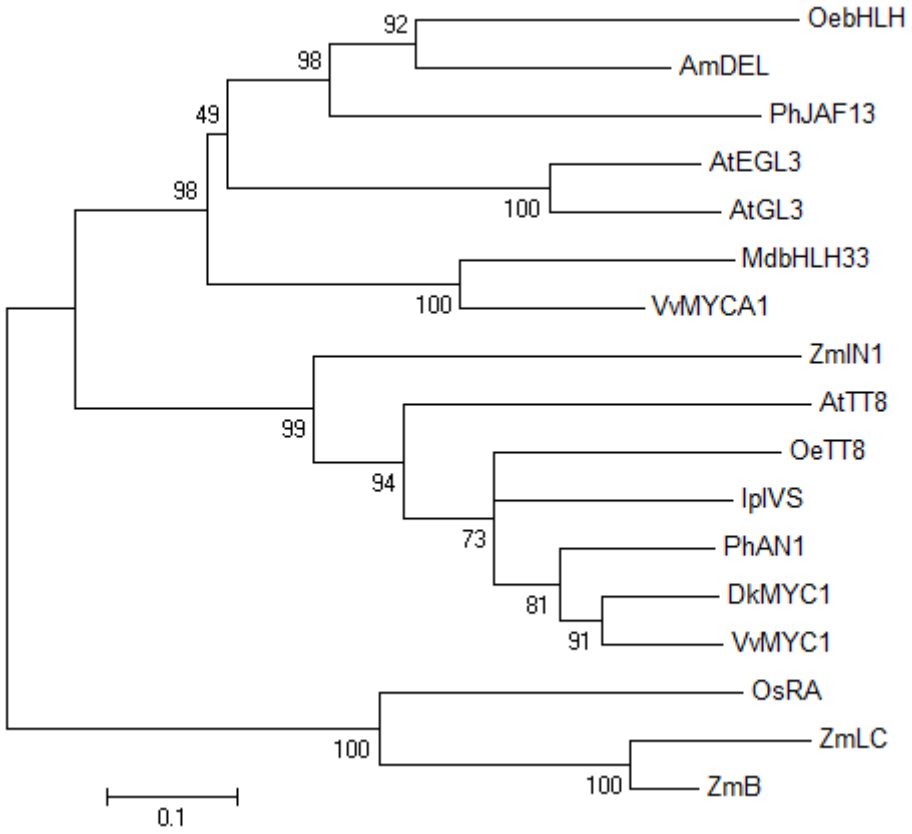

Figure 19. Phylogenetic tree of bHLH proteins regulating the flavonoid pathway in plants. The bootstrap values out of 1000 retrials are indicated at each branch. The scale bar represents the number of substitutions per site. Protein accession were obtained from NCBI database: PhAN1(AAG25928), AtTT8(CAC14865), ZmB (CAA40544), ZmLc(ABD72707), OsRa(AAC49219), AmDEL (AAA32663), PhJAF13(AAC39455), MdbHLH33

(ABB84474), AtEGL3(NP_176552) and AtGL3(NP_680372) VvMYCA1(ABM92332), VvMYC1(ABR23669), together with identified olive bHLH protein OebHLH and partial OeTT8.

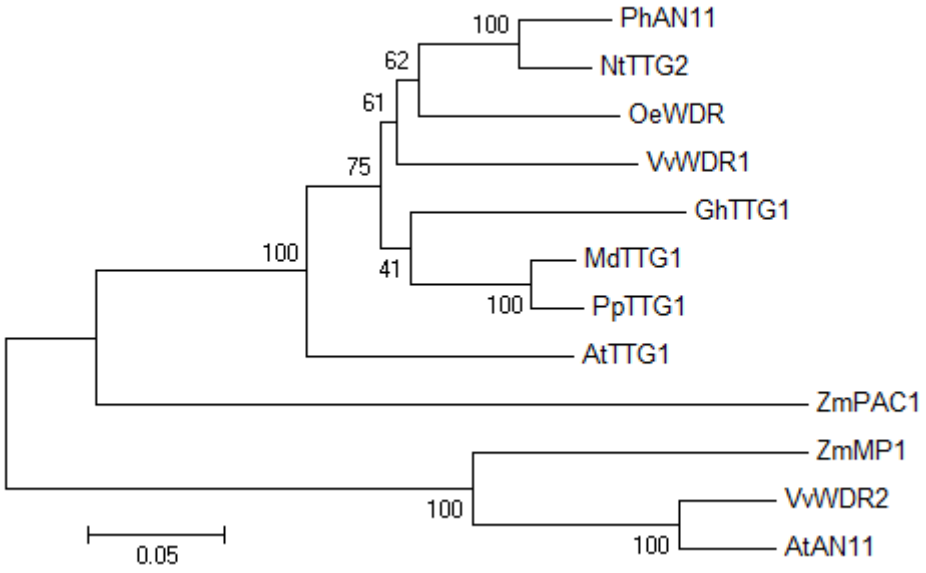

Figure 20. Phylogenetic tree of WDR proteins regulating the flavonoid pathway in plants. The bootstrap values out of 1000 retrials are indicated at each branch. The scale bar represents the number of substitutions per site. Protein accession were obtained from NCBI database: ZmMP1(AAR01949), GhTTG1 (AAM95641), AtAN11(AAC18912), ZmPAC1(AAM76742), AtTTG1 (NP_851070), MdTTG1(AAF27919), PhAN11(AAC18914), VvWDR1(ABF66625) and VvWDR2 (ABF66626).

2.20 TEMPORAL EXPRESSION OF GENES ENCODING STRUCTURAL GENES AND TRANSCRIPTION FACTORS DURING OLIVE FRUIT DEVELOPMENT AND RIPENING

Transcriptional regulation of gene coding for upstream flavonoid pathway enzymes closely mirrored the developmental accumulation of total flavonoids. Transcript levels of *OePAL* (*Figure 21a*) encoding a phenylalanine-ammonia-lyase enzyme, that produces cinnamoyl-CoA, the first metabolic intermediate for phenylpropanoid and flavonoid biosynthesis, resulted higher during the early stage of drupe development and then progressively declined until ripening in both cvs Leccino and Leucocarpa. However, *OePAL* resulted about 2-fold more expressed in drupe of cv Leccino in all four stage analyzed. A similar trend of expression during drupe development has been also observed for *Oe4CL* gene, coding for 4-coumarate ligase, *OeC3H* coding for *p*-coumarate-3-hydroxylase (*Figure 21b, c)*. However, these genes did not differ significative between the two cultivars, suggesting they could have only a secondary role in determining mutant phenotypes of cv Leucocarpa. Interesting, the chalcone synthase isoform *OeCHS1* (*Figure 21d*) has shown an increased expression at stage III (color change) resulting 2-fold more abundant in cv Leccino respect to Leucocarpa.

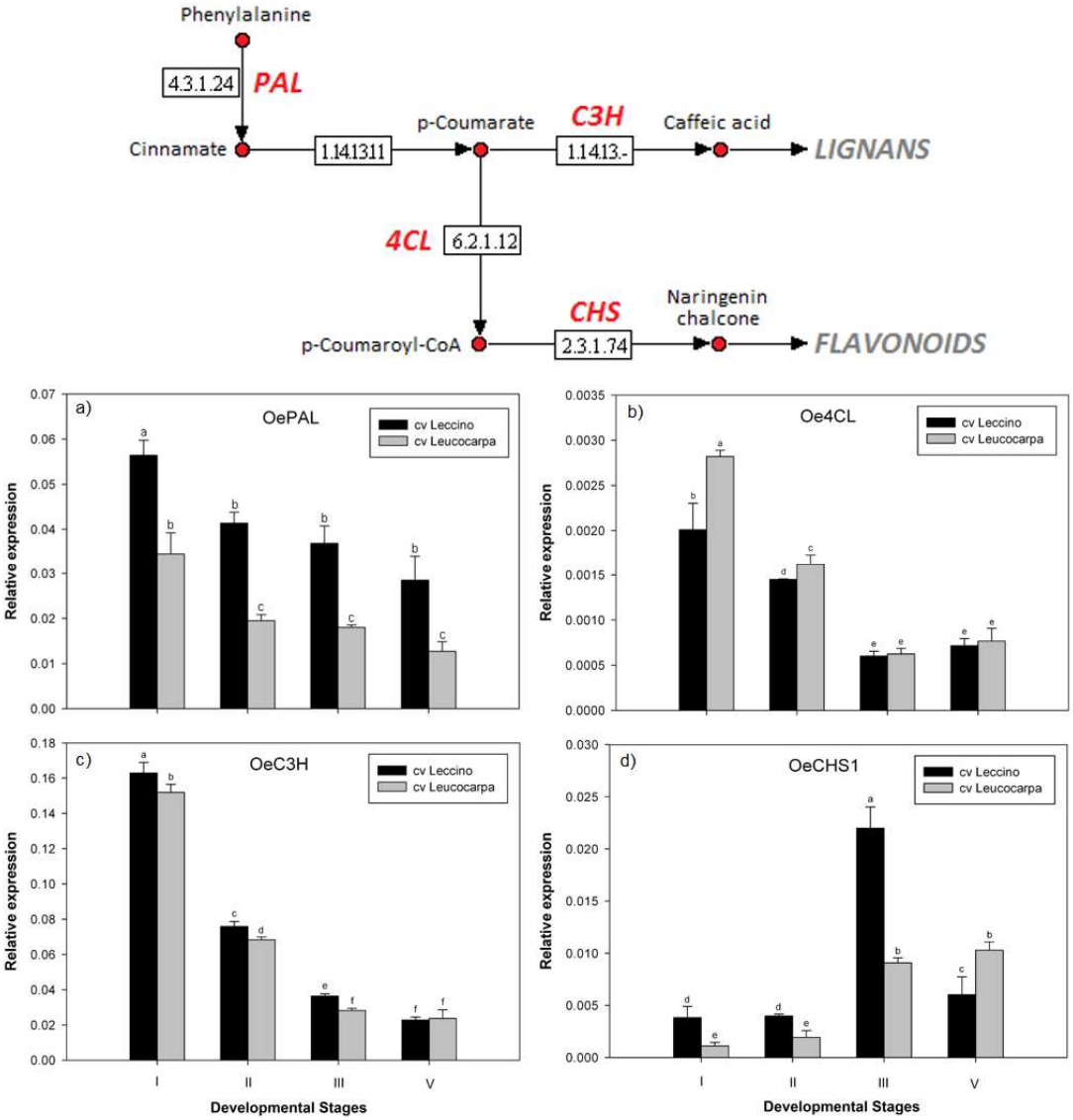

Figure 21. Expression pattern of genes coding early structural enzyme of flavonoid pathways in cvs Leccino and Leucocarpa along drupe development. Histograms are the mean of three biological replicates and bar represent standard error. Letters indicate statistical significant difference for p<0.01 (SNK test)

In cv Leccino, *OeCHI* gene, coding for chalcone isomerase, resulted highly expressed during early stage of fruit development, strongly decreased at mature green stage and then re-increased at color change reached highest amount at maturity (*Figure 22b*). A similar regulatory trend was observed in cv Leucocarpa along fruit development, however, expression level of *OeCHI* resulted about 3-fold lower than Leccino, independently from sampling stage. *OeF3H* gene, coding for flavanone-3-hydroxylase, resulted up regulated at the onset of ripening in cv Leccino, even if gene was expressed at comparable level since early stage of drupe development (*Figure 22c*). Important, *OeF3H* gene resulted very low expressed in cv Leucocarpa. The same was observed even for *OeDFR* (coding for a dihydroflavonol reductase) and *OeANS* (coding for anthocyanidin synthase) genes, which were strongly up-regulated at color change and maturity stages, but only in drupe of cv Leccino,

resulting barely detectable (*OeDFR*) or even absent (*OeANS*) in the colorless cv Leucocarpa (*Figure 22d, e*).

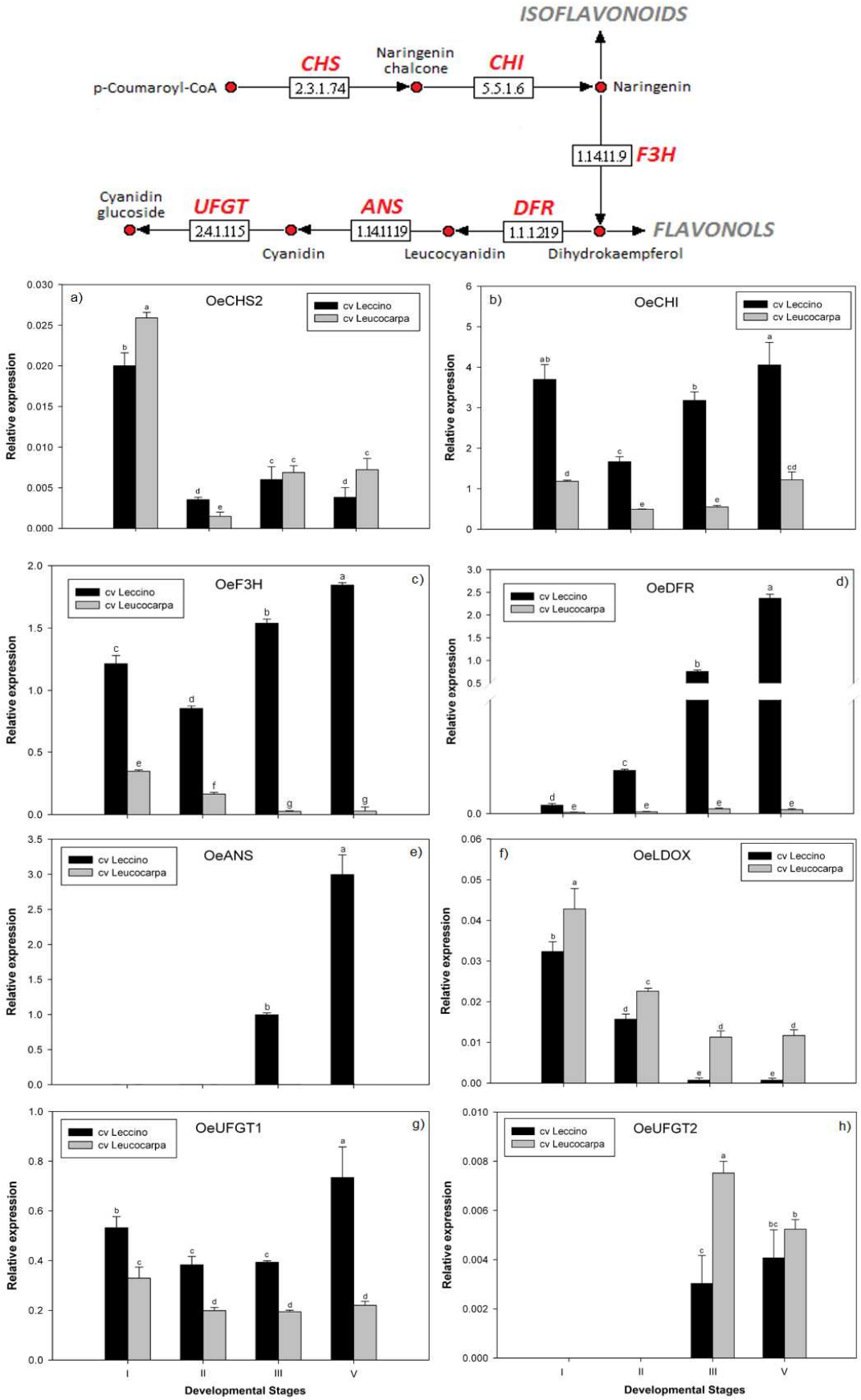

Figure 22. Expression pattern of genes coding structural enzyme of flavonoid pathways leading to anthocyanins biosynthesis in cvs Leccino and Leucocarpa along drupe development. Histograms are the mean of three

biological replicates and bar represent standard error. Letters indicate statistical significant difference for p<0.01 (SNK test).

Interesting, *OeLDOX* gene, encoding an anthocyanidin synthase isoform, result higher expressed in drupes of Leucocarpa, (*Figure 22f*) although this gene was expressed at very low level compared to *OeANS*. as Surprisingly, *OeUFGT1* gene, coding for a flavonoid-3-glycosil transferase and regulating the last step in anthocyanins biosynthesis, resulted to be expressed since early stage of drupe development in both cultivars, when detected anthocyanin concentration was very low ((Figure 22, g)). Subsequently, transcripts level decreased until ripe stage, when they increased again but only in drupe of cv Leccino. Even for this gene was observed a general lower expression in cv Leucocarpa, even if differences with cv Leccino were lower with respect to that observed for *OeF3H*, *OeDFR* and *OeANS*. Finally, we analyzed expression patterns of putative genes involved in flavone and flavonol biosynthesis. In particular, the flavone luteolin-7-glucoside and the flavonol quercetin-3-rutinoside (also known as rutin), both representing an important flavonoid fraction of olive drupe. As reported in bioinformatic analysis section, we identified in fruit and flower EST, transcripts coding for a flavonoid-3-hydroxylase (*OeF3'H*) and a type-II flavone synthase (*OeFNSII)* putatively involved in luteolin biosynthesis; a flavonol synthase (*OeFLS*) and a few characterized flavonol-3-glucoside L-rhamnosyltransferase (*OeUGT73C6*), putatively involved in last step of rutin biosynthesis. Except for *OeFNSII*, which did not appear differently regulated during drupe development, *OeFLS*, *OeF3'H* and *OeUGT73* resulted main expressed during early stage of drupe development and declined along drupe ripening. Moreover, we observed a higher expression of *OeFLS* and *OeUGT73* in cv Leucocarpa, and these results were somewhat surprising, considering that we found only traces of rutin compound in ripe drupes of cv Leucocarpa.

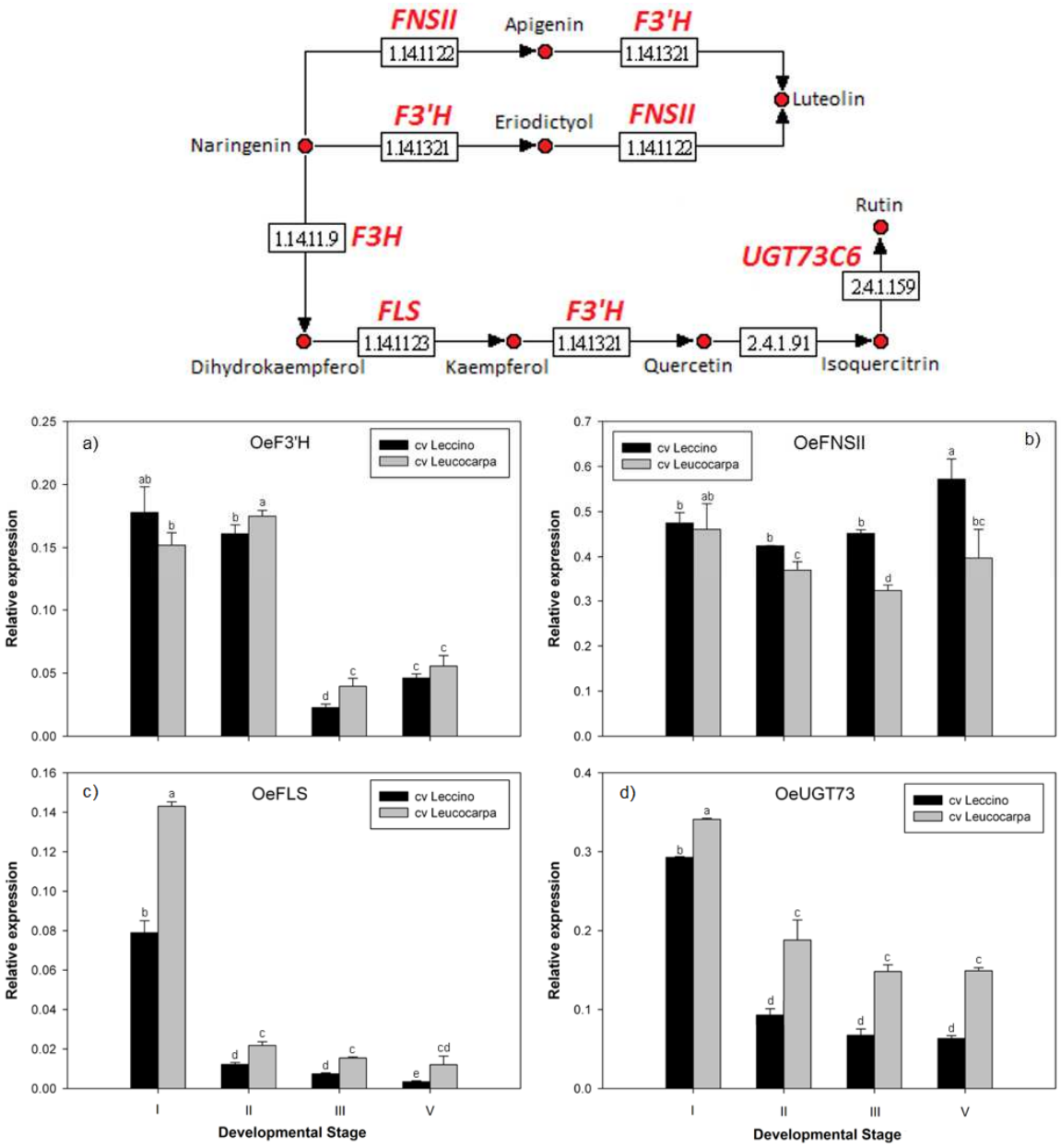

Figure 23. Expression pattern of genes coding structural enzyme of flavone and flavonols biosynthesis pathways in cvs Leccino and Leucocarpa along drupe development. Histograms are the mean of three biological replicates and bar represent standard error. Letters indicate statistical significant difference for p<0.01 (SNK test)

As previously described in bioinformatics section, we identified several olive orthologs genes coding for R2R3-MYB, bHLH and WDR transcription factors. Therefore, we analyzed their expression patterns during drupe development Despite we did not identify transcripts having high homology degree with anthocyanin-related R2R3-MYB subclade; three olive putative members of flavan3-ols related R2R3-MYB subclade have been identified, showing high degree of identity with VvMYBPA1 protein. Interesting, *OeMYBPA1-1* was about 10-fold more expressed respect to *OeMYBPA1-2*, independently from sampling stage (*Figure 24a, b*), suggesting it could be the main active *MYBPA1* isoform in olive

fruit. In contrast, transcripts coding for *OeMYBPA1-3* were not detect in drupe tissues (data not shown). *OeMYBPA1-1* and *OeMYBPA1-2* resulted up-regulated in young fruit in both cultivars Leccino and Leucocarpa and appeared correlated with accumulation of total flavonoids, higher in early stage of drupe development. Successively, transcripts level *OeMYBPA1-2* progressively decline along drupe ripening, reaching the lowest level at maturity. In contrast, transcripts level of *OeMYBPA1-1* strongly decreased at mature green stage, but re-increasing again starting from color change and until maturity. To get a more complete picture of olive flavonoid-related R2R3-MYB expression pattern in fruit, we also analyzed a flavonol-related R2R3-MYB (*OeMYBF1*), a putative olive tannin-related MYB (*OeMYB10*), a C2-repressor MYB (*OeMYBC2*) and an orthologs MYB of AtGL1 clade (*OeMYB2*). *OeMYBF1* resulted more expressed during early stage of fruit development and then strongly declined at mature green stage, remaining almost constant until drupe maturity (*Figure 24d*). Interesting, *OeMYBF1* was about 2-fold more expressed in Leucocarpa in all analyzed fruit developmental stage. Interesting, *OeMYBC2* gene resulted more expressed during early and middle stages of fruit development (until mature green stage) with no differences between Leccino and Leucocarpa (*Figure 24c*). However, at stage III, *OeMYBC2* transcript resulted to be strongly down regulated in both cultivars. *OeMYB10* resulted to be mainly expressed at stage I (early fruit development) and strongly declined already at mature green stage, resulting undetectable already at stage III (color change) (*Figure 24e*). Finally, we did not detect substantial differences in *OeMYB2* expression patterns (*Figure 24f*). This gene appear expressed at the same level in all fruit developmental stage, without differences between drupe of cv Leccino and Leucocarpa.

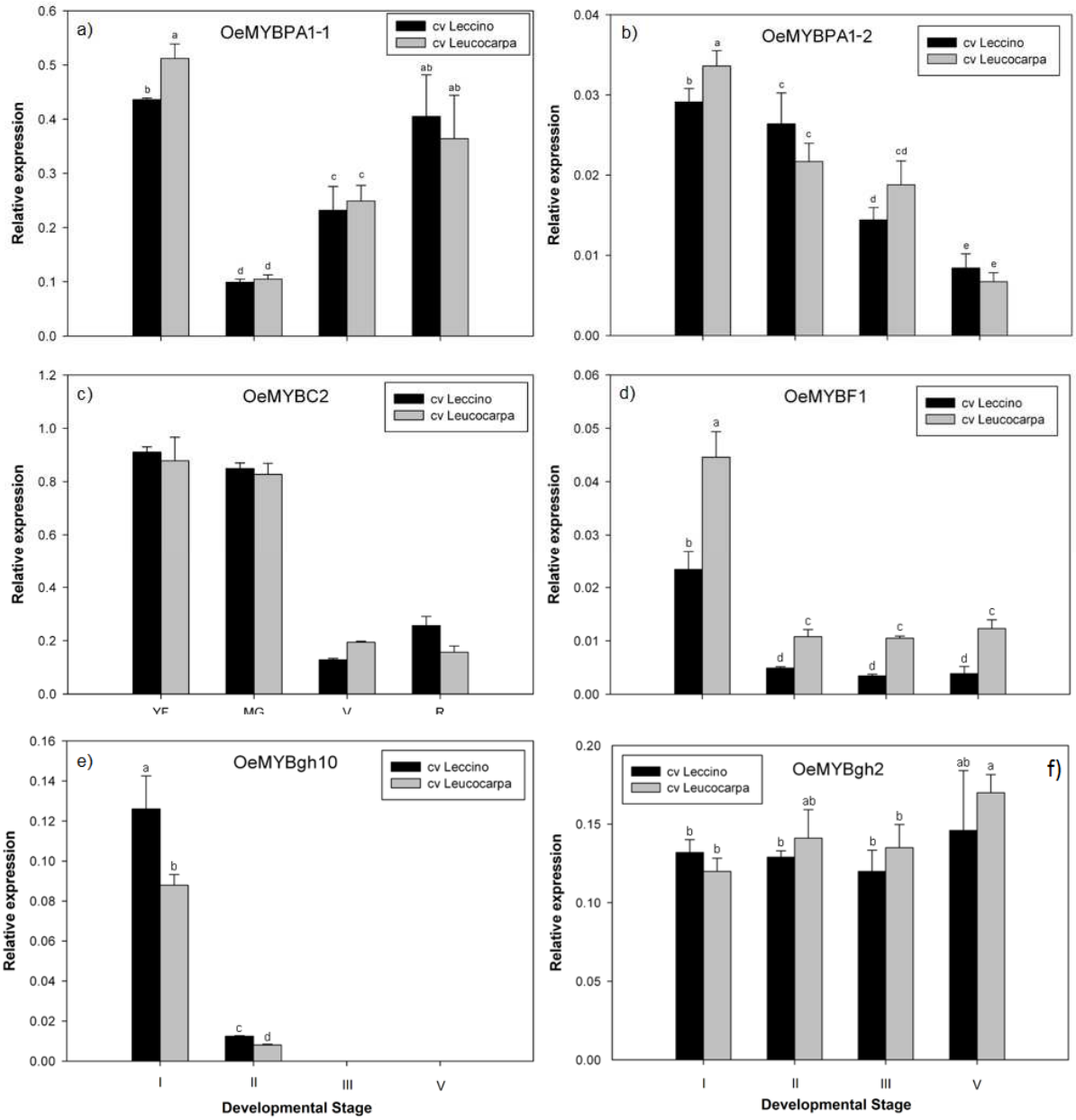

Figure 24. Expression pattern of genes coding olive R2R3-MYB transcription factors, putatively involved in the regulation of flavonoid pathways, in cv Leccino and Leucocarpa, along drupe development. Histograms are the mean of three biological replicates and bar represent standard error. Letters indicate statistical significant difference for p<0.01 (SNK test)

The two identified members of R clade of olive beta-HLH family protein, *OebHLH* and *OeTT8* coding for putative partners of MBW regulatory complex, have shown a distinct expression patterns along fruit development. *OeTT8* gene transcript was most abundant in young fruit, strongly declined already at mature green stage, resulting absent during ripening stages. On the contrary, *OebHLH* was most abundant in young fruit, as observed even for *OeTT8*, progressively decreased until color change and then re-increased again in ripe fruit. We did not observe significative differences in expression levels between the two cultivars Leccino and Leucocarpa. Finally, we analyzed also expression pattern of

the third putative member of MBW complex, *OeWDR*, coding for a WD-repeat protein. Expression pattern of *OeWDR* along fruit development resembled that observed for *OeMYBPA1-1* and *OebHLH*: transcripts were most abundant in young fruit, progressively declined until color change re-increasing again in ripe fruit.

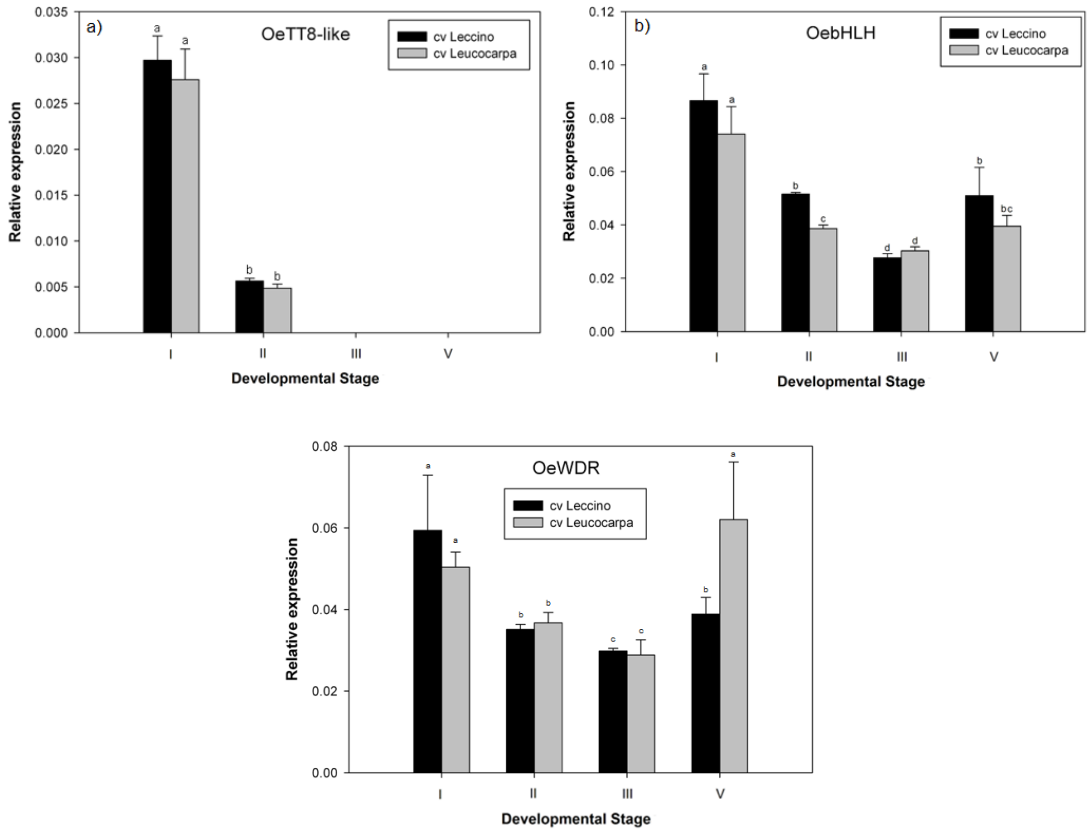

Figure 25. Expression pattern of genes coding best olive WDR and bHLHs candidates for flavonoids pathway regulation in cv Leccino and Leucocarpa, along drupe development. Histograms are the mean of three biological replicates and bar represent standard error. Letters indicate statistical significant difference for p<0.01 (SNK test)

The pivotal role of *OeDFR* and *OeANS* genes in the regulation of anthocyanin biosynthesis has been further confirmed by analyzing their expression pattern during drupe ripening in cv Buscionetto. Indeed, *OeDFR* and *OeANS* transcript levels strongly increased only at stage V (*Figure 26c, d*), when anthocyanin content dramatically increased. Instead, no significant difference have been found in *F3H* transcript levels. Interesting, the putative upstream regulator *OeMYBPA1-1* resulted up-regulated at stage V (*Figure 26e*) while, on the contrary, *OeMYBC2* was strongly down-regulated at this stage (*Figure 26f*). This general trend of regulation for *OeMYBC2* has also been observed in cv Leccino and Leucocarpa, suggesting that they could have a role in the negative regulation of anthocyanins biosynthesis. Finally, no significant differences have been found in other putative members of MBW complex, such as *OebHLH* and *OeWDR* genes during drupe ripening (*Figure 26g, h*)

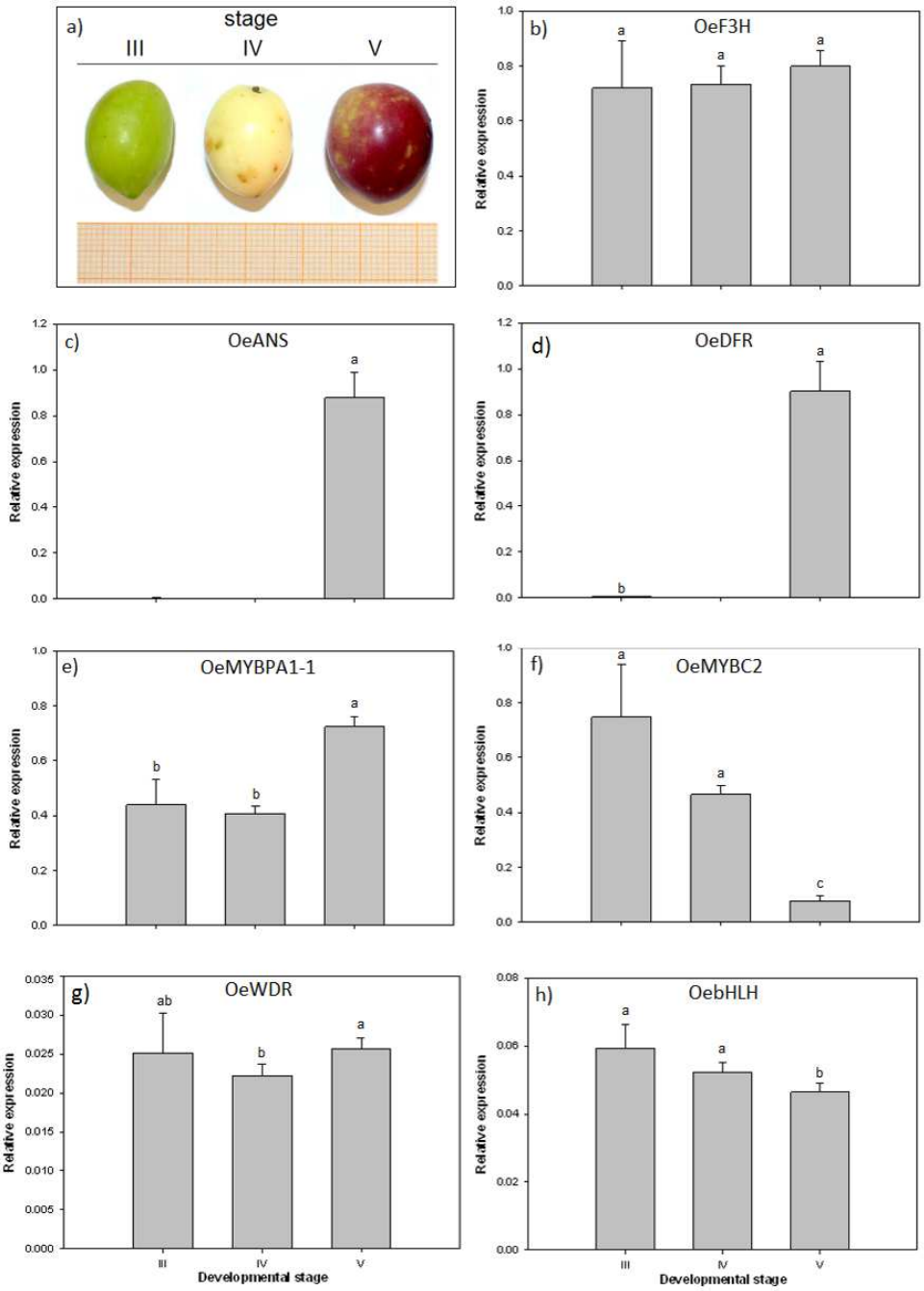

Figure 26. Expression pattern of genes and transcription factors putatively involved in anthocyanin biosynthesis in cv Buscionetto, along drupe development. Histograms are the mean of three biological replicates and bar represent standard error. Letters indicate statistical significant difference for p<0.01 (SNK test)

2 DISCUSSION

Drupe color-based indexes represent one of the most used ripening marker in many fruits, including olive (Roca et al., 2001). Anthocyanins compounds are the main pigments in olive fruit, conferring their typical black-purple color at maturity. Although, drupe color represents an important quality parameter for table olive production, however, this attributes play a role in oil quality compared to other pigments, such as chlorophylls and carotenoids. As reported by Roca et al. (2001), overall

evolution of pigments profile of drupe, during ripening, strongly depends on variety and it is influenced by environmental conditions. Different olive cultivars show a peculiar dynamics of chlorophyll and carotenoids degradation and the appearance of anthocyanins, which are associated with the pigmentation, could be link to a sharp drop in chlorophylls content. In this study, the dynamics of chlorophylls degradation resulted to be different among the drupes of cvs Leccino, Leucocarpa and Buscionetto during ripening, while the degradation of carotenoids did not show any significant differences. In the drupe of cv Leccino, a sharp change in chlorophyll degradation was observed at color change (stage III), in contrast to the drupe of cv Buscionetto, in which it occurs prior to color appearance. Therefore, color evolution might be consider a suitable marker for cv Leccino, because its tight association with satisfactory chlorophylls content, but not for cv Buscionetto, since color appearance occurs later, when chlorophylls and carotenoids content could be inadequate for quality oil production. The kinetics of chlorophylls degradation in drupe of cv Leucocarpa resulted very similar to that of cv Buscionetto, although in the first cultivar no anthocyanin accumulation was observed at any stage of drupe ripening. Therefore, for these two cultivars, the appearance of a light-green color could be a useful marker for harvest, particularly for olive production (Pasqualone et al., 2012).

As reported by many authors (Amiot et al., 2003; Servili et al., 2009; Alagna et al., 2012), qualitative and quantitative evolution of phenolic compounds in olive fruit during ripening is strongly cultivar dependent. The level of phenolic compounds detected in drupes of cv Leucocarpa resulted higher compared to that found by Pasqualone et al. (2012) in the same cultivar. Moreover, phenolics content of cv Leucocarpa resulted to be higher than cv Leccino, considered a high phenolics cultivar (Alagna et al., 2012). Instead, drupe of cv Buscionetto is a typical low phenolics cultivar (Caruso et al., 2007). The oleuropein and 3,4-DHPEA-EDA compounds usually represented the most abundant fraction of phenolic, and their content decreased during drupe ripening. Interesting, the three different cultivars have shown important qualitative differences in phenolic composition. Drupes of cv Leccino had a high content of demethyloleuropein, in contrast to the low amounts detected in cv Buscionetto and Leucocarpa. As also reported by Alagna et al. (2012), other cultivars such as Tendellone, Bianchella and Dritta, contain only trace amount of demethyloleuropein, while in Dolce d'Andria, Nocellara del Belice and Nocellara Etnea, it was completely absent. Moreover, drupe of cv Buscionetto has been characterized by the complete absence of verbascoside, particularly intriguing, since in phenols extract have been found both secoiridoids and flavonoids precursors (data not shown), suggesting therefore a block in the last step of reaction leading to its synthesis. In drupes of cv Leucocarpa the almost completely absence of flavones (such as luteolin or apigenin), flavonols (such as rutin) and anthocyanins, and the concomitant presence of lignans and phenolic acids, suggest a block in downstream flavonoid pathways reaction.

To unravel if the difference observed in cv Leucocarpa is under the genetic control, namely to clarify the mechanisms regulating flavonoid biosynthesis, genes encoding enzymes and transcription

factors have been identified. The expression analysis of structural enzymes of flavonoid pathways clearly highlighted a general down-regulation of many of them, such as *OePAL*, *OeCHI*, *OeF3H*, *OeDFR* and *OeANS* in the colorless cv Leucocarpa. The block in the transcription observed might responsible for the lack of anthocyanins and flavonols accumulation in drupes of Leucocarpa, and in opposite way the high expression of *OeDFR* and *OeANS* genes found in drupes of cv Leccino confirm their pivot role in the anthocyanins biosynthesis in the acquisition of color of the fruit in this cultivar. Martinelli and Tonutti (2012) have previously observed that these two structural genes are expressed only during drupe ripening, when anthocyanins begins to be accumulate. In contrast, *OeUFGT1*, which regulates anthocyanidin glycosylation, the last biosynthetic step, resulted to be expressed during fruit development and therefore apparently uncorrelated with the onset of anthocyanins accumulation. Moreover, the high number of structural genes miss-expressed in Leucocarpa suggested that a mutation could not affect a single particular structural gene, but more likely a taskmaster regulator such as one or more of MYB, bHLH or WDR transcription factors. However, strong differences between cv Leccino, Leucocarpa and Buscionetto, have been not observed regarding the transcriptional regulation of most important candidate TFs such as *OeMYBPA1-1*, *OeMYBPA1-2*, *OebHLH* or *OeWDR*. All these candidate genes resulted expressed at comparable level between the three cultivars. Despite this, *OeMYBPA1-1*, belonged to R2R3-MYB subgroup 5, might have a broad role in regulating structural genes of flavonoid pathways and therefore could represent a good candidate causing cv Leucocarpa mutant phenotype and thus, the main transcription factor regulating anthocyanin biosynthesis in olive drupe. Some evidences supported this hypothesis. The pattern of *OeMYBPA1-1* expression, together with their putative partner in MBW complex, *OebHLH* and *OeWDR*, appear correlated with total flavonoids accumulation in fruit. Comparing the expression pattern of some structural gene in cv Leccino and Leucocarpa, a general lower expression of *OePAL*, *OeCHI* and *OeF3H* genes have been observed in this last cultivar and in all analyzed fruit developmental stages. Thus, the gene/s hypothetically responsible for the mutant phenotype, appear expressed throughout fruit development and not restricted to ripening events. Moreover, as demonstrated in grape berry by Bogs et al. (2007), *VvMYBPA1*, together with a *bHLH* partner, is able to regulate not only promoter activity of *VvANR* and *VvLAR* genes, specific of flavan-3-ols branch, but also other structural genes of flavonoid pathways such as *VvANS/LDOX*, *VvCHI* and *VvF3'5'H* genes. In addition, flavan-3-ols were not detected in olive mesocarp and pericarp tissues and transcripts coding for olive orthologs of *OeANR* and *OeLAR* genes were not identify in olive EST library. Despite this, the possibility that other MYB or other class of transcription factors are involved in the regulation of flavonoid pathways could not be excluded. For example, the role of *OeMYBC2* gene is intriguing, since it resulted strongly down regulated at color change, when anthocyanins biosynthesis begins in cv Leccino. Thus, regulatory trend of MYBC2 suggest that it might negatively regulate *OeDFR* and *OeANS* activation, maybe competing with *OeMYBPA1-1* for their promoter binding site, as observed for other members of this *MYB* clade (Persak et al., 2014) (*Figure 30a, b*). Regarding 'Leucocarpa'

phenotype, based on molecular data, we argue the hypothesis that a non-sense mutation could occur in coding region of *OeMYBPA1-1* gene, the most transcribed isof0orm, and/or in putative partner of MBW complex, such as *OebHLH* and *OeWDR*. Interesting, a discrete number of aminoacidic substitution have been found in *OeMYBPA1-1* gene, in particular an Asp/His substitution inside R2 domain, which could modify protein functionality and thus, might be unable to activate *OeDFR* and *OeANS* genes, as well as other structural genes of the flavonoid pathways (*Figure 30c, d*).

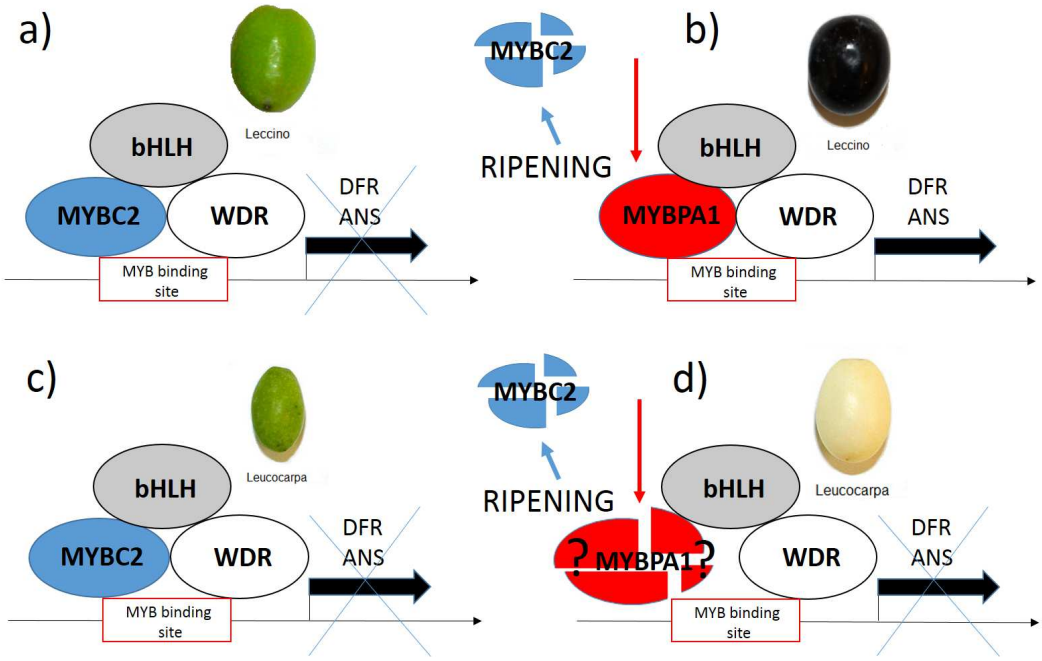

Figure 30. Proposed model for anthocyanin biosynthesis regulation in olive. In cv Leccino, at green maturation and during early stages of fruit development (a), MYBC2 might function as transcriptional repressor competing with MYBPA1-1 for ANS and DFR promoter binding site. At ripening (b), developmental cues might down-regulate MYBC2 gene, allowing MYBPA1-1 to activate DFR and ANS genes, ultimate leading to anthocyanin biosynthesis. In Leucocarpa, a putative loss-of-function might occur in genes forming MBW complex, in particular in MYBPA1-1 protein, which prevent the activation of DFR and ANS genes (d) and thus the anthocyanin biosynthesis.

The evaluation of the optimal ripening stage of olive fruit through rapid and cost-effective methods is a new frontier for olive producers. Pigments and phenolic compounds represent the most important substances determining quality attributes of VOO and, thus, they could be considered an important analytical marker for the evaluation of optimal harvest date. Non-destructive measurement of important olive quality parameter through NIR spectroscopy has been already applied in olive fruit for the prediction of parameters such as olive moisture, dry matter, oil content, oil free acidity and phenolics content (Cayuela et al., 2010; Marquez et al., 2005; Bellincontro et al., 2012). In this study, NIR spectroscopy has been applied for the modeling and prediction of total chlorophylls, carotenoids, anthocyanins and flavonols, the most important pigments in olive fruit and other important phenolic compounds. The results are quite promising in terms of correlations and cross-validation for the

different classes of pigments, although further studies are needed to confirm these early results, increasing data set number. In particular, for drupe firmness prediction model, a very high R^2 value of 0.99 has been found, and low RMSEC/RMSECV values. This result is encouraging, since NIR spectroscopy for firmness analysis has been encounters considerable difficulties, as highlighted by some studies in other fruit (Nicolaï et al., 2008; Zude et al., 2006). These difficulties are usually due to different factors, including variability of firmness and the high instrumental error of the penetrometer. The employment of more accurate tools for texture analysis, such as Instron, appear to improve the predictive capabilities of NIR, although, clearly, an additional number of olive samples are required to further validate the models. The addition of sample might improve its robustness, better if samples will be collect in different seasons and productive areas.

2 CONCLUSION AND PERSPECTIVES

This research represents the first in dept molecular investigation of flavonoid biosynthesis regulation in olive drupe. As a result this research has identified some molecular targets of the genetic determinants of olive colour, demonstrating that anthocyanins biosynthesis in olive is regulated by a specific subset of structural gene, such *OeDFR* and *OeANS*, temporally regulated during olive drupe development and ripening. Moreover, bioinformatic analysis suggest that anthocyanin biosynthesis in olive fruit could be more intricate than other well-characterized species such as grape or apple. Although the model of regulation presented here is not complete, the addition of the molecular information obtained from this research will aid considerably future efforts to identify the color determinants of olive. Finally, this research has been evaluating the potential use of NIR spectroscopy to measure olive firmness and pigments content. Although additional number of sample will be required to improve robustness of created predictive models, promising results have been obtained, particularly for firmness prediction.

SECTION III

IDENTIFICATION AND CHARACTERIZATION OF APPLE AND OLIVE SMALL RNA WITH POTENTIAL ROLE IN HUMAN HEALTH

3. STATE-OF-THE-ART

3.1 EFFECT OF PLANT MIRNA ON HUMAN HEALTH

The horizontal transfer of genetic material is one of the most exciting biological issue. Recently, some contradictory studies give new emphasis to the research in this field. Zhang et al (2012a) demonstrated that plant miRNAs is about 5% of the total small RNAs population in the human serum (*Figure 1a*), probably coming from food intake. Unlike those human, plant miRNAs are 2′-O-methyl modified at their 3′ end, which offers the possibility to use periodate-resistance to confirm their vegetal origin. The hypothesis that plant small RNAs derived from food intake was confirmed by analyzing serum of rice-fed mice, compared with chow diet-fed ones (*Figure 1b*). In fact, plant mature miRNAs were mainly detected in plasma microvesicles (MVs), and in various tissues, including liver, intestine and lung. MVs organelles are usually shared among many of the cell types and selectively interact with specific target cells to mediate intercellular communication, transporting lipids, RNA and proteins. The most common plant miRNAs are accumulated differently from one tissue to another, reaching up to one tenth of the most abundant human miRNA.

Zhang and collaborators (2012a) focused their studies to rice *miR168* (*osa-miR168*), regulating plant *AGO1* mRNA, which encodes the core component of the plant RNA silencing complex (RISC complex). Unexpectedly, *osa-miR168* exhibits a high degree of complementarity with the exon 4 of mammalian *Low Density Lipoprotein Receptor Adapter Protein 1* (*LDLRAP1*) gene, a liver-enriched mRNA encoding a protein that facilitates the removal of LDL Low Density Lipoprotein (LDL) from the blood circulatory system (*Figure 1c*). Although, the gene transcripts level was not affected, however, a reduced level of LDLRAP1 protein was found, in rice-fed mice compared with chow diet-fed mice, indicating that plant miR168 might acts at post-transcriptional stage, inhibiting physically the translation of the gene, as likewise occur for the activity of human miRNA. Indeed, the effect of *osa-miR168* resulted to be sequence specific, as it has been resulted in a test where *LDLRAP1* transcript linked to a luciferase reporter, in cells co-transfected with *miR168*, a luciferase activity decreased (*Figure 1d*). Furthermore, when the recognized *situ*, which is present in the *LDLRAP1*, was modified the *osa-miR168* was not able to recognize the target *situ* and the silencing effect was abolished. A similar reduction of LDLRAP1 protein amount was detected in luciferase assay using the precursor of *osa-miR168* (*pre-osa-miR168*). However, neither plant *pri-osa-miR168* nor plant *pre-osa-miR168* has been detected in the sera and tissues of mice. Authors hypothesized that epithelial cells in the intestine might up-take miRNAs from food, package them into MVs and release them into the blood circulatory system. The secreted MVs could then deliver exogenous plant miRNAs to target

organs where they could regulate cognate mRNAs. This hypothesis has been tested in human HepG2 cells by delivering *osa-miR168* through MVs, which have been produced transfecting human intestinal epithelial Caco-2 cells with the same *miR168*. Immunoprecipitation tests revealed that *osa-miR168* and *LDLRAP1* mRNA resulted to be associated with human RNA RISC silencing complex in HepG2 cells. As consequence of this event, the LDLRAP1 protein level decreased in HepG2 cells, indicating that MVs carried a functional *miR168* to specific cells, evocating a possible functional role of small RNA in target organs. Consistent with the silencing effect of plant *miR168* on LDLRAP1 protein synthesis, LDL levels in mouse plasma were elevated following *miR168* uptake. This effect was specific to *miR168* because injection of an anti-*miR168* oligonucleotide blocked the increase in LDL levels.

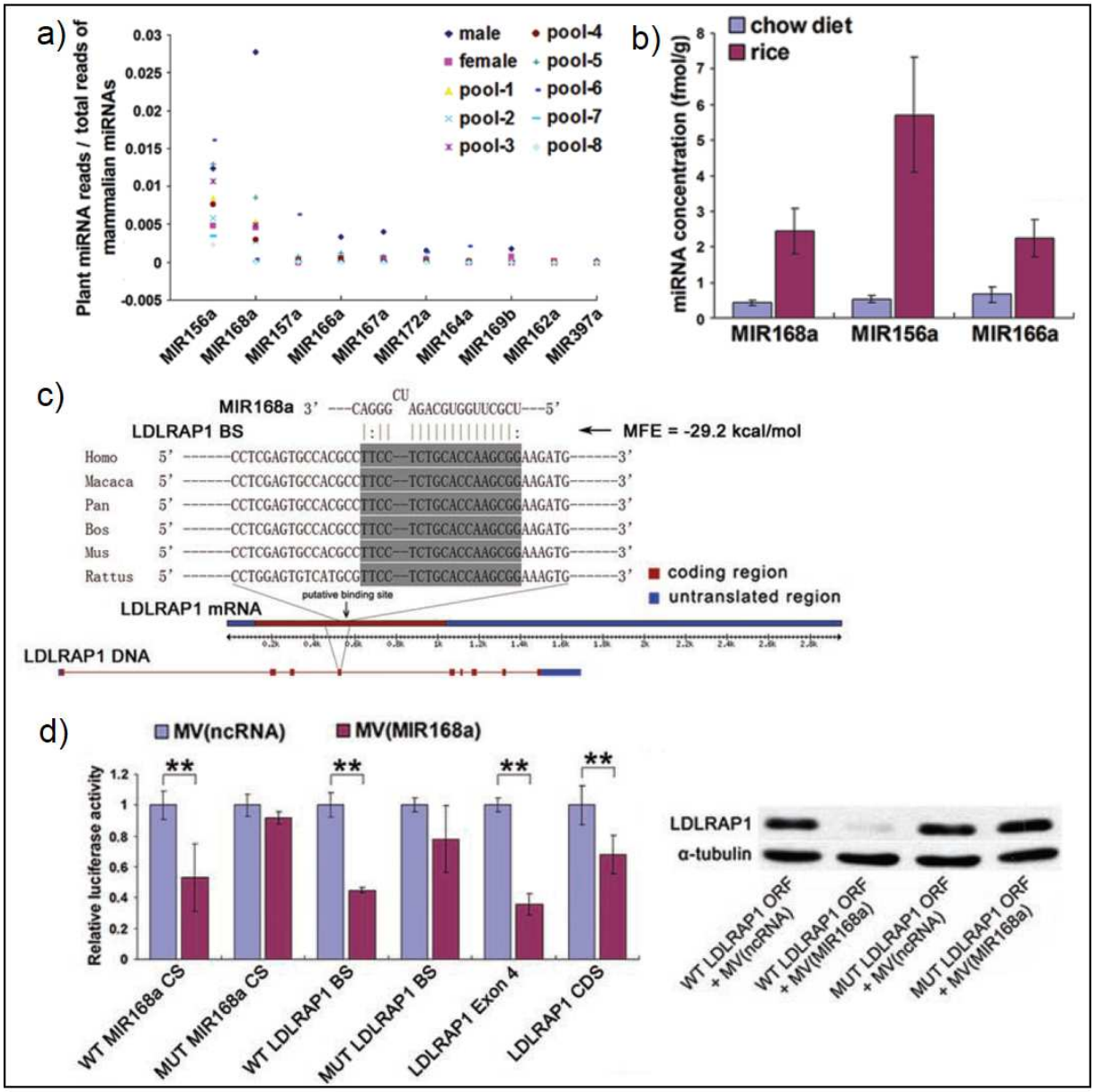

Figure 1. All information reported in this figure came from Zhang et al. (2012) paper. a) Relative abundance of ten plant miRNAs as detected by Solexa sequencing in human sera of healthy Chinese men and women, and as detected in eight pooled samples of ten healthy Chinese human. For normalization, the sequencing frequency of

each plant miRNA was normalized to the total amount of mammalian miRNAs. b) L*evels of miR168a, miR156a, and miR166a as detected by qRT-PCR in mouse sera fed with fresh rice and chow diet (n = 6). miR16 and miR150 mammalian miRNAs have been used served as internal controls to normalize the level of transcripts. UD, undetectable. c)* Hypothetical alignment *duplexes miRNAs:mRNA formed by interactions between the exon 4 of LDLRAP1gene and plant miR168a. Paired bases are indicated by vertical lines and G:U pairs by two dots. The predicted free energy of the hybrid is indicated by the arrow. Tthe potential binding site of miR168a to LDLRAP1 mRNA is highly conserved across species. d)* L*uciferase activities as detected in luciferase reporter-transfected HepG2 cells treated with or without Caco-2 MVs (n = 9).*

The previously described findings have been criticized by studies that have highlighted the possibility of occasionally plant miRNA contamination of different animal serum by laboratory procedures (Zhang et al., 2012b). Also feeding trials of monkeys (Witwer et al., 2013), humans and mice (Snow et al., 2013) failed to demonstrate any biologically relevant uptake of plant-derived small RNAs. Moreover, Dickinson et al. (2013), running the same Zhang's experiment (2012a), have not obtained the same results, concluding that no apparent uptake of plant *miR168* occurred. It is noteworthy, this study provided strong evidence that nutritional differences and experimental variation, rather than ingested miRNAs, were responsible for the observed changes reported in the earlier mouse feeding studies.

3.2 RNA INTERACTION WITH POLYPHENOL MOLECULES

Despite the controversy opened on the possibility that small RNAs are transferred from the food, a strong interest is growing up with the aim to find efficient delivery systems of these molecules through the human organism, for pharmaceutical aims. Indeed, evidences suggest that miRNA-based therapies, either restoring or repressing endogenous miRNAs and mRNA expression or activity, hold great promise for many pathologies, including some type of cancer (Iorio et al., 2012; Rothschild, 2014) and cardiac regeneration (Eulalio et al., 2012). A large number of different miRNA delivering methods have been tested, from chemical modification of synthetic oligonucleotides to nanotechnologies (Zhang et al., 2013, for a detailed review). Plant secondary metabolites might represent a relatively unexplored delivery system, in fact many evidence, in particular from phenolics compounds, are present that shown they have the property to bind nucleic acids molecules. Indeed, Kuzuhara et al. (2006) clearly demonstrated the ability of green tea monomer flavan-3-ols, such as catechins and epicatechins, to bind both single and double strand DNA and RNA oligomers *(Figure 2)*.

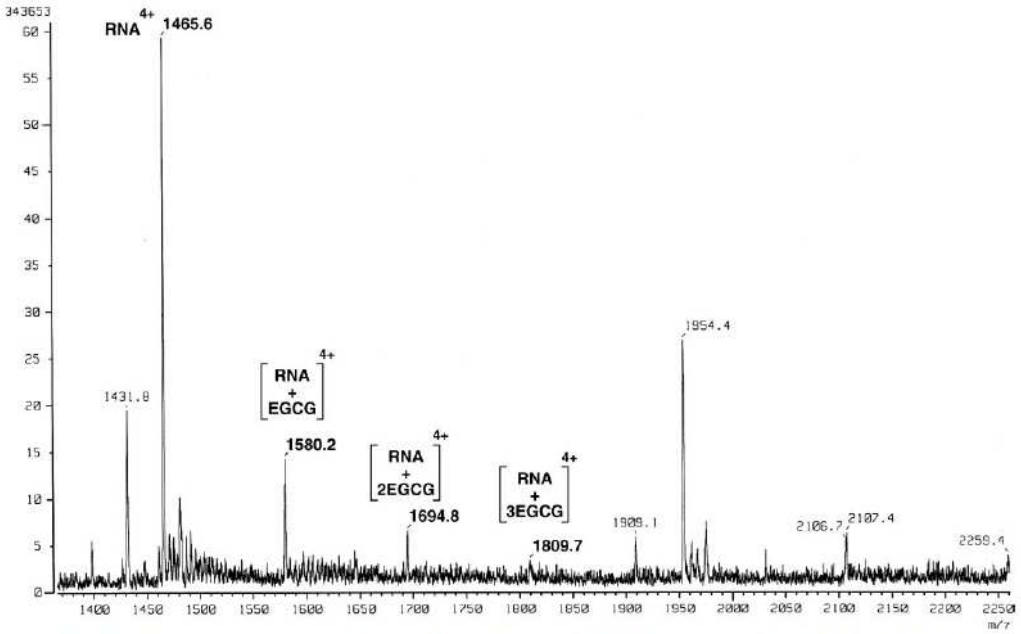

FIGURE 4. **Direct binding of EGCG to ssRNA oligomers determined by CSI-MS analysis.** EGCG and oligomer RNA were mixed and applied to CSI-MS. Peaks are estimated by the indicated molecular weights.

Figure 2. Direct binding of ssRNA oligomers to green tea flavan-3-ols monomers (image taken from the article of Kuzuhara et al., 2006).

3.3 BIOINFORMATICS PREDICTION OF PUTATIVE HUMAN TARGET GENES

In order to unravel the role of each miRNA on gene regulation, several bioinformatics algorithms have been developed in last decade, in order to identify the target gene. These computational approaches implement experimental studies and allow high-throughput prediction of miRNA target genes. In vertebrates, miRNA-target prediction is particularly difficult because the complexity of recognition mechanism. Indeed, miRNA:mRNA duplexes often contain several mismatches, gaps and G:U base pairs in many positions, which limits the maximum length of contiguous sequences of perfect nucleotide matching. This is in contrast to miRNA function in plants, where targets are usually recognized by perfect complementarity along the length of the miRNA sequence. A key step in the computational identification of miRNA target is the selection of predictive features, such as base-pairing interaction between 2-8 nucleotides at 5'–end of miRNA and target, defined as *seed region* (Lewis et al., 2003), evolutionary conservation of *seed region* binding site (Friedman et al., 2009), secondary structure accessibility (Kertesz et al., 2007), dinucleotide composition of flanking sequence (Nielsen et al., 2007) and thermodynamic stability of binding sites (Rehmsmeier et al., 2004). In particular, *seed region* of miRNA and target gene represent an important determinant for recognition, together with phylogenetic conservation of miRNA binding sites. *Seed region* increases binding affinity for target sequences relative to other parts of the miRNA (Gaidatzis et al., 2007). Many algorithms have been developed for miRNA target prediction, such as miRanda (Betel et al., 2008), microCOSM Targets (Griffiths-Jones et al., 2008), DIANA-MicroT (Maragkakis et al., 2009), TargetScan (Friedman et al., 2007) and many others.

Although these algorithms were developed on similar principles, they often provide different results, and researchers need to crosscheck multiple algorithms to get an additional layer of confidence for the true positive targets. Although computational methods have successfully predicted many miRNA target sites, these approaches inevitably produce a certain number of false-positive predictions.

3.4 MIRANDA SOFTWARE

The miRanda algorithm (Betel et al., 2008) is one of the first miRNA target prediction algorithms to be developed. This algorithm relies on a stepwise progression through target prediction, free-energy calculation to estimate the thermodynamics of the most probably interactions between miRNA and target, and evolutionary conservation. The target prediction component of the algorithm consists of using dynamic programming to search for maximal local complementarity alignments between the mature miRNA sequence and all possible positions in each gene 3'-UTR. A score of +5 is assigned for G:C and A:T pairs, +2 for G:U wobble pairs, and -3 for all other nucleotide pairs. The software could insert single o more gap, to ensure maximum base pair complementarity between miRNA and the target. The insertion of single gap has a score penalty of -8, adding one or more gaps close to the first the penalty will score -2 penalty for each additional gap (*Figure 2*).

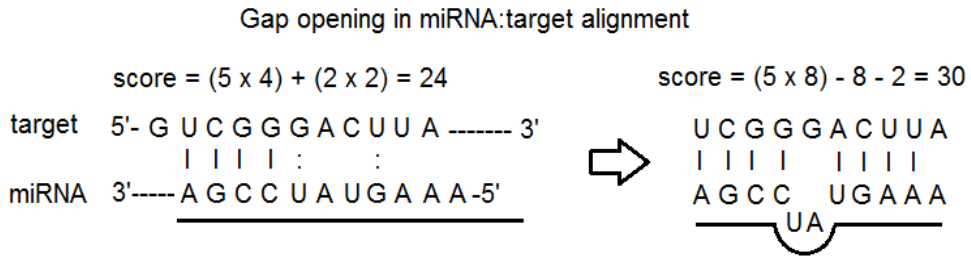

Figure 2. Example of gap opening by miRanda algorithm within miRNA:target sequence alignment. In this case, the gap insertion improve miRNA:target alignment and consequently the score (for simplicity, mismatch were not considered in score calculation).

Moreover, the miRanda algorithm recognizes the importance of the *seed region* through a scaling factor optimized on the bases of experimental information about functional validated miRNAs *seed region*. To estimate the thermodynamic stability of the predicted miRNA: mRNA duplex, the miRanda algorithm uses folding routines from the Vienna package. The free energy of the duplex is estimated and checked against a threshold value. Previous implementations of this algorithm have used G < -17 kcal/mol or G < 0-14 kcal/mol as cut-off values. Finally, miRanda algorithm searches for conservation of the target site between orthologous species. After passing the conservation filter, predicted target sites for each miRNA are sorted according to alignment score primarily and free energy secondarily.

3 AIMS OF THIS STUDY

The main objective of this study was to deepen the knowledge about the presence and abundance of specific classes of plant small-RNA that might have the putative ability to bind human gene and consequently regulate them posttranscriptional activity, in *O. europaea* and *M. domestica* fruit and their-derived products. The integration of food technology with recent advances in human nutrition may help to expand the concept of fruit quality beyond primary and secondary metabolites composition, including others molecules, such as specific classes of small-RNA, characterized by a potential benefit for human health.

Results reported in the following section are generated in collaboration with the Biology Department of Tor Vergata University (Rome, Italy) and with the academic spin off MirNat srl (www.mir-nat.com), a start-up company devoted to investigate the role of plant miRNAs in human and animal physiopathology. For patent reason, the nomenclature of specific plant miRNAs identified to regulate the expression of specific human genes is not disclosure.

3 RESULTS

3.1 BIOINFORMATICS PREDICTIONS OF OLIVE HOMOLOGUES OF HUMAN MIRNAS

A multi-step workflow has been designed to identify a stringent number of *O. europaea* miRNAs, having functional homology with human miRNAs. For candidates search, it has been assumed that ectopic miRNA would be processed by host cell machinery MirCompare software, developed by Dr. Stefano Pirrò - bioinformatics expert at MirNat startup Company, has been used to identify a restricted number of *Olea europaea* microRNAs with a putative role in cross-kingdom interaction. A specific filter series, implemented into MirCompare algorithm, allow identifying 18 candidates.

The computational analysis described relies on the assumption that ectopic miRNA mimics native miRNA processing mechanism, including binding at 3'UTR of target genes and translation inhibition. However, as described previously, Zhang et al. (2012a) identified a different mechanism of action of ectopic miRNAs, as for example plant *miR168* binding site is located on fourth exon of *LDLRAP1* transcript. Thus, the regulation of ectopic miRNA of host target gene might be only not restricted to 3'UTR region. In fact, plant *miR168* exhibited a high level of complementary with its target. For this reason, it has been used a diverse bioinformatics approach to identify putative human target of apple *miR858 (mdo-miR858)*. Therefore, miRanda software has been applied for an initial screening of putative target genes, which discriminate on alignment score (>140) and thermodynamic properties. This initial screening identify about 150 miRNA candidates. Subsequently, the identified candidates have been filtered considering the global number of conserved nucleotides between miRNA:mRNA, high seed complementary and at least 2/3 nt in the region comprised between 13-16nt (from 3'). This further filtering step reduced candidates target to 11 (*Table 1*). Among the putative targets of *mdo-miR858*, is interesting signal the presence of *VAV2* and *SPN* genes. The *VAV2* gene

encodes GDP/GDT exchange factors (GEFs) critical to Rho GTPase activity. Together with VAV3, this protein play important roles in the initiation and development of some types of disease, including skin cancer (Mejia, 203) and ovarian tumor cell migration (Bourguignon et al., 2001). Leukosialin also known as sialophorin or CD43 (cluster of differentiation 43) is a transmembrane cell surface protein that in humans is encoded by the *SPN* gene (Pallant et al., 1989). Recently, *CD43* silencing by siRNA-targeting has demonstrated the potential effect on lung cancer therapy (Fu et al., 2013).

gene ID	gene name	alignment region	score	energy kCal/Mol	miR858: transcript alignment
NP_001245135.1	hsVAV2	1112-1133	174	-27,07	3' agTCCAGCTTG-TCTGTTGCTt 5' 5' cgAGGTCAAGCGAGACAACGAg 3'
NP_060601.3	hsCEP55	305-325	171	-25,82	3' agTCCAGCTTGTCTGTTGCTt 5' 5' acAGCTGGAAGAGACAACGAg 3'
BAA76764.2	hsKIAA0920	3380-4000	162	-25,41	3' agTCCAGCTT-GTCTGTTGCTT 5' 5' ccAGGAGGAAGAAGACAACGAA 3'
NP_003114.1	hsSPN	390-410	161	-25,38	3' agTCCAGCTT-GT-CTGTTGCTT 5' 5' acAGGTGGAACCATAACAACGAA 3'
NP_115698.3	hsRFN135	450-471	164	-21,68	3' agtccAGCTTGTCTGTTGCTT 5' 5' gaatcTGGACCAGACAACGAA 3'
BAA08084.1	hsCP	689-710	166	-21,99	3' agTCCAGCT-TGTCTGTTGCTT 5' 5' gaAAGTTGACAAAGACAACGAA 3'
NP_004628.4	hsRAB7A	533-553	166	-24,62	3' agTCCAGCTTGTC-TGTTGCTT 5' 5' ggAGGTGGAGCTGTACAACGAA 3'
NP_003160.2	hsSPT5a	2016-2031	167	-26,53	3' agTCCAGCTTGTCTGTTGCTT 5' 5' cgGGGCCGGAGGGACAACGAA 3'
NP_001166988.1	hsMAP7.3	2120-2141	162	-23,03	3' agTCCAGCT-TGTCTGTTGCTT 5' 5' agAGGCTGAGGCTGACAACGAA 3'
NP_036336.2	hsGTF3C4	779-800	166	-26,18	3' agTCCAGCTTGT-CTGTTGCTT 5' 5' gcAGGTCAAGCATAACAACGAA 3'
AAP36638.1	hsTUBA1A	600-620	149	-18,12	3' agtccagcTTGTCTGTTGCTT 5' 5' gccttcatGGTGGACAACGAA 3'

Table 1. Results of bioinformatic prediction with miRanda software of mdo-miR858 putative human target genes.

Among the olive miRNAs predicted by MirCompare software, *oeu-miRX* was tested for *in vitro* target validation. Transfection experiment demonstrated the ability of *oeu-miRX* to mimics the endogenous human miRNA, negatively regulating SIRT1 and NOTCH1 protein levels. SIRT1 is an NAD-dependent deacetylase that regulates apoptosis in response to oxidative stress, and recent data suggests that may function as an oncogene (Yamaguchi et al., 2008). NOTCH1 signaling pathways is involved in maintaining the balance between cell proliferation and differentiation, and altered Notch signaling

has been associated with various disorders, including cancer (Bae et al., 2012). The results of functional validation of transfected human mature miRX (Figure 3), showing a very high homology the plant-derived miRNA, suggests that the plant *oeumiRx* could play a role in human target genes regulation, when transfected. However, a different mechanism respect to that hypothesized by Zhang and colleagues (2012a).

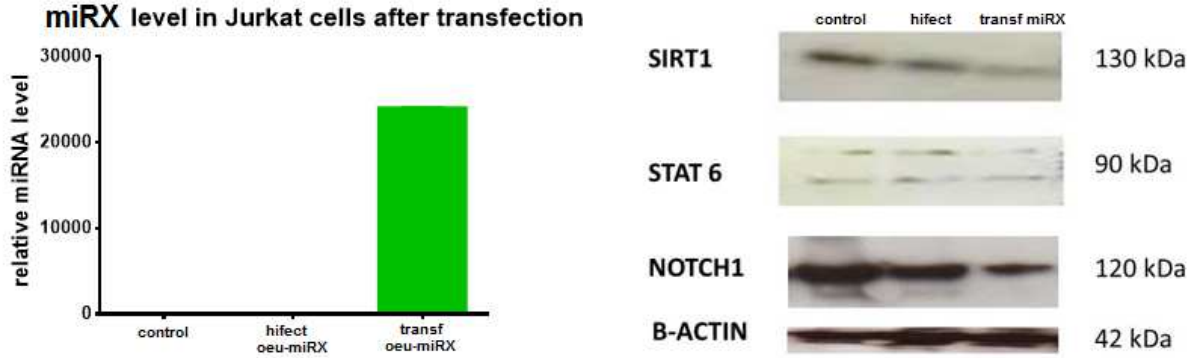

Figure 3. In vitro validation experiment of miRx human target (image reprinted with permission of MirNat Start-Up Company, Rome, Italy).

3.2 OLIVE MIRNA ABUNDANCE IN DRUPE, FILTERED AND NON-FILTERED OLIVE OIL AND OLIVE PATÈ

Although *in-vitro* experiment confirmed the ability of *oeu-miRX* to mimics endogenous *hsa-miRXa*, *in vivo* feeding-experiments are necessary to assess effective *oeu-miRX* uptake by human organism. However, for the correct planning of feeding-experiment, detailed information about the presence and amount of *oeu-miRX* in olive fruit based-foods are required. Therefore, we analyzed the presence and abundance of *oeu-miRX* in olive products, such as fresh drupes, extra-virgin olive oil and olive '*patè*', waste product obtained from olive mill by the innovative two-phase system of olive processing. In addition to *oeu-miRX*, we analyzed the abundance of *oeu-miR168*, homologs of *osa-miR168*, and *oeu-miR166*, one of the most abundant class in olive miRnomes.

Firstly, abundance of *oeu-miRX*, *oeu-miR168* and *oeu-miR166* were tested in nucleic acids extracted from fresh drupes of cultivars Canino and Leucocarpa, sampled at commercial harvest on November 4 and November 22, respectively (*Figure 4, a*). The candidates miRNAs *oeu-miR168*, *oeu-miR166* and *oeu-miRX* were detected in both cultivars, although transcript levels of *oeu-miRX* was very low compared to *oeu-miR168* and *oeu-miR166*, expressed at similar levels. The lower transcript level of *oeu-miRX* was not surprising since only a very low number of reads were found in olive fruit small-RNAs libraries (*Table 3*).

Extra-virgin olive oils contains only very low amount of nucleic acids, however, including highly degraded RNA molecules, below fluorometer or agarose gel electrophoresis detection limits (data not shown). Despite this, we tested miRNAs presence in nucleic acids extracted from extra-

virgin olive oils and olive mills derived from the same drupes of cv Canino above descripted. Surprisingly, trace amount of *oeu-miR168* and *oeu-miR166* were detected in non-filtered oils (*Figure 4, c*) but not in filtered ones, neither preserved in glass bottle or can (*Figure 4, d*). On the contrary, *oeu-miRX* were not detected in any of tested oils samples (*Figure 4, c*). It is been resulted that in the lyophilized *paté* an higher amount total RNA is contained respect to than of extra-virgin oil, as visualized on electrophoresis gel and the total quantity detected was up to 15 ng/g of lyophilized *paté*; therefore in the last product the highest abundance of the three tested miRNAs has been found (*Figure 4b*). Despite this, relative transcript level of *oeu-miR168*, *oeu-miR166* and *oeu-miRX* resulted 10 times less than that found in pith of fresh drupes.

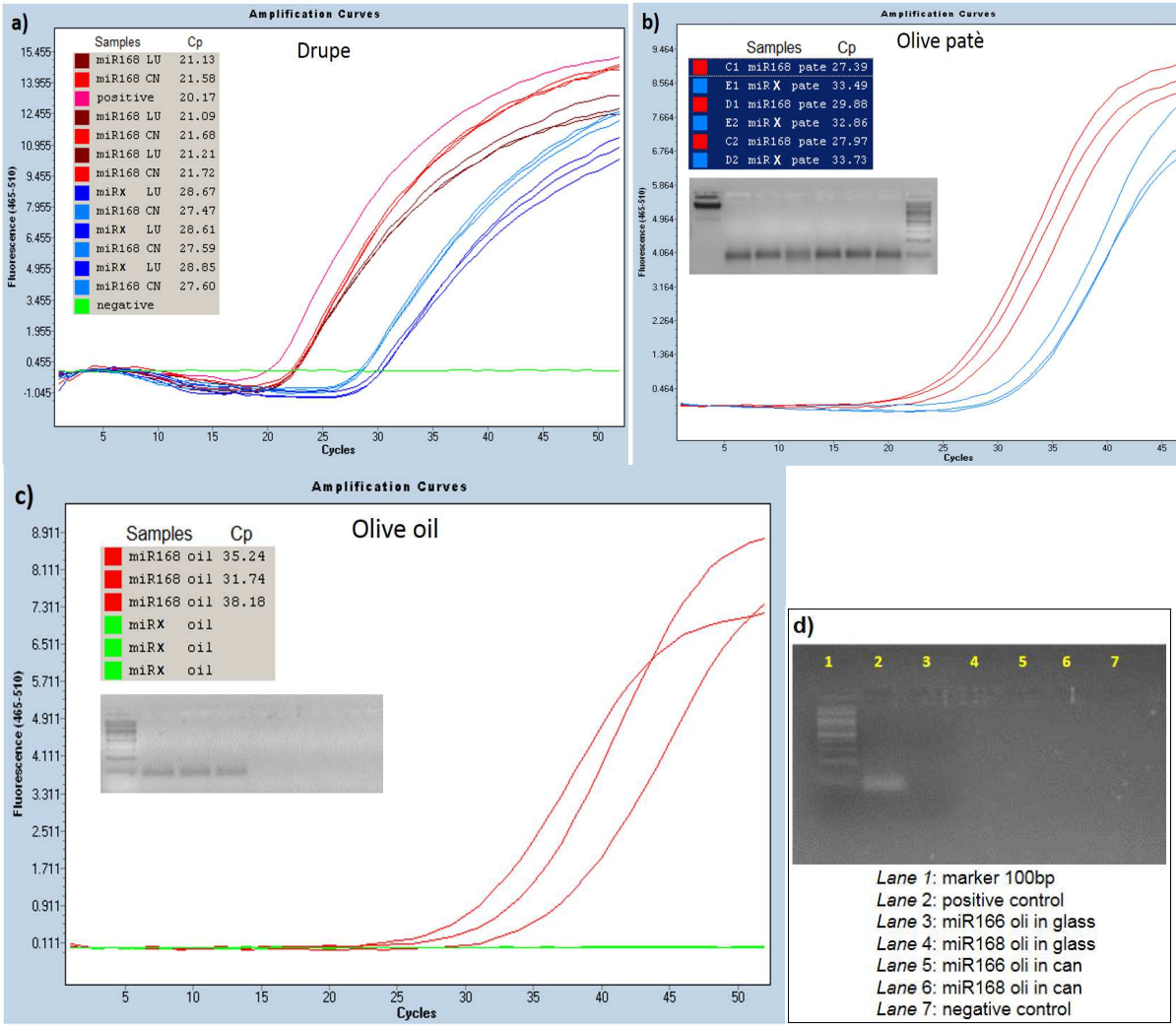

Figure 4. a) Real-time amplification of oeu-miR168 and oeu-miRX in mature drupe of cvs Canino and Leucocarpa. Values of crossing point are shown in the grey box, on the left. b) *Real-time amplification of oeu-miR168 and oeu-miRX in olive paté samples of cv Canino. Values of crossing point and visualization of amplified products onto agarose gel are shown in the two boxes, on the left. c) Real-time amplification of oeu-miR168 and oeu-miRX in non-filtered extra-virgin oil samples of cv Canino. Values of crossing point and*

visualization of amplified products onto agarose gel are shown in the two boxes, on the left. d) Visualization of amplified products onto agarose gel of oeu-miR166 and oeu-miR168 in filtered extra-virgin olive oil cv Canino samples, preserved in glass bottles or cans for two weeks. Positive control is represented by amplification of miR160 in Canino olive dupes.

sRNA library tissue/organ	NCBI accession	references	total reads number	oeu-miRX	
				hits	identity (nts)
juvenile lateral bud	GSM669402	Donaire et al., 2011	89,945	1	21/21
dormant lateral bud	GSM669403	Donaire et al., 2011	66,978	-	-
unripe fruit	GSM1054347	Yanik et al., 2013	15,260,014	-	-
ripe fruit	GSM1054348	Yanik et al., 2013	13,817,321	-	-
leaf	GSM1054349-52	Yanik et al., 2013	63,745,958	20	21/21
fruit*	unpublished	-	11,769,043	3	21/21; 18/21; 18/21

*Table 3. Abundance of oeu-miRX in small-RNAs libraries available at NCBI database. *Unpublished mature drupe sRNA libraries.*

Finally, the presence of the three miRNA has been investigate in nucleic acids extracted from polyphenols matrices in turn extracted from filtered olive oils and lyophilized olive patè of cv Canino (*Figure 5*). Interesting, low amount of *oeu-miR168* and *oeu-miR166* has been detected in polyphenols extracts from olive patè, while they have been not detected in extra-virgin olive oil extracts. On the contrary, *oeu-miRX* has been not detected in any of the two different polyphenol matrices (data not shown).

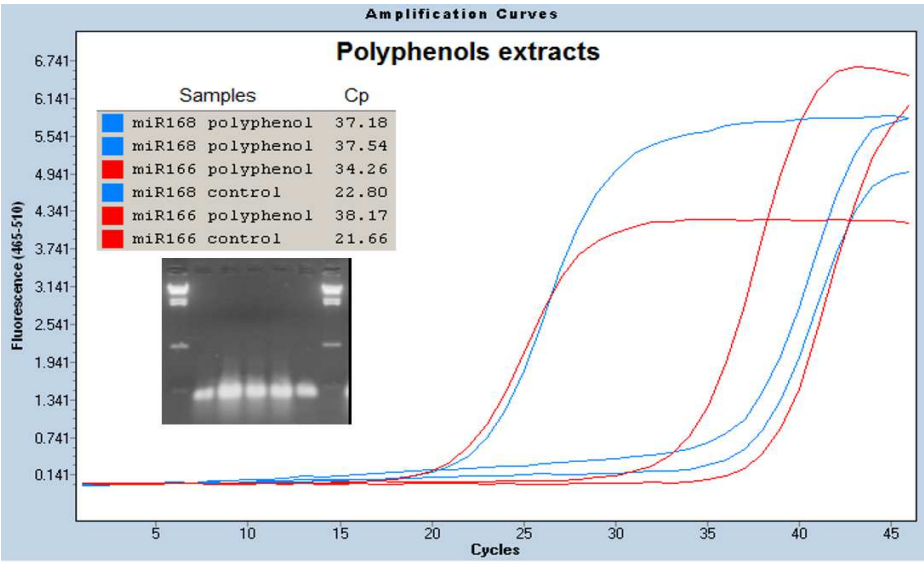

Figure 5. Real-time amplification of oeu-miR168 and oeu-miR166 in polyphenols extracts from lyophilized paté of cv Canino. The crossing point values and the visualized qPCR products onto agarose gel are shown inside the box, on left side.

3.3 APPLE MIR858 ABUNDANCE IN LYOPHILIZED APPLE AND TOTAL POLYPHENOLS EXTRACTED FROM APPLE FLESH

Presence and abundance of *mdo-miR858* has been investigated in nucleic acids extracted from fresh apple, lyophilized apples and polyphenols matrices extracted from the same lyophilized products, of Italian Red Passion C15 line.

The lyophilization procedure did not affect *mdo-miR858* stability in apple of C15 line (*Figure 6*), although a similar but quite lower transcripts level has been detected compared to fresh tissues. More interesting, also polyphenols extracts from lyophilized apples contained low amount of nucleic acids (ranged from 2 to 9 ng/ 1g of lyophilized tissue) and most important, detectable levels of *mdo-miR858* (*Figure 6a*).

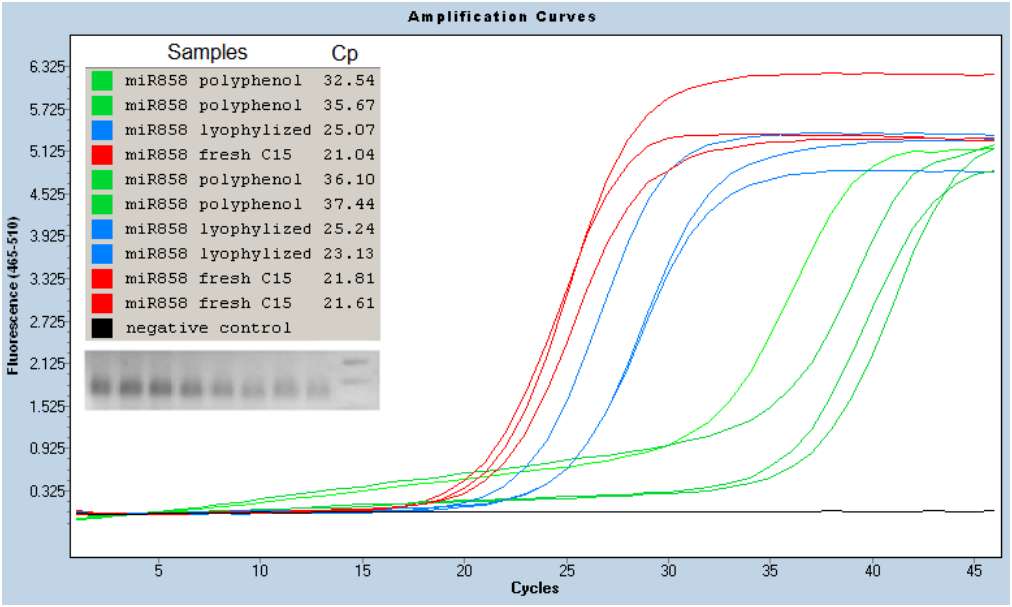

Figure 6. Real-time amplification of mdo-miR858 in fresh apples, lyophilized apples and polyphenols extracted from lyophilized apples of C15 line. In the boxes, on the left, crossing point and visualization of amplified products onto agarose gel.

3 DISCUSSION AND CONCLUSION

Although still controversial, the hypothesis of a cross-kingdom gene regulation played by food–derived small-RNAs might have in the recent future a dramatic impact on agriculture and on technology of food industry. However, many further studies should be perform to confirm this intriguing hypothesis, considering that scarce are the knowledge about the presence and abundance of small-RNA molecules in common food, including those from fruits and their derivate.

In this work, in addition to *miR168*, we have investigate the presence of olive *miRX* and apple *miR858*, identified through different bioinformatics approaches. The *oeu-miRX* was identified using a novel algorithm (MirCompare) developed to scan plant specific miRNAs, which mimics endogenous human miRNAs. Through this approach, several olive miRNAs have been identified. Functional validation through *in vitro* cell transfection experiment, demonstrated the *oeu-miRX* ability to mimics endogenous human *miRNA*, inhibiting translation of *SIRT1* and *NOTCH1* target transcripts. Instead,

putative targets of *mdo-miR858* have been identified by searching miRNA pairing inside gene coding regions, however conserving some typical features of human miRNAs mechanism of action. Following this approach, a discrete number of putative *mdo-miR858* targets have been identified, including the two oncogenes *hsaSPN/CD43* and *hsaVAV2* genes, which will be functional validated in the next future.

Beyond bioinformatic predictions and *in vitro* experimental target validation, the effective uptake through diet of *oeu-miRX*, as well as other plant-derived miRNAs, remained to verify. As pointed out by several researches (Witwer et al., 2013; Snow et al., 2013), the planning of a correct feeding-experiment is crucial to assess the effective relevance of food-delivery plant miRNAs. In this way, the presence and abundance of *oeu-miRX*, *oeu-miR168* and *mdo-miR858* has been analyzed in different food source. Not surprisingly, highest abundance of candidates miRNAs have been found in fresh fruit compared to fruit-derived product. However, the presence of miRNAs in non-filtered olive oils, olive patè and lyophilized apples indicate that a greater chemical stability of these molecules in these matrices compared to others RNA forms.

In addition, despite they are not conclusive; we obtained initial evidences that permit to speculate the strict linkage between miRNAs and polyphenols, particularly the most hydrophilic fraction of these molecules. Recent findings revealed that polyphenols (in particular flavonoids) could affect the expression of many classes of human microRNAs, regulating important biological functions, such as apoptosis, inflammation and anticancerogenesis (Milenkovic et al., 2013). For example, Tunca et al. (2012) demonstrated the properties of olive leaf extract, containing high amount of polyphenols, to modulate the expression of some class of human miRNA in glioblastoma cells. However, the mechanism underlying miRnomes regulation by polyphenols molecules are still largely unknown. Therefore, the delivering of plant miRNA in human organism through polyphenols might be more than a suggestive hypothesis, particularly considering the assessed ability of some phenolic class to bind nucleic acids (Kuzuhara et al., 2006).

REFERENCES

Aharoni A, De Vos CHR, Wein M, Sun ZK, Greco R, Kroon A, Mol JNM, O'Connell AP (2001) The strawberry FaMYB1 transcription factor suppresses anthocyanin and flavonol accumulation in transgenic tobacco. *Plant J* 28: 319–332.

Alagna F, Mariotti R, Panara F, Caporali S, Urbani S, Veneziani G, Esposto S, Taticchi A, Rosati A, Rao R, Perrotta G, Servili M and Baldoni L (2012) Olive phenolic compounds: metabolic and transcriptional profiling during fruit development. *BMC Plant Biol* 12:162-183.

Akagi T, Ikegami A, Tsujimoto T, Kobayashi S, Sato A, Kono A, Yonemori K. (2009) DkMyb4 is a Myb transcription factor involved in proanthocyanidin biosynthesis in persimmon fruit. *Plant Physiol* 151:2028–2045.

Aldrich L and Blisard N (1998) Consumer acceptance of biotechnology: Lessons from the rbST experience. *Current Issues in Economics of Food Markets* 747:1-5.

Amiot MJ, Fleuriet A, Macheix JJ (1986) Importance and Evolution of Phenolic Compounds in Olive during Growth and Maturation. *J Agric Food Chem* 34:823-826.

Aparicio-Ruiz R, Gandul-Rojas B, Roca M (2009) Pigment Profile in Non-Spanish Olive Varieties (*Olea europaea* L. Var Coratina, Frantoio, and Koroneiki) *J Agric Food Chem* 57:831-836.

Arts I, Harnack L, Gross M, Folsom A (2001) Dietary catechins in relation to coronary heart disease among postmenopausal women. *Epidemiology* 12: 668-675.

Axelson LE & Axelson J (2000) Hypercompetition on horticultural markets Acta Horticulturae, 536, 485-492

Ban Y, Honda C, Hatsuyama Y, Igarashi M, Bessho H and Moriguchi T (2007) Isolation and functional analysis of a MYB transcription factor gene that is a key regulator for the development of red coloration in apple skin. *Plant Cell Physiol* 48: 958-970.

Baudry A, Heim MA, Dubreucq B, Caboche M, Weisshaar B and Lepiniec L (2004) TT2, TT8, and TTG1 synergistically specify the expression of BANYULS and proanthocyanidin biosynthesis in Arabidopsis thaliana. *Plant J* 39: 366–80.

Bellincontro A, Taticchi A, Servili M, Esposto S, Farinelli D and Mencarelli F (2012) Feasible application of a portable NIR-AOTF tool for on-field prediction of phenolic compounds during the ripening of olives for oil production. *J Agric Food Chem* 60: 2665−2673.

Ben-Yehuda G, Korchinsky R, Redel G, Ovadya R, Oren-Shamir M and Cohen Y (2005) Colour accumulation patterns and the anthocyanin biosynthetic pathway in 'Red Delicious' apple variants. *J Hortic Sci Biotechnol* 80: 187-192.

Betel D, Wilson M, Gabow, A, Marks D, Sander C (2008) The micrornaorg resource: Targets and expression *Nucleic Acids Res* 36:149–153.

Bisignano G, Tomaino A, R Lo Cascio (1999) On the In-vitro Antimicrobial Activity of Oleuropein and Hydroxytyrosol. *J Pharm Pharmacol* 51: 971-974.

Bogs J, Jaffé FW, Takos AM, Walker AR, Robinson SP (2007) The grapevine transcription factor *VvMYBPA1* regulates proanthocyanidin synthesis during fruit development. *Plant Physiol* 143: 1347-1361.

Borevitz JO, Xia YJ, Blount J, Dixon RA, Lamb C (2000) Activation tagging identifies a conserved MYB regulator of phenylpropanoid biosynthesis. *Plant Cell* 12: 2383-2393.

Bourguignon LY, Zhu H, Zhou B, Diedrich F, Singleton PA, Hung MC (2001) Hyaluronan promotes CD44v3-

Vav2 interaction with Grb2-p185 (HER2) and induces Rac1 and Ras signaling during ovarian tumor cell migration and growth *J Biol Chem* 11:23-29.

Boyer J, Liu RH (2004) Apple phytochemicals and their health benefits. *Nutr J* 3:5-8.

Bracalente B, Cossignani M, Mulas A (2009) Statistica aziendale, Mc-Graw-Hill", Milano.

Brand-Williams W, Cuvelier ME, Berset C (1995) Use of free radical method to evaluate antioxidant activity. *Lebensm Wiss Technology* 28:25-30.

Brenes M, García A, García, P, Ríos J, Garrido A (1999) Phenolic compounds in Spanish olive oils. *J Agric Food Chem* 47:3535-3540.

Calinsky R, Harabasz J (1974) A dendrite method for cluster analysis. *Communications in Statistics* 3:1-27

Carrasco-Pancorbo A, Gómez-Caravaca AM, Cerretani L, Bendini A, Segura-Carretero A, Fernández-Gutiérrez A (2006) Rapid quantification of the phenolic fraction of spanish virgin olive oils by capillary electrophoresis with UV detection. *J Agric Food Chem* 54:7984-7991.

Caruso T, Cartabellotta D, Motisi A (2007) Cultivar di olivo siciliane. Pages: 202. Regione siciliana, Assessorato Agricoltura e Foreste Palermo, Italy.

Cayuela JA, Pérez-Camino MC (2010) Prediction of quality of intact olives by near infrared spectroscopy. *Eur J Lipid Sci Technol* 112: 1209−1217.

Cefarelli G, D'Abrosca B, Fiorentino A, Izzo A, Mastellone C, Pacifico S (2006). Free radical scavenging and antioxidant activities of secondary metabolites from reddened cv. Annurca apple *J Agric Food Chem* 54(3): 803–809.

Chagné D, Carlisle C, Blond C, Volz R, Whitworth C, Oraguzie N, Crowhurst R, Allan A, Espley R, Hellens R, and Gardiner S (2007) Mapping a candidate gene (MdMYB10) for red flesh and foliage colour in apple. *BMC Genomics* 8: 212-219

Cherubini C, Migliorini M, Mugelli M, Viti P, Berti A, Cini E, Zanoni B (2009) Towards a technological ripening index for olive oil fruits. *J Sci Food Agr* 89:671-682.

Chiou A, Kalogeropoulos N, Boskou G, Salta FN (2012) Migration of health promoting microconstituents from frying vegetable oils to French fries. *Food Chem* 133: 1255–1263.

Chun OK, Kim DO and Lee CY (2003) Superoxide radical scavenging activity of the major polyphenols in fresh plums. *J Agric Food Chem* 51: 8067-8072.

Cimato A, Baldini A, Moretti R (2001) L'olio di oliva.Cultivar, ambiente e tecniche agronomiche ARSIA, Regione Toscana, Firenze.

Cocciolone SM, Cone KC (1993) Pl-Bh, an anthocyanin regulatory gene of maize that leads to variegated pigmentation. *Genetics* 135:575-588

Collard BC, Mackill DJ (2007) Marker-assisted selection: an approach for precision plant breeding in the twenty-first century. *Philos Trans R Soc Lond B Biol Sci* 7:15-23.

Conde C, Delrot S, Gerós H (2008) Physiological, biochemical and molecular changes occurring during olive development and ripening. *J Plant Physiol* 165:1545-1562.

Coni E, Di Benedetto R, Di Pasquale M, Masella R, Modesti D, Mattei R and Carlini EA (2000) Protective effect of oleuropein, an olive oil biophenol, on low density lipoprotein oxidisability in rabbits. *Lipids* 35:45-54

Criado MN, Motilva MJ, Ramo T, Romero MP (2006) Chlorophyll and carotenoid profile and enzymatic

activities (chlorophyllase and lipoxygenase) in olive drupes from the fruit-setting period to harvest time. *J Am Soc Hortic Sci* 131:593-600.

Criado MN, Motilva MJ, Goñi M, Romero MP (2007) Comparative study of the effect of the maturation process of the olive fruit on the chlorophyll and carotenoid fractions of drupes and virgin oils from Arbequina and Farga cultivars. *Food Chem* 100:748-755.

Crozier A, Jaganath IB (2009) Dietary phenolic: chemistry, bioavailability and effects on health. *Nat Prod Rep* 26(8): 1001-1043.

Czemmel S, Stracke R, Weisshaar B, Cordon N, Harris NN, Walker AR, Robinson SP, Bogs J (2009) The grapevine R2R3-MYB transcription factor *VvMYBF1* regulates flavonol synthesis in developing grape berries. *Plant Physiol* 151: 1513-1530.

Dag A, Kerem Z, Yogev N, Zipori I, Lavee S, Ben-David E (2011) Influence of time of harvest and maturity index on olive oil yield and quality. *Sci Hortic* 127:358-366.

Dare AP, Tomesa S, Cooney JM, Greenwooda DR and Hellens LP (2013) The role of enoyl reductase genes in phloridzin biosynthesis in apple. *Plant Physiol Biochem* 72: 54–61.

Davin LB, Wang HB, Crowel AL, Bedgar DL, Sarkanen S, Lewis NG (1997) Stereoselective bimolecular phenoxy radical coupling by an auxiliary (dirigent) protein without an active center. *Science* 275:362-366.

DeFelice SL The nutraceutical revolution: its impact on food industry. *Trends Food Sci Technol* 6:59–61.

Deluc L, Bogs J, Walker AR, Ferrier T, Decendit A, Merillon JM, Robinson SP, Barrieu F (2008) The transcription factor *VvMYB5b* contributes to the regulation of anthocyanin and proanthocyanidin biosynthesis in developing grape berries. *Plant Physiol* 147: 2041-2053.

Dillard CJ, German JB (2000) Phytochemicals: nutraceuticals and human health. *J Sci Food Agric* 80(12): 1744–1756.

Dubcovsky J (2004) Marker-Assisted Selection in Public Breeding Programs: The Wheat Experience. *Crop Sci* 44:6.

Dubos C, Stracke R, Grotewold E, Weisshaar B, Martin C, Lepiniec L (2010) MYB transcription factors in Arabidopsis. *Trends Plant Sci* 15:573-581.

Dzhangaliev AD (2003) The wild apple tree of Kazakhstan. *Hort Rev* 29: 63-30.

Ehrenkranz JR, Lewis NG, Kahn CR, Roth J (2005) Phlorizin: A review. *Diabetes/Metabolism Research and Reviews* 21: 31–38.

Espley R, Brendolise C, Chagné D, Kutty-Amma D, Green R, Volz J, Putterill H, Schouten S, Gardiner R, Hellens RP and Allan A (2009) Multiple repeats of a promoter segment causes transcription factor autoregulation in red apples. *Plant Cell* 10: 1105.

Espley R, Hellens RP, Putterill J, Stevenson DE, Kutty-Amma S and Allan AC 2006 Red colouration in apple fruit is due to the activity of the MYB transcription factor, MdMYB10. *The Plant Journal* 49: 414-427.

Espley RV, Bovy A, Bava C, Jaeger SR. (2013) Analysis of genetically modified red-fleshed apples reveals effects on growth and consumer attributes. *Plant Biotechnol. J* 11:408–419.

Esti M, Cinquanta L, La Notte E (1998) Phenolic compounds in different olive varieties. *J Agric Food Chem* 46:32-35.

Fabbris L (1997) Statistica multivariate, McGraw-Hill, Milano.

FAO (Food and Agriculture Organization of the United Nations), (2011) FAOSTAT http://faostatfaoorg/site/339/defaultaspx

Fardet A, Chardigny JM (2013) Plant-based foods as a source of lipotropes for human nutrition: a survey of in vivo studies. *Crit Rev Food Sci Nutr* 53:535–90.

Feskanich D, Ziegler R, Michaud D, Giovannucci E, Speizer F, WIllett W, Colditz G (2000) Prospective study of fruit and vegetable consumption and risk of lung cancer among men and women *J Natl Cancer Inst* 92: 1812-1823.

Francini A and Sebastiani L (2013) Phenolic compounds in apple (*Malus x domestica Borkh*): compounds characterization and stability during postharvest and after processing. *Antioxidants* 3: 181–193.

FreshPlaza 2008 Global fresh produce and Banana news 2008 NFG develops redfleshed apple http://freshplaza/news.html

Friedman R, Farh K, Burge C, Bartel D (2009) Most mammalian mRNAs are conserved targets of microRNAs *Genome Res* 19:92–105.

Fu Q, Cash SE, Andersen JJ, Kennedy CR Oldenburg D G, Zander VB, Foley GR and Shelley CS (2013) CD43 in the nucleus and cytoplasm of lung cancer is a potential therapeutic target. *Int J Cancer* 132: 1761–1770

Gaidatzis D, Nimwegen E, Hausser J, Zavolan M (2007) Inference of miRNA targets using evolutionary conservation and pathway analysis. *BMC Bioinformatic*, 69 :1–69

Galtier O, Dupuy N, Le Dréau Y, Ollivier D, Pinatel C, Kister J, Artaud J (2007) Geographical origins compositions of virgin olive oils determined by chemometric analysis of NIR spectra. *Anal Chim Acta* 595: 136-144.

García JM, Seller S, Pérez-Camino MC (1996) Influence of fruit ripening on olive oil quality. *J Agric Food Chem* 44:3516-3520.

German JB and Watkins SM (2004) Metabolic assessment—a key to nutritional strategies for health. *Trends in Food Science & Technology* 11: 541.

Goodman MM (2004) Plant Breeding Requirements for Applied Molecular Biology. *Crop Sci* 44:6.

Gosch C, Halbwirth H, Kuhn J, Miosic S, Stich K (2009) Biosynthesis of phloridzin in apple (*Malus domestica Borkh*). *Plant Sci* 176:223–231.

Gosch C, Stich K, Halbwirth H (2010) Cloning and heterologous expression of glycosyltransferases from *Malus x domestica* and *Pyrus communis*, which convert phloretin to phloretin 2-O-glucoside (phloridzin). Plant Sci. 178: 299–306

Griffiths-Jones S; Saini H; Dongen S, Enright A (2008) Mirbase: Tools for microRNA genomics *Nucleic Acids Res* 36:154–158.

Guyot S and Bourvellec CL (2002) Procyanidins are the most abundant polyphenols in dessert apples at maturity. *LWT- Food Sci Technol* 35: 289-291.

Hajjar R and Hodgkin T (2007) The use of wild relatives in crop improvement: a survey of developments over the last 20 years. *Euphytica* 156: 1-13.

Hampson CR, Quamme HA, Hall JW, MacDonald RA, King MC and Cliff MA (2000) Sensory evaluation as a selection tool in apple breeding. *Euphytica* 111: 79-90

Harker FR, Gunson FA and Jaeger SR (2003) The case for fruit quality: An interpretive review of consumer attitudes, and preferences for apples. *Postharvest Biol Technol* 28: 333-347.

Harker FR, Kupferman EM, Marin AB, Gunson FA and Triggs CM (2008) Eating quality standards for apples based on consumer preferences. *Postharvest Biol Technol*, 50: 70-78.

Henry-Kirk RA, McGhie TK, Andre CM, Hellens RP and Allan AC (2012) Transcriptional analysis of apple fruit proanthocyanidin biosynthesis. *J Exp Bot* 63: 5437–5450.

Holton TA and Cornish EC (1995) Genetics and biochemistry of anthocyanin biosynthesis. *Plant Cell* 7: 1071-1083.

Iñón FA, Garrigues JM, Garrigues S, Molina A, Guardiã M (2003) Selection of calibration set samples in determination of olive oil acidity by partial least squares– attenuated total reflectance–Fourier transform infrared spectroscopy. *Anal Chim Acta* 489: 59-75.

Jaeger SR, Andani Z, Wakeling IN and MacFie HJH (1998) Consumer preferences for fresh and aged apples: A cross-cultural comparison. *Food Quality and Preference* 9(5): 355-366.

Janick JN, Cummins J, Brown SK and M. Hemmat (1996) Apples, p1-51. In J. Janick, and J.N. Moore (eds.). Fruit breeding. Volume 1. Tree and tropical fruits. John Wiley & Sons, Inc. New York.

Jin H, Cominelli E, Bailey P, Parr A, Mehrtens F, Jones J, Tonelli C, Weisshaar B, Martin C (2000) Transcriptional repression by AtMYB4 controls production of UV-protecting sunscreens in Arabidopsis. *EMBO J* 19 (22):6150-61.

Jiménez A, Rodríguez R, Fernández-Caro I, Guillén R, Fernández-Bolaños J, Heredia A (2001a) Olive fruit cell wall: Degradation of cellulosic and hemicellulosic polysaccharides during ripening. *J Agric Food Chem* 49:2008-2013

Jiménez A, Rodríguez R, Fernández-Caro I, Guillén R, Fernández-Bolaños J, Heredia A (2001b) Olive fruit cell wall: Degradation of pectic polysaccharides during ripening. *J Agric Food Chem* 49:409-415.

Jones P, Messner B, Nakajima J, Schäffner AR and Saito K (2003) UGT73C6 and UGT78D1, glycosyltransferases involved in flavonol glycoside biosynthesis in Arabidopsis thaliana. *J Biol Chem* 45: 43910–43918

Joseph JA, Shukitt-Hale B, Denisova NA, Bielinski D, Martin A, McEwen JJ and Bickford PC (1999) Reversals of age-related declines in neuronal signal transduction, cognitive, and motor behavioral deficits with blueberry, spinach, or strawberry dietary supplementation. *J Neurosci* 19: 8114-8121

Ju Z, Liu C and Y Yuan (1995) Activities of chalcone synthase and UDPGal: flavonoid-3-O-glycosiltransferase in relation to anthocyanin synthesis in apple. *Sci Hortic* 63: 175-185.

Ju Z, Yongbing Y, Chenglian L, Yongzhang W and Xiaopeng T (1997) Dihydroflavonol reductase activity and anthocyanin accumulation in 'Delicious', 'Golden Delicious' and 'Indo' apples. *Sci Hortic* 70: 31-43.

Judgé H, Nguy D, Moller I, Cooney JM, Atkinson RG (2008) Isolation and characterization of a novel glycosyltransferase that converts phloretin to phlorizin, a potent antioxidant in apple. *FEBS Journal* 275: 3804-3814

Kertesz M, Iovino N, Unnerstall U, Gaul U, Segal E (2007) The role of site accessibility in microrna target recognition. *Nat Genet* 39:1278–1284.

Kim SH, Lee JR, Hong ST, Yoo YK, An G, Kim SR (2003) Molecular cloning and analysis of anthocyanin biosynthesis genes preferentially expressed in apple skin. *Plant Sci* 165: 403-413.

Knekt P, Jarvinen R, Hakkinen R, Reunanen A, Maatela J (1996) Flavonoid intake and coronary mortality in Finland: a cohort study. *BMJ* 312: 478-481.

Knoops KTB, de Groot LC, Kromhout D, Perrin AE, Moreiras-Varela O, Menotti A, van Staveren WA. (2004) Mediterranean diet, lifestyle factors, and 10-year mortality in elderly European men and women: *The HALE project JAMA* 292: 1433–1439

Kobayashi S, Goto-Yamamoto N, Hirochika H (2004) Retrotransposon-induced mutations in grape skin color. *Science* 304: 982-982.

Koes R, Verweij W, Quattrocchio F (2005) Flavonoids: a colorful model for the regulation and evolution of biochemical pathways. *Trends Plant Sci* 10: 236-242.

Kondo S, Hiraoka S, Kobayashi C, Honda and Terahara N (2002) Changes in the expression of anthocyanin biosynthetic genes during apple development. *J Am Soc Hortic Sci* 127: 971-976.

Kubista M, Andrade JM, Bengtsson M, Forootan A, Jonak J, Lind K (2006). The real-time polymerase chain reaction. *Mol Aspects Med* 27:95–125.

Kumar S, Nei M, Dudley J, Tamura K (2008) MEGA: a biologist-centric software for evolutionary analysis of DNA and protein sequences. Brief Bioinform, 9: 299-306.

Lawless HT and Heymann H. (1998). Descriptive analysis. Sensory evaluation of food, principles and practices. 1st Edition. USA: Chapman & Hall.

Le Marchand L, Murphy S, Hankin J, Wilkens L, Kolonel L (2000) Intake of flavonoids and lung cancer. *J Natl Canc Inst* 92:154-160.

Lewis B, Shih I, Jones-Rhoades M, Bartel D, Burge C (2003) Prediction of mammalian microRNA targets. *Cell* 115:787–798.

Lila MA (2004) Plant pigments and human health In Plant pigments and their manipulation. KM Davies ed. CRC Press, pp 246-274.

Lin-Wang K, Bolitho K, Grafton K, Kortstee A, Karunairetnam S, McGhie TK, Espley RV, Hellens RP, Allan AC (2010) An R2R3 MYB transcription factor associated with regulation of the anthocyanin biosynthetic pathway in *Rosaceae*. *BMC Plant Biol* 10:50.

Mancinelli AL, Yang CPH, Lindquist P, Anderson OR and Rabino I (1975) Photocontrol of anthocyanin synthesis. III.The action of streptomycin on the synthesis of chlorophyll and anthocyanin. *Plant Physiol* 55: 251–25.

Maragkakis M, Reczko M, Simossis V, Alexiou P, Papadopoulos G (2009) Diana-MicroT web server: Elucidating microRNA functions through target prediction. *Nucleic Acids Res* 37:273-276.

Martens S and Mithöfer A (2005) Flavones and flavone synthases. *Phytochemistry* 66:2399–2407.

Martinelli F and Tonutti P (2012) Flavonoid metabolism and gene expression in developing olive (*Olea europaea* L) fruit. *Plant Biosystems* 1:1–7

Matsui K, Umemura Y and Ohme-Takagi M (2008) AtMYBL2, a protein with a single MYB domain, acts as a negative regulator of anthocyanin biosynthesis in Arabidopsis. *Plant J* 55: 954–967.

Matsumoto H, Nakamura Y, Tachibanaki S, Kawamura S and Hirayama M (2003) Stimulatory effect of cyanidin 3-glycosides on the regeneration of rhodopsin. *J Agric Food Chem* 51: 3560-3563

McCracken VA, Maier B, Boylston T and Worley T (1994) Development of a scheme to evaluate consumer apple variety preference. Washington State 21 University. 34th Annual conference presentation of the food distribution research society, *J. Food Distr. Research*. 56-63.

Mehrtens F, Kranz H, Bednarek P, Weisshaar B (2005) The Arabidopsis transcription factor MYB12 is a

flavonol specific regulator of phenylpropanoid biosynthesis. *Plant Physiol* 138(2):1083-1096.

Mejia R (2013) Vav Proteins' Role in Skin Cancer. *PLoS Biol* 11:7.

Milenkovic D, Jude B, Morand C (2013) miRNA as molecular target of polyphenols underlying their biological effects. *Free Radic Biol Med* 64: 40–51.

Montedoro GF; Servili M, Baldioli M, Miniati E (1992) Simple and hydrolyzable phenolic compounds in virgin olive oil 2 Initial characterization of the hydrolyzable fraction. *J Agric Food Chem* 40:1577–1580.

Moran R (1982) Formulae for determination of chlorophyllous pigments extracted with NN-dimethylformamide. *Plant Physiol* 69:1376-1381.

Morelló JR, Vuorela S, Romero MP, Motilva MJ, Heinonen M (2005) Antioxidant activity of olive pulp and olive oil phenolic compounds of the arbequina cultivar J Agric Food Chem, 53, 2002-2008

Muleo R, Colao MC, Miano D, Cirilli M, Intrieri MC, Baldoni L, Rugini E (2009) Mutation scanning and genotyping by high- resolution DNA melting analysis in olive germplasm. *Genome* 52:252–260.

Murata J, Roepke J, Gordon H, De Luca V (2008) The leaf epidermome of Catharanthus roseus reveals its biochemical specialization. *Plant Cell*, 20(3):524–542.

Murkovic M, Lechner S, Pietzka A, Bratacos M, Katzogiannos E (2004) Analysis of minor components in olive oil. *J Biochem Methods* 61:155-160.

Nesi N, Jond C, Debeaujon I, Caboche M, Lepiniec L (2001) The Arabidopsis TT2 gene encodes an R2R3 MYB domain protein that acts as a key determinant for proanthocyanidin accumulation in developing seed. *Plant Cell* 13: 2099-2114.

Neveu V, Perez-Jimenez J, Vos F, Crespy V, du Chaffaut L, Mennen L, Knox C, Eisner R, Cruz J, et al. (2010) PhenolExplorer: an online comprehensive database on polyphenol contents in foods. Database (Oxford). Available at http://www.phenol-explorer.eu/.

Nguyen-Dumont T, Pope BJ, Hammet F, Southey MC, Park DJ (2013) A High-Plex PCR approach for massively parallel sequencing. *BioTechniques* 55: 69-74.

Nielsen C, Shomron N, Sandberg R, Hornstein E, Kitzman J, Burge C (2007) Determinants of targeting by endogenous and exogenous microRNAs and siRNAs *RNA;13:1894–1910*

O'Rourke AD (2011) World Apple Review Washington, USA: Belrose Inc, Pullman

Obied HK, Prenzler PD, Ryan D, Servili M, Taticchi A, Esposto S, Robards K (2008) Biosynthesis and biotransformations of phenol-conjugated oleosidic secoiridoids from Olea europaea L *Nat Prod Rep* 25(6):1167–1179.

Obied HK, Prenzler PD, Omar SH, Ismael R, Servili M, Esposto S, Taticchi A, Selvaggini R, Urbani S; Fishbein JC, Heilman JM (2012) Pharmacology of Olive Biophenols In Advances in Molecular Toxicology Eds; Elsevier: Amsterdam, The Netherlands; Volume 6: 195–223.

Pallant A, Eskenazi A, Mattei MG, Fournier RE, Carlsson SR, Fukuda M, Frelinger JG (1989) Characterization of cDNAs encoding human leukosialin and localization of the leukosialin gene to chromosome 16 *Proc Natl Acad Sci USA 86 (4): 1328–32*

Pasqualone A, Di Rienzo V, Blanco A, Summo C, Caponio F, Montemurro C (2012) Characterization of virgin olive oil from Leucocarpa cultivar by chemical and DNA analysis. *Food Res Int* 47(2):188–193.

Paz-Ares J, Ghosal D, Wienand U, Peterson PA, Saedler H (1987) The regulatory c1 locus of Zea mays encodes a protein with homology to myb proto-oncogene products and with structural similarities to transcriptional activators. *EMBO J* 6: 3553-3558.

Peck G and Merwin I (2010) A Grower's Guide to Organic Apples NYS IPM Publication No 223 Cornell University Cooperative Extension

Pelletier MK, Burbulis IE, Winkel-Shirley B (1999) Disruption of specific flavonoid genes enhances the accumulation of flavonoid enzymes and end products in Arabidopsis seedlings. *Plant Mol Biol* 40: 45-54.

Pelletier MK, Murrell J, Shirley BW (1997) Arabidopsis flavonol synthase and leucoanthocyanidin dioxygenase: further evidence for distinct regulation of early and late flavonoid biosynthetic genes. *Plant Physiol* 113: 1437–1445

Pelletier MK, Shirley BW (1996) Analysis of flavanone 3-hydroxylase in Arabidopsis seedlings: coordinate regulation with chalcone synthase and chalcone isomerase. *Plant Physiol* 111: 339–345.

Peneau S, Hoehn E, Roth HR, Escher F and Nuessli J (2006) Importance and consumer perception of freshness of apples. *Food Quality Prefer* 17: 9-19.

Persak H and Pitzschke A (2014) Dominant repression by Arabidopsis transcription factor MYB44 causes oxidative damage and hypersensitivity to abiotic stress Int J Mol Sci, 15, 2517-2537

Prasanna V, Prabha TN, Tharanathan RN (2007) Fruit ripening phenomena – An overview. *Crit Rev Food Sci Nutr* 47:1-19.

Rehmsmeier M, Steffen P, Hochsmann M, Giegerich R (2004) Fast and effective prediction of microRNA/target duplexes RNA; 10:1507–1517

Reid M & Buisson D (2001) Factors influencing adoption of new apple and pear varieties in Europe and the UK *International Journal of Retail & Distribution Management*, **29**, 315-327

Reinhart BJ, Weinstein EG, Rhoades MW, Bartel B and Bartel DP (2002). MicroRNAs in plants. *Genes Dev.* 16:1616–1626.

Roberfroid MB (1999) Concepts in functional foods: the case of inulin and oligofructose. *J Nutr* 129 (7 Suppl):1398S–1401S.

Robinson C (1997) Genetically modified foods and consumer choice. *Trends Food Scie Technol* 8:84–8.

Roca M, Mínguez-Mosquera MI (2001) Unusual Carotenogenesis in Fruits with Pronounced Anthocyanic Ripening (Olea europaea Var Arbequina). *J Agric Food Chem* 49:4414-4419.

Romani A, Mulinacci N, Pinelli P, Vincieri FF, Cimato A (1999) Polyphenolic content in five Tuscany cultivars of Olea europaea L. *J Agric Food Chem* 47:964-967.

Rotondi A, Bendini A, Cerretani L, Mari M, Lercker G, Gallina Toschi T (2004) Effect of olive ripening degree on the oxidative stability and organoleptic properties of cv. Nostrana di Brisighella Extra Virgin Olive Oil. *J Agric Food Chem* 52:3649-3654.

Russo M, Tedesco I, Iacomino G, Palumbo R, Galano G, Russo GL (2005) Dietary phytochemicals in chemoprevention of cancer. *Curr Med. Chem Immunol Endocr Metab Agents* 5:61–72.

Ryan D, Antolovich M, Herlt T, Prenzler PD, Lavee S, Robards K (2002) Identification of phenolic compounds in tissues of the novel olive cultivar hardy's mammoth J Agric Food Chem, 50(23):6716–6724

Schirrmacher G, Schempp H (2003) Antioxidative potential of flavonoid-rich extracts as new quality marker for different apple varieties *J App Bot*, 77: 163–166

Schwinn KE, Davies KM (2004) Flavonoids In: Davies KM, editor Plant pigments and their manipulation Annual Plant Reviews Vol 14 Boca Raton FL: CRC Press, Blackwell Publishing; pp 92–149

Selvaggini R, Servili M, Urbani S, Esposto S, Taticchi A, Montedoro GF (2006) Evaluation of phenolic compounds in virgin olive oil by direct injection in high-performance liquid chromatography with fluorometric detection. *J Agric Food Chem* 54:2832–8.

Servili M, Baldioli M, Selvaggini R, Miniati E, Macchioni A, Montedoro GF (1999) High-Performance Liquid Chromatography evaluation of phenols in olive fruit, virgin olive oil, vegetation waters and pomace and 1D- and 2D-Nuclear Magnetic Resonance characterization. *J Am Oil Chem Soc* 76: 873–882.

Servili M & Montedoro G (2002) Contribution of Phenolic Compounds to Virgin Olive Oil Quality European. *Eur J Lipid Sci Technol* 104 (9-10):602-613.

Servili M, Esposto S, Fabiani R, Urbani S, Taticchi A, Mariucci F, Selvaggini R, Montedoro GF (2009) Phenolic compounds in olive oil: Antioxidant, health and organoleptic activities according to their chemical structure *Inflammopharmacology* 17: 1–9.

Sesso H, Gaziano JM, Liu S, Buring J (2003) Flavonoid intake and risk of cardiovascular disease in women *Am J Clin Nutr* 77: 1400-1408.

Shin WH, Park SJ and Kim EJ (2006) Protective effect of anthocyanins in middle cerebral artery occlusion and reperfusion model of cerebral ischemia in rats. *Life Sci* 79: 130-137.

Smith MAL, Marley KA, Seigler D, Singletary K and Meline WB (2000) Bioactive properties of wild blueberry fruits. *J Food Sci* 65: 352-356.

Snow JW, Hake AE, Isaacs SK, Baggish AL, Chan SY (2013) Ineffective delivery of diet-derived microRNAs to recipient animal organisms *RNA Biology; 10:1107-16;*

Stracke R, de Vos RC, Bartelniewoehner L, Ishihara H, Sagasser M, Martens S, Weisshaar B (2009) Metabolomic and genetic analyses of flavonol synthesis in Arabidopsis thaliana support the in vivo involvement of leucoanthocyanidin dioxygenase. *Planta*; 229:427–445

Stracke R, Ishihara H, Barsch GHA, Mehrtens F, Niehaus K, Weisshaar B (2007) Differential regulation of closely related R2R3-MYB transcription factors controls flavonol accumulation in different parts of the Arabidopsis thaliana seedling. *Plant J* 50: 660-677

Takos AM, Jaffe FW, Jacob SR, Bogs J, Robinson SP and Walker AR (2006) Light-induced expression of a MYB gene regulates anthocyanin biosynthesis in red apples. *Plant Physiol* 142: 1216-1232.

Tamura K, Stecher G, Peterson D, Filipski A and Kumar S (2013) MEGA6: Molecular Evolutionary Genetics Analysis Version 6.0. *Mol Biol Evol* 30(12):2725–2729.

Tapp HS, Defernez M, Kemsly EK (2003) FTIR spectroscopy and multivariate analysis can distinguish the geographic origin of extra virgin olive oils. *J Agric Food Chem* 51:6110-6115.

Tomás-Barberán FA and Clifford MN (2000) Flavanones, chalcones and dihydrochalcones – nature, occurrence and dietary burden. *J Sci Food Agr* 80:1073-1080.

Treutter D (2001) Biosynthesis of phenolic compounds and its regulation in apple. *Plant Growth Regul* 34(1): 71-89.

Truter AB, Eksteen GJ, Van Der Westhuizen, AJM, Peereboom Voller C (1985) Evaluation of maturity indices to determine optimum picking stage of apples. *Hort Sci* 2: 19-25.

Tsao, R and Yang R (2003) Polyphenolic profiles in eight apple cultivars using high-performance liquid chromatography (HPLC). *J Agric Food Chem* 51: 6347-6353.

Tunca B, Tezcan G, Cecener G, Egeli U, Ak S, Malyer H, Tumen G and Bilir A (2012) Olea europaea leaf extract alters microRNA expression in human glioblastoma cells. *J Cancer Res Clin Oncol* 138(11):1831-44.

Ubi BE, Honda C, Bessho H, Kondo S, Wada M, Kobayashi S and Moriguchi T (2006) Expression analysis of anthocyanin biosynthetic genes in apple skin: Effect of UV-B and temperature. *Plant Sci* 170, 571-578

Uceda M and Frías L (1975) Harvest dates Evolution of the fruit oil content, oil composition and oil quality In Proceedings of II Seminario Oleícola Internacional; International Olive Oil Council: Cordoba, Spain, 125-130

van Nocker S, Berry G, Najdowski J, Michelutti R, Luffman M, Forsline P, Alsmairat N, Beaudry R, Nair MG and Ordidge M (2012) Genetic diversity of red-fleshed apples (*Malus*) *Euphytica* 185: 281-293.

Vaucheret, H. et al. (2004) The action of ARGONAUTE1 in the miRNA pathway and its regulation by the miRNA pathway are crucial for plant development. *Genes Dev*. 18:1187–1197.

Velasco, R., A. Zharkikh, J. Affourtit, A. Dhingra, A. Cestaro et al., (2010) The genome of the domesticated apple (*Malus x domestica* Borkh.). *Nat Genet* 42: 833-839.

Volz R (2006) Red-fleshed apple a silver bullet? *Orchardist* 79: 18-55.

Volz R, Oraguzie N, Whitworth C, How N, Chagnè D, Carlisle C and Gardiner S (2009) Red flesh breeding in apple—progress and challenges. *Acta Hort* 814: 337–342

Volz RK, White AG, Brookfield PL, Weskett R, Legg S, Koorey R, Tustin DS, Hughes J and White M (2004) Breeding and development of the new apple cultivar 'JazzTM'. *Acta Hort* 663: 891-894.

Wang, J, and Mazza, G (2002) Effects of anthocyanins and other phenolic compounds on the production of tumor necrosis factor alpha in LPS/IFN-gamma-Activated RAW 2647 macrophages. *J Agric Food Chem* 50: 4183-4189.

Wesley IJ, Barnes RJ, McGill AEJ (1995) Measurement of adulteration of olive oils by near-infrared spectroscopy. *J Am Oil Chem Soc* 72: 289-292.

Witwer KW, McAlexander MA, Queen SE, Adams RJ (2013) Real-time quantitative PCR and droplet digital PCR for plant miRNAs in mammalian blood provide little evidence for general uptake of dietary miRNAs: Limited evidence for general uptake of dietary plant xenomiRs. *RNA Biology* 10:2-8.

Woods R, Walters H, Raven J, Wolfe R, Ireland P, Thien F, Abramson M (2003) Food and nutrient intakes and asthma risk in young adults. *Am J Clin Nutr* 78:414-421.

Xia R, Zhu H, An YQ, Beers EP, Liu Z (2012) Apple miRNAs and tasiRNAs with novel regulatory networks. *BMC Gen Biol* 13(6):47.

Xie DY, Sharma SB, Dixon RA (2004) Anthocyanidin reductases from Medicago truncatula and *Arabidopsis thaliana*. *Arch Biochem Biophys* 422: 91–102

Yonekura-Sakakibara K, Tohge T, Niida R, Saito K (2007) Identification of a flavonol 7-O-rhamnosyltransferase gene determining flavonoid pattern in Arabidopsis by transcriptome coexpression and reverse genetics. *J Biol Chem* 282:14932–14941.

Yousfi K, Cayuela JA, García JM (2008) Reduction of Virgin Olive Oil Bitterness by Fruit Cold Storage. *J Agric Food Chem* 56:10085-10091.

Zhang L, Hou D, Chen X; Li D, Zhu L, Zhang Y, Li J, Bian Z, Liang X, Cai X, Yin Y, Wang C, Zhang T, Zhu D, Zhang D, Xu J, Chen Q, Ba Y, Liu J, Wang Q, Chen J, Wang J, Wang M, Zhang Q, Zhang J, Zen K, Zhang CY (2011) Exogenous plant MIR168a specifically targets mammalian LDLRAP1: evidence of cross-kingdom regulation by microRNA *Cell research* 22: 107–26

Zhao J, Pang Y, Dixon RA (2010) Update on biosynthesis of proanthocyanidins. The mysteries of proanthocyanidin transport and polymerization. *Plant Physiol* 153:437-443.

APPENDIX

Lists of published papers and poster communications

Abdollahi H, Luziatelli F, Cirilli M, Frioni E, Rugini E, Ruzzi M and Muleo R (2014) Involvement of Hypersensitive-like reaction in tolerance to fire blight in pear (*Pyrus communis* L.). African Journal of Biotechnology 13: in press.

Distefano G., **Cirilli M.**, Las Casas G., La Malfa S., Continella A., Rugini E., Thomas B., Long G., Gentile A., Muleo R.(2013). Ectopic expression of Arabidopsis phytochrome B in Troyer citrange affects photosynthesis and plant morphology. *Scientia Horticulturae*. Vol. 159, Pages 1-7

Iacona C., **Cirilli M.**, Zega A., Frioni E., Silvestri C., Muleo R. (2013) A somaclonal myrobalan rootstock increases waterlogging tolerance to peach cultivar in controlled conditions. *Scientia Horticulturae*. Volume 156, 1-8.

Pistelli L., Iacona C., Miano D., **Cirilli M.**, Colao M.C., Mensuali-Sodi A., Muleo R. (2012). Novel Prunus rootstock somaclonal variants with divergent ability to tolerate waterlogging. *Tree Physiology*. Volume 32, Pages 355-368.

Cirilli M., Bellincontro A., De Santis D., Botondi R., Colao M.C., Muleo R., Mencarelli F. (2012). Temperature and water loss affect ADH activity and gene expression in grape berry during postharvest dehydration. *Food Chemistry*. Volume 132, Pages 447–454.

Mencarelli F., Bellincontro A., Nicoletti I., **Cirilli M.**, Muleo R., Corradini D. Chemical and Biochemical Change of Healthy Phenolic Fractions in Wine grape by Means of Postharvest Dehydration. *J. Agric. Food Chem*. 2010, 58, 7557–7564.

Muleo R., Colao M.C., Miano D., **Cirilli M.**, Intrieri M.C., Baldoni L., Rugin, E. Mutation scanning and genotyping by high-resolution DNA melting analysis in olive germplasm. Genome 52 (2009): 252–260.

Cirilli M., Caporali S., Frioni E., Paoletti., A., Zega A., Latini G., Rapoport H., Perrotta G., Rosari A., Muleo R (2013). I geni OeCNR regolano la dimensione della drupa di olivo sin dalle prime fasi dello sviluppo dell'ovario?. In: (a cura di): Bonghi C., Sambo P., Riassunti dei lavori, X giornate Scientifiche SOI, Padova, 25-27 giugno 2013. *ACTA ITALUS HORTUS*, vol. 12, p. 88, Firenze: Società di Ortoflorofrutticoltura Italiana (SOI), ISBN: 978-88-905628-3-9, Padova, 25-27 giugno 2013

Cirilli M., Giampetruzzi A., Frioni E., Saponari M., Muleo R (2013). I microRNA e l'architettura della pianta in Olivo. In: (a cura di): Bonghi C., Sambo P., Riassunti dei lavori, X giornate Scientifiche SOI, Padova, 25-27 giugno 2013. *ACTA ITALUS HORTUS*, vol. 12, Firenze: Società di Ortoflorofrutticoltura Italiana (SOI), ISBN: 978-88-905628-3-9, Padova, 25-27

Iacona C., **Cirilli M.,** Frioni E., Latini G., Zega A., Zecchini M., Muleo R (2013). La qualità della luce e il fotoperiodo regolano lo sviluppo della pianta in vitro e in extra vitro tramite il sistema di segnalazione del fitocromo. In: (a cura di): Bonghi C., Sambo P., Riassunti dei lavori, X giornate Scientifiche SOI, Padova,

25-27 giugno 2013. *ACTA ITALUS HORTUS*, vol. 12, p. 145, Firenze: Società di Ortoflorofrutticoltura Italiana (SOI), ISBN: 978-88-905628-3-9, Padova, 25-27

Zega A., Sgamma T., Iezzi G., Massiah A., Luziatelli F., Silvestri C., **Cirilli M.**, Frioni E., Latini G., Rugini E., Ruzzi M., Muleo R, Thomas B. (2013). La qualità della luce modula l'infezione e la risposta di difesa al colpo di fuoco batterico (Fire Blight).. In: (a cura di): Bonghi C., Sambo P., Riassunti dei lavori, X giornate Scientifiche SOI, Padova, 25-27 giugno 2013. *ACTA ITALUS HORTUS*, vol. 12, p. 72, Firenze: Società di Ortoflorofrutticoltura Italiana (SOI), ISBN: 978-88-905628-3-9, Padova, 25-27

Latini G., Zega A., **Cirilli M.**, Cristofori V., Frioni E., Luziatelli F., Ruzzi M., Muleo R (2013). Mele a polpa rossa Italian Red Passion: un incremento di antociani e di polifenoli totali determina un'azione antimicrobica ed un potenziale effetto salutistico.. In: (a cura di): Bonghi C., Sambo P., Riassunti dei lavori, X giornate Scientifiche SOI, Padova, 25-27 giugno 2013. *ACTA ITALUS HORTUS*, vol. 12, p. 109-110, Firenze: Società di Ortoflorofrutticoltura Italiana (SOI), ISBN: 978-88-905628-3-9, Padova, 25-27

Muleo R, **Cirilli M.**, Caboni E., Iacona C., Frioni E., Zega A., Latini G. (2013). Ringiovanire dalla fase adulta: il meccanismo genetico e epigenetico in pesco.. In: (a cura di): Bonghi C., Sambo P., Riassunti dei lavori, X giornate Scientifiche SOI, Padova, 25-27 giugno 2013. *ACTA ITALUS HORTUS*, vol. 12, p. 91, Firenze: Società di Ortoflorofrutticoltura Italiana (SOI), ISBN: 978-88-905628-3-9, Padova, 25-27 giugno 2013.

Frioni E., Caruso G., **Cirilli M.**, Zega A., Gennai C., Ruzzi M., Servili M., Gucci R., Bonocore V., Poerio E., Muleo R (2013). Stato idrico della pianta e catabolismo dei polifenoli in Olea europaea.. In: (a cura di): Bonghi C., Sambo P., Riassunti dei lavori, X giornate Scientifiche SOI, Padova, 25-27 giugno 2013. *ACTA ITALUS HORTUS*, vol. 12, p. 76, Firenze: Società di Ortoflorofrutticoltura Italiana (SOI), ISBN: 978-88-905628-3-9, Padova, 25-27

E. Rugini, C. Silvestri, V. Cristofori, G. Musco, M- Zecchini, M.C. Colao, **M. Cirilli**, G. Pannelli, R. Muleo. Phenotypical observations of novel olive genotypes suitable for an intensive plantation. In: OLIVEBIOTEQ 2011, Chania (Greece) 31 October- 4 November 2011

Cirilli M., Colao M.C., Rugini E., Caboni E. and Muleo R. Go back from adult phase. Proceeding of the Joint Meeting AGI-SIVB-SIGA, Assisi, 12-22 September 2011, Oral Communication.

Cristofori V., **Cirilli M.**, Montagnini D., Jacob F., Senni S., Rugini E., Muleo R. Il germoplasma di ciliegio del territorio dell'alto Lazio, aspetti bioagronomici e molecolari. Convegno Nazionale Del Ciliegio, Rocca di Vignola 8-10 Giugno 2011

Cirilli M., Bellincontro A., Nicoletti I., Mencarelli F., Colao M.C., Muleo R. Temperature and water loss differently affect gene expression in grape berry cv "Aleatico" during post-harvest dehydration. Proceeding of the Joint Meeting SIGA. Matera 27-30 Settembre 2010. Poster Presentation.